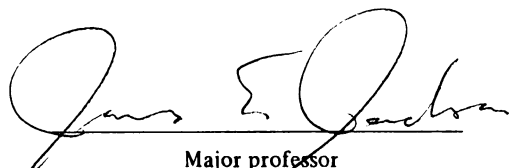




This is to certify that the
thesis entitled
Molecular Magnets from Stable Organic Free Radicals:
An Ion-Binding Approach

presented by
Sei-Hum Jang

has been accepted towards fulfillment
of the requirements for
Ph.D. degree in Chemistry


Major professor

Date 10/22/93

LIBRARY
Michigan State
University

PLACE IN RETURN BOX to remove this checkout from your record.
TO AVOID FINES return on or before date due.

DATE DUE	DATE DUE	DATE DUE
FEB 06 1996	_____	_____
_____	_____	_____
_____	_____	_____
_____	_____	_____
_____	_____	_____
_____	_____	_____
_____	_____	_____

MSU is An Affirmative Action/Equal Opportunity Institution

c:\circ\database.pm3-p.1

Molecular Magnets from Stable Organic Free Radicals:
An Ion-Binding Approach

by

Sei - Hum Jang

A DISSERTATION

Submitted to
Michigan State University
in partial fulfillment of the requirements
for the degree of

DOCTOR OF PHILOSOPHY

Department of Chemistry

1993

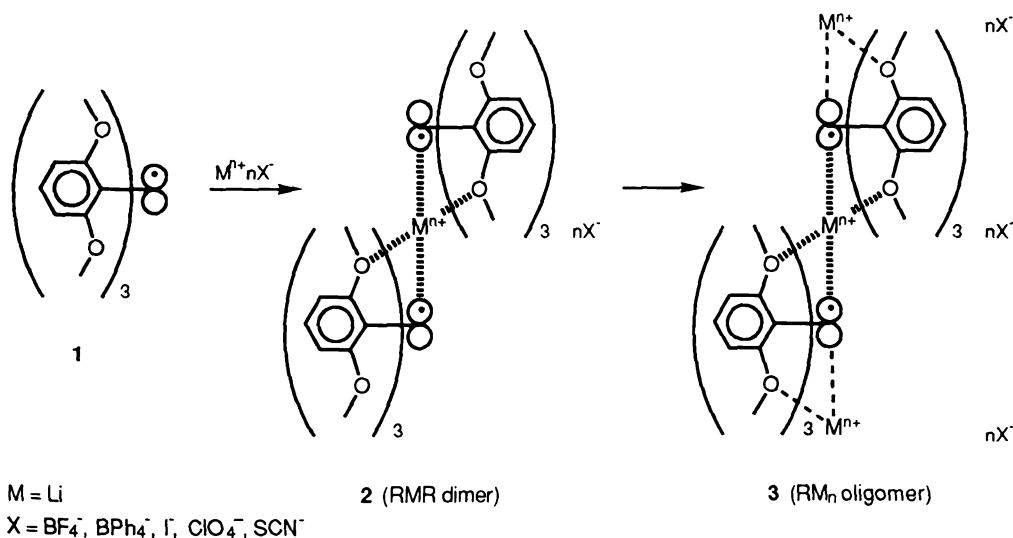
ABSTRACT

Building Organic Magnets from Stable Organic Free Radicals: An Ion-Binding Approach

by

Sei - Hum Jang

Structural studies of the propeller-shaped radical **1** and related triaryl-X species show pairs of binding sites comprising tripods of ether oxygens. The preorganized nucleophilic pockets have enough flexibility to accept a range of metal ion sizes. By coordination with small alkali metal cations the radicals may stack to make extended chains of interacting electron spins as shown below. In fact, mixtures of tris(2,6-dimethoxyphenyl)methyl **1** and LiBF₄ form solids with weak ferromagnetic behavior and solids from **1** and CdCl₂ show clear antiferromagnetic behavior.



NMR, pulsed EPR, UV-Vis, and electrochemical studies of radicals and diamagnetic analogs show behavior consistent with ion binding to form complexes. In addition, by varying substituents on the aryl rings of **1**, it is

possible to adjust redox and binding properties and thus the radical's electronic and structural nature. Such adjustments are significant tools for fine tuning radicals for effective ion binding and electron coupling.

Extended oligomeric arrays are difficult to characterize, so model compounds that form well-defined molecular complexes were devised to separate and characterize the metal-radical, metal-radical-metal, and radical-metal-radical relationships. Because magnetism is a bulk property that arises from a three-dimensional structure, potential chain-coupling di- and tri-radical building blocks were devised by utilizing m-phenylene as a high spin coupling unit.

Magnetic measurements with a Superconducting Quantum Interference Device (SQUID) magnetometer show that, unlike $1 \cdot \text{LiX}$, some of monomeric complexes show simple paramagnetism, with independent electron spins. Control over magnetic properties can be achieved by varying the metal cation, thus complex $1 \cdot \text{LiX}$ shows weak ferromagnetism while complex $1 \cdot \text{CdCl}_2$ shows antiferromagnetic coupling.

Electron Spin Echo Envelope Modulation (ESEEM) studies of complexes in the radical ionophoric system **28** in frozen matrices yield the number of metal ions bound and their distances to the radical center. Molecular mechanics and semiempirical molecular orbital (MO) calculations coincide remarkably well with the spectroscopic findings. Complexation studies in solution support these ideas while *Ab Initio* calculations on a linear $\text{H}_3\text{C} \cdot \text{Li}^+ \cdot \text{CH}_3$ model show that high-spin (ferromagnetic) electron coupling is favored for a wide range of radical- Li^+ distances. Model *Ab Initio* MCSCF computations on the same system offer an explanation for high-spin complexation-induced magnetic coupling of radicals.

Attempts to assemble and characterize a series of triarylmethyls and their metal ion complexes were made. Triaryl-X frameworks are new to the ion binding field, so the complexation abilities of **1** and its congeners were studied by UV-Vis, electrochemistry, NMR and EPR methods. ESR, SQUID, and X-ray studies on these systems were used to assess inter-electron communication. Besides addressing structural and theoretical issues of magnetic coupling, the requirements for the design of molecular solids with long-range structure induced by ion complexation were probed.

To my Parents

ACKNOWLEDGMENTS

My sincere thanks are given to Professor James E. Ned Jackson whom I believe to be one of the great chemists. It was my honor to be his first student and is going to remain as a happy memory in my heart. Numerous discussions with him on my research and others made me realize the meaning of learning how to learn.

I would like to thank Professor Bart E. Kahr, Professor John McCracken, and Hong-In Lee for their help in my research and Professor James L. Dye, Professor William Reusch, and Professor Daniel G. Nocera for serving on my committee.

I am grateful to the National Science Foundation, the United States Air Force, and the Michigan State University Center for Fundamental Materials Research for financial support in the form of teaching and research assistantships. I would like to thank to the Department of Chemistry for its excellent research environment. I also owe special thanks to many friends in the Chemistry and Physics departments for their friendships.

Last, I would like to thank my wife and family for love and patience throughout my study.

TABLE OF CONTENTS

Chapter	page
LIST OF TABLES	viii
LIST OF FIGURES	x
INTRODUCTION	1
1. Macromolecular Chemistry and Molecular Engineering.....	4
2. Stable Organic Radicals	6
2.1. Tri- and Diphenylmethyl Radicals	
Historical Background.....	7
2.1.1. Gomberg's Triphenylmethyl Radical	7
2.1.2. Schlenk, Chichibabin, and Thiele's Hydrocarbon.....	9
2.1.3. Ballester's Stable Triarylmethyl Radicals	11
2.1.4. Jackson and Kahr's Lithium Complex of Triarylmethyl.....	13
2.2. Nitrogen Centered Radicals	15
2.2.1. Hydrazyl Radicals.....	15
2.2.2. Nitroxyl Radicals.....	17
2.3. Aroxyl Radicals.....	21
3. Magnetism.....	23
3.1. Diamagnetism	23
3.2. Paramagnetism.....	24
3.3. Curie-Weiss Law.....	28
3.4. Pairwise Magnetic Exchange.....	30
3.5. One-Dimensional or Linear Chain Systems.....	31
3.6. Alternating Linear Heisenberg Chain.....	35
4. Molecular Magnets.....	37
4.1. Molecular Magnet models.....	37
4.1.1. McConnell Model	37
4.1.2. Mataga Model	39
4.1.3. Ovchinnikov Model	41
4.1.4. Breslow Model.....	42
4.1.5. Torrance Model	44
4.1.6. Kahn's Proposal	44

4.2.	Metal Based Molecular Magnets	46
4.2.1.	Single Atom Bridged Bimetals	46
4.2.2.	Molecule Bridged Bimetals.....	48
4.2.3.	Metal and Organic Radical Based Systems	49
4.2.4.	Charge Transfer Complex Based Systems.....	54
4.3.	Galvinoxyl and Nitroxyl Radical Based systems	55
4.3.1.	Galvinoxyl Radicals	55
4.3.2.	Nitroxyl Radicals.....	58
4.4.	Alternant Hydrocarbon Based Polyradicals.....	63
4.4.1.	Triplet Diradicals	66
4.4.2.	Perchlorinated Triphenylmethyl Radicals.....	68
4.4.3.	Polyphenyl Carbenes.....	72
5.	Molecular Magnets by Macromolecular Chemistry	75
5.1.	Long-range Magnetic Interactions in Organic Radicals	77
5.2.	Through Space Magnetic Interactions in Organic Radical Complexes	81
5.3.	Design of Molecular Magnets by Ion-Binding.....	83
RESULTS AND DISCUSSION		90
CHAPTER I. Triarylmethyl Radicals.....		90
1.	Structure of Triarylmethyl Radical	90
1.1.	Structure of Triarylmethyl Radical.....	92
1.2.	Structure of Triarylmethyl Cation.....	95
1.3.	Structure of Triarylmethyl Borane.....	96
1.4.	Hexachloro Triphenylmethyl Radical and Borane.....	100
2.	Substituent Effects.....	102
2.1.	Hexamethoxy Triphenylmethyl Radicals.....	104
2.2.	The Cyclized Xanthenol	120
2.3.	Tetramethoxy Triphenylmethyl Radicals	121
2.4.	Rotational Barriers	131
3.	Ion-Binding	137
3.1.	Borane	137
3.2.	Double faced Paramagnetic Ionophore.....	141
3.3.	Tetramethoxy Triphenyl amines.....	153
3.4.	Ammonium Complexes by Hydrogen bonding.....	160
3.5.	Metal Ions.....	165

CI

1.

2.

3.

4.

5.

C

C

S

1

2

3

E

1

2

3

4

R

CHAPTER II. Magnetism of Triarylmethyl Radical Complexes.....	167
1. Calculations on Pairwise Interaction of Methyl Radicals.....	167
2. Antiferromagnetic Interaction and Dimer of The Radical.....	169
3. Magnetic Behavior of Radicals and Complexes.....	171
3.1. Diamagnetism of Methane and Metal Salts.....	173
3.2. Paramagnetism of Radicals and Radical Complexes	175
3.3. Ferromagnetism of Complexes.....	184
3.4. Antiferromagnetism of Radical Complexes.....	187
4. Design of Molecular Magnets by Other Ion-Binding	192
5. Introduction of Cross-Linkers	195
CONCLUSIONS AND SUGGESTIONS FOR FUTURE WORK.....	199
Conclusions.....	199
Suggestions for future work	201
1. Aromatic Linked Biradicals	201
2. Magnetic Coupling through Hydrogen Bonds	202
3. Ion-Binding in Various Nitroxyl Radicals.....	204
EXPERIMENTAL	208
1. General Procedures.....	208
2. Solvents and Chemicals.....	209
3. Equipment and Procedures.....	209
CV Measurements.....	209
VT-EPR Measurements.....	210
SQUID Measurements.....	210
4. Synthesis	212
REFERENCES	242

Ta

1.

2.

3.

4.

5.

6.

7.

8.

9.

10

LIST OF TABLES

Table	page
Aryl ring twists in tripod binding sites.....	99
Crystal structure determination and refinement data for tris (2,6-dimethoxyphenyl)methyl 1 , tris(2,6-dimethoxyphenyl)methyl tetrafluoroborate 62 , tris(2,6-dimethoxyphenyl)borane 63	99
Summary of electrochemical data for derivatives of tris(2,6-dimethoxyphenyl)methyl 1	105
Correlation of $E_{1/2}$ and σ -values for derivatives of tris(2,6-dimethoxyphenyl)methyl 1	108
Summary of hyperfine constants for derivatives of tris(2,6-dimethoxyphenyl)methyl 1	116
Summary of electrochemical data for derivatives of phenyl-bis(2,6-dimethoxyphenyl)methyl 77	123
Correlation of $E_{1/2}$ and σ -values for derivatives of phenyl-bis(2,6-dimethoxyphenyl)methyl 77	125
Summary of hyperfine constants for derivatives of phenyl-bis(2,6-dimethoxyphenyl)methyl 77	126
Summary of VT-NMR results for tris(2,6-dimethoxy- phenyl)methyl ammonium tetrafluoroborate 72 , tris(2,6- dimethoxy-3,5-dichlorophenyl)methyl ammonium tetrafluoroborate 75 , tris(3,5-dichloro-2,6-dimethoxy phenyl)methane 76	133
Complexation data from ESEEM for tris(2,6-di(2-methoxy ethoxy)phenyl)methyl 86 •2MX	150

Summary of electrochemical data for tris(2-(methoxyethoxy)-6-methoxyphenyl)methyl 85 and tris(2,6-di-(methoxyethoxy)phenyl)methyl 86	151
Summary of electrochemical data for bis(2,6-dimethoxyphenyl)-4-chlorophenyl amine 87 , bis(2,6-dimethoxyphenyl)-3,5-dimethoxyphenyl amine 88 , tris(3,5-dimethoxyphenyl)amine 89	155
Crystal structure determination and refinement data for tris(2,6-dimethoxyphenyl)methyl ammonium tetrafluoroborate 72 and tris(3,5-dichloro-2,6-dimethoxyphenyl)methyl ammonium tetrafluoroborate 75	162

Fi

1.

2.

3.

4.

5.

6.

7.

8.

9.

10.

11.

12.

13.

14.

LIST OF FIGURES

Figure	page
Temperature dependence of the paramagnetic susceptibility	25
The molar susceptibility for ferro- and antiferromagnets.....	29
Bleaney Bowers susceptibilities compared with the Curie law.....	31
Ising susceptibilities compared with Curie law	34
Ising "perpendicular" susceptibilities.....	34
Heisenberg linear chain susceptibilities	36
Illustration of the oligomeric chain of tris(2,6-dimethoxyphenyl)methyl 1 with M^+ ions	87
MM2 optimized structure of an RMR dimer 2 calculated	87
Stereo view of the X-ray structure of the radical tris(2,6-dimethoxyphenyl)methyl 1	94
Space-filling views of the binding site for tris(2,6- dimethoxyphenyl)methyl 1 and tris(2,6-dimethoxyphenyl) methyl tetrafluoroborate 62	96
Ball & Stick representations of the binding site for tris(2,6-dimethoxyphenyl)methyl 1 and tris(2,6-dimethoxy phenyl)borane 63	97
Stereo view of the packing diagram of tris(2,6-dimethoxy phenyl)borane 63	98
MM2 calculated structure of tris(3,5-dichloro-2,6-dimethoxy- phenyl)borane 64 dimer with Li^+	101
Cyclic voltammogram of tris(3,5-dichloro-2,6-dimethoxyphenyl) borane 64 in methylene chloride	101

15. *Ch...*
...
16. *A...*
17. *A...*
...
18. *P...*
...
19. *P...*
...
20. *T...*
...
21. *A...*
22. *P...*
...
23. *P...*
...
24. *P...*
...
25. *P...*
...
26. *S...*
...
27. *V...*
...
28. *V...*
...

5. Cyclic Voltammogram of tris(2,6-dimethoxyphenyl) methyl 1 in THF.....	103
6. $\Delta E_{1/2}(V)$ vs σ in THF for HMTP methyl radicals.....	108
7. EPR spectrum of tris(2,6-dimethoxyphenyl)methyl 1 in THF with simulations	117
8. EPR spectrum of tris(3,5-dichloro-2,6-dimethoxyphenyl) methyl 65 in THF with simulations.....	118
9. EPR spectrum of tris(4-chloro-2,6-dimethoxyphenyl) methyl 66 in THF with simulations.....	119
10. The X-ray structure of cyclized tris(2,6-dimethoxy phenyl)methyl carbinol.....	120
11. $\Delta E_{1/2}(V)$ vs σ in THF for TMTP methyl radicals.....	124
12. EPR spectrum of phenyl-bis(2,6-dimethoxyphenyl) methyl 77 in THF with simulations.....	127
13. EPR spectrum of phenyl-bis(2,6-dimethoxyphenyl) methyl 77 in toluene with simulations.....	128
14. EPR spectrum of bis(2,6-dimethoxyphenyl)-4-chlorophenyl methyl 78 in THF with simulations.....	130
15. EPR spectrum of bis(2,6-dimethoxyphenyl)-3,5-dimethoxy phenyl methyl 84 in THF with simulations	130
16. Stereo view of the X-ray structure of tris(2,6-dimethoxyphenyl) methane 73	131
17. VT 300 MHz 1H NMR spectrum of tris(2,6-dimethoxy- 3,5-dichlorophenyl)methyl ammonium tetrafluoroborate 75	134
18. VT 300 MHz 1H NMR spectrum of tris(2,6-dimethoxy- 3,5-dichlorophenyl)methane 76	135

2

3

3

3.

3.

34

35

36

37

38

39

40.

41.

UV-Vis spectra showing ion-binding in tris(2,6-dimethoxyphenyl)borane 63	139
Mass Spectrum of a dimer 2 of tris(2,6-dimethoxy- phenyl)methyl 1 •Na ⁺ • 1	140
EPR spectrum of tris(2,6-di(methoxyethoxy)phenyl) methyl 86 with simulations.....	143
ESEEM spectrum of tris(2,6-di(methoxyethoxy)phenyl) methyl 86 •2LiBF ₄	145
ESEEM spectrum of tris(2,6-di(methoxyethoxy)phenyl) methyl 86 •2NaBPh ₄	147
Summary of ESEEM and MNDO results of tris(2,6- di(methoxyethoxy)phenyl)methyl 86 •2LiBF ₄	149
Stereo view of the MNDO calculated structure of tris(2,6-di(methoxyethoxy)phenyl) methyl 86 •2LiBF ₄	149
¹ H NMR spectra for ion-binding of bis(2,6-dimethoxyphenyl)- 4-chlorophenyl amine 87 with LiI.....	156
¹³ C NMR spectra for ion-binding of bis(2,6-dimethoxyphenyl)- 4-chlorophenyl amine 87 with LiI.....	157
¹ H NMR spectra for ion-binding of bis(2,6-dimethoxyphenyl)- 3,5-dimethoxyphenyl amine 88 with LiI.....	158
¹³ C NMR spectra for ion-binding of bis(2,6-dimethoxyphenyl)- 3,5-dimethoxyphenyl amine 88 with LiI.....	159
Stereo views of the X-ray crystal structure of tris(2,6- dimethoxyphenyl)methyl ammonium BF ₄ 72 and tris(3,5- dichloro2,6-dimethoxyphenyl)methyl ammonium BF ₄ 75	161
¹ H NMR spectrum of complex of tris(2,6-dimethoxyphenyl) borane 63 •NH ₄ I in CD ₃ CN.....	163

42.

43.

44.

45.

46.

47.

48.

49.

50.

51.

52.

53.

54.

55.

56.

57.

^1H NMR spectrum of complex of tris(2,6-dimethoxy-3,5-dichlorophenyl)borane 64 • NH_4I in CD_3CN	164
Qualitative MO diagram for orbital interactions in MeLi^+Me	167
Curie-Weiss behavior of tris(2,6-dimethoxyphenyl)methyl 1	169
The X-Ray structure of head-to-tail peroxydimer 91	170
Plot of magnetization M vs H for tris(2,6-dimethoxyphenyl)methyl 1 and 1 • LiBF_4	172
Plot of magnetization M vs H for tris(2,6-dimethoxyphenyl)methane 73 and CdCl_2	174
Plot of $1/\chi$ vs T and χT vs T for tris(2,6-dimethoxyphenyl)methyl 1	176
Plot of M vs. H and $1/\chi$ vs T for tris(2,6-di(methoxyethoxy)phenyl)methyl 86 • 2LiBF_4	179
Plot of μ_{eff} vs T for tris(2,6-dimethoxyphenyl)methyl 1 • 2LiI	180
Plot of $1/\chi$ vs T for tris(2,6-dimethoxyphenyl)methyl 1 • NH_4I ...	181
Plot of Brillouin functions calculated for $S=1/2$ to $7/2$	182
The saturation magnetization of the complex of tris(2,6-dimethoxyphenyl)methyl 1 • LiI at 1.8K	184
Plot of magnetization M vs H for tris(2,6-dimethoxyphenyl)methyl 1 • LiBF_4 and 1 • ZnCl_2	186
Plot of χ vs T for tris(2,6-dimethoxyphenyl) 1 • CdCl_2 with Bleaney-Bowers fit	189
Alternating dimer and linear chain Heisenberg fit for tris(2,6-dimethoxyphenyl) 1 • CdCl_2	190
X-ray powder patterns of 1 and 1 • CdCl_2	191

in
co
19
dr
re
m
el
m
ch
as
the

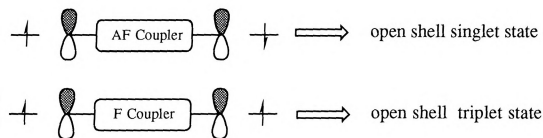
Or
mo
fre
ove
and
fur
inte
sta
the
are

INTRODUCTION

Organic materials science is in a stage of infancy compared to its inorganic sibling. The difficulties are associated mainly with the lack of control of structure in the organic solid state. Since the Nobel prize in 1987¹, interest in macromolecules and their self-assembly has increased dramatically. Attention has focused not only on the fundamental molecular recognition processes of the macromolecules but also on the design of molecular devices using various intermolecular interactions such as electrostatic, hydrogen bonding, van der Waals forces, etc. Organic materials chemistry requires the resources of traditional molecular chemistry combined with an understanding of non-covalent interactions so as to form macromolecular entities that possess structures as well defined as those of molecules themselves.

One of the greatest challenges to materials science is the design of molecular magnetic materials. Simple paramagnetic organic compounds—free radicals,² triplet carbenes,³ biradicals^{4,5}—have been well studied over the last 30 years, and their magnetic characteristics can be adequately analyzed in terms of current theory.⁶ Molecular magnets represent a fundamentally new class of materials in which a defined magnetic exchange interaction has been imposed on adjacent paramagnetic entities in the solid state.⁷ In spite of significant growth in the field of molecular magnetism, the mechanisms of colligative magnetic properties such as ferromagnetism are incompletely understood.⁸

Interest in organic and molecular magnetism has grown so much in the last ten years that special ACS symposia on the subject were held in 1989 and 1992,⁹ yet to date there are only a few molecular magnets that clearly exhibit long-range ferromagnetic interactions.¹⁰



In an isolated atom or molecule, a pair of electron spins may be coupled to yield closed-shell singlet, open-shell singlet, or triplet states. In other words, we can relate the magnetic interaction between two organic radicals to their chemical bonding interactions. Strong interactions between two radicals will result in electrons pairing up in a closed shell singlet state (σ -bond), while very weak interactions between two radicals will result in a pair of open shell doublet states (isolated paramagnets). We can view an antiferromagnetic coupling as a weak bonding interaction between radicals.

In extended odd-electron systems, the three modes above correspond to diamagnetic (closed-shell singlet), antiferromagnetic (open-shell singlet), and ferromagnetic coupling (triplet), respectively.¹¹ Several mechanisms have been discussed by which high-spin states of molecular materials may be stabilized.^{12,13} However, there is still no predictive theory that can accurately forecast the magnitude or even the sign of magnetic coupling in a generic chemical system of known structure. Magneto-structural

c
e
c
s

l
p
r
d
s
d
p
c
h
o

sh
of
m
sh
di
str
rac
ex

correlations are best described among structural homologs, and even then, experts do not always agree on the mechanisms of coupling. This thesis describes an approach to this problem that uses structurally well defined systems made of stable organic radicals.

The principles developed in selective ion binding studies of polyether ligands¹⁴ suggest that the methoxy groups in tris(2,6-dimethoxyphenyl)methyl radical can serve as binding sites for metal cations. Two radicals may "sandwich" a cation of appropriate size between them in a distorted octahedral pocket,^{15,16} fixing their relative orientation. The spatial relationships in such controlled radical aggregation can, in turn, dictate intermolecular electron coupling in "interrupted σ - bonds"—radical pairs or oligomers in which electron interactions are mediated by metal cations. Extended stacks formed by this complexation mechanism would have at their cores a linear array of one-electron carbon-centered *p*-orbitals interacting through metal ions.

In writing the first dissertation on this project in the Jackson group, I shall have a rather extended introductory chapter to give a detailed picture of current molecular magnetism research, a brief overview of the theory of magnetism, and a historical review of stable organic radical chemistry. I shall give the rationale behind our research, followed by results and discussion. Results and discussion will be divided into three parts: building structural bases for the formation of complexes; magnetic studies on radicals and complexes; and attempts at the introduction of linkers for extended magnetic structures.

th
in
fo
en
co
en
int
de
sel
inc
and

mo
pos
of
ent
tha
latt
coc
con
the

1. Macromolecular Chemistry and Molecular Engineering

In contrast to molecular chemistry, which is predominantly based on the covalent bonding of atoms, supramolecular chemistry is based on intermolecular interactions. Supramolecular interactions are the foundation for highly specific biological processes, such as substrate binding by enzymes or receptors, formation of protein complexes, intercalation complexes of nucleic acids, and immunology. An exact knowledge of the energetic and stereochemical characteristics of these non-covalent, multiple intermolecular interactions within defined structural motifs should allow the design of artificial enzymes or receptors, which bind substrates strongly and selectively.¹⁷ There are many examples of such receptor or enzyme models including cyclodextrins,¹⁸ and cyclophanes based on biphenyl¹⁹, terphenyl, and triphenylmethyl²⁰ frameworks, and cryptophanes.²¹

Molecular materials are characterized by being made up of discrete molecules. The structural properties of molecular materials offer many possibilities to modulate the bulk electrical, magnetic, and optical properties of the material by choosing appropriate molecules as the macromolecular entities. At the same time, it is a challenge to develop synthetic strategies that allow the control of the spatial distribution of the molecules in the lattice. The bulk properties of materials are always determined by cooperative interactions between the constituting molecules, which consequently must be assembled in the lattice in such a way as to maximize the bulk response.²²

a
c
t
r

r
P
n
a
c
m
c

ar
m
re
te
th
D
re
su
co

Beyond the basic problem of establishing correlations between structure and a given property, molecular materials appear promising for development of new characteristics through the combination and linking of their properties. The recognition of inter- and intramolecular interaction in macromolecules is the basis for the design of molecular materials.⁷

An organic crystal is perhaps the most precise example of molecular recognition, since molecular chemistry blends with intermolecular forces to propagate a periodic molecular array.²³ The almost perfect alignment of molecules in an organic crystal usually results in highly regular physical and chemical properties of the molecules, which in turn justify efforts in crystal engineering. Of course, phenomena such as hydrogen bonding and molecular complexation have been known for decades. However, ideas concerning molecular recognition have only been refined in recent years.

The research on organic materials with nonlinear optical properties and the studies on organic conductors and superconductors are some of the most active areas in the field. Much of the motivation for the increased research activity in conducting materials has been based on the potential for technological applications. Conducting, light-weight, soluble, and thermoplastic materials are of great industrial and economic interest. During the past ten years, there has been a very significant international search effort as a result of the search for higher T_c organic superconductors, much of it stimulated by the discovery of the high T_c copper oxide ceramic superconductors.^{24,25}

1

2

3

4

5

6

7

8

9

10

11

12

13

14

15

16

17

18

19

20

21

22

2. Stable Organic Radicals

A free radical is an atom, molecule or complex which contains one or more unpaired electrons. Free radicals can be obtained in a variety of ways; those which can be isolated and exist as stable, pure substances may be prepared by conventional chemical methods but the more reactive radicals are produced by thermal or photochemical bond cleavage, decomposition, irradiation, mechanical degradation, or by electron transfer reactions. The majority of free radicals obtained by these methods are highly reactive and have lifetimes measurable in terms of micro- or milliseconds unless they are stabilized by trapping in some inert matrix or on the surface of a solid.

The concept of stability in organic radicals depends on the chemical circumstances; for example, the methyl radical can be stabilized indefinitely in an argon matrix at very low temperatures although it disappears irreversibly on warming the matrix. Diphenylpicrylhydrazyl (DPPH) can exist permanently as a free radical in the solid state at room temperature; it can be crystallized, isolated and treated as a normal organic compound but when exposed to other organic radicals it usually reacts rapidly to give diamagnetic products. The word "stable" should only be used to describe a radical so persistent and so unreactive to air, moisture, etc., under ambient conditions that the pure radical can be handled and stored in the lab with no more precautions than would be used for the majority of commercially available organic chemicals.^{26,27}

1

n

P

A

U

n

w

k

a

U

th

l

he

m

th

ch

G

th

tri

2.1. Tri- and Diphenylmethyl Radicals: Historical Background

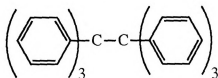
2.1.1. Gomberg's Triphenylmethyl Radical

In 1900 Gomberg discovered triphenylmethyl, the first organic free radical. The historical significance of the discovery was reflected in "The History of Organic Chemistry in The United States, 1875-1955" by D. S. & A. T. Tarbell.²⁸

" Without question, the single most important piece of work from the United States in the beginning of the century and the one which aroused the most interest abroad was the discovery by Moses Gomberg of structures which contained trivalent carbon. Gomberg was an example of the best kind of American success story. " " Coming to this country from Russia as a child with his penniless father, he eventually worked his way through the University of Michigan at Ann Arbor and received a doctorate in chemistry here in 1894." "During a year of study with Victor Meyer at Heidelberg in 1897, he synthesized tetra-phenyl methane, and after his return to Michigan, he studied the preparation of the hexaphenylethane by the action of various metal salts and metals on triphenylmethyl chloride. He obtained, instead of the expected hexaphenylethane, a compound whose composition and chemical properties corresponded to the peroxide."

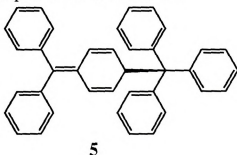
Gomberg suggested in his first paper that the highly reactive substance from the reaction of silver metal with triphenylmethyl chloride contained trivalent carbon. Gomberg's interpretation of the triphenyl methyl was

against the classical structural theory of tetravalent carbon. From the same reaction under nitrogen, he isolated the first product and showed that it had the composition corresponding to hexaphenylethane by elemental analysis. However, the structure of the first product was not proven by Gomberg to be hexaphenylethane. The elegance and serendipity of Gomberg's experiments in 1900 have made the discovery familiar to many organic chemists. The significance of the claim of an isolable trivalent carbon molecule was immediately recognized, and leading chemists of the day entered the debate on the nature of Gomberg's hydrocarbon **4**.



Gomberg Dimer **4**

The hypothesis of an equilibrium between triphenylmethyl radicals and hexaphenylethane had been accepted as certainly as that of tetrahedral carbon until the discovery by Lankamp, Nauta, and MacLean in 1968 that "hexaphenyl ethane" in fact had the unsymmetrical quinoid structure **5** which Jacobson had proposed for it in 1904.²⁹



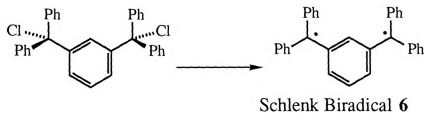
5

So far, Gomberg's hexaphenylethane has not been synthesized except for the derivative hexakis(3,5-di-*t*-butyl-4-biphenyl) ethane by Winter in 1978 and hexakis(3,5-di-*t*-butylphenyl) ethane by Mislow and Kahr in

1986.³⁰ The realization that trivalent carbon could exist as a relatively stable structure made chemists more ready to accept free radicals as intermediates in reactions in solutions even when the individual radicals could not then be identified.

2.1.2. Schlenk, Chichibabin, and Thiele's Hydrocarbon

On dehalogenating 1,3-bis(diphenylchloromethyl)benzene Schlenk and Brauns obtained a colorless product whose elemental analysis accorded with the molecular formula of Schlenk biradical **6**. Investigation showed the biradical to be associated into a polymer.³¹



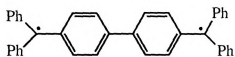
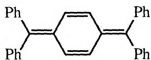
Sümmermann produced the monomeric Schlenk biradical by electrochemical reduction of the corresponding dication with a rotating platinum electrode and assigned the triplet EPR spectrum with the zero-field splitting parameters of $D = 0.0079 \text{ cm}^{-1}$, $E \leq 0.0005 \text{ cm}^{-1}$ for $\Delta m = 1$.

The zero-field splitting parameters D and E can be determined directly from the triplet EPR spectrum; D and E values provide information on the distance between radical centers and the molecular symmetry of the triplet, respectively. The three levels of a triplet EPR spectrum (according to x , y , and z axis) are split even in the absence of an external magnetic field. This zero field splitting (zfs) arises from a dipolar coupling of the two spins that

creates an internal magnetic field in the molecule, which splits the energy levels.

Sümmermann could not detect the half field transition, a hallmark of a high spin state, from the spectrum of Schlenk biradical.³² The "half-field spectrum" corresponds to $\Delta m=2$ transitions in a triplet EPR spectra. This transition is quantum-mechanically forbidden, but in most organic diradicals, the zero field splitting relaxes the selection rule and the transition can be observed. It is a critical spectral feature because its presence unambiguously signals that one is observing a triplet state.

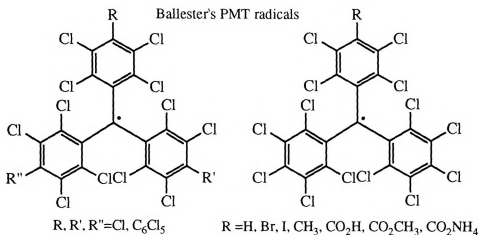
Shortly after Gomberg's preparation of the triphenylmethyl radical in 1900, Chichibabin attempted to synthesize the analogous diradical **7**.³³ He obtained a blue-violet compound that reacted rapidly with oxygen, yielding a polymeric peroxide. Early studies on Chichibabin's hydrocarbon **7** led to speculation as to whether it existed as a singlet, a triplet, or a mixture of the two spin states.³⁴ Numerous attempts to observe triplet spectra in solution have failed; doublet spectra were found, however. Platz discussed existing experimental inconsistencies and assigned a singlet ground state to Chichibabin's hydrocarbon. Montgomery reported a crystal structure of Chichibabin's hydrocarbon and concluded that it has a singlet ground state with an unusually large amount of "diradical character" by comparing each bond length in the molecule with di-*p*-xylylene framework.³⁵ He only recorded a singlet EPR spectrum even with the single crystal of the radical used for the X-ray structure determination.

Chichibabin's Biradical **7**Thiele's Hydrocarbon **8**

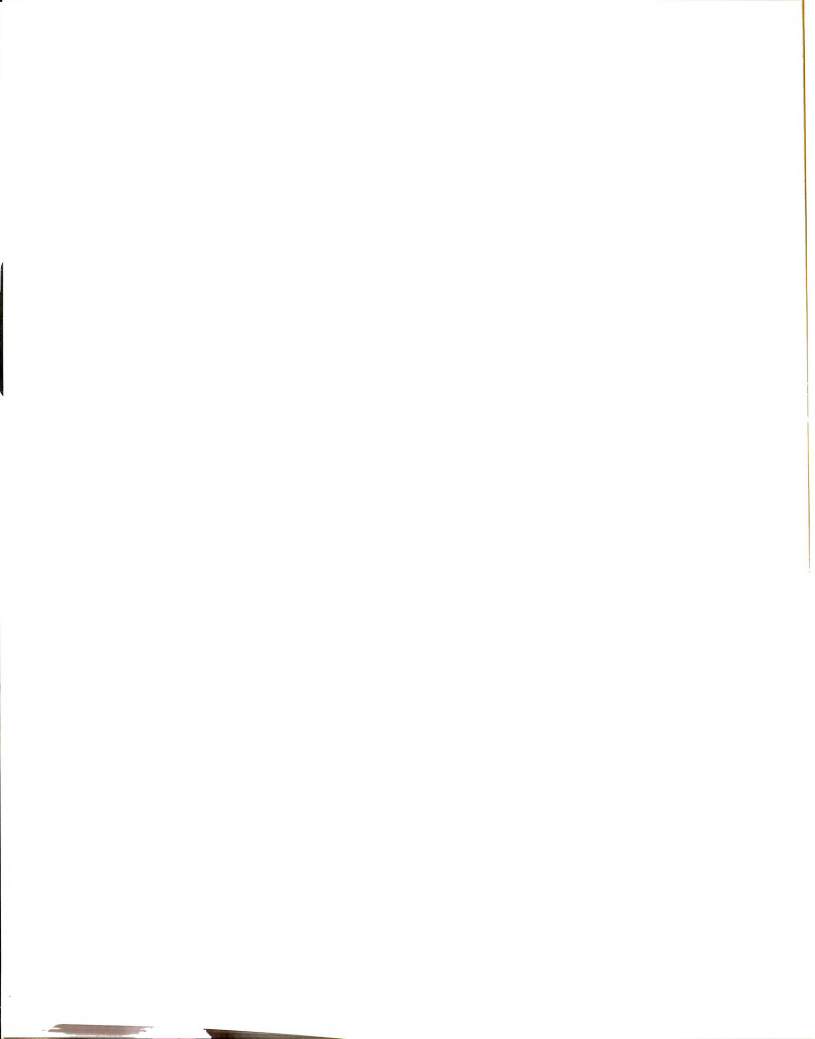
Thiele synthesized the first isolable derivative of p-xylylene **8** in 1904, after attempts to prepare the unsubstituted compound failed.³⁶ Thiele's hydrocarbon **8** reacted with oxygen, but could be manipulated without elaborate precautions. The Thiele's hydrocarbon has been examined by a variety of physical methods, and there seems to be little doubt that the molecule has a singlet ground state. Montgomery reported a crystal structure of Thiele's hydrocarbon and concluded that it has a singlet ground state.

2.1.3. Ballester's Stable Triarylmethyl Radicals

Since Gomberg's discovery of the first free radical a great number of stable organic radicals have been detected and isolated. Although carbon centered free radicals are highly reactive species, some of them show remarkable stability, the best example being Ballester's perchlorotriphenylmethyl radical series shown below.³⁷ Some of these radicals have half-lives of decades in the air, and withstand typical radical reagents like nitric oxide, hydroquinone, quinone, and even highly aggressive chemical species like concentrated sulfuric, nitric acids, sodium hydroxide, or halogen, with little or no alteration. Also, they possess a remarkably high thermal stability, up to 300 °C. They are all completely dissociated in solution.

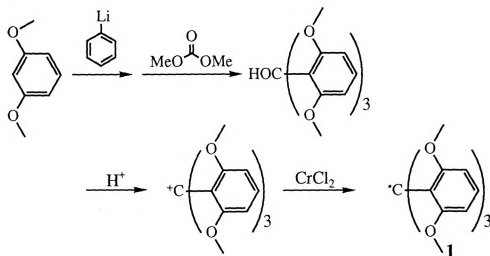


These radicals have distorted D_3 propeller structures (C_2) in the solid state, and their high stabilities have been traced predominantly to the shielding of the trivalent carbon atom by their phenyl rings with a propellerlike conformation and the six ortho chlorines. Thermal and chemical stabilities of free radicals are governed by two main factors: resonance and steric hindrance.³⁸ The inhibition of resonance and steric hindrance frequently cause high thermal stability and chemical inertness of the aromatic chlorocarbons.³⁹ The perchlorotriphenylmethyl radical has twist angles of 6.3, 53.4, and 53.8° between the phenyl groups and the reference plane of the central carbon in the solid state. The effect of the absence of ortho or meta chlorines on the twist angles of the rings, and therefore on their stability, has been assessed by direct comparison of X-ray structures of various derivatives of Ballester's radical by Veciana and coworkers. The results were consistent with the steric shielding of chlorine atoms being the main reason for the observed stabilities of these radicals.



2.1.4. Jackson and Kahr's Lithium Complex of Triarylmethyl

Tris(2,6-dimethoxyphenyl)methyl **1**, originally synthesized by J. C. Martin, is a remarkably stable organic free radical.⁴⁰ It can be synthesized efficiently using the procedure shown below. It is air-stable, presumably due to the fact that in its D_3 propeller conformation the central trivalent carbon is protected from above and below by six ortho-methoxy groups similar to Ballester's radicals. Martin reported detailed EPR studies of the radical **1** and its ^2D and ^{13}C (central carbon) derivatives with the correlation of hyperfine coupling constants and the average twists of aryl rings of 47° in solution.



In 1985 Jackson and Kahr treated solutions of the radical **1** with solutions of lithium salts in order to study the possibility of complex formation between the radical **1** and metal cations. Precipitates formed upon mixing that frequently gave unusual, intense ESR spectra. Some of the spectra were very broad, others had considerable fine and hyperfine structure, and often g -values deviated markedly from the free electron value.⁴¹ During the following year they unsuccessfully tried to establish a structural basis for

the surprising magnetic behavior of their precipitates by growing single crystals from the precipitated solids. Results at that time suggested colligative magnetic properties as a possible explanation for their puzzling and highly variable ESR spectra.

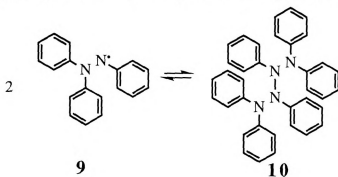
Their proposed model did not include any of the structural elements suggested by available strategies for achieving ferromagnetic coupling of spins between carbon centered radicals.^{42,43} The general line of research was set aside because, at the time of the initial discoveries, the principle investigators were graduate students whose chief responsibilities were unrelated to the present subject or the chemical system described. However, in 1989, Professor Jackson reexamined precipitates of $\mathbf{1} \cdot \text{LiBF}_4$ and $\mathbf{1} \cdot \text{LiClO}_4$ with a Superconducting Quantum Interference Device (SQUID) magnetometer in the Department of Chemistry (Professor Dye's SQUID) at Michigan State University.

While a polycrystalline sample of $\mathbf{1}$ behaved as a paramagnet, the susceptibility of the "salted" precipitates showed a ferromagnetic field-dependent hysteresis, signatures of colligative magnetic behavior. Surprised by these new results Professor Jackson revived investigations of organic magnetism with the aim of establishing a rational basis for the observed magnetic phenomena. We are now pursuing this research with the expectation that a deeper understanding of electron coupling between simple paramagnets will result.

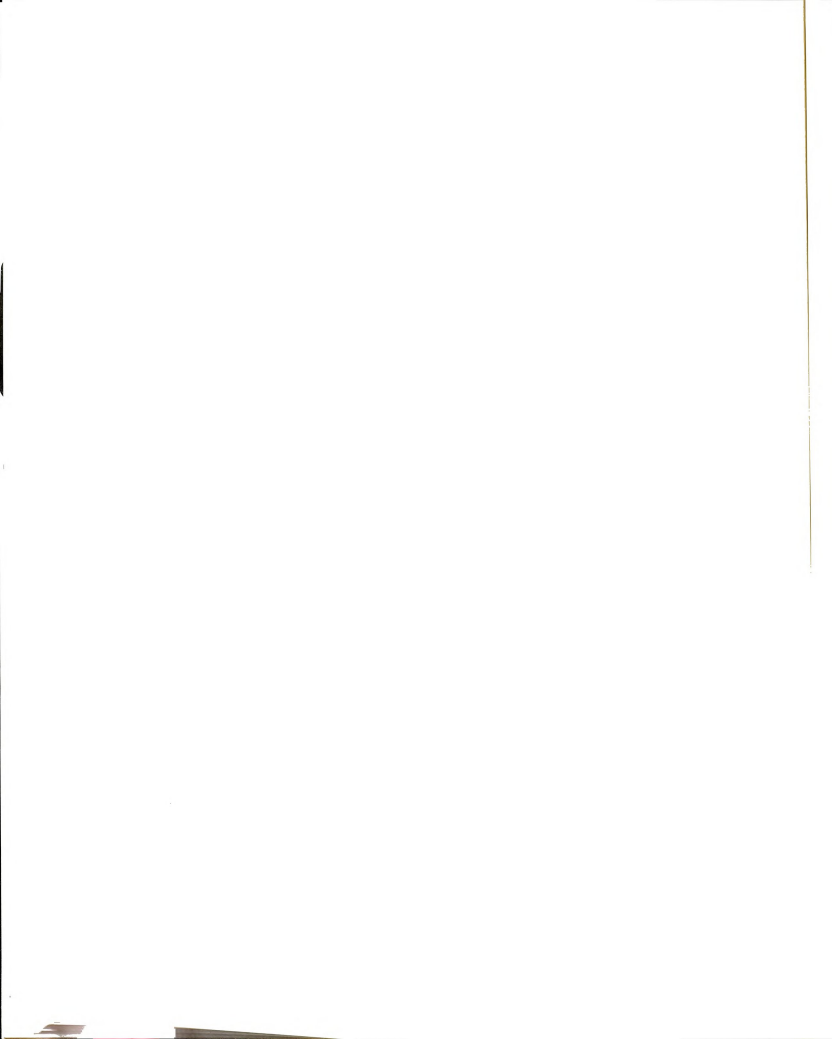
2.2. Nitrogen Centered Radicals

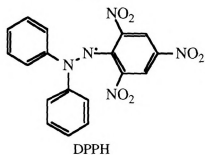
2.2.1. Hydrazyl Radicals

The discovery and early investigations of hydrazyl radicals were made mainly by Goldschmidt and coworkers during the period of 1920 to 1929.⁴⁴ From his original observation that treatment of triphenylhydrazine with lead dioxide in ether gave a deep blue solution which rapidly changed to green and then a red-brown, he proposed that the labile blue intermediate was triphenylhydrazyl **9** and the final product hexaphenyltetrazene **10**.

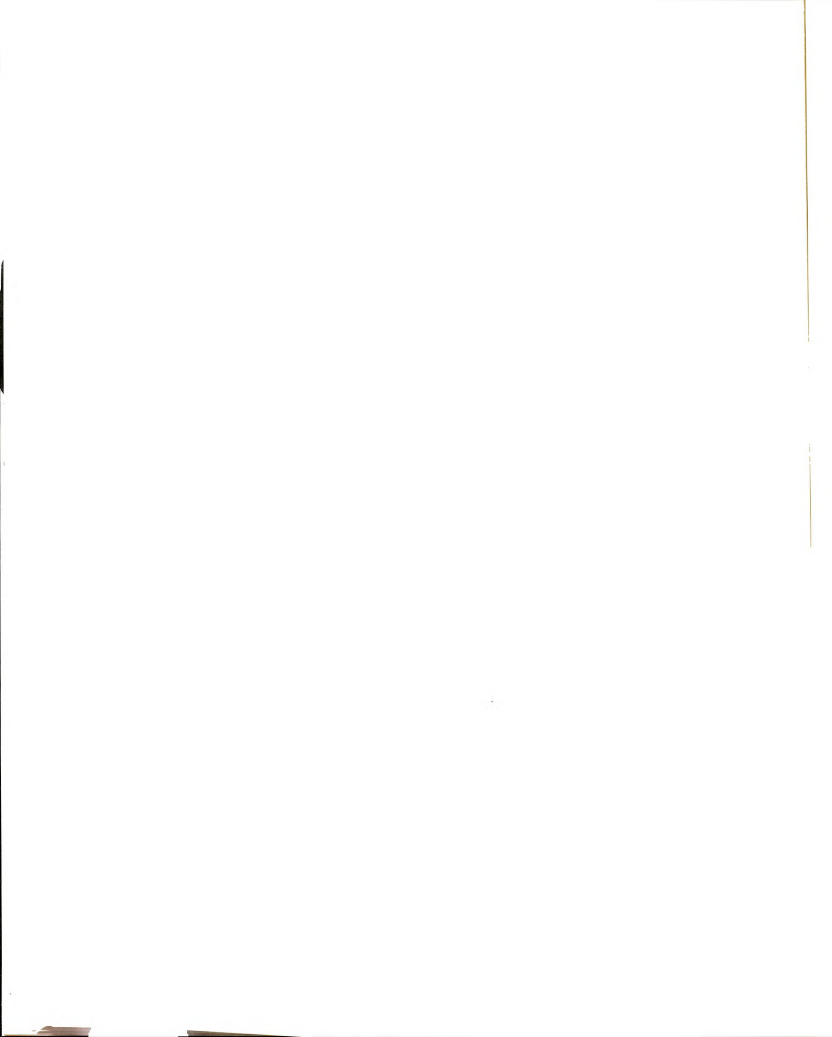


The equilibrium between radical and dimer was further confirmed by the dependence of the blue color on the polarity and temperature of the solvent. Goldschmidt also prepared and characterized various hydrazyl radicals including the remarkably stable, 2,2-diphenyl-1-picrylhydrazyl (DPPH); shown on the next page which shows no tendency to dimerize in the solid state or in solution even at room temperature.⁴⁵ Because of its applications, interest in hydrazyl chemistry has been focused on DPPH. It has been used since 1950 as a radical scavenger in polymer chemistry and radiolysis and to a lesser extent in synthetic organic chemistry.⁴⁶

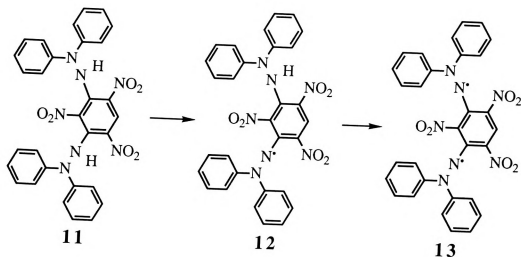




Very early magnetic susceptibility measurements established that under various conditions DPPH was essentially 100% free radical.⁴⁷ It has been used as a reference radical frequently in connection with EPR spectroscopy because of its availability and stability. The EPR spectrum of crystalline samples of DPPH was measured and found to consist of one narrow line about 1.7 gauss wide, but in a dilute benzene solution it shows a five line spectrum which was originally attributed to equal coupling of the unpaired electron with the two nitrogen atoms, $a_{N1}=a_{N2}= 8.9$ gauss. More refined analysis of the spectrum revealed that the two nitrogens in DPPH were not equivalent and had coupling constants of 9.35 and 7.85 gauss. The larger of these two constants was shown to be associated with the picryl nitrogen by ^{15}N labeling studies.⁴⁸ Apparently, for some reason, there are no studies on these radicals as base radicals for organic magnetic systems. They should have significant potential for such applications in comparison with other nitro functionalized organic radicals.

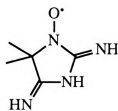
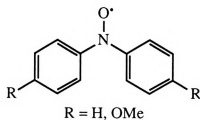


Oxidation of the dihydrazine **11** with lead dioxide yields unstable pentaphenyl picryl mono hydrazyl (PPPMH) **12** which has hyperfine coupling constants similar to other meta-substituted picryl hydrazyls. Further oxidation gives the very unstable "pentaphenyl picryl dihydrazyl (PPPDH)" **13**, which is considered to be diamagnetic below $-30\text{ }^{\circ}\text{C}$ from EPR and NMR measurements. Some workers claim to have obtained the EPR spectrum of the biradical form shown below.⁴⁹

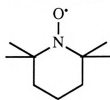
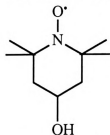


2.2. Nitroxyl Radicals

Porphyrexide **14** was the first organic nitroxyl radical to be isolated and characterized even though it was formulated as a "derivative of trivalent nitrogen."⁵⁰ A number of diarylnitroxides **15** were subsequently prepared and characterized as radicals which do not dimerise in the solid state or in solution ($\text{R}=\text{OMe}$).⁵¹

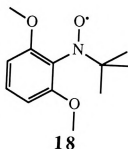
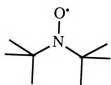
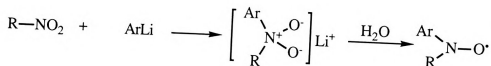
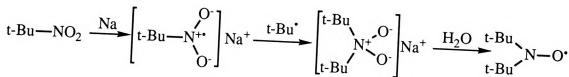
**14****15**

2,2,6,6-tetramethylpiperidine-N-oxyl (TEMPO) **16** has been studied extensively, and its Lewis basicity has been studied mainly by Drago.⁵² EPR spectra of TEMPO in solution have been reported to be solvent sensitive. Drago tried to explain the facts by the correlation of changes in the hyperfine coupling constant on adduct formation with enthalpies of interaction and with changes in the infrared spectra of the hydrogen-bonding acid upon interaction. The nitrogen hyperfine coupling constant is found to increase with the enthalpy of adduct formation. Quite a few variations on this sterically hindered nitroxyl have been reported, mainly from France and Russia including 4-hydroxy TEMPO (TEMPOL) **17**.⁵³

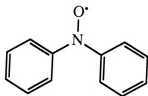
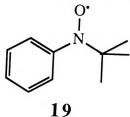
**TEMPO 16****TEMPOL 17**

K. Hoffmann reported a series of t-butyl nitroxides prepared by electrochemical or sodium reduction of nitrobutane in glyme, with a proposed mechanism shown below, in 50% yield. The method was not general for the preparation of other di-t-alkyl nitroxides, but, t-butyl-2,6-dimethoxyphenyl nitroxide **18** is prepared by hydrolysis of the reaction

mixture obtained from 2,6-dimethoxyphenyl-lithium and nitrobutane in 17.8% yield.

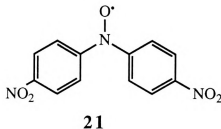
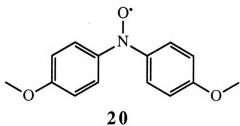


Diphenylnitroxide **15** (R=H) is only stable in dilute solution. In concentrated solution or in the solid state it behaves like *t*-butylphenylnitroxide **19**, decomposing spontaneously. Thus, the increase in unpaired electron delocalization, which occurs as a result of replacing a *t*-butyl group by a phenyl group, merely increases the number of reactive sites in the molecule and not its stability.

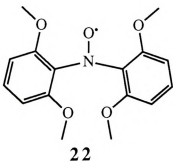


in the *t*-alkyl aryl series, however, stable diarylnitroxides are produced when C-O dimerization is prevented by the presence of blocking groups in the para-positions, thus, di-*para*-anisyl nitroxide **20** which is believed to be the first organic radical studied by single crystal X-ray and 4,4'-

dinitrodiphenyl nitroxide **21** are stable for months. In this respect the chlorine substituted system is apparently inadequate since it decomposes rapidly. Di-(*p*-tolyl)nitroxide (di-*p*-methyl) is sufficiently stable to be isolated but decomposes within hours.⁵⁴

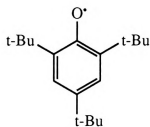
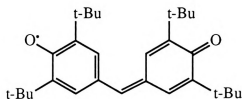


Ortho-substituents in diaryl nitroxide stabilize the radical probably by forcing the phenyl groups out of conjugation with the radical center, thereby reducing unpaired electron density at the para-positions.⁵⁵ Of particular interest is bis-(2,6-dimethoxyphenyl) nitroxide **22** shown below. It has a very interesting structure not only by the similarity to our diarylmethyl systems, but also for the natural extension of our rationale in designing molecular magnets by ion-bindings which I will discuss later.

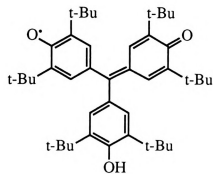
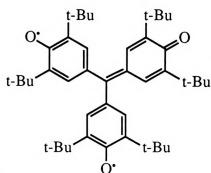


2.3. Aroxyl Radicals

It has long been appreciated that aroxyl radicals are intermediates in many phenol oxidations, and interest in these radicals has been enhanced by the fact that they play a role in many biological oxidations. Since the discovery of 2,4,6-tri-*t*-butylphenoxyl radical **23**, attention has been given largely to hindered phenoxyl radicals such as galvinoxyl **24**, some of which have been isolated and are sufficiently stable to be used as reagents.⁵⁶

**23**Galvinoxyl **24**

Of special interest are a number of stable aroxyl biradicals. Oxidation of the quinone methide with lead dioxide gives first the mono-radical **25**, its EPR spectrum shows interaction of the unpaired electron with the four equivalent ring protons of the conjugated rings ($a_H=1.3$ gauss). On further oxidation Yang's biradical **26** is obtained in which there is delocalization between the three rings giving seven lines from the six ring protons ($a_H=0.86$ gauss).⁵⁷

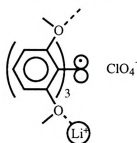
**25**Yang's Biradical **26**

Yang's biradical **26** is the best characterized stable biradical with high spin multiplicities among conjugated systems.⁵⁸

3. Magnetism

3.1. Diamagnetism

If a sample is placed in a magnetic field H , the observed field with a sample will generally differ from the free space value. If the observed field with a sample is reduced, the substance is said to be diamagnetic.⁵⁹ The molar susceptibility of a diamagnetic material is negative, and rather small (-1 to -100×10^{-6} emu/mol). Diamagnetic susceptibilities do not depend on field strength and are independent of temperature. Since organic compounds with unpaired electrons also have a number of filled shells, they have a diamagnetic contribution to their susceptibility. Diamagnetic susceptibilities of atoms in molecules are largely additive, and this provides a method for the estimation of the diamagnetic susceptibilities of ligand atoms and counter ions in a complex like $1 \cdot MX$.



Li^+	: -1.0×10^{-6} emu/g atom
ClO_4^-	: -32.0×10^{-6} emu/g atom
C_{25}	: -6.0×10^{-6} emu/g atom $\times 25$
H_{27}	: -2.93×10^{-6} emu/g atom $\times 27$
O_6	: -4.61×10^{-6} emu/g atom $\times 6$
	<hr/>
	-2.89×10^{-4} emu/mol

The Pascal constants provide an empirical method for this procedure. One holds the atomic susceptibility of each atom, as well as the constitutive correction to take account of such factors as π -bonds as shown above for the complex $1 \cdot LiClO_4$. This procedure is only of moderate accuracy, and the values given could change from compound to compound. Greater accuracy

can be obtained by the direct measurement of the susceptibility of a diamagnetic analogue of the paramagnetic compound.

3.2. Paramagnetism

A paramagnet concentrates the lines of force provided by an applied magnet and thereby moves into regions of higher field strength. This results in a measurable gain in weight in Gouy or Faraday balances. Paramagnetic susceptibility is generally independent of the field strength, but it is temperature dependent. To a first approximation at high temperature, the susceptibility χ varies inversely with temperature, which is the Curie Law:

$$\chi = \frac{C}{T}$$

C is called the Curie constant, and T is the absolute temperature. Since $\chi^{-1} = T/C$, a plot of χ^{-1} vs. T is a convenient procedure for the determination of the Curie constant; note that the line goes through the origin for paramagnetic materials in **Figure 1**.

Since the magnitude of magnetic susceptibility at room temperature is an inconvenient number, it is common among chemists to report the effective magnetic moment, μ_{eff} , which is defined as

$$\mu_{\text{eff}} = \left(\frac{3k}{N}\right)^{\frac{1}{2}} (\chi T)^{\frac{1}{2}} = [g^2 S(S+1)]^{\frac{1}{2}} \mu_B$$

Here, k is the Boltzmann constant, 1.38×10^{-16} erg/K, N is Avogadro's number, 6.022×10^{23} /mol and $\mu_B = |eh/2mc| = 9.27 \times 10^{-21}$ erg/G is the Bohr magneton. (the units of μ_{eff} is μ_B).

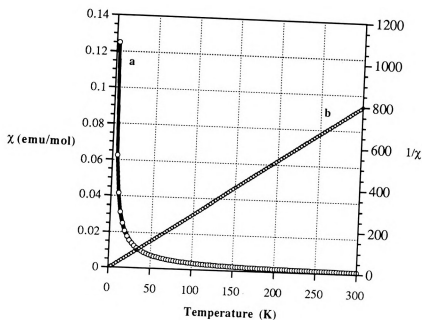


Figure 1. The molar susceptibility (χ_{mol}), **a**, and the reciprocal susceptibility (χ^{-1}_{mol}), **b**, as a function of temperature for $g=2$, $S=1/2$.

When an isolated radical is placed in an external magnetic field H (the Zeeman perturbation), the field will resolve the degeneracy of the various states according to the magnetic quantum number m_s , which varies from $-S$ to $+S$ in steps of unity. The energy of each of the sub levels in field becomes $E = m_s g \mu_B H$, where g is a Landé constant, characteristic of each system, which is equal to 2.0023 when $S=1/2$ and $L=0$ (total angular magnetic quantum number).

7

8

9

10

11

12

13

14

15

16

17

18

19

20

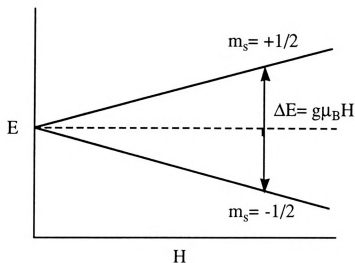
21

22

23

24

25



Thus, at a given external field, the distribution (population) of radicals among the various states can be calculated from the Boltzmann relation,

$$\frac{N_i}{N_j} \propto \exp\left(\frac{-\delta E_i}{kT}\right)$$

δE_i being the energy level separation between the level i and the ground state j . This model provides a basis for a simple derivation of the Curie law, which states that a magnetic susceptibility varies inversely with temperature. For an organic free radical ($S=1/2$) in zero field, the two levels $m_s = \pm 1/2$ are degenerate, but split when a field H_z is applied.

The magnetic moment of a radical in the level n is given as

$$\mu_n = \delta E_n / \delta H = -m_s g \mu_B$$

The molar macroscopic magnetic moment M is obtained as the sum over magnetic moments weighted according to the Boltzmann factor and it can be approximated as following:

St
in
fol

Thi
Ref

It is
large
inde
satu
situ
appl

$$M \sim N g^2 \mu_B^2 H_z / 4kT$$

Static molar magnetic susceptibility is defined as $\chi_{\text{mol}} = M_{\text{mol}}/H$ which is in the form of the Curie law where the Curie constant can be expressed as following when $S=1/2$.

$$\chi = \frac{M}{H_z} = \frac{N g^2 \mu_B^2}{4kT} = \frac{C}{T}$$

$$C = N g^2 \mu_B^2 / 4k = 0.125 g^2 S(S+1) \text{ cm}^3 \text{ K} / \text{mol}$$

This is a special case of the more general spin-only formula, where $\mu_{\text{eff}}^2 = g^2 \mu_B^2 S(S+1)$ is the square of the "magnetic moment".

$$\chi = \frac{N g^2 \mu_B^2 S(S+1)}{3kT} = N \frac{\mu_{\text{eff}}^2}{3kT}$$

It is interesting to examine the behavior of M in the other limit, of very large fields and very low temperatures, the magnetization becomes independent of field and temperature, and becomes the maximum or saturation magnetization M_{sat} which the spin system can exhibit. This situation corresponds to the complete alignment of magnetic dipoles by the applied field.

$$M_{\text{sat}} = N g \mu_B S$$

3.3. Curie-Weiss Law

The Curie law is the magnetic analog of the ideal gas law, which is expressed in terms of the variables p , V , T . For magnetic systems, one uses H , M , T and the thermodynamic relations derived for a perfect gas can be translated to a magnetic system by replacing p by H and V by $1/M$.

There are many situations in which the Curie law is not strictly obeyed. One source of the deviations can be the presence of an energy level whose population changes significantly over the measured temperature interval (magnetic phase transition); another source is the magnetic interactions which can occur between paramagnetic centers.

To the simplest approximation, this behavior is expressed by a small modification of the Curie law, to the Curie-Weiss law, where the correction term, θ , has the units of temperature.

$$\chi = \frac{C}{(T + \theta)}$$

When θ is negative in sign it is called antiferromagnetic; when θ is positive, it is called ferromagnetic. The constant, θ , characteristic of any particular sample, is best evaluated when $T > 10K$, as curvature of χ^{-1} usually becomes apparent at smaller values of T .

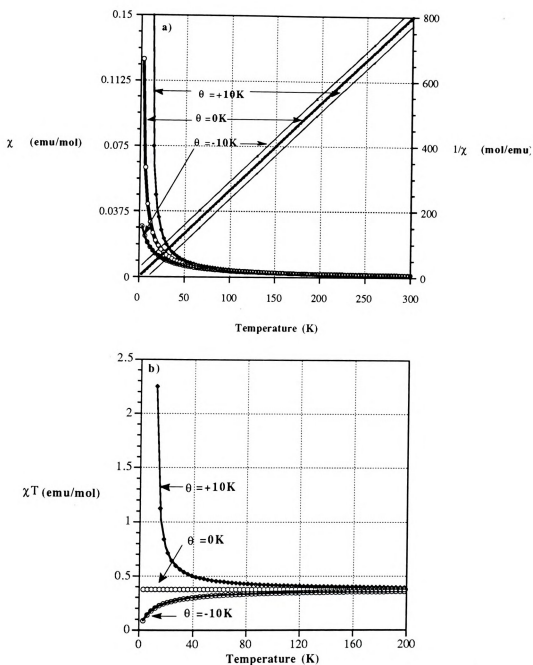


Figure 2. a) The reciprocal susceptibility, χ^{-1} , extrapolated from the high temperature data; b) χT , as a function of temperature. These plots represent a system in which $g=2$, $S=1/2$, as well as ferromagnetically coupled ($\theta = +10\text{ K}$) and antiferromagnetically coupled ($\theta = -10\text{ K}$) systems.

3.4.

Blea

Blea

For r

by se

at J/k

susce

This

zero

positi

the C

low w

2 whi

mole

The s

couple

the sa

broad,

decrea

3.4. Pairwise Magnetic Exchange

The magnetic susceptibility per mole of dimers was calculated by Bleaney and Bowers via the application of Van Vleck's equation (the Bleaney-Bowers equation).

$$\chi = \frac{(2Ng^2\mu_B^2 / kT)}{3 + \exp(-2J / kT)}$$

For negative J (antiferromagnetic), χ has a maximum. This may be found by setting $d\chi / dT = 0$. With the definitions used here, the maximum occurs at $J/kT_m \sim -4/5$. For $-J/k \ll T$ (or $T \gg T_m$) (at high temperature), the susceptibility follows a Curie-Weiss law, $\chi = 3/[4(T - \theta)]$ with $\theta = J/2k$. This is a specific instance of the more general connection between a non-zero Weiss constant and the presence of exchange interaction. When J is positive, the susceptibilities calculated according to the above equation and the Curie law for spin $S=1/2$ do not differ greatly until temperatures very low with respect to $2J/k$ are achieved; this is because of the extra factor of 2 which enters when comparing a mole of uncoupled $S=1/2$ spins with a mole of dimers.

The susceptibilities for a pair of $S=1/2$ radicals antiferromagnetically coupled are described in **Figure 3**. While the low temperature behavior is the same, the temperature of maximum χ increases with decreasing θ . A broad, featureless peak is observed because of the continuous population decrease of the various levels as temperature decreases.

3.5.

classi
dimer
with
behav

There
descri
system
chains

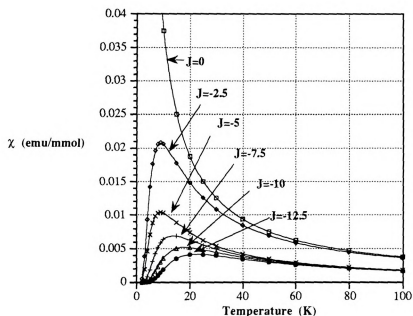


Figure 3. The Bleaney Bowers susceptibilities compared with the Curie law; plots for $J=0, -2.5, -5, -7.5, -10, -12.5 \text{ cm}^{-1}$.

3.5. One-Dimensional or Linear Chain Systems

Much of what has been covered so far could come under the classification of short-range order. The physical meaning implied by low dimensional magnetism is that radicals are assumed here to interact only with their nearest neighbors in a particular spatial sense. This magnetic behavior follows directly from the structure of the various compounds.

There are good theories and extensive experimental data available which describe the thermodynamic properties of one-dimensional magnetic systems, at least for $S=1/2$; for systems of metal ions linked into uniform chains. In order to discuss exchange at the atomic level, one must

intro

Ham

This

mod

when

The

of th

situat

the I

Heise

pract

There

for a

chara

in 1D

exten

system

Since

calcul

predic

introduce quantum mechanical ideas and we need to use the following Hamiltonian.

$$H = -2J \sum S_i \cdot S_j$$

This is an isotropic Hamiltonian and is often referred to as the Heisenberg model. A very anisotropic expression, called the Ising model is obtained when γ is set equal to zero in the following equation.

$$H = -2J \sum [\gamma(S_{1x}S_{2x} + S_{1y}S_{2y}) + S_{1z}S_{2z}]$$

The Heisenberg model, which corresponds to using all the spin-components of the vectors S_1 and S_2 , is obtained when $\gamma=1$. This appears as an artificial situation, and yet the Ising model is important, in part, because solutions of the Ising Hamiltonian are far more readily obtained than those of the Heisenberg Hamiltonian. Both of these Hamiltonians are restricted in their practical application to nearest-neighbor interactions.

There are no exact or closed-form solutions for the Heisenberg model, even for a $S=1/2$ one-dimensional system. But, calculations are available which characterize Heisenberg behavior to a high degree of accuracy, particularly in 1D systems. Furthermore, one-dimensional short-range order effects are extended over a much larger region in temperature for the Heisenberg systems than for the Ising systems.

Since the Heisenberg model is an isotropic one, the susceptibility is calculated to be isotropic. A broad maximum in the susceptibility is predicted for a linear chain antiferromagnet. For an infinite linear chain,

S
v
r
[
a
i

T
L

M
sa
T

T
ex
qu
str
an

Bonner and Fisher calculate that the susceptibility maximum will have a value $\chi_{\max}/(N g^2 \mu_B^2 / |J|) \sim 0.07346$ at the temperature $kT_{\max}/|J| \sim 1.282$.

The best example of an antiferromagnetic Heisenberg chain compound is $[\text{N}(\text{CH}_3)_4]\text{MnCl}_3$, TMMC. The crystal consists of chains of $J=5/2$ manganese atoms bridged by three chloride ions. The antiferromagnetic 1D behavior in this nearly ideal Heisenberg system has been reviewed.⁶⁰

The zero-field susceptibilities have been derived by Fisher for the $S=1/2$ Ising chain.

$$\chi_{\text{par}} = \frac{N g_{\text{par}}^2 \mu_B^2}{2J} (J / 2kT) \exp(J / kT),$$

$$\chi_{\text{per}} = \frac{N g_{\text{per}}^2 \mu_B^2}{4J} [\tanh(J / 2kT) + (J / 2kT) \text{sech}^2(J / 2kT)].$$

Many susceptibility measurements are made on powdered paramagnetic samples, so that only the average susceptibility, $\langle \chi \rangle$, is obtained.

The average susceptibility $\langle \chi \rangle$ is defined as

$$\langle \chi \rangle = \frac{(\chi_{\text{par}} + 2\chi_{\text{per}})}{3}$$

The meaning of the symbols "parallel" and "perpendicular" refer to the external magnetic field direction with respect to the direction of spin-quantization or alignment within the chains, rather than to the chemical or structural arrangement of the chains. The zero-field susceptibilities for χ_{par} and χ_{per} are plotted in **Figures 4 and 5**.

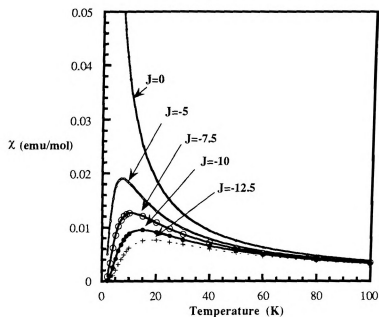


Figure 4 The Ising "*parallel*" susceptibilities compared with Curie law; plots for $J = -2.5, -5, -7.5, -10, -12.5 \text{ cm}^{-1}$.

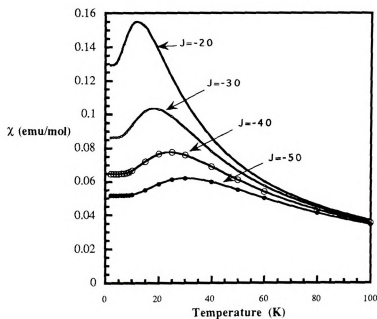


Figure 5 The Ising "*perpendicular*" susceptibilities for $J = -20, -30, -40, -50 \text{ cm}^{-1}$.

3.

int

alc

An

He

be

co

W

int

an

ex

fer

tw

sus

On

alte

alte

the

der

1/k

3.6. Alternating Linear Heisenberg Chain

The models discussed so far are uniform linear chain systems. The intrachain exchange constant has been assumed not to vary with position along the chain, and it is assumed that there is no interchain interaction.

$$H = -2J \sum_i [S_{i-1} \cdot S_i + \alpha S_i \cdot S_{i+1}]$$

An alternating chain is defined by letting α be less than one. For a Heisenberg alternating linear chain, $-2J$ is then the exchange interaction between a spin and one of its nearest neighbors, and $-2\alpha J$ is the exchange constant between the same spin and the other nearest neighbor in the chain. When $\alpha=0$, the model reduces to the dimer model with pairwise interactions (the Bleaney-Bowers model). The alternating linear chain antiferromagnet with $S=1/2$ has been studied in detail both theoretically and experimentally.⁶¹ In 1955 Oguchi developed a general theory of ferromagnetism and antiferromagnetism, based on the Heisenberg model of two-spin clusters. Ohya-Nishiguchi later extended this theory to the susceptibility of interacting spin-pair systems.

One of the important susceptibility results for an antiferromagnetic alternating Heisenberg linear chain is a broad maximum for all values of the alternation parameter α . The susceptibility curves decrease exponentially as the temperature approaches zero.⁶² The zero-field susceptibilities have been derived by Fisher for the $S=1/2$ linear Heisenberg chain where $u=(\coth K - 1/K)$ with $K=3J/2kT$.

Each
suscep
derive
 J' is t
suscep
chain

$$\chi = \frac{Ng^2\mu_B^2}{4kT} \left[\frac{1 + \coth\left(\frac{3J}{2kT}\right) - 1 / \left(\frac{3J}{2kT}\right)}{1 - \coth\left(\frac{3J}{2kT}\right) + 1 / \left(\frac{3J}{2kT}\right)} \right]$$

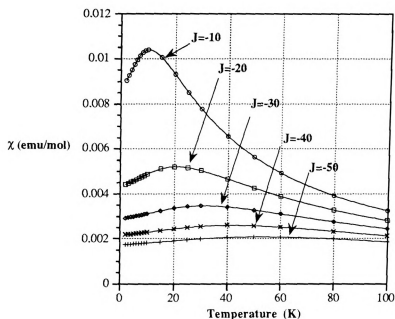


Figure 6. The Heisenberg linear chain susceptibilities for $J = -10, -20, -30, -40, -50 \text{ cm}^{-1}$.

Each of the magnetic models described above (Heisenberg and Ising chain susceptibilities) can be modified by the addition of a mean-field correction derived by Carlin where Z is the number of neighboring dimers or chains, J' is the coupling constant between dimers or chains, and χ is the molar susceptibility. The Bleaney-Bowers model turns into the alternating linear chain model with the mean-field correction when $Z=2$.

$$\chi' = \frac{\chi}{1 - (2ZJ' / Ng^2\mu_B^2)\chi}$$

4. Molecular

4.1. Molecu

4.1.1. McC

In 1963
on the studies
proposal was
hydrogen mol
free radicals (
negative atom
radicals may s
of positive sp
density in nei
interaction fav
molecules.⁶⁴

If we conside
interaction bet
the Hamiltonia

4. Molecular Magnets

4.1. Molecular Magnet models

4.1.1. McConnell Model

In 1963 McConnell proposed a model for organic ferromagnets based on the studies by Edelstein and Mandel,⁶³ of solid organic free radicals. His proposal was based on the Heitler-London spin exchange principle for a hydrogen molecule. He pointed out that in certain aromatic and olefinic free radicals (especially odd-alternant radicals) there are large positive and negative atomic π -spin densities, and it is possible that in special cases these radicals may stack on top of one another in the crystal lattice so that atoms of positive spin density are exchange coupled to atoms of negative spin density in neighboring molecules, resulting in a ferromagnetic exchange interaction favoring parallel total spin angular momentum on neighboring molecules.⁶⁴

If we consider only two center exchange integrals, then the exchange interaction between two aromatic radicals A and B can be approximated by the Hamiltonian

$$H^{AB} = - \sum_{ij} J_{ij}^{AB} S_i^A \cdot S_j^B$$

where S_i^A is the
electron spin
in the form

where S_A and
are the π -spin
McConnell and
coupling in so
are usually positive
for aromatic molecules

He later
superexchange
"If an ionic molecule
whose neutral
transfer to lead
molecules. The
acceptor molecule
coupling of the
possibility."

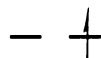
where S_i^A is the π -electron spin on atom i of molecules A , and S_j^B is the π -electron spin on atom j of molecule B . The equation above can be written in the form

$$H^{AB} = -S^A \cdot S^B \sum_{ij} J_{ij}^{AB} \rho_i^A \cdot \rho_j^B$$

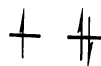
where S_A and S_B are the total spin operators for A and B , and ρ_i^A and ρ_j^B are the π -spin densities on atoms i and j of molecules A and B .

McConnell attributed the dominant tendency toward antiparallel spin coupling in solid free radicals to the fact that the spin densities ρ_i^A and ρ_j^B are usually positive, and the largest exchange integrals J_{ij}^{AB} are negative for aromatic molecules that are stacked on top of one another in crystals.

He later proposed another recipe for molecular magnets using superexchange in charge transfer complexes.⁶⁵ He stated in this paper, "If an ionic molecular crystal $D+A^-$ could be formed with a donor molecule whose neutral ground state was a triplet, then one would expect back charge transfer to lead to ferromagnetic coupling of the spins on adjacent ion molecules. The same effect could be achieved if, instead, the neutral acceptor molecule A had a triplet ground state. Thus, ferromagnetic coupling of the spins of free radicals in certain ionic molecular crystals is a possibility."



D^+

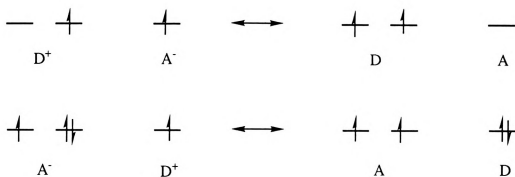


A^-

The result of s
spins on two r
transfer can le
such charge tra
be parallel to
parallel to both
to a ferromagn
could be two-di

4.1.2. Matag

In 1968,
some extended
systems which
topological natu
the mechanism
possible routes
next page, are
number of the g



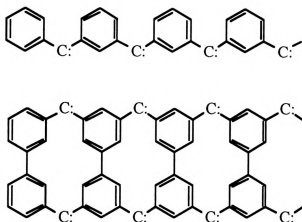
The result of such charge transfer will be to favor a system in which the spins on two neighboring species $D^{+\bullet}$ and $A^{\bullet-}$ are parallel, so that charge transfer can lead to the favored triplet state of one of the partners. Since such charge transfer can go in either direction, the spin on a given $A^{\bullet-}$ will be parallel to the spins on both neighboring $D^{+\bullet}$, which in turn must be parallel to both other neighboring $A^{\bullet-}$. Such parallel spin correlation leads to a ferromagnetic domain; if the charge transfer is not only linear there could be two-dimensional or three-dimensional domains.

4.1.2. Mataga Model

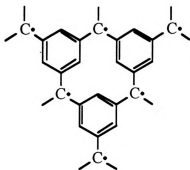
In 1968, Mataga proposed several possible ferromagnetic states of some extended hypothetical hydrocarbons with conjugated π -electron systems which will show ferromagnetic spin alignment due to the topological nature of the MO's. Qualitative discussions have been given for the mechanism of couplings in the "ferromagnetic state", as well as some possible routes for their preparation..⁶⁶ These compounds, shown on the next page, are all alternant hydrocarbons (even or odd according to the number of the groups and atoms).

These are poly
and they are a
assumed that
participates in
remains as a "
these compound

These meta-sub
to the Hückel M
Orbitals (NBM
electrons as ind
If the orbital e
sufficiently sma



These are polymeric carbenes or extensions of the triphenylmethyl radical, and they are all meta-substituted compounds. In the case of carbenes, it is assumed that one of the unpaired π -electrons of the divalent carbon participates in conjugation with the ring π -electrons while the other of them remains as a "n-orbital." For the sake of simplicity, Mataga assumed that these compounds are all co-planar.



These meta-substituted hydrocarbons have non-bonding π -MO's according to the Hückel MO theory and the number of such π -Non Bonding Molecular Orbitals (NBMO) is equal to the number of carbon atoms with unpaired electrons as indicated in the structure.

If the orbital energy differences between the non-bonding orbitals are sufficiently small, all unpaired electrons will have parallel spin according to

Hund's rule
extended over
relatively con
electronic stru
like, and the '
electron spins

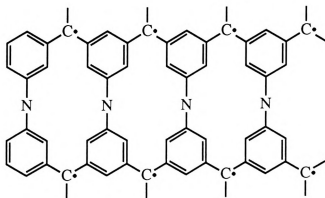
4.1.3. Ovch

In 1978
multiplicity of
conjugated bor
the class of al
two groups are
than zero. He
shown below I
electrons in a n
gives very little

Hund's rule (extended to a molecule). Although the π -NBMO's are extended over the whole molecule, the electron density in a π -NBMO is relatively concentrated on each trivalent atom. In this situation, the electronic structure on each carbon with the n-orbital may be rather atom-like, and the "intra-atomic" interactions probably induce alignments of the electron spins in all the n-orbitals.

4.1.3. Ovchinnikov Model

In 1978 Ovchinnikov proposed an organic magnet model based on the multiplicity of the ground state of large alternant organic molecules with conjugated bonds which are similar to Mataga's model. He showed that for the class of alternant hydrocarbons in which the numbers of atoms in the two groups are unequal (i.e., for the odd alternants) the total spin is more than zero. He presented some possible planar and linear molecules such as shown below having the full spin proportional to the number of unpaired electrons in a molecule.⁶⁷ This model is basically similar to Mataga's and it gives very little insight into how or why high-spin is expected.



4.1.4. Bres

In 1982

ions as buildin

proposal (char

conjugated sys

states. If stab

crystallize as r

be used to pre

and to the ferr

Over the year

which have ap

shown to exist

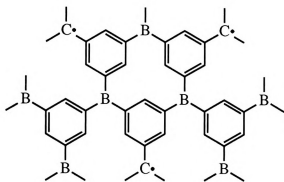
been shown to

salt of this cat

showed a typic

an E value of

being examine



4.1.4. Breslow Model

In 1982 Breslow proposed a series of stable high spin molecules or ions as building block for molecular magnets based on McConnell's second proposal (charge transfer model).⁶⁸ He suggested that cyclic $4n$ π -electron conjugated systems with C_3 or greater symmetry should have triplet ground states. If stable examples of such systems could be prepared they might crystallize as molecular magnets. He outlined a theory of how triplets could be used to prepare ferromagnets. Synthetic approaches to stable triplets, and to the ferromagnetic system were described.

Over the years, the Breslow group has examined a number of systems which have appropriate symmetry and electron count and which have been shown to exist to some extent as triplets. The simplest of these, which has been shown to exist as a ground state triplet is cyclopentadienyl cation. A salt of this cation **27**, prepared from 5-bromocyclopentadiene and SbF_5 , showed a typical triplet EPR spectrum, with a D value of 0.1865 cm^{-1} and an E value of 0. The zero value of E indicates that the triplet molecule being examined has a plane polygonal geometry, as expected by symmetry.

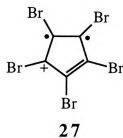
The rather large
average fairly

Unfortunately
for the ground
simple ideas
temperature de
of pentapheny
state lying 0.2
energy gap t
equilibrium wi
unsubstituted
down to 4K, so

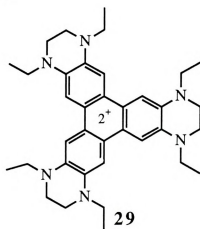
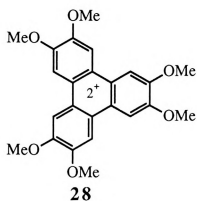


Although the
triplet EPR sp
requirements

The rather large D value indicate that the two unpaired electrons are on the average fairly close.



Unfortunately, even in a symmetrical $4n-\pi$ -electron molecule, it is possible for the ground state to be a singlet, in contrast to expectations based on simple ideas about orbital degeneracy and Hund's rules. From the temperature dependence of the EPR signal it was seen that the ground state of pentaphenylcyclopentadienyl cation is actually a singlet, with a triplet state lying 0.35 to 1.15 kcal/mole higher in energy. With such a small energy gap there was a detectable population of triplets in thermal equilibrium with the singlet at essentially all temperatures. By contrast, the unsubstituted cyclopentadienyl cation triplet followed the Curie-Weiss law down to 4K, so it is a ground state triplet.



Although the dication (28 and 29) of the triphenylene shown above have triplet EPR spectra and the charge-transfer solid appears to have met the requirements of Breslow's model for ferromagnetism, these dication

systems were
dependence st

4.1.5. Torra

In 198
containing sta
with iodine at
phase to form
The reaction
reproducible.
structure show
analyses. F
ferromagnetic

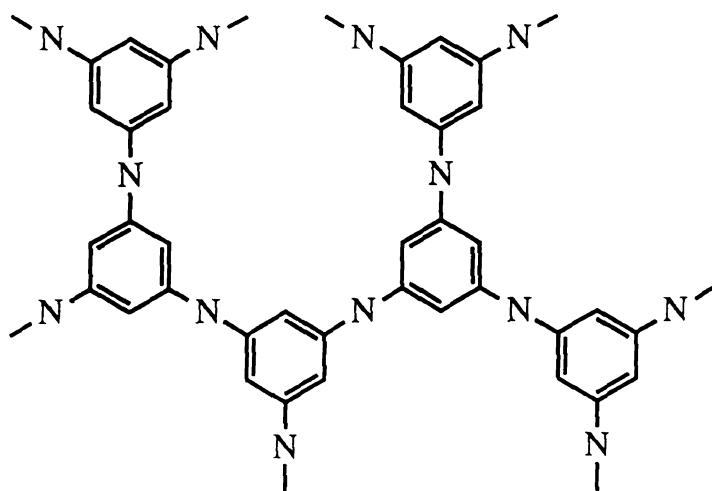
4.1.6. Kahn

Kahn ha
McConnell m

systems were also found to be ground-state singlets based on temperature dependence studies with a Faraday balance.⁶⁹

4.1.5. Torrance Model

In 1987 Torrance proposed a model for organic ferromagnets containing stacks of radical ions.⁷⁰ Symmetrical triaminobenzene reacts with iodine at room temperature in a variety of solvents and in the vapor phase to form a black, insoluble polymer of radical cations of aryl amines. The reaction is complex and the resulting polymer was not very reproducible. He proposed a possible precursor of "unoxidized" polymeric structure shown below which was consistent with IR data and chemical analyses. However, the extreme lack of reproducibility of the ferromagnetic material has made characterization troublesome.



4.1.6. Kahn's Proposal

Kahn has recently presented a careful and detailed discussion of the McConnell mechanism for the possible mixing of ground and charge-

transfer confi
states. He sho
transfer mixin
for the triplet
stabilized trip
energies and c
organic magn
success. In ad
stacks is sugg
might be obt
molecules in th

transfer configurations of a donor-acceptor pair for both singlet and triplet states. He showed that in contrast to McConnell's assumption, more charge-transfer mixing terms are available for the stabilization of the singlets than for the triplet in the charge-transfer complexes. For the superexchange-stabilized triplet to be favored, a delicate balance of magnetic orbital energies and overlaps must be achieved, which suggests that approaches to organic magnets based on the above strategy have little probability of success. In addition, a modification of McConnell's mechanism for uniform stacks is suggested. Kahn proposed that a triplet ground state of the dimer might be obtained only for a highly symmetrical arrangement of the molecules in the stack.⁷¹

4.2. Metal

It is m
magnetism in
appeared rece
charge transfe

Studies on ma
and Bowers
copper(II) ace
established a t
magnetic suscep
the energy par
ions in dimeric
were synthes
comparing the
and more resear
in the light of
and magnetic
understanding o

4.2.1. Single

The sing
Kahn et al.⁷⁵ a
ligands. In this

4.2. Metal Based Molecular Magnets

It is my intention to summarize the current state of molecular magnetism in this section even though many excellent reviews have appeared recently from the leaders in their areas-mainly bimetallic and charge transfer systems.⁷²

Studies on magnetic polynuclear complexes started in 1952, when Bleaney and Bowers demonstrated that the magnetic and EPR properties of copper(II) acetate were due to the dimeric nature of the molecule. They established a theoretical expression (the Bleaney Bowers equation) for the magnetic susceptibility of such a system as a function of the temperature and the energy parameters J characterizing the interaction between the Cu^{2+} ions in dimeric copper (II) acetates.⁷³ Numerous polynuclear complexes were synthesized, and their coupling parameters J determined by comparing the observed magnetic data with the theoretical values. More and more researchers then attempted to rationalize observed magnetic data in the light of structural data. This allowed correlations between structural and magnetic properties to be made, and provided a step toward an understanding of the mechanisms of interaction between metal centers.⁷⁴

4.2.1. Single Atom Bridged Bimetals

The single atom bridged bimetallic systems have been followed by Kahn et al.⁷⁵ and Drillon et al.⁷⁶ who used metal ions bridged by organic ligands. In this case, one-dimensional ferrimagnets (incomplete cancellation

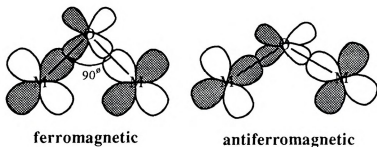
of spins by the
which in some
highest ferromagnetic

Bimetallic compounds
compared to
coupled). The
based molecular
atom bridging
have been attributed
magnetic orbital
of oxygen and
interactions in

Anderson discussed
interactions and
as electron density
increase in electron
coupling. This
coworkers, 78

of spins by the differences in magnitude of interacting spins) were obtained, which in some cases ordered ferromagnetically at low temperature. The highest ferromagnetic phase transition temperature was reported to be 14K.

Bimetallic complexes exhibiting a spin-triplet ground state are very rare as compared to those with spin-singlet ground state (antiferromagnetically coupled). There are three known cases of ferromagnetically coupled metal based molecular magnetic systems, two of which are bridged by a single atom bridging ligand.⁷⁷ The ferromagnetic properties of these compounds have been attributed either to accidental or to strict orthogonality of their magnetic orbitals or to spin-polarization effects using Hund's rule for both of oxygen and nitrogen ligands. Thus, it is very rare to have ferromagnetic interactions in single atom bridged bimetallic systems.



Anderson discussed the influence of ligand substituents on superexchange interactions and concluded that the antiferromagnetic interaction decreases as electron density is removed from the bridging atoms. Conversely, an increase in electron density raises the ligand levels and enhances the AF coupling. This conclusion was also reached by Hodgson, Hatfield, and their coworkers.⁷⁸

4.2.2. Mole

The ab
interaction be
demonstrated

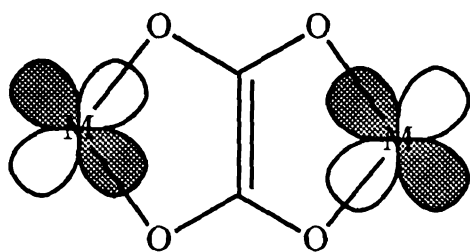


The symmetri
was understo
value of -193
tetraamineeth
However, due
carboxylato b
exhibited a J/k

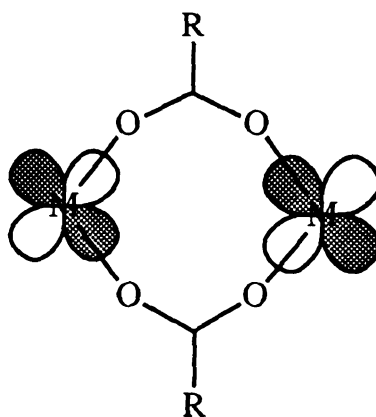
Tsipis reporte
Cu(II) binucle
proposed two
goes through
very few bim
magnetic inter

4.2.2. Molecule Bridged Bimetals

The ability of the carboxylate group to mediate the exchange interaction between two Cu(II) ions separated by more than 5 \AA has been well demonstrated in the case of (oxalato) copper (II) compounds shown below.⁷⁹



oxalate bridge



dicarboxylate bridge

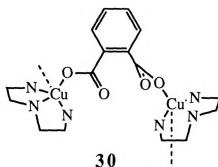
The symmetric orientation of magnetic orbitals in the bimetallic complexes was understood as a reason for a large antiferromagnetic J/k coupling value of -193 cm^{-1} in $[(\text{tetraamineethylenediamine}(\text{H}_2\text{O})\text{Cu}(\text{C}_2\text{O}_4)\text{Cu}(\text{H}_2\text{O})\text{tetraamineethylene diamine})(\text{ClO}_4)_2]$ with a Cu-Cu separation of 5.14 \AA . However, due to the unfavorable magnetic orbital configuration of its carboxylato bridge, the $[\text{Cu}(\text{NH}_3)_2(\text{CH}_3\text{COO})\text{Br}]$ polymeric complex exhibited a J/k value of -4.3K .⁸⁰

Tsipis reported magnetic studies on a ferromagnetic phthalato-bridged Cu(II) binuclear complex **30** with its Cu(II) ions separated by 6.7 \AA . He proposed two possible pathways for spin-orbital couplings, one of which goes through two carboxylate and aromatic π -orbitals. This is one of a very few bimetallic molecular bridged systems showing very long-range magnetic interactions.⁸¹

Least-squares
susceptibility
energy gap of
bridged Cu(II)
obtained for a
orbital interpre
ferromagnetic
atom-bridging

4.2.3. Metal

One of
magnets is bas
and stable org
radicals have
chemistry has
has weak Lew
metal ions.
paramagnetic r



Least-squares fitting of the variable-temperature (4.2-295K) magnetic susceptibility data to the Bleaney-Bowers equation indicated a singlet-triplet energy gap of $80 \pm 10 \text{ cm}^{-1}$, $g=2.10$, and $J = -1.81 \text{ cm}^{-1}$ for the phthalato-bridged Cu(II) binuclear complex. However, no direct EPR evidence was obtained for a triplet state (half field transition). From the standpoint of orbital interpretation of the coupling, this is a new situation leading to ferromagnetic interaction between magnetic centers separated by multi-atom-bridging units.

4.2.3. Metal and Organic Radical Based Systems

One of the most unique approaches to the design of molecular magnets is based on a model of directly interacting paramagnetic metal ions and stable organic radicals, such as nitroxides, by Gatteschi et al.⁸² These radicals have been widely used as spin probes, and their coordination chemistry has been reviewed previously.⁸³ The oxygen atom of the radical as weak Lewis basicity, and can serve as a ligand toward many different metal ions. When a nitroxide binds through its oxygen atom to a paramagnetic metal ion, the spins can orient anti-parallel to each other or

parall

coupl

The s

easily

orbita

signif

orthog

In the

The l

radica

has b

Antife

where

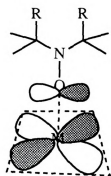
O-N a

coupli

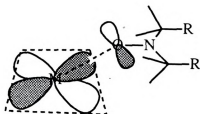
magne

parallel to each other, resulting in antiferromagnetic or ferromagnetic coupling.

The sign of the coupling of a nitroxide directly bound to a metal ion is easily predicted on the basis of orbital overlap considerations.⁸⁴ If the orbitals containing the unpaired electrons on the metal and the radical have significant overlap, the coupling is antiferromagnetic, while if they are orthogonal to each other, the coupling is ferromagnetic.



ferromagnetic



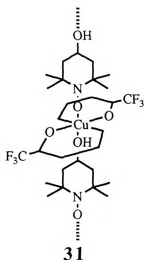
antiferromagnetic

In the ferromagnetic case, the two orbitals are orthogonal to each other. The latter situation occurs in a copper(II) nitroxide complex, where the radical is in an axial coordination site, and experimentally the triplet state has been found to lie $10 - 70 \text{ cm}^{-1}$ below the singlet state. Antiferromagnetic coupling occurs in copper(II)-nitroxide complexes where the radical coordinates in an equatorial coordination site. If the M-O-N angle is not 180° (very rare case), substantial overlap can occur and the coupling becomes antiferromagnetic. This expectation was confirmed by magnetic measurements showing singlet ground states for these systems.

It
Cu
ma
con
the
fer
pa

T
exp
ad
the
the
pa
ten
bro
alte
a v
sup

It has recently been demonstrated that the coordination polymer $\text{Cu}(\text{hfac})_2 \cdot 2\text{TEMPOL}$ **31**, shown below, behaves like an alternating linear magnetic chain.⁸⁵ At high temperature, the magnetic behavior of the complex shows characteristics of two independent spin $S=1/2$ moieties. As the temperature of the sample is decreased, the spins interact ferromagnetically, leading to a triplet ground state for the copper nitroxyl pair.

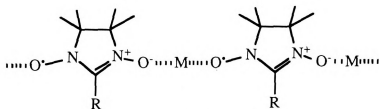


The exchange constant, based on an analysis using the Bleaney-Bowers expression, was found to be $2J/k = 19 \pm 7\text{K}$. The average g value for the adduct was found to be 2.08. At a temperature of 4.2K and below, one therefore expects the system to consist of spin $S=1$ units with $g=2.08$, and the question was asked whether there is a weak magnetic link between the pairs via the saturated ligand and the "hydrogen bond". At lower temperatures the magnetic susceptibility data increase and go through a broad maximum at about 80mK; these data have been explained as an alternating Heisenberg linear chain with $g=2.2$ and $2J'/k = -78\text{mK}$, which is a very weak exchange constant but is reasonable given the proposed lengthy superexchange path.

with t
differ
yieldin
two d
bind t
nitrox

Accor
three-
report
comp
ordere
and e
20K v
transi
coaxia
of me
coils
tempe

Nitronyl nitroxides show very interesting coordination chemistry with transition metal ions.⁸⁶ It has been found that they can bind in several different ways: they can bind via one oxygen atom to one metal ion, yielding mononuclear complexes; they can bind via the two oxygen atoms to two different metal ions to form magnetic chains. In these cases the radicals bind to the metal ions, keeping their radical nature; the π^* orbital of the nitroxide has a weak overlap with the magnetic orbitals of the metal ions.



R = Ph, Me, Et, Py, etc.,

According to this model, ferrimagnetic chains have been obtained and three-dimensionally ordered ferromagnets have been reported. Gatteschi reported the magnetic properties of the $\text{Mn}(\text{hexafluoroacetoacetate})_2$ complex of nitronitronyl nitroxide shown above, which is ferromagnetically ordered at 8K, and of the $[\text{Mn}(\text{pentafluorobenzene})_2]_2$ complex of methyl and ethyl nitronyl nitroxide, which show bulk ferromagnetism at 24 and 20K with a Weiss constant of 25K. He characterized the magnetic phase transition using *ac* susceptibility measurements (sample is placed within a coaxial set of coils and a low-frequency signal is applied with a few gaussess of measuring (*ac*) magnetic field; the change in mutual coupling between the coils is proportional to magnetic susceptibility) and reported low temperature EPR spectra that show apparent short-range order effects,

providing info

he was not ab

The 4-
acetylaceton

acetoacetate)

the basis of

complexes ex

groups as sh

assignment w

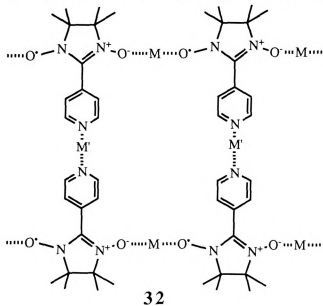
pyridine nitro

might form a

order ferroma

providing information on the preferred spin arrangements. Unfortunately, he was not able to get the X-ray structure of the dimetal complexes.⁸⁷

The 4-Pyridyl nitronyl nitroxide reacts with metal hexafluoroacetylacetonates forming compounds of formula $Mn_2M(\text{hexafluoroacetoacetate})_6(4\text{-pyridylnitronyl nitroxide})_2$ **32**, with $M = Mn, Co, Ni$. On the basis of magnetic and IR evidence, Gatteschi reported that all these complexes exist as chains of radicals bridged to metal ions through NO groups as shown below. Unfortunately, he was not able to confirm this assignment with the X-ray structure of the complex. He proposed that the pyridine nitrogen donors bind the metal M to connect different chains and might form a ladder-like two dimensional structure. These compounds order ferromagnetically below 10K when M and M' are Mn.



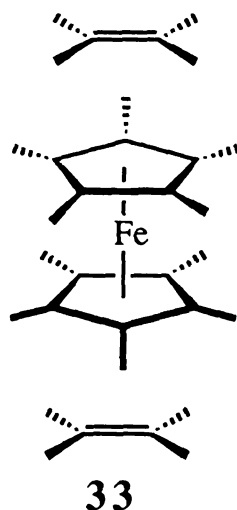
4.2.4. Characterization

The charge transfer band at 450 nm in the second molecule was observed. The compound synthesized a ferromagnetic complex. The magnetic moment calculated using the spin-only formula is 1.73 BM, which is suggested to be a high-spin state. The mechanism of the complex formation is suggested to be the coordination of the compound to the metal ion.

The charge transfer band at 450 nm in the second molecule was observed. The compound synthesized a ferromagnetic complex. The magnetic moment calculated using the spin-only formula is 1.73 BM, which is suggested to be a high-spin state. The mechanism of the complex formation is suggested to be the coordination of the compound to the metal ion.

4.2.4. Charge Transfer Complex Based Systems

The charge transfer complex based systems motivated by McConnell's second molecular magnet model have been studied by Miller who synthesized a compound of formula $[\text{Fe}(\text{Me}_5\text{Cp})_2](\text{TCNE})$ **33** which orders ferromagnetically at 4.8K and has a coupling constant of $J = 19 \text{ cm}^{-1}$ as calculated using an empirical linear chain Heisenberg model. In this case, it is suggested that the parallel alignment of the spins is achieved through a mechanism of virtual charge transfer between the two different spin centers of the compound.⁸⁸



The charge transfer complex superexchange model of Miller which had driven much of the synthetic activity in the field has recently been thoroughly reanalyzed and questioned by Kahn, as mentioned earlier.⁸⁹ He proposed to apply McConnell's first magnetic model of spin polarization instead of the second charge transfer model to explain the observed magnetic behavior in the decamethylferrocenium tetracyanoethenide complex of Miller. He argued that the unpaired electrons of the metallocenium ions localized on the metal induce a negative spin density on the Cp rings which interacts antiferromagnetically with the unpaired

electron in
polarization

4.3. Galvin

Stable
used in buildi
this country.
magnet was a
stable organi
density induc
hydrocarbons
possible to bu
many experts
Japan and Mi

4.3.1. Galv

Galvino
1-ylidene]met
itself. Awa
intermolecula
interaction ext
6 cm⁻¹. The c
in the context

electron in the π^* LUMO of the acceptor molecule TCNE by spin polarization to give ferromagnetic interactions.

4.3. Galvinoxyl and Nitroxyl Radical Based systems

Stable organic radicals such as galvinoxyls and nitroxyls have been used in building organic magnetic systems by several groups in Japan and in this country. As discussed earlier, McConnell's first proposal for organic magnet was a simple suggestion for the possibility of magnetic interaction in stable organic radical in the solid state by the interaction of negative spin density induced by spin polarization between radical centers in alternant hydrocarbons. He did not propose or explain in detail "how or why" it is possible to build such a system. Galvinoxyl radical is a stable radical that many experts in the field pursued including Awaga, Kinoshita, and Mukai in Japan and Miller in this country.

4.3.1. Galvinoxyl Radicals

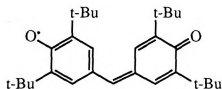
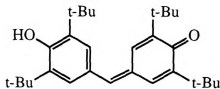
Galvinoxyl, (4-[[3,5-bis(1,1-dimethylethyl)-4-oxo-2,5-cyclohexadien-1-ylidene]methyl]-2,6-bis(1,1-di-methyl)phenoxy] **24**, is ferromagnetic by itself. Awaga and Kinoshita reported evidence for ferromagnetic intermolecular interaction in crystalline galvinoxyl and proved that this interaction extends one-dimensionally with an exchange constant J of about 5 cm^{-1} . The condition of the ferromagnetic couplings have been discussed in the context of spin-unrestricted INDO calculations.⁹⁰

O₂

t-Bu

The calculation
at room tem
hydrogen ato
allows them
explained the
from charge
and β -spin on
(NHOMO) an
suggested tha
stabilized rela
In order to o
transfer conf
interacting o
which the fer
that the ferro
orbital (SO
intramolecula

Awaga
measuremen
measurements
it was found

**24****33**

The calculation was based on the molecular structure determined by X-ray at room temperature, except that all the *t*-butyl groups are replaced by hydrogen atoms.⁹¹ The nearly planar molecular structure of Galvinoxyl allows them to separate the π -type and the σ -type orbitals and they explained the observed ferromagnetism by a dimeric interaction derived from charge transfer between radicals. The large splittings between the α - and β -spin orbitals in the non bonding highest occupied molecular orbital (NHOMO) and non bonding lowest unoccupied molecular orbital (NLUMO) suggested that the energies of triplet charge transfer configurations are well stabilized relative to those of singlet ones by spin polarizations.

In order to obtain the magnitudes of the transfer integrals for the charge transfer configurations, the intermolecular overlap integrals between the interacting orbitals were calculated based on one-dimensional stacks, in which the ferromagnetic interactions were found to work. They concluded that the ferromagnetic interactions result from singly occupied molecular orbital (SOMO) -NHOMO and SOMO-NLUMO interactions and intramolecular spin polarizations.

Awaga and Kinoshita reported another interesting magnetic measurements which was later confirmed by Miller. From the measurements of the temperature dependence of the magnetic susceptibility, it was found that the ferromagnetic intermolecular interactions, which are

lost below 8
maintained d
hydrogalvino
in the high te
offering mec
measured the
transitions in

For the purpo
SQUID at M
measurement
Chemical Co.
any problem c
hydrogalvino
and a Weiss c
to 15.7 K fo
Miller gave an

"No apparent
of these stru
structure obt
structure of
disintegration
suggests a ma
of the crystal;

lost below 85K in pure galvinoxyl because of a phase transition, are maintained down to 2K in mixed crystals of 6:1 and 4:1 galvinoxyl and hydrogalvinoxyl **33**. They reported Weiss constants of 19, 13, 14, and 13K in the high temperature region in 19:1, 9:1, 6:1, and 4:1 mixtures without offering mechanisms for the observed magnetic behaviors. They also measured the temperature dependence of the EPR intensities of half-field transitions in those mixed crystals.

For the purpose of comparing magnetic data obtained by others with our SQUID at Michigan State University, I ran the temperature dependence measurements on a polycrystalline sample of galvinoxyl from Aldrich Chemical Co. at 200G and 500G and found a Weiss constant of 19K without any problem of phase transitions, presumably due to contamination of some hydrogalvinoxyl in the crystals. Miller reported a value for J of 8.7 cm^{-1} , and a Weiss constant θ of 15.2K for pure galvinoxyl; he also found $\theta = 12.6$ to 15.7 K for a mixture of crystals in proportion $x:1-x$ ($x=0.85\pm0.02$). Miller gave an interesting conclusion in his paper as follows:⁹²

"No apparent change in the crystal structure was detected when the results of these structures are compared to each other and the earlier reported structure obtained at room temperature. Attempts to obtain the crystal structure of hydrogalvinoxyl-free sample were unsuccessful due to disintegration of the crystals as the samples were cooled through T_{max} . This suggests a major transformation occurs which leads to the loss of integrity of the crystal; thus, this mysterious phase transition remains unsolved."

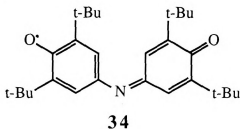
One m
analogue nitr
butyl-4-oxoc
contrast to gal
antiferromagn
of a phase tra

It has been su
are paired up
triplet separa
was observed
structure of E
instead, it has
galvinoxyl an

4.3.2. Nitr

A
extensively a
nitronyl nitro
because they
interaction th
considered as

One more related magnetic measurement is that of the structural analogue nitrogen substituted galvinoxyl radical, 2,6-di-*t*-butyl-4-(3,5-di-*t*-butyl-4-oxocyclohexa-2,5-dienylidene amino) phenoxyl (BIP) **34**.⁹³ In contrast to galvinoxyl, the magnetic susceptibility of the BIP radical exhibits antiferromagnetic behavior with a broad maximum at 54K and no evidence of a phase transition.



It has been suggested that the unpaired electrons on neighboring molecules are paired up by exchange interactions to form dimers and the singlet-triplet separation was estimated to be 60.5 cm^{-1} . No half-field transition was observed over the accessible temperature range. The single crystal structure of BIP was reported recently not to be coplanar like galvinoxyl; instead, it has significant twist between the two aromatic rings so that the galvinoxyl and amino galvinoxyl are not crystallographically isostructural.

4.3.2. Nitroxyl Radicals

As mentioned earlier, nitronyl nitroxides have been used extensively as precursors for molecular magnets. Nitroxides, especially nitronyl nitroxides are good candidates as molecular magnet precursors because they show significant spin polarization and provide possibilities for interaction through conjugation.⁹⁴ The Nitroxyl functionality may be considered as an odd electron bonded system with a σ -bond and a 3-electron

π -bond between

small dipole moment

R

For organic

convenient, a

nitrogen atom

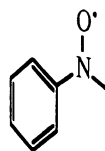
the odd electron

the nitrogen

electron arrangement

effects which

part in preventing



For this reaction

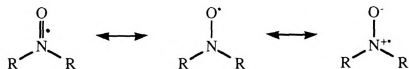
unpaired electron

while others

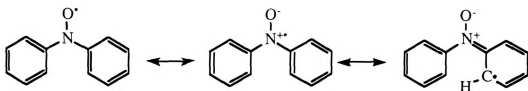
believed to be

20% on the oxygen

π -bond between nitrogen and oxygen. Such a structure is supported by the small dipole moment, the bond length, and the infrared spectrum.⁹⁵



For organic purposes the resonance hybrid representation is most convenient, and nitroxides with aryl or conjugated groups attached to the nitrogen atom are best described by a series of resonance forms in which the odd electron is delocalized over the conjugated system as well as over the nitrogen and oxygen atoms. An inherent stability comes from an electron arrangement around the nitrogen and oxygen atoms, and steric effects which arise from the groups attached to the nitrogen atom play little part in preventing dimerization.



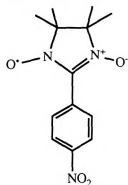
For this reason, there is a controversy concerning the exact amount of unpaired electron density on nitrogen or oxygen. Some claim $\rho_{\text{N}} \sim 0.3$, while others claim $\rho_{\text{N}} \sim 0.9$.⁹⁶ In the case of TEMPO the electron is believed to be delocalized approximately 80% on the nitrogen atom and 20% on the oxygen atom.

Awaga
dependence of
nitrophenyl)-
35 in several

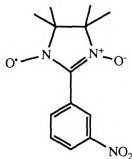
The temperature
the Curie-Weiss
and Weiss constants
respectively.
more rapid
presence of
shown that
temperature
antiferromagnetic

The radical
interesting
 N^+ and O^-
using an M
dominated by

Awaga and Kinoshita reported the temperature dependence and field dependence of the magnetic susceptibility of the organic free radical, 2-(4-nitrophenyl)-4,4,5,5-tetramethyl-4,4-dihydro-1H-imidazolyl-1-oxy 3-oxide **35** in several crystalline phases.



para-NITNPh

35

meta-NITNPh

The temperature dependence of the susceptibility of **32** was found to follow the Curie-Weiss law over a temperature range of 2 to 250K, and the Curie and Weiss constants are determined to be $C=0.375$ emuK/mol and 0.9K, respectively. The magnetization curves of **35** at 2, 2.9, and 4.5K exhibit a more rapid saturation than that of a $S=1/2$ spin entity, which supports the presence of ferromagnetic intermolecular interaction. Furthermore, it was shown that magnetization comes to saturation more rapidly as the temperature decreases. The structural isomer, meta nitroxide exhibits antiferromagnetic intermolecular interactions.

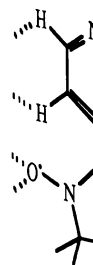
The radical **35** has several crystal phases; the best characterized and most interesting phase was found to be the two-dimensional network linked by N^+ and O^- reported by Awaga. MO calculations have been carried out using an MNDO RHF-doublet method and they suggest a mechanism dominated by the Coulombic attractions. The results of the calculation also

indicated that
side of the n
ring, wherea
nitrophenyl r

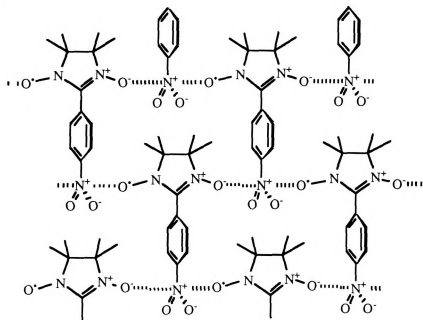
· · O

O

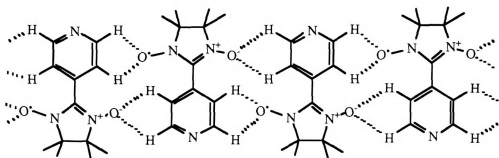
They suggest
much smaller
NLUMO at t
interactions
coupling. Th
to the SOMO



indicated that the unpaired electron occupying the SOMO is localized on the side of the nitronyl nitroxide and has little population in the nitrophenyl ring, whereas the NHOMO and NLUMO are distributed mainly in the nitrophenyl ring.



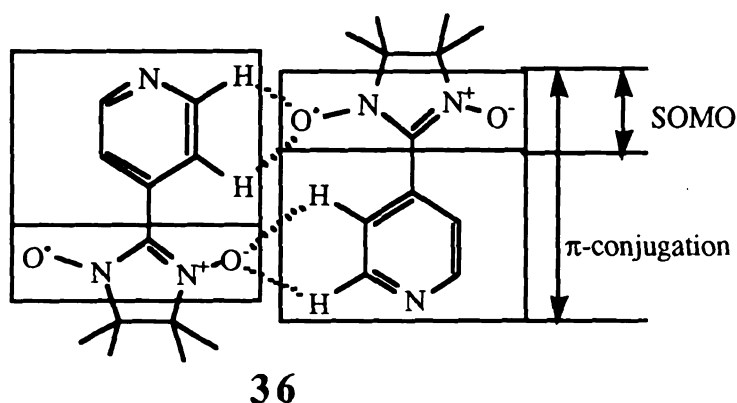
They suggested that the intermolecular overlap between SOMOs could be much smaller than those between SOMO-NHOMO and/or between SOMO-NLUMO at the contact points in the 2-D network and the intermolecular interactions between SOMOs would mainly result in antiferromagnetic coupling. Thus, the ferromagnetic interactions of NITNPh were attributed to the SOMO-NHOMO and/or SOMO-NLUMO interactions.



The SO
have been eva
radical shown
shown to be
"hydrogen-bo
between the S
frontier orbita

The ferroma
nitroxide (3-
Weiss constan
relationship w
to the case of
diagram were
though they d

The SOMO-NHOMO and/or SOMO-NLUMO interaction arguments have been evaluated again by Awaga in the para-pyridyl nitronyl nitroxide radical shown above. The para-pyridyl nitronyl nitroxide **36** has been shown to be a ferromagnetic linear chain with $J/k=0.27$ K through "hydrogen-bonding" interactions. There is little overlap in this radical between the SOMOs, while the overlaps between the SOMO and the other frontier orbitals are rather large.

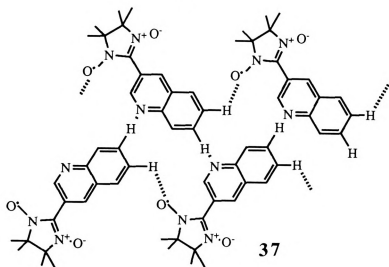


The ferromagnetic intermolecular interaction in 3-quinolyl nitronyl nitroxide (3-QNNN) **37** has been reported by Kinoshita.⁹⁷ The reported Weiss constant was 0.27K and the crystal structure was described and the relationship with the intermolecular interaction is discussed as being similar to the case of radical **36**. The main interactions according to their packing diagram were again through hydrogen bond between the radicals, even though they did not take account of the hydrogen bond explicitly.

4.4. Altern

Advanc
allowed the s
past 30 years
understood in
basis of Hun
themselves i
different spa
two non bon
the ground st
HOMO-LUM
electrons in t
singlet will b

The questio
degenerate p



37

4.4. Alternant Hydrocarbon Based Polyradicals

Advances in the observation of transient open-shell species have allowed the study of numerous types of π -conjugated diradicals over the past 30 years. Many EPR spectra of π -conjugated diradicals have been understood in terms of Hund's rule. Electron repulsion is the underlying basis of Hund's rule. Two non-bonding electrons will prefer to distribute themselves in different degenerate orbitals, since they will then occupy different spatial regions and minimize their electrostatic repulsion. If the two non bonding orbitals are split by a small amount, the triplet can still be the ground state because of its minimal electron repulsion. However, if the HOMO-LUMO splitting is large, the energy benefit of placing both electrons in the HOMO will outweigh the electron repulsion factor, and the singlet will be the ground state.

The question remains whether all diradicals with two electrons in a degenerate pair of NBMOs would prefer triplet high spin state. Berson

proposed that
criterion. Me
triplet ground

There are s
polyradical s
(EHMO) trea
questionable
there is no
molecule.

In 1936, H
coefficients
junction link
at the HMO
of Hund's ru

In 1977 and
the concept
violate Hund
molecule, th
repulsion tha

The m-Quin
triplet by a
around a be
earlier for S

proposed that having such orbitals is neither a necessary nor a sufficient criterion. Meta-Xylylene and meta-quinomethane have been shown to have triplet ground states even though they lack degeneracy at the HMO level.

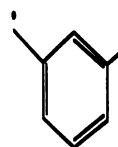
There are several controversies on theoretical treatments in organic polyradical systems including the Extended Hückel Molecular Orbital (EHMO) treatment. Most importantly, the applicability of Hund's rule is questionable for heteroatom substituted alternant hydrocarbons in which there is no symmetry-induced degeneracy of NBMOs and even for a molecule.

In 1936, Hückel pointed out that some hydrocarbons with zero HMO coefficients at the joint (disjoint) do not follow Hund's rule. Since the junction links two sites with zero coefficients, the exchange energy vanishes at the HMO level of approximation, and the normal basis for the application of Hund's rule vanishes with it.

In 1977 and 1978, Borden and Davidson's theoretical studies strengthened the conceptual basis for identifying which π -conjugated molecules might violate Hund's rule. If the NBMOs are confined to separate regions of the molecule, they are said to be disjoint. This property erases the Coulombic repulsion that usually destabilizes the singlet in π -conjugated biradicals.

The *m*-Quinodimethane (*m*-xylylene) biradical has been predicted to be a triplet by all levels of theory and the quinodimethyl biradical topology around a benzene ring (*o*, *m*, or *p*) produces different results as discussed earlier for Schlenk, Thiele, and Chichibabin's hydrocarbons.

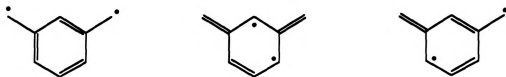
There is no st
degenerate no
MO (HMO) t
only if the
degeneracy ge



Since these an
models can b
meaning that
starred—such
A variety of s
been derived
coupling thro
powerful para

In recent year
been reporte
building bloc
are based on
units when th
of all electron

There is no stable Kekulé structure from meta-Xylylene. There is a pair of degenerate non bonding molecular orbitals (NBMOs) at the level of Hückel MO (HMO) theory. At higher levels of theory, the NBMOs are degenerate only if the system has a threefold symmetry axis, although a near degeneracy generally exists in the absence of such symmetry.



Since these are planar π systems, HMO theory and a variety of other simple models can be applied. Most of the systems are alternant hydrocarbons, meaning that the atoms can be divided into two sets—starred and non starred—such that no two atoms of the same set are connected to each other. A variety of simple rules concerning orbital energies and coefficients have been derived for alternant hydrocarbons. The realization that meta coupling through a benzene ring is always high spin has provided a powerful paradigm for the design of very high spin molecules.

In recent years, a series of organic molecules with spin as high as $S=9$ has been reported, in which meta coupled di-phenyl carbenes provide the building blocks toward ever higher spin states.⁹⁸ These delocalized systems are based on a design which predicts high spin coupling between adjacent units when the contiguous π topology of the molecule precludes the pairing of all electrons into bonds (non-Kekulé structures, Mataga model).⁹⁹

4.4.1. Triple

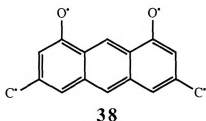
The π -
heteroatoms a
Berson and L
xylylene and
tetra radical
semiempirical

m-Benzoquin
high level of
state about 10
experimental
MNDO-UHF
fixed geomet
and relative e

Lahti a
design of bui
phenylnitrene
 π -conjugated

4.4.1. Triplet Diradicals

The π -topology of organic diradicals and diradicaloids with heteroatoms allows one to construct building blocks for organic magnets. Berson and Lahti reported properties of organic diradicals such as meta-xylylene and its heteroatom diradicaloid analogues **38**; they built the quintet tetra radical shown below and analyzed its electronic structure using semiempirical molecular orbital theory.¹⁰⁰



m-Benzoquinodimethane (meta-xylylene) has been treated at a relatively high level of SCF-MO-CI *ab initio* theory, by which it has a triplet ground state about 10 kcal/mol below the singlet state in qualitative agreement with experimental EPR results.¹⁰¹ Berson and Lahti found the combination of MNDO-UHF and INDO-CISD (semiempirically parameterized methods at fixed geometries) computations to be effective in giving both geometries and relative energies for spin states of diradical and diradicaloid systems.

Lahti and Iwamura independently reported a unique approach to the design of building blocks for molecular magnets through the linkage of two phenylnitrene units by π -conjugated linker groups.^{105,102} These open-shell π -conjugated systems with the general structure of $:N:-Ph-X-Ph:N:$ have

been studied

linkers and co

For 1,1-bis(4

with zero-fiel

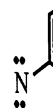
0.0029 cm⁻¹

with zfs param

results suppo

qualitative co

hydrocarbon



Dough

between two

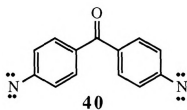
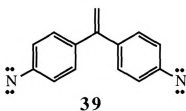
combining

trimethylene

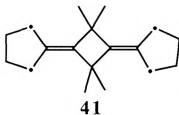
radical **41** by

been studied by variable temperature EPR with various cross-conjugating linkers and connectivity types.

For 1,1-bis(4-nitrenophenyl)ethene **39**, a quintet ground state was found with zero-field splitting (zfs) parameters $|D/hc| = 0.151 \text{ cm}^{-1}$ and $|E/hc| = 0.0029 \text{ cm}^{-1}$. For 4,4'-dinitrenobenzophenone **40**, a quintet ground state with zfs parameters of $|D/hc| = 0.156 \text{ cm}^{-1}$ and $|E/hc| = 0.0046 \text{ cm}^{-1}$. These results support the idea that minor heteroatom substitution does not reverse qualitative connectivity-based exchange coupling effects (extended alternant hydrocarbon model).



Dougherty reported an alternative ferromagnetic coupling mechanism between two triplets to give the higher spin state quintet ($S=2$). By combining derivatives of the classic non-Kekulé diradical, trimethylenemethane (TMM), he was able to build and study the tetra radical **41** by EPR.¹⁰³



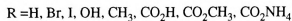
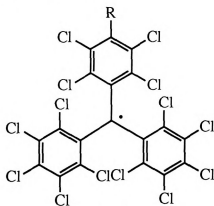
4.4.2. Perc

As mer
Ballester (Bal
called an in
triphenyl me
properties hav
magnetic pro
they provide
according to

For example
interactions i
of acid and
bonding inte
and -I to
intermolecul
acid and este
for -Cl, -Br
functionalize

4.4.2. Perchlorinated Triphenylmethyl Radicals

As mentioned earlier, the perchlorinated triphenyl methyl radical of Ballester (Ballester's radical) is a very stable organic radical which has been called an inert radical.⁴³ A series of functionalized polychlorinated triphenyl methyl radicals have been synthesized and their magnetic properties have been analyzed.¹⁰⁴ Among the various systems reported, the magnetic properties of monofunctionalized radicals are interesting because they provide a collection of possible dimeric magnetic interactions according to their functional groups.



For example, we can expect to see the effects of hydrogen-bonding interactions in the groups $-CO_2H$, CO_2NH_4 . Also, by comparing the cases of acid and ester, we can estimate the contribution of each hydrogen bonding interaction involved and compare the differences between $-Cl$, $-Br$, and $-I$ to find any trends to follow in determining the possible intermolecular interactions. As expected, there are differences between acid and ester in Weiss constants of 0.9 and $-3.8K$ and 2.1, -3.4 , and $-4.4 K$ for $-Cl$, $-Br$, and $-I$, respectively. The Weiss constant for the CO_2NH_4 functionalized radicals has been reported to be $0K$, in contrast to most of

them being an
without havin
radical has a
metal salts of
phenomena.¹⁰

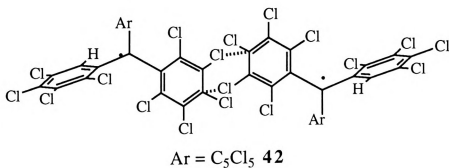
The -2.
studied by X-
has been disc
term of McC
been assigne
crossed inter
pentachloropl



The perchlor
fluorenyl **44**
to have Wei
structural exp

them being antiferromagnetic. This result is unique and difficult to interpret without having the single crystal structure. The hydroxy functionalized radical has a problem of forming quinoidal structures and various alkali metal salts of this radical have been shown to have interesting association phenomena.¹⁰⁵

The -2H substituted perchloro triphenylmethyl radical **42** has been studied by X-ray analysis and its observed antiferromagnetic susceptibility has been discussed and related to molecular packing and spin densities in term of McConnell's theory.¹⁰⁶ The interaction sites between radicals have been assigned to be the two para-carbons and two meta-chlorines through a crossed interaction pattern with closest distances of 3.64 Å between two pentachlorophenyl groups.



The perchloro-9-phenylfluorenyl **43** and dodecachloro-3-methoxy-9-phenylfluorenyl **44** radicals shown below have been studied by EPR and reported to have Weiss constants θ of -14.5 and -17.5K, respectively, without any structural explanation of the magnetic interactions.

Cl-

C

Triple

reported by V

strategies. 1

meta-xylene

stable solids

and enantio

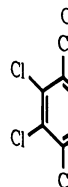
reported zfs

meso and 1D

suggest sign

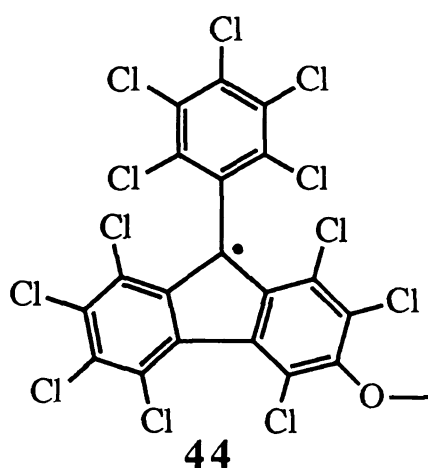
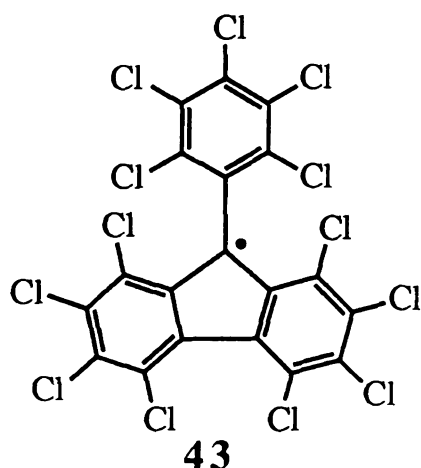
although it is

C

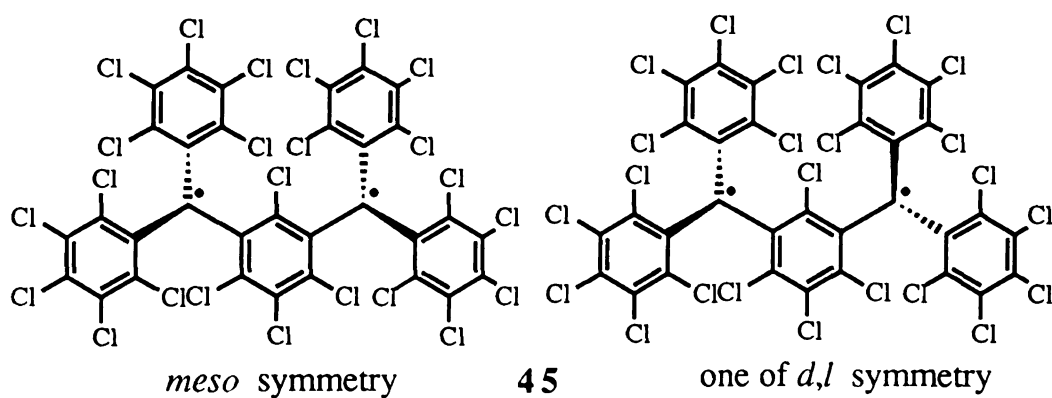


Magnetic s

diastereoisom



Triplet biradical homologues of Ballester's radical have been reported by Veciana and Riera using π -conjugated meta-xylylene diradical strategies.¹⁰⁷ The biradical **45** and its corresponding monoradical of meta-xylylene diradical derivatives have been synthesized and isolated as stable solids at ambient condition. The biradical forms a mixture of *meso* and enantiomeric *dl* forms which can be differentiated by EPR. The reported zfs parameters were $|D/hc| = 0.0152$ and $|E/hc| = 0.0051$ cm⁻¹ for *meso* and $|D/hc| = 0.0085$ and $|E/hc| \leq 0.003$ cm⁻¹ for the *dl* isomer which suggest significantly stronger coupling in the *meso* form than in the *dl*, although it is not clear why this should be true.



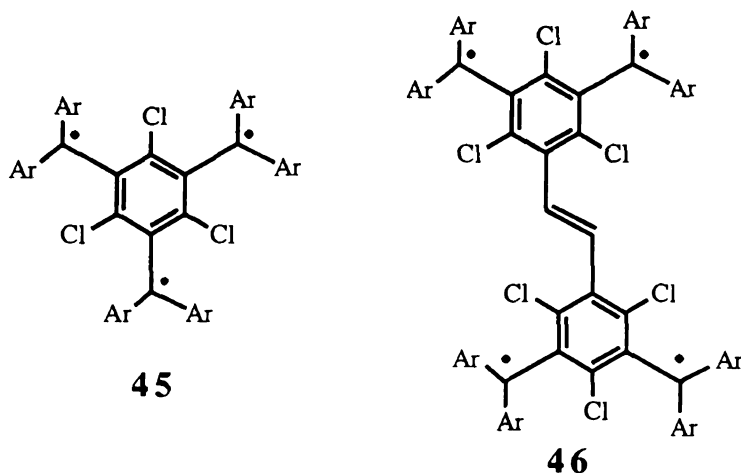
Magnetic susceptibility and magnetization measurements of the diastereoisomers in solid state show "quasi-ideal $S = 1$ paramagnetic

behavior" do
multiplicities
of the lack o
interactions.
and 46) show
biradical.

Althou
spin organi
dimensional
mechanism
radical syste
understandin
based on t
Ovchinnikov

A seri
high spin m
radical, he e
methyl rad
polyradical.

behavior" down to 4.2K. They suggest that the prediction of ground state multiplicities in any non-disjoint alternant hydrocarbon are true regardless of the lack of planarity and changes in the symmetries in intramolecular interactions. They extended these strategies to the tri- and tetra radicals (**45** and **46**) shown below, with results consistent with the findings for the biradical.



Although the above approach is successful for construction of high spin organic molecules, it is inappropriate for assembly of three dimensional structures which would show ferromagnetism unless there is a mechanism for intermolecular interaction. Most studies of reported poly radical systems have concentrated on building molecules themselves without understanding the nature of their intermolecular interactions. They are based on the proposed organic magnet mechanism of Mataga and Ovchinnikov which were discussed earlier.

A series of polyradicals has been assembled by Rajca¹⁰⁸ in building high spin molecules using similar strategies. Instead of using Ballester's radical, he employs homologous derivatives of t-butyl substituted triphenyl methyl radicals. Although there is little structural data on these polyradicals, the crystal structure and magnetic property of the related

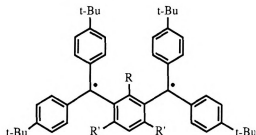
tris(3,5-di-t-bu
expected, tris(
intermolecular
with $S=1/2$.

Rajca was ab
above diradi
dependences
measurement
R=i-Pro) acc
without show
Bleaney-Bov
dimeric inte
polyradicals

4.4.3. Pol

Iwami
is controlle
incorporate

tris(3,5-di-*t*-butylphenyl)methyl radical has been reported by Kahr.¹⁰⁹ As expected, tris(3,5-di-*t*-butylphenyl)methyl radical does not show significant intermolecular magnetic interaction and behaves as a simple paramagnet with $S=1/2$.



R = H, Me
R' = Me, *i*-Pro

47

Rajca was able to correlate the sign of the exchange interactions in the above diradicals **47** in the solid state. He reported temperature and field dependences of these diradicals using SQUID measurements. The measurements showed anti-ferro or ferromagnetic interactions (when $R=H$, $R'=i\text{-Pro}$) according to interactions which he claimed to be intermolecular without showing the mechanism. He was unsuccessful in applying the Bleaney-Bowers equation to their data which means that it is not a simple dimeric interaction. More recently, he reported an extension of these polyradicals to hepta- and decaradicals with $S=7/2$ and $S=5$, respectively.

4.4.3. Polyphenyl Carbenes

Iwamura reported a novel dicarbene system in which spin multiplicity is controlled by the overlap modes of spin-distributed benzene rings incorporated in the rigid [2,2] paracyclophane framework.¹¹⁰ According

to McConnell
interaction be
product of sp
negative in si
organic radica

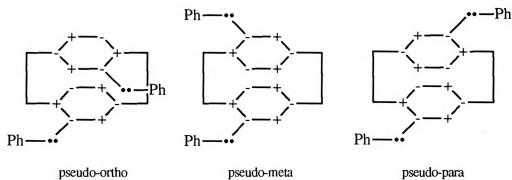


pse

Among three
the pseudo-c
spin density
spin distribu
cyclophanes,
of the dicarb
the π -electro

Iwamura and
series of hig
polycarbene
known (dete

to McConnell's theory on intermolecular magnetic interactions, exchange interaction between two aromatic radicals can be ferromagnetic when the product of spin densities at two interacting sites on different molecules is negative in sign, since the exchange integral is usually negative between organic radicals at the van der Waals contact distance .



Among three isomers of bis(phenylmethylene)[2.2]para-cyclophanes only the pseudo-ortho and pseudo-para isomers are expected to have negative spin density at each interacting site between the two benzene rings and the spin distribution is expected to result in quintet ground states for these cyclophanes, as confirmed by EPR. These differences in spin multiplicity of the dicarbenes are the first experimental examples of overlap control of the π -electron magnetic interactions in layered aromatic radicals.

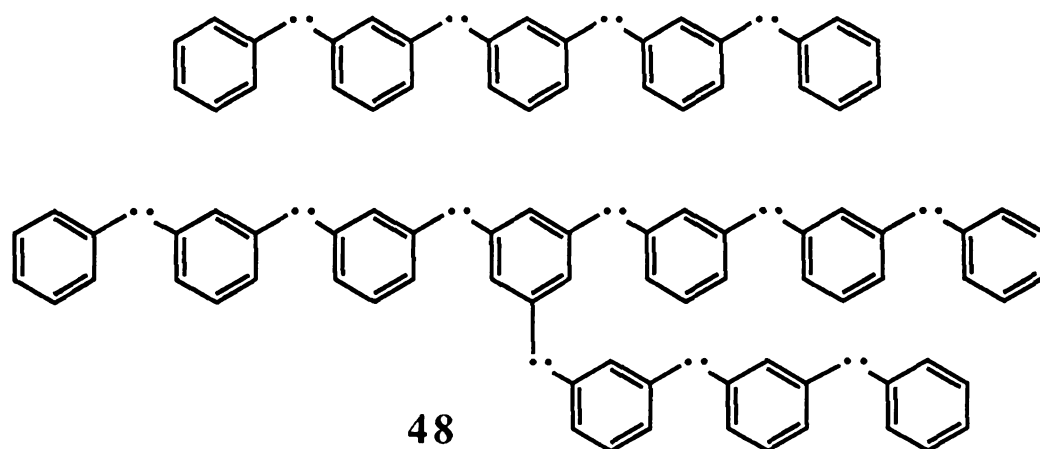
Iwamura and Itoh extended the meta-xylylene π -conjugation topology into a series of high spin poly carbenes of $S=4$ and Iwamura reported 2-D extended polycarbenes **48** of $S=9$ which is highest spin molecular system currently known (determined by saturation magnetization experiments).¹¹¹



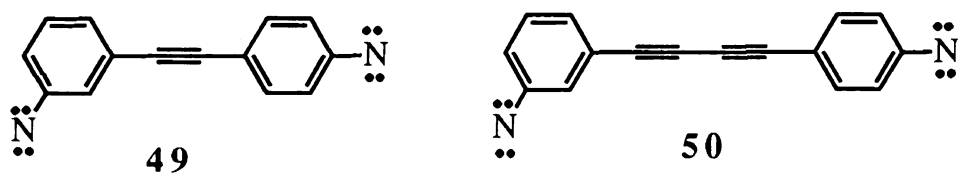
Iwamura also
the expected
obeyed a Cur



It is clear th
from alterna
intramolecul
available. 11



Iwamura also reported the dinitrenes (**49** and **50**) shown below which show the expected high spin multiplicities (quintet) and magnetic behaviors which obeyed a Curie law in the temperature range 12-85 K.¹¹²



It is clear that successful strategies to design magnetic molecular materials from alternate hydrocarbons will require a far more precise knowledge of intramolecular and intermolecular exchange interactions than is presently available.¹¹³

5. Molecular

As we
present in the
different from
radicals surr
depend on th
radicals throu
either a spin
said to be a
interactions a
involved (3-4

The nature a
by carefully
and by the s
radicals and
be utilized f

The design
in a geome
unit not onl
coupler. A
ferromagne
based on th
system.

5. Molecular Magnets by Macromolecular Chemistry

As we have seen in many examples, when two organic radicals are present in the same molecular entity, the magnetic properties can be quite different from the sum of the magnetic properties of two such mono radicals surrounded by their nearest neighbors. These new properties depend on the nature and the magnitude of the interaction between the radicals through the coupling unit. The molecular state of lowest energy is either a spin singlet or a spin triplet. In the former case, the interaction is said to be antiferromagnetic, in the latter case ferromagnetic. These interactions are often termed superexchange because of the large distances involved (3-5 Å) between the radical centers.¹¹⁴

The nature and the order of magnitude of the interaction can be engineered by carefully choosing the interacting organic radicals and the coupling unit and by the symmetry and the delocalization of the orbitals centered on the radicals and occupied by the unpaired electrons. The same strategy could be utilized for designing molecular ferromagnets.

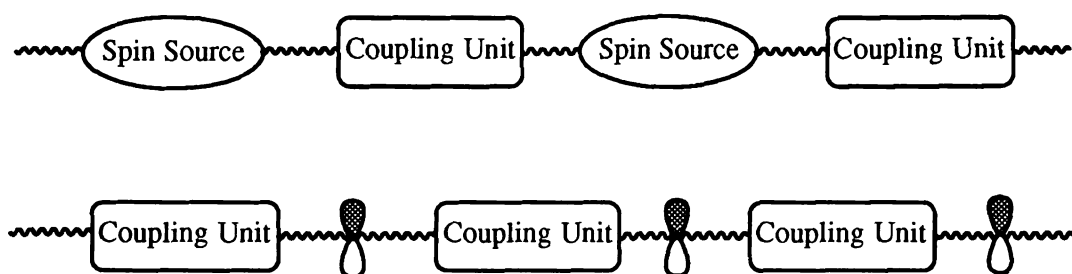
The design of extended magnetic structures requires the alignment of spins in a geometrically well defined environment, where the proper coupling unit not only plays a role as a physical linkage but also as a ferromagnetic coupler. As noted by Dougherty, the design of an extended molecular ferromagnet can be naively envisioned by the following simple diagram based on the spin sources and the magnetic coupling units in a linear chain system.

Spin

Coupling

There are several
system: The
characterized
The coupling
themselves, s
spin sources
to form a li
molecule inc

We have sel
and metal ca
of building
through spa
organic di
interactions
induce throu
crown ether
these dimer
where the
macromolec



There are several points that we should address in building such a magnetic system: The spin sources should be stable and magnetically well characterized, and they might form a linear chain with the coupling units. The coupling units, which could be diamagnetic or paramagnetic themselves, should be able to couple spin sources ferromagnetically. The spin sources could be any stable organic radical with proper functionalities to form a linear chain, and the coupling units could be any atom or molecule including stable organic radical and poly radical.

We have selected tris(2,6-dimethoxyphenyl)methyl radical **1** as a spin base and metal cations as the magnetic coupling unit. I will introduce our design of building organic magnets followed by examples of through bond and through space magnetic interactions in organic radicals: examples of organic diradicals showing long-range (superexchange) magnetic interactions through σ -bonds; examples of stable organic radicals used to induce through-space magnetic interactions by ion-binding of spin labeled crown ethers. Our design of molecular magnets will be given by extending these dimeric interactions in organic radicals into a linear chain and further where the geometrical control and magnetic coupling are achieved by macromolecular chemistry.

5.1. Long-

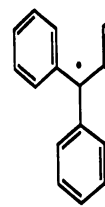
As me
the first org
were studied
been examin
bond and th
suggested in
ferro- or an
through-bon
general phe
transfer pro
through-spa
magnetic in
very useful

In 19
 π -conjugate
below,¹¹⁵
system sho
diradicals li
orbital on t
for the oxy
was greater
1, 2, 3, 4) .

5.1. Long-range Magnetic Interactions in Organic Radicals

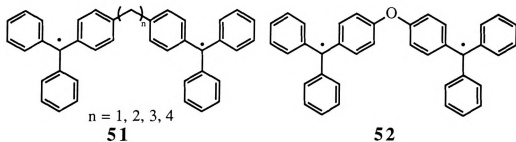
As mentioned earlier, Chichibabin and Schlenk hydrocarbons were the first organic diradicals in which intramolecular magnetic interactions were studied. Since then, numerous examples of polyradical systems have been examined by many renowned chemists. The orbital nature of through-bond and through-space interactions for magnetic coupling has been suggested initially by Hoffmann and many examples of diradicals showing ferro- or antiferro-magnetic interactions have been reported. Still, the through-bond and through-space magnetic interactions are not accepted as general phenomena in organic radicals even though electron and energy transfer processes are often analyzed in terms of through-bond and through-space interactions. It is my intention to show here that long-range magnetic interactions in organic radicals are not only possible but can be very useful tools in building molecular magnets.

In 1956, Sloan and Vaughan reported stable organic biradicals with π -conjugated and nonconjugated magnetic coupling linkers such as shown below.¹¹⁵ They found that the unpaired electrons in the oxygen-linked system shown below are less insulated from one another than in the diradicals linked by simple aliphatic chains because of the existence of a π -orbital on the oxygen. To their surprise, they obtained an EPR spectrum for the oxygen linked diradical **52** with a g -value of 2.0031 ± 0.0004 which was greater than the 2.0025 ± 0.0004 for the aliphatic linked diradicals ($n=1, 2, 3, 4$) **51**.



The EPR spectrum shows
 the relative intensities of the
 coupling constants. The lines
 interact with the magnetic field
 situations: The spectrum shows
 lines with separation J . If
 J is much smaller than the
 if each electron has a different
 constant) is the same. The
 separation of the lines is
 highly sensitive to the
 (hyperfine coupling).

In general, the spectrum is
 or held rigid. The spectrum
 three lines are observed. The
 nor rigid. The spectrum shows
 dinitroxides.

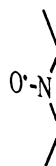


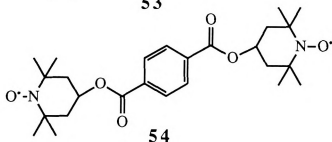
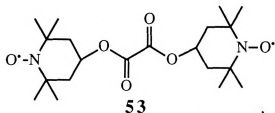
The EPR spectrum obtained from a biradical in solution depends largely on the relative magnitudes of the exchange interaction and the hyperfine coupling constants. For a bisnitroxyl in which the two unpaired electrons interact with two equivalent nitrogen atoms, there are three possible situations: The biradical may behave like two mono radicals and show three lines with separation of a (hyperfine constant) when the exchange coupling J is much smaller than the hyperfine coupling. The biradical may behave as if each electron spends half of its time on each nitrogen when a (hyperfine constant) is much smaller than J and five line spectra are then obtained with separation of a (hyperfine constant)/2. More complicated spectra which are highly sensitive to solvent and temperature are obtained when J and a (hyperfine constant) are about the same in magnitude.

In general, when the two nitroxide groups in nitroxyl radicals are far apart or held rigidly apart then the exchange interaction tends to be small and three lines are observed, while if the linking group is neither especially long nor rigid five lines or more appear in the spectrum. There are several dinitroxides which belong to latter category.¹¹⁶

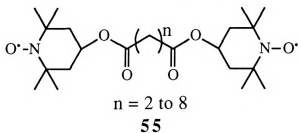
The EPR sp
150 °C. Sim
of biradicals
from interra

The biradic
7.4 gauss,
correspondi

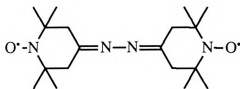
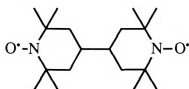




The EPR spectrum of diradicals **53** and **54** show five line spectra at 140-150 °C. Similarly, as the number of methylene groups increase in the series of biradicals **55** the intensities of the additional spectral lines which come from interradsical interactions in the corresponding spectra decrease.

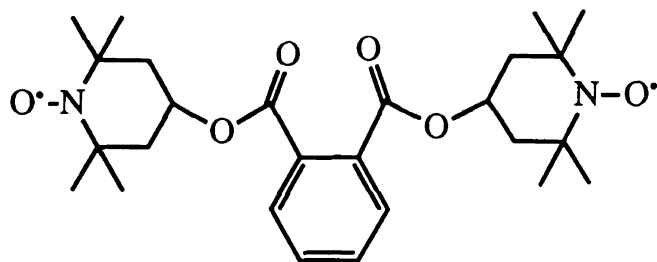


The biradicals shown below all gave spectra with five lines in which $a_N = 7.4$ gauss, which is half of that in an analogous mononitroxide, corresponding to the situation of $J \gg a$.

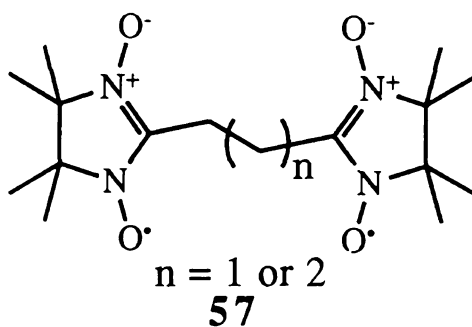
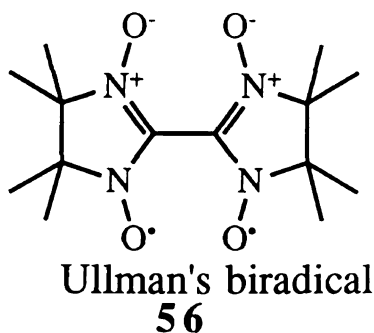


Ullman
geometrical
Bulk magnet
which meas
reference pe
By compari
showed "75
Ullman clai
spins.¹¹⁸

Very recent
by Rey.
measureme
Ullman's b
l via the B.
Lahti repo
polyradica



Ullman reported a conjugated nitronyl-nitroxide biradical **56** with geometrical evidence which showed particularly strong dipolar interactions. Bulk magnetic susceptibility measurements by Evans' NMR method¹¹⁷ which measures the amount of paramagnetic shifts of NMR peaks to a reference peak such as TMS gave 49 % triplet character for the radical **56**. By comparison, the unconjugated trimethylene-bis-nitronyl nitroxide **57** showed "75% triplet character" with a half field transition spectrum. Ullman claimed that the value correspond to a weakly interacting free spins.¹¹⁸



Very recently Ullman's biradical **56** and its derivatives have been studied by Rey. He reported X-ray structures and magnetic susceptibility measurements showing antiferromagnetic intramolecular interaction for the Ullman's biradical. The singlet-triplet energy gap estimated was as -311 cm^{-1} via the Bleaney-Bowers equation.

Lahti reported computational modeling studies of various π -conjugated polyradicals using the AM1 semiempirical molecular orbital method with

configuration
alternant hydrocarbons
polyradical mechanism
variety of compounds
groups as in
Nitrene. 119

5.2. Thro Complexes

A series of complexes
constructed from
nitroxyl, and
radicals as p
use of spin
summarize
complexes
interactions
a complex
binding pr
complex w
below. If th
centers, the
specific al
ferromagne

configuration interactions which give theoretical basis for the heteroatom alternant hydrocarbons. He has been interested in synthesis of π -conjugated polyradical model systems based upon coupling of phenoxyl radicals by a variety of connecting spacer groups, such as heteroatoms and olefinic spacer groups as in the general model of Phenoxy-X-Phenoxy and Nitrene-X-Nitrene.¹¹⁹

5.2. Through Space Magnetic Interactions in Organic Radical Complexes

A series of spin labeled crown ethers (15-crown-5) have been constructed by Mukai using stable organic radicals such as galvinoxyl, nitroxyl, and verdazyl (**58**, **59**, **60**, and **61**) with the goal of using these radicals as probes for biological systems.¹²⁰ There are good reviews on the use of spin labeled organic molecules for a biological probes and I will summarize mainly the systems with magnetic interactions. The alkali metal complexes of these radical crown ethers show interesting magnetic interactions in solution EPR.¹²¹ When the spin labeled crown ethers form a complex with alkali metal salts in solution according to the general ion-binding properties of crown ethers, 15-crown-5 can only form a 1:1 complex with sodium salts but a 2:1 complex with potassium salts; as shown below. If there are significant magnetic interactions between the two radical centers, the EPR spectra of 2:1 complexes would reflect the interactions; specifically, a triplet spectrum would result when they are ferromagnetically coupled.

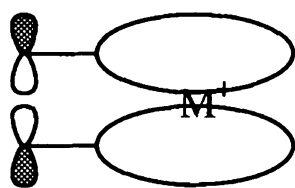


Triplet spec
galvinoxyl
observed in
system which
instead of p
characterist
verdazyl ra
triplet spec
complexes
systems wi
potential ic
great exten

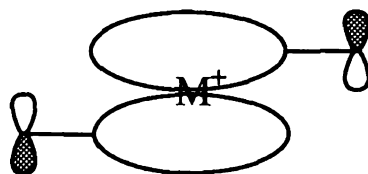
$\text{O}^{\bullet}-\text{N}$

t-l

t-

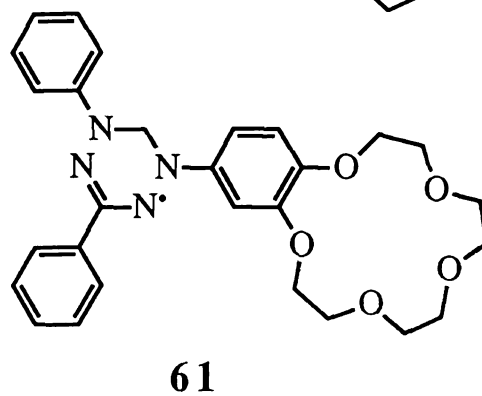
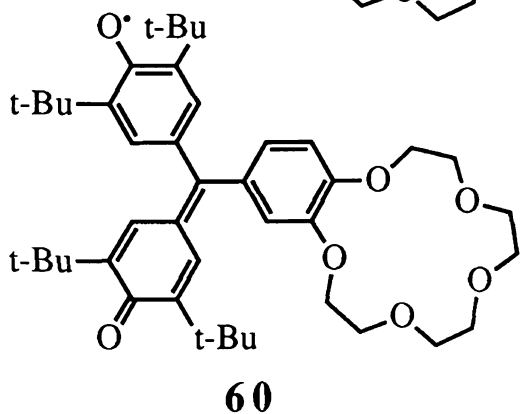
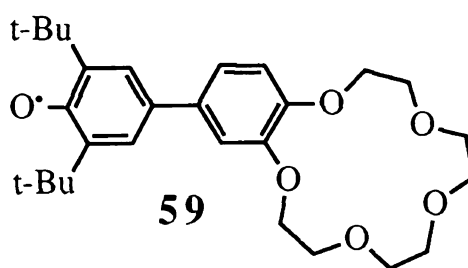
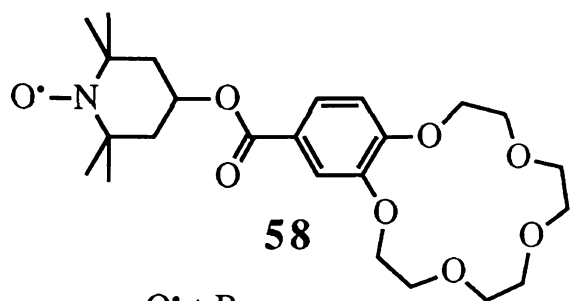


Syn



Anti

Triplet spectra have been reported for 2:1 complexes of nitroxyl **58**, galvinoxyl **59**, and phenoxyl radicals **60**. Half field transitions were observed in all complexes except for the verdazyl labeled 15-crown-5 system which was reported as triplet coupled when sodium salts were used instead of potassium salts which is in contrast to the general ion-binding characteristics of 15-crown-5. The question remains whether the triphenyl verdazyl radical **61** itself forms a 2:1 complex with sodium cation to give a triplet spectrum. Furthermore, there is the possibility of forming complexes with different conformations (syn or anti) even in the above systems with triplet EPR spectra. Finally, the role of the oxy radicals as potential ion-binding sites for alkali metals has not been explored to any great extent.



5.3. Design

The th
traditionally
it has been r
ions in bimetal
interaction,
overlap inte
orbitals.

More recent
such analysis
species, with
earlier. In t
superexchan
were made
metal cente
or π -electro
link between
energies be
extended H
bimetallic c
two-electro
of the calc
observe in

5.3. Design of Molecular Magnets by Ion-Binding

The theoretical interpretation of superexchange interactions has traditionally been based on ideas developed for infinite solid lattices. Since it has been realized empirically that the bridging atoms between the metal ions in bimetallic systems determine the sign and magnitude of the exchange interaction, these qualitative treatments focus on the various types of overlap interactions between the ligand atomic orbitals and the metal d orbitals.

More recently there have been theoretical treatments which seek to extend such analyses to the cases involving molecular, rather than atomic bridging species, with special interest in molecular bimetallic complexes as discussed earlier. In this context a broader theoretical framework for the analysis of superexchange interactions has been proposed by Hoffmann.¹²² Attempts were made to show a connection between antiferromagnetically coupled metal centers and the phenomenon of through bond coupling of lone pairs or π -electron systems in organic molecules.¹²³ Hoffmann established the link between antiferromagnetic exchange interactions and the difference in energies between degenerate MO's using the orbital energies obtained from extended Hückel calculations (the simplest all valence-electron model) in bimetallic complexes. Although these calculations do not explicitly include two-electron interactions in organic radicals, he suggested that the behavior of the calculated orbital energies are expected to reflect what one would observe in more sophisticated calculations.

The effect of
exchange in
geometrical
bond angle v
same symme
the metal orb
earlier in bir

Photoelectro
pair and π -
interactions
complexes
affects the
these splitt
metal-ligan
respond to

The effect of the metal-single-atom-ligand-metal bridge angle on the exchange interaction has been studied extensively by Kahn.¹²⁴ Such geometrical considerations lead one to expect a large AF coupling for a 180° bond angle when the metal orbitals can interact with a ligand orbital of the same symmetry, and a ferromagnetic coupling for a 90° bond angle when the metal orbitals are interacting through orthogonal ligand orbitals, as seen earlier in bimetallic systems.

Photoelectron spectroscopy has provided evidence for the splitting of lone pair and π -levels as a consequence of through-space or through-bond interactions such as shown below. The bridging groups in dimetal complexes provide orbitals of a certain symmetry type, and this in turn affects the splitting of the metal orbitals. The interaction which leads to these splittings has a strong conformational dependence (180° angle for metal-ligand-metal) and metal centers coordinated to such systems should respond to the energy splitting by showing sizable magnetic coupling.

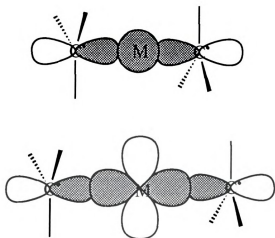


Along the same
possible magnitude
the electron
between organic
substituents

As discussed
organic free
carbon, the
bulk of the
ion binding
can serve
dimethoxy
size between
orientation

The spatial
dictate inter

Along the same line we might expect the systems shown below to have a possible magnetic coupling via bridging diamagnetic metals. Furthermore, the electron density on the metal may affect the degree of interaction between organic radicals as we have seen in reviewing the effect of substituents on bridging ligands in dimetal complexes.



As discussed earlier, tris(2,6-dimethoxyphenyl)methyl **1** is a stable organic free radical and in its D_3 propeller conformation around the central carbon, the unpaired electron is protected from above and below by the bulk of the six methoxy groups.¹²⁵ The principles developed in selective ion binding studies of polyether ligands suggest that these methoxy groups can serve as binding sites for metal cations. Two of the tris(2,6-dimethoxyphenyl)methyl radicals can "sandwich" a cation of appropriate size between them in a distorted octahedral pocket, fixing their relative orientation.

The spatial relationships in such controlled radical aggregation can, in turn, dictate intermolecular electron coupling^{126,127} in "interrupted σ - bonds",

radical pairs
metal cation
would have
orbitals inter
with Kahn's

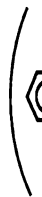
"The orbita
easier to ac
respects the
up-down ty
space intera
weak excep
each other.

We are wo
higher olig
enforced b
might acco
cations to
them para
exclusivel
working m

radical pairs or oligomers in which electron interactions are mediated by metal cations. Extended stacks formed by this complexation mechanism would have at their cores a linear array of one-electron carbon-centered *p*-orbitals interacting through metal ions.¹²⁸ This idea happens to coincide with Kahn's recent suggestions for designing molecular magnets.¹²⁹

"The orbital approaches based on the spin polarization effect might be easier to achieve. This approach is particularly attractive. Indeed, it respects the strong tendency of nature to favor local spin interactions of the up-down type." "To conclude, we would also like to stress that the through-space interactions on which we have focused in this Account are generally weak except when *p* atomic orbitals belonging to adjacent molecules point to each other."

We are working to exert control over electron coupling in radical pairs or higher oligomers designed so that electron interactions are mediated and enforced by metal cations with varying electron densities. Various metals might accomplish this task, from diamagnetic alkali metal and alkaline earth cations to those of transition metals in various oxidation states, some of them paramagnets in their own right. Our efforts have focused almost exclusively on diamagnetic salts. The following scheme illustrates our working model:



M =
X = E

Figure
assoc

Figure
Mol
radi

Fig
oligomers
structures
tripod bin
radical di

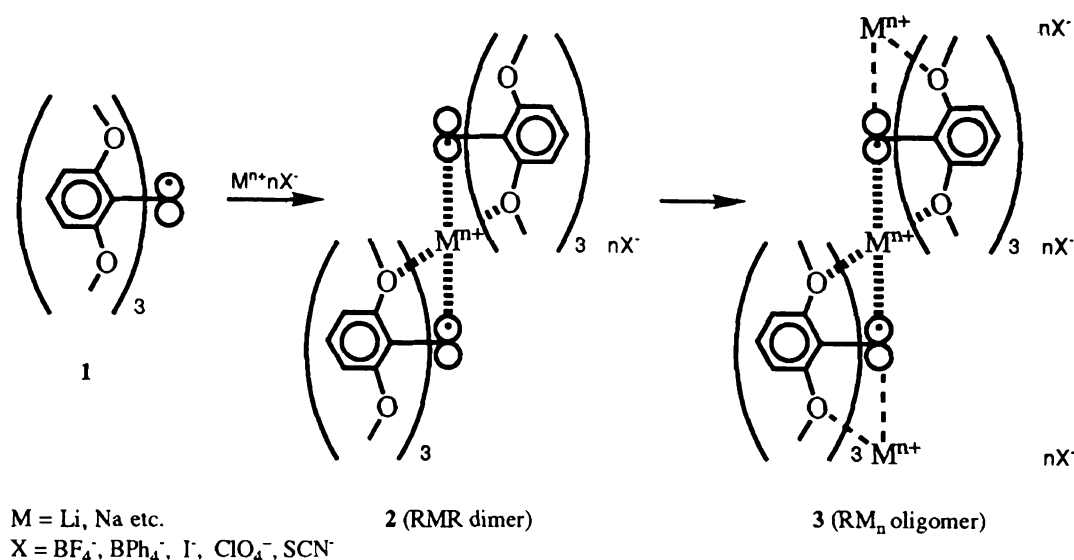


Figure 7. Schematic illustration of the dimeric and oligomeric association of tris(2,6-dimethoxyphenylmethyl) 1 with M^+ ions.

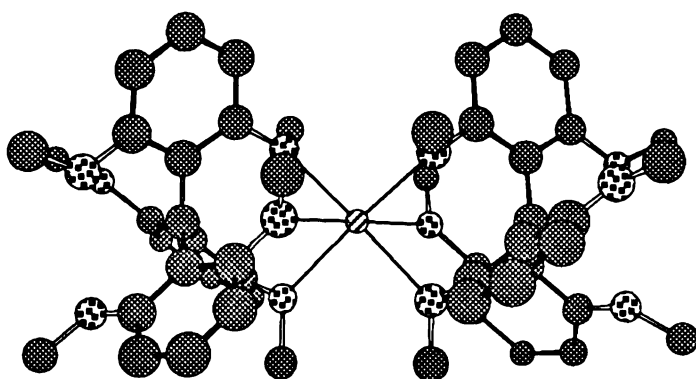


Figure 8. Optimized structure of an RMR dimer 2 calculated by the Molecular Mechanics methods in PCModel. Here the individual radicals adopt a homochiral, staggered conformation.

Figure 7 portrays these "interrupted σ -bonds" in radical pairs 2 or oligomers 3. CPK models, molecular mechanics calculations, and X-ray structures (*vide infra*) of related species support the metal ion-radical ether tripod binding. **Figure 8** displays an illustration of a radical-metal ion-radical dimeric such as 2 as calculated by molecular mechanics.

The a
magnetic p
paramagnet
straightforw
rings and in
paramagnet
stoichiomet
2:1, or 1:2
examples c
molecule c
possibility

Thes
structure c
electrons r
mechanica
electron.
of structu
organic r
applicatio
for devel
favor a p
model sy
gave the

The above strategy targets rationally engineered materials whose magnetic properties result from collective interactions between simple paramagnetic centers. The basic structure of radical **1** allows for a range of straightforward modifications at the *meta* and *para*-positions of the aryl rings and in the group bound to the ether oxygen. By careful assembly of paramagnetic radical ligands, metal ions, counterions, and their respective stoichiometries, a variety of novel complexes may be accessible. Simple 1:1, 2:1, or 1:2 complexes between metal ions and **1** in solution are monomeric examples of the desired types. Ultimately, extended chains in which each molecule of **1** is coordinated to two metal ions and vice versa offer the possibility of a designed molecular solid with unique magnetic properties.

These would be fundamentally new materials, whose composition and structure can be easily varied to vary their bulk properties. With their unpaired electrons residing on light atom centers, organic free radicals are quantum mechanically simple with $S=1/2$ and g values close to that of the free electron. Our work may therefore shed light on the fundamental interplay of structure and magnetic character in materials.¹³⁰ Since the problem of organic magnetism is essentially a problem in electronic structure, application of *ab initio* and semiempirical computational methods is essential for developing a detailed understanding of the electronic interactions that favor a positive exchange integral. Preliminary *ab initio* calculations on a model system $\text{CH}_3\text{Li}^+\text{CH}_3$ have been conducted by Professor Jackson which gave the triplet as a ground state.

The X-ray s
in building
ligand associ
Visible spec
radical 1 w
are thought
interaction
synthesized
We have pu
of our syst
SQUID me
markedly
susceptibi
aniferroma

Detailed r
single crys
structure a
robust ma

I will pres
the struc
properties
terms of
interaction
at introd
conclusio

The X-ray structures of related monomers provided structural information in building ligands for better ion-binding. Determination of the metal-ligand association processes in solutions are evidenced by NMR, EPR, UV-Visible spectrophotometry and cyclic voltammetry. The redox properties of radical **1** which can be adjusted by varying substituents of the aryl rings, are thought to be important in superexchange-mediated magnetic interactions. Thus, various substituted-triarylmethyl radicals were synthesized and studied electrochemically to determine the redox properties. We have pursued SQUID and EPR studies to examine the magnetic behavior of our systems as a function of temperature and magnetic field strength. SQUID measurements on various complexes of triarylmethyl radicals show markedly nonlinear Curie-Weiss behavior and high paramagnetic susceptibilities, while polycrystalline powders of **1**•CdCl₂ shows aniferromagnetic behavior.

Detailed magnetic characterization of well-defined materials, ideally as single crystals, will enhance our understanding of the relationships between structure and odd-electron coupling. We hope these efforts will lead to a robust materials with controllable magnetic properties.

I will present the results and discussion in the following order: i) building a the structural basis for complex formation; ii) studies on electronic properties of substituted radicals; iii) evidence for complex formation in terms of ion-bindings; iv) theoretical basis for pairwise magnetic interactions; v) magnetic behavior of radicals and complexes; vi) attempts at introduce magnetic cross couplers in building extended structures; vii) conclusions and suggestions for future studies.

CHAPTER

1. Struct

Under
is critical to
materials d
properties.
prediction
analyzing
determined
molecular

The effect
triphenyl
estimated
from EPR
carbon. T
at the p
McConne
for all a
gauss, 131

RESULTS AND DISCUSSION

CHAPTER I. Triarylmethyl Radicals

1. Structure of Triarylmethyl Radical

Understanding the structures of organic compounds in the solid state is critical to the engineering of physical properties. The search for organic materials demands understanding of the forces that determine structure and properties. Such understanding should lead to improved methods for the prediction and design of organic crystal structures. The major challenge in analyzing the structure of molecular organic solids is that the structures are determined by summation of the many contributing weak intra and inter molecular forces.

The effects of ortho or meta substituents on the twist angles of the rings in triphenylmethyl radicals, and therefore on their stability, have been usually estimated by comparison of the experimental hyperfine coupling constants from EPR spectra with theoretically calculated spin densities on para carbon. The comparison can be achieved by the calculation of spin density at the para carbon from the hyperfine coupling constants using McConnell's equation, where Q is a factor that is approximately constant for all aromatic hydrocarbons and has an empirical value of -22.5 gauss.¹³¹

$$a_i = Q \rho_i$$

The twist an
between the
where β is
aromatic rin
rings and t
densities an
from hyper
only ^1H hy

A systema
electronic
X-ray stru
while crys
ions have
of the ch
compared
by Veciar

To
tris(2,6-d
frustrate
 O_2 to y
crystal g
structura
diffracti
structura

The twist angle is introduced by using $\beta \cos \theta$ for the resonance integral between the central carbon atom and the adjacent carbon atom in each ring, where β is the resonance integral between neighboring carbon atoms in aromatic ring and θ is the angle between the plane of one of the phenyl rings and the reference plane of the central carbon and its bonds. Spin densities are then obtained as functions of θ . But, these calculated angles from hyperfine coupling constants are not reliable enough, at least when only ^1H hyperfine coupling constants are compared.

A systematic study of the influence of substitution on geometries and electronic structures of chlorinated triphenylmethyl radicals based on their X-ray structures has been started by Veciana and coworkers in 1987¹³² while crystal structure determinations of many triphenylmethyl carbonium ions have been reported since 1965.¹³³ The hyperfine coupling constants of the chlorinated triphenylmethyl radicals have been calculated and compared with those obtained in isotropic solution using INDO calculations by Veciana and coworkers.

To date we have not obtained single crystals of metal complexes of tris(2,6-dimethoxyphenyl)methyl radical **1**. Our efforts have in part been frustrated by the fact that Li^+ catalyzes the oxidization of the radicals by O_2 to yield the cation and the persistent cation in solution hampers the crystal growth process which I will discuss later. Consequently, our structural studies have focused on characterizations of the binding site via diffraction studies of the uncomplexed monomeric species and some close structural analogues and pulsed EPR studies.

1.1. Structure

Tris(2,6-dimethoxyphenyl)amine is a remarkable compound which has been traced mainly in the literature. The rings which are attached to the central six ortho methoxy groups are coupled to the central nitrogen atom. The rings in the molecule are compared by comparing the triphenylamine, nitrophenyl, and Martin ester. The dimethoxy triphenylamine is a 1. He proposed a substantial substitution of delocalization of the propoxy methoxy groups.

We were able to obtain a solution of the angles of the using various

1.1. Structure of Triarylmethyl Radical

Tris(2,6-dimethoxyphenyl)methyl **1**, originally reported by Martin, is a remarkably stable organic free radical. The high stability has been traced mainly to the shielding of the trivalent carbon atom by the phenyl rings which are strongly twisted in a propellerlike conformation and the six ortho methoxy groups. Martin correlated observed EPR hyperfine coupling constants of the radical **1** with the twist angles of the aromatic rings in tris(2,6-dimethoxyphenyl)methyl radical in solution. By comparing the calculated twist angle of 30° for Gomberg's triphenylmethyl ($a_{\text{Hpara}}=2.77$), the X-ray structure of tris(4-nitrophenyl)methyl ($\theta=30^\circ$), and a Hückel Molecular Orbital calculation, Martin estimated the increase in angle of twist to be 17° for tris(2,6-dimethoxy-phenyl)methyl ($a_{\text{Hpara}}=2.26$) over that of Gomberg's triphenylmethyl resulting in an estimated twist angle of 47° for the radical **1**. He pointed out that the reduction in a_{para} from 2.77 to 2.26 is substantially larger than would be expected for simple methoxy substitutions in triphenylmethyl radicals and that the decrease in spin delocalization should therefore be attributed to the increase in the pitch of the propeller conformation of the radical **1** induced by the six ortho methoxy groups.

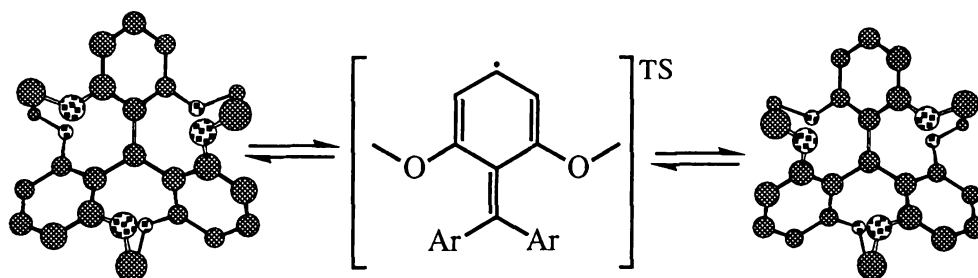
We were able to directly compare the solution and solid structures by using solution EPR and the X-ray structure of the radical **1**. The estimated twist angles of the radical **1** in solution were nearly identical to Martin's values using various experimental conditions and solvents such as THF or diethyl

ether (solu
initially by
Michigan S
were obtain
radicals ad
twisted out
two rings a
the way t
pathway¹
unpreceden
triarylmeth



Increased
substituen
temperatu
sterically
fully mini
kcal/mol
We believ
stable sol
conforma

ether (solution EPR). The X-ray structure of radical **1** was determined initially by Professor Kahr at Purdue University and repeated here at Michigan State University later. Brick-red monoclinic prisms of radical **1** were obtained by fast evaporation of an ether solution under argon. The radicals adopt an unusual conformation in the solid state. One aryl ring is twisted out of the central methyl carbon plane by only 12° while the other two rings are twisted by 61° . This structure represents a point well along the way to the transition state for the two-ring flip racemization pathway¹³⁴ and its large deviation from the D_3 ground state is unprecedented for triaryl-X propellers, especially in a perorthosubstituted triarylmethyl radical.



Increased racemization barriers are consistent with large ortho-substituents; perchlorotriphenylmethyl does not racemize on the room temperature time scale.¹³⁵ However, methoxy groups are substantially less sterically demanding than chlorine atoms, and AM1 calculations on **1** at the fully minimized and X-ray twist angles show an energy cost of less than 3 kcal/mol for this distortion.

We believe that the X-ray structure of the radical **1** represent a kinetically stable solid state structure which may be far from the relaxed solution conformation. Because of the dissymmetric twists of the rings, the ether

tripod binding
radical.

The
average dis
But, as note
of energies

Fig

In p
small mol
or other
results in
the chara
been con
Removal
radical.

Pr
the Li^+
methoxy

tripod binding site is poorly represented by the crystal structure of the radical.

The crystal structure of the radical **1** is shown in **Figure 9**. The average distance between the oxygen atoms of a tripod pocket is 3.7 Å. But, as noted above, this distance can vary substantially over a small range of energies as a function of the three aryl rings' rotations.

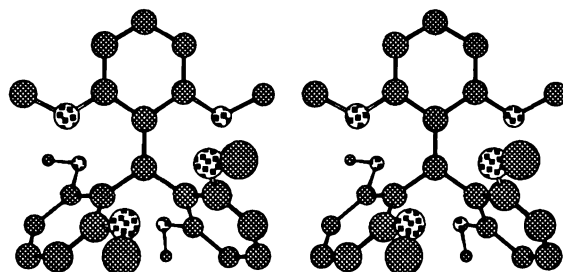


Figure 9. Stereo view of the X-ray structure of the radical **1**.

In pure solution, radical **1** is air stable; this suggests that even such a small molecule as O_2 is sterically excluded. However, addition of $LiBF_4$ or other lithium salts to air-saturated THF or ether solutions of radical **1** results in nearly instantaneous oxidation of the red radical solution to give the characteristic purple color of the triarylmethyl cation. This process has been confirmed by Jackson and Kahr to be inhibited by excess 12-crown-4. Removal of air and reduction with acidic $Cr(II)$ salts regenerates the radical.

Professor Jackson proposed several possible interpretations. First, the Li^+ ion may bind, as shown in the Scheme below, to the tripod of methoxyl oxygens in radical **1**, inducing a conformational change which

opens up a

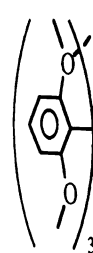
binding site

O₂ itself, a

molecule.

simply acti

O₂ radical a



As r

concerning

the sensi

1.2. Str

A r

crystal st

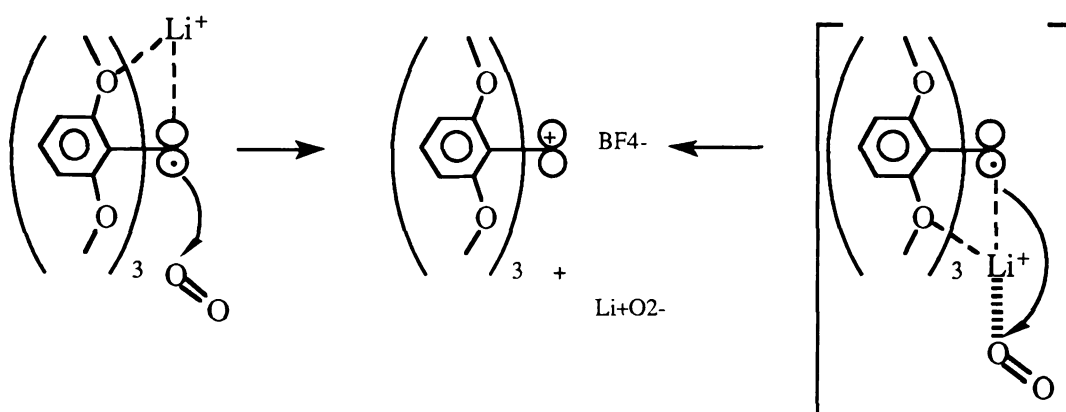
deviates

propeller

and Blou

(MMP2)

opens up access for O_2 to the radical center. Alternatively the fourth binding site on the (normally tetrahedrally coordinated) Li^+ ion may bind O_2 itself, serving as a bridge between the radical center and the O_2 molecule. Finally, the presence of the Li^+ ion in an organic solvent may simply activate electron transfer (ET) by strongly stabilizing the product O_2 radical anion via ion pairing.



As mentioned above, our attempts to obtain structural information concerning complexes of radical **1** with metal salts have been hampered by the sensitive redox chemistry of this system.

1.2. Structure of the Triarylmethyl Cation

A more realistic picture of the binding site than **1** is provided by the crystal structure of the related cation tetrafluoroborate salt **62** which deviates from D_3 symmetry in the lattice but can still be described as a propeller. The comparison of the X-ray structure (determined by Kahr and Blount at Princeton University) of the cation **62** and a calculated (MMP2) structure of the radical **1** is shown in **Figure 10**.

As a consequence
groups are
pockets with
cavity.



Fig
state
(from

1.3. Stru

Since
avoid some
circumve
complexa
dimethox
boron rep
following
handled i
structure

As a consequence of the propeller conformations of **1** and **62** the methoxy groups are arranged in such a way that they form a pair of nucleophilic pockets with the oxygens' lone pairs projecting toward the center of a small cavity.

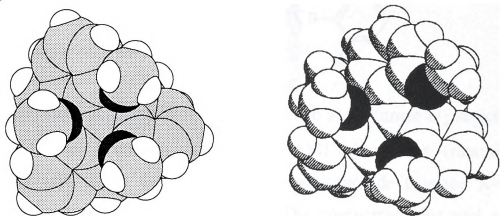


Figure 10. Space-filling views of the binding site: MMP2 ground state conformation of radical **1** (left) and X-ray structure of **62** (from **62** •BF₄, right).

1.3. Structure of Triarylmethyl Borane

Since small metal ions catalyze oxidation of **1** by O₂, it is difficult to avoid some oxidation in all our preparations of complexes. Wishing to circumvent these difficulties while still gaining structural data on complexation, we have synthesized the diamagnetic compound tris(2,6-dimethoxyphenyl)methyl borane **63**, a structural analogue to **1** in which boron replaces the central carbon atom. This compound is easily prepared following a modified Martin's procedure as shown below; it is easily handled in the absence of Brønsted acids, it crystallizes easily, and its X-ray structure is shown in **Figure 11**, along with an MMP2 calculated structure

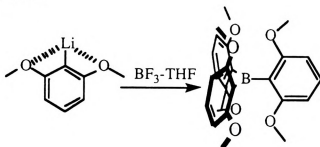
of radical
shown in F

This neutral
in the solid
barrier for
structure of
twists in tr
crystal st
dimethoxy
tris(2,6-di



Fig
ray
con

of radical **1** for comparison. A stereo view of the packing diagram is shown in **Figure 12**.



This neutral isostructural analogue of **1** gives an approximate D_3 structure in the solid state. From this structure and AM1 calculations (rotational barrier for aryl rings; 4-6 kcal/mol),¹³⁶ we conclude that the X-ray structure of the radical **1** is anomalous. The comparison for aryl ring twists in tripod binding sites are summarized in **Table 1** and a summary of crystal structure determination and refinement data for tris(2,6-dimethoxyphenyl)methyl **1**, tris(2,6-dimethoxyphenyl)borane **63**, and tris(2,6-dimethoxyphenyl)methyl cation **62** are summarized in **Table 2**.

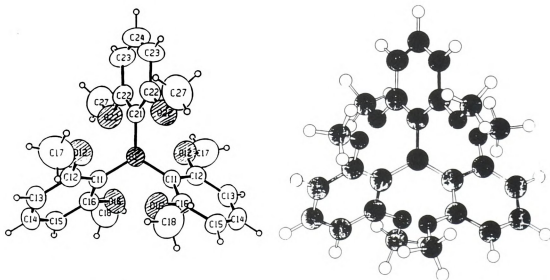
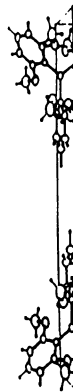


Figure 11. Ball and Stick representations of the binding site: X-ray structure of borane **63** (left), and MMP2 ground state conformation of radical **1** (right).



Figure

It was shown
 trimesitylb
 identical. I
 structural c
 compound
 by a tend
 triarylbor
 difference
 only a sin
 significan
 should no

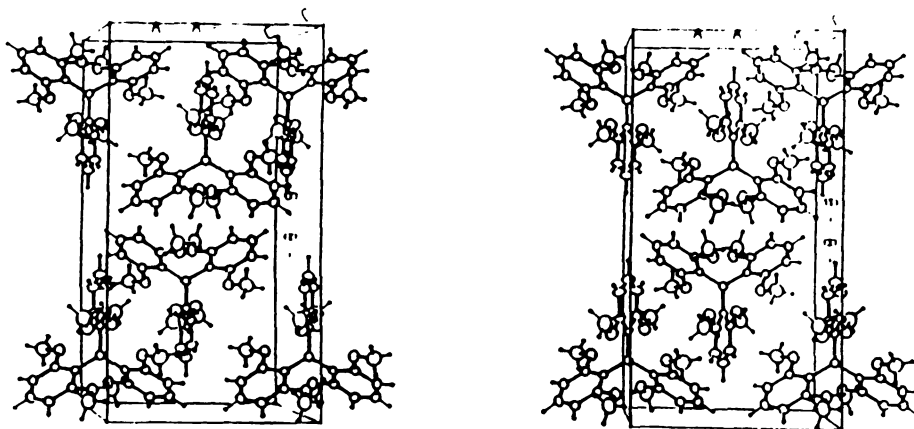


Figure 12. Stereo view of packing diagram of borane **63**.

It was shown by Power that the solid state conformations of trimesitylborane and the trimesitylborane radical anion are virtually identical.¹³⁷ The conclusion of this comparative study was that the structural consequences of the addition of one electron into the LUMO of a compound of the type Ar_3X are trivial. While this conclusion is supported by a tendency toward D_3 symmetry in many reported structures of triarylboranes, triarylmethyls, and triarylamines, there are gross differences in the crystal conformations of **1** and **62**, which also differ by only a single electron. Similarly, the isoelectronic species **62** and **63** are significantly different. These results caution that simple generalization should not be drawn from a comparison of only two crystal structures.

Tabl

^aTw
soul
solu

Tal
tris
bor

Cr

Sp
Z*
Te
a
b*
c*
 α
 β
 γ
 μ

*
s

Table 1. Aryl ring twists in tripod binding sites (in degrees)^a

1	12.3	61.0	61.0	C ₂ Axis
1^b	47	47	47	D ₃
1^c	45	45	45	D ₃
63	62.8	64.2	64.2	C ₂ Axis
62	32.6	46.1	48.9	General site

^aTwists out of central atom plane; coplanar = 0.0° ^bDetermined in solution by Martin using EPR measurements. ^c Determined in solution by Ishizu and Mukai using ENDOR measurements.¹³⁸

Table 2. Crystal structure determination and refinement data for tris(2,6-dimethoxyphenyl)methyl **1**, tris(2,6-dimethoxyphenyl)borane **63**, and tris(2,6-dimethoxyphenyl)methyl cation **62**.

Crystal data	63	62	1
Space group	C2/c	P1	P2/n
Z*	4	2	2
Temperature	295	110	295
a (Å)**	11.076	7.214	10.405
b**	20.839	12.931	9.429
c**	9.944	13.633	11.767
α (°)**	90	83.13	90
β**	98.40	77.70	102.120
γ**	90	80.56	90
μ (cm ⁻¹)***	0.80 (Mo Kα)	9.7 (Cu Kα)	0.83 (Mo Kα)

*number of molecules in the unit cell, ** Cell dimensions, ***X-ray source.

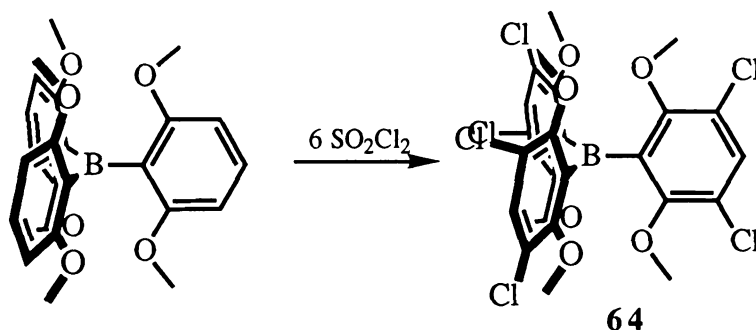
1.4. Hex

Tris
dimethoxy
various me
groups wh
sterically
position i
substituen
ether oxy
ligand's b

Borane 6
63 with
methoxy
Borane
ferrocen
voltamr
tetraflu
potentia
conditio

1.4. Hexachloro Triphenylmethyl Radical and Borane

Tris(2,6-dimethoxy-3,5-dichlorophenyl) borane **64** and tris(2,6-dimethoxy-3,5-dichlorophenyl)methyl radical **65** were synthesized with various modifications. The chlorine substituents are vicinal to the methoxy groups which form the ether tripod binding sites; they may therefore sterically perturb the methoxy groups, twisting them out of their preferred position in the aryl ring plane. These sites also position a vicinal substituent to withdraw or donate electron density by resonance with the ether oxygens, potentially modifying their Lewis basicity and hence the ligand's binding abilities, without perturbing the radical center.



Borane **64** show remarkable stability toward protic acid compare to borane **63** with better preorganization for ion binding because of the twisting of methoxy groups out of the binding cavities as shown in **Figure 13**. Borane **64** shows a reversible redox potential of -2.14V (referenced to ferrocene oxidation) for the process of $B \rightleftharpoons B^{\cdot\cdot}$ in cyclic voltammetry in methylene chloride with tetrabutylammonium tetrafluoroborate as a supporting electrolyte. Determination of the redox potential for borane **63** was unsuccessful under a variety of experimental conditions.

Fig
with
ion-
twis

Fi
so
pc

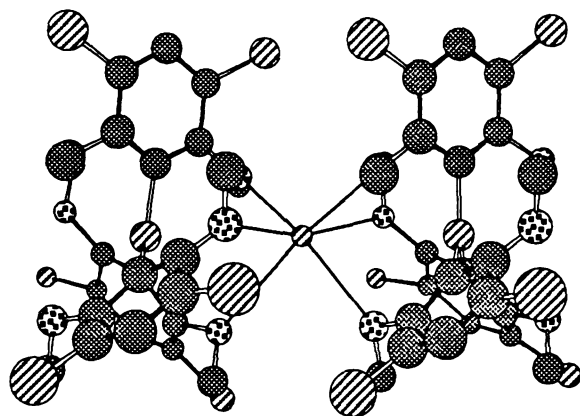


Figure 13. MM2 calculated structure of borane **64** dimer with lithium cation showing improved preorganization for a ion-binding over that in borane **63** by twisting methoxy group twistings out of conjugation with the aryl rings.

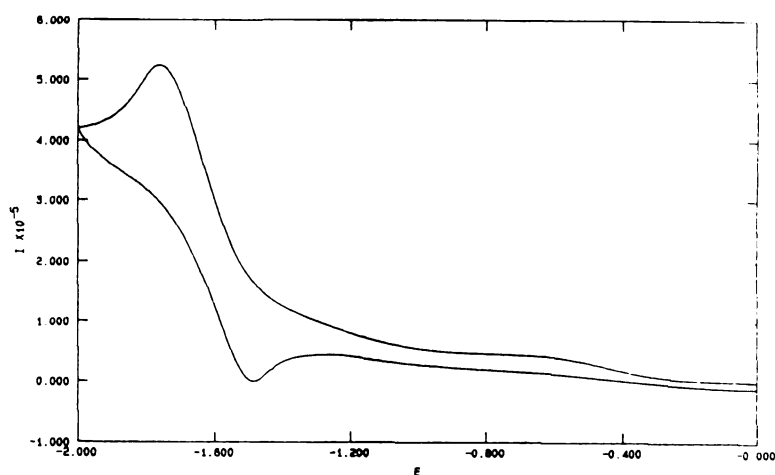


Figure 14. Cyclic voltammogram of **64** in methylene chloride solution of tetrabutylammonium tetrafluoroborate. The redox potential was referenced to the oxidation of ferrocene.

2. Subst

It is
scheme, th
the centra
magnetic
therefore
substituted

The cycli
conveys i
consists o
unstirred
this worl
saturated
(Ag/AgC
solvents
Calomel
of which

Our res
and me
oxidatio
voltamm
examin
examin

2. Substituent Effects.

It is reasonable to suppose, based on our paramagnet coupling scheme, that variations in the odd electron's availability (spin density) at the central carbon and methoxy oxygen will affect the formation and magnetic properties of crystallized complexes of these radicals. We have therefore synthesized and examined the redox properties of various substituted analogues of the radical **1** using cyclic voltammetry (CV).

The cyclic voltammogram is analogous to a conventional spectrum in that it conveys informations as a function of an energy scan. Cyclic voltammetry consists of cycling the potential of an electrode, which is immersed in an unstirred solution, and measuring the resulting current. The potential of this working electrode is controlled by a reference electrode such as a saturated calomel electrode (SCE) or a silver/silver chloride electrode (Ag/AgCl). The accessible potential ranges for common electrochemical solvents have been studied and found to be -3.0 to 1.4 V vs SCE (Saturated Calomel Electrode) for THF and -1.8 V to 1.9 V vs SCE for CH₂Cl₂, both of which are wide enough for our measurements.¹³⁹

Our results show reversible oxidation and reduction waves for **1** in THF and methylene chloride as shown in **Figure 15**, indicating that all three oxidation states are stable, at least on the time scale of our cyclic voltammetry scans (50-200mV/sec). Various supporting electrolytes were examined, including tetraalkylammonium and alkali metal salts, in order to examine their effects on redox potential for ion-bindings.

Fig
kin
rad
res
sec

One stre
compon
binding
accessib
mediated
valuable
choice o
electron
focused
then pro

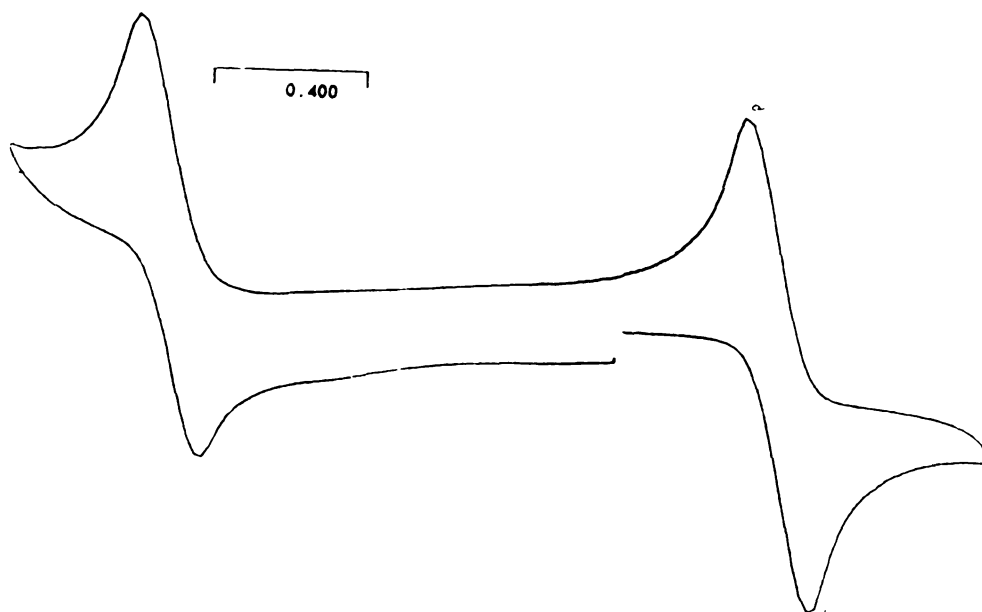


Figure 15. Cyclic Voltammogram of **1** in THF. Note that kinetically reversible electron transfer was found for both radical/cation and anion/radical couples (-0.49 V and -2.05V respectively vs. ferrocene oxidation), at scan rates of 200mV sec⁻¹.

One strength of our approach to magnetic materials is that the organic components can be modified in synthesis to adjust the redox and ion-binding properties of these multidentate radicals. As the range of accessible oxidation states is thought to be related to superexchange-mediated magnetic coupling in stacked materials, such control may prove valuable.^{140,141} This tuning of the paramagnetic ligands, combined with choice of metal couplers, promises broad control over the magnetic and electronic characteristics of our extended complex materials. I have focused first on simple modifications to make derivatives of radical **1**, and then progressed to the more complicated systems.

2.1. Hex

Mar

made min

approach

targets, I

procedure

withdraw

reagents.

devoted

the desire



E

systems

oxidation

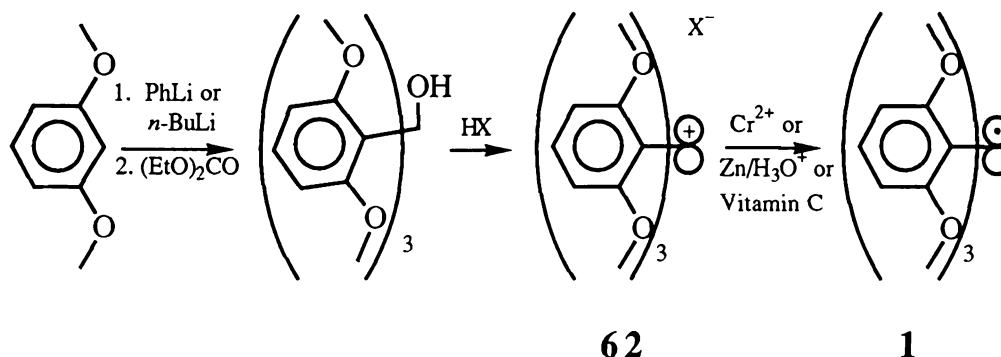
derivati

Based

charac

2.1. Hexamethoxy Triphenylmethyl Radicals.

Martin's synthesis of **1** is simple and economical. Although we have made minor modifications in building derivatives of radical **1**, our approach is basically unchanged from the original work. In selecting new targets, I initially focused on substituents which can tolerate the synthetic procedures. However, many of the most potentially interesting electron withdrawing substituents cannot survive treatment with organolithium reagents. Such substituents are of particular interest and we have therefore devoted substantial effort to developing new syntheses in order to access the desired range of substituted radicals.



Electrochemical studies on simple *para*-substituted triphenylmethyl systems have shown that the substituents can substantially alter their oxidation and reduction potentials.^{142,143} Functionalization of **1** to make derivatives similarly varies the redox properties of this family of radicals. Based on simple resonance pictures, the electron donor or acceptor character of 4-substituents in aromatic rings should strongly affect the

energy C
perturbin

X

T:

ra

a,

X

F

C

C

F

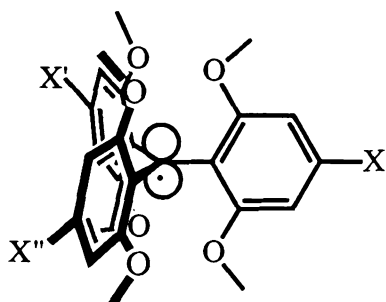
t

N

C

C

energy of the singly occupied MO (the SOMO) without significantly perturbing the oxygens of the methoxy groups.



- 1** : X = X' = X'' = H
66 : X = X' = X'' = Cl
67 : X = X' = X'' = OCH₃, OBu
68 : X = X' = X'' = CH₃
69 : X = X' = X'' = Ph
70 : X = CH₃

Table 3. Summary of electrochemical data for derivatives of radical **1** in THF a) and CH₂Cl₂ b).

a)

X	X'	X''	$R^+ \rightleftharpoons R^\bullet$	$R^\bullet \rightleftharpoons R^-$
H	H	H	-0.49 V	-2.05 V
Cl	Cl	Cl	-0.30 V	-1.84 V
OMe	OMe	OMe	-0.89 V	-2.29 V
Ph	Ph	Ph	-0.50 V	-1.90 V

THF Solvent; Reference: Ferrocene oxidation

b)

H	H	H	-0.44 V	-2.07 V
Cl	Cl	Cl	-0.34 V	-1.84 V
OMe	OMe	OMe	-0.93 V	-2.31 V
CH ₃	CH ₃	CH ₃	-0.72 V	-2.19 V
Ph	Ph	Ph	-0.53 V	-1.88 V
CH ₃	H	H	-0.61 V	-1.99 V

CH₂Cl₂ Solvent; Reference: Ferrocene oxidation

By using
oxidation
property.
orbital en
might fin
helpful.
and 70, s
radicals
while ele
expected
are only
condense

The red
between
of the su
where k
(meta or

ρ is a c
peculia
correlat
where l
unsubst

By using electron withdrawing substituents in **1**, we may produce oxidation-resistant derivatives of **1** which still retain **1**'s ion-binding property. On the other hand, if triplet coupling is promoted by better orbital energy matching between radical and lithium cation orbitals, we might find donor or resonance delocalized substituents to be especially helpful. As a start on these studies, we have synthesized **66**, **67**, **68**, **69**, and **70**, simple derivatives of **1**. It is clear that electron donor substituted radicals **67**, **68**, and **69** are more vulnerable to air oxidation than is **1**, while electron acceptor substituted radical **66** is less so. As might be expected, yields vary from good to poor as some of the substituents studied are only marginally tolerant of the ortho lithiation conditions required to condense the intermediate triarylmethyl carbinol.

The redox potentials in **Table 3** can be examined for a possible relation between half-wave potential (for the one-electron reduction) and the nature of the substituent. One such relation is expressed in the Hammett relation where k and k° represent rate or equilibrium constants for substituted (meta or para) and unsubstituted compounds, respectively.

$$\log \frac{k}{k^\circ} = \rho \sigma$$

ρ is a constant characteristic of the reaction series, and σ is a constant peculiar to the substituents; σ_H is generally set equal to zero. The correlations of electrochemical data are made using the following equation where $E_{1/2}^R$ and $E_{1/2}^H$ are the half-wave potentials for the substituted and unsubstituted compounds. Note that in the equation, ρ is expressed in volts.

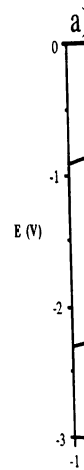
The intr
electrode
many or
wave po
reduction
cation/r
couples.

Examin
graphic
 σ valu
values
becaus
involv
correla
correla
cation
induct
contri
correl
worse
times

$$\Delta E_{\frac{1}{2}} = E_{\frac{1}{2}}^R - E_{\frac{1}{2}}^H = \rho\sigma$$

The intrinsic difficulties of attempting $E_{1/2}$ - σ correlations when the electrode reactions are irreversible have been stated.¹⁴⁵ Unfortunately, many organic reductions and oxidations are irreversible and hence half-wave potentials cannot have thermodynamic significance. However, the reduction potential measured in this work are generally reversible for the cation/radical couples and reversible or nearly so for the radical/anion couples.

Examination of a relation between half-wave potential and σ may be done graphically merely by linear plotting of one against the other using known σ values.¹⁴⁶ The correlations between half-wave potential and sigma values are not so good as we can see in the least-squares fit in **Table 4** because of the complexities of reactions and conformational effects involved. It has been suggested that the cation stability should be correlated with σ^+ values, whereas anion and radical stabilities are to be correlated with σ or σ^- values.¹⁴⁷ It appears as if substituents affect the cation with resonance and/or hyperconjugation terms in addition to inductive and polarizability terms, whereas only the polarizability contributes substantially to radical and anion stability. An attempt to correlate our experimental data with σ^+ or σ^- was unsuccessful and gave worse correlation parameters than with σ (the values were summed three times for the trisubstituted radicals for the correlation).



Fi
Th

T
an

-

-

C

C

C

C

.

a

.

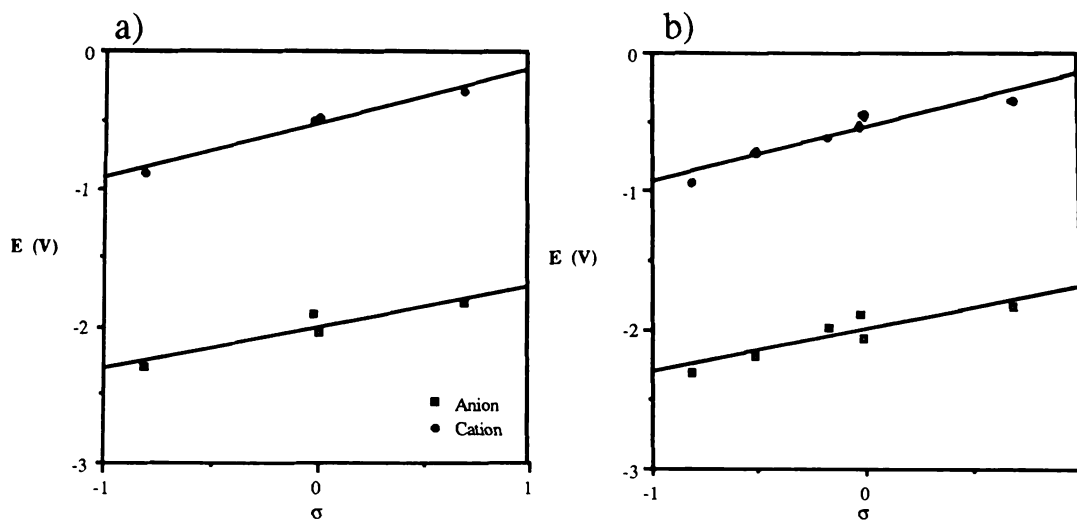


Figure 16. $\Delta E_{1/2}$ (V) vs σ in THF for HMTP methyl radicals a) in THF and b) in CH_2Cl_2 .

Table 4. Least-squares fit of Correlation for half-wave potential and sigma values for HMTP methyl radicals. $\Delta E_{1/2} = \rho X - E'_{1/2}$

	ρ	$E'_{1/2}$	# ^a	R ^b
σ (Cation) ^c	0.3969	-0.53	4	0.965
σ (Anion) ^c	0.3019	-2.00	4	0.852
σ (Cation) ^d	0.3912	-0.54	6	0.905
σ (Anion) ^d	0.3177	-2.00	6	0.805

^a Number of experimental points used. ^b Correlation coefficient. ^c THF solution. ^d CH_2Cl_2 solution.

Bank pro

radical sy

simple su

first of th

triphenyl

balanced

monomet

are repor

expect si

function

stabilizin

maximal

stabilizin

unsubsti

methyl a

Bank su

system

withdra

effect;

substitu

exactly

Direct

variety

comme

limited

Bank proposed that substituent effects detected in CV of triarylmethyl radical systems are not likely due to conformational changes but rather to simple substituent contributions. He recorded the largest change for the first of the three methyl substitutions for H in the para position of the triphenylmethyl system. Steric and conjugative effects are said to be balanced in each case to provide the optimum stabilities. For para monomethylated triarylmethyl anion, the twist angles for the phenyl rings are reported to be 19.7° , 30.6° , and 44.8° , respectively.¹⁴⁸ Thus, we can expect significant differences in the degree of conjugation of aryl rings as a function of substitution. For the electron-deficient cation the greater stabilizing effect can occur when the donor methyl group is in the maximally conjugated ring. Similarly for the electron rich anion better stabilizing effects are achieved when the maximally conjugated ring is unsubstituted. This analysis is based on the electron donor properties of methyl and the differential ring conjugation.

Bank suggested that the preferred ring conjugation of the triarylmethyl system should be determined by various substituents. In fact an electron-withdrawing group should reverse the pattern of sequential substituent effect; thus, for the anion, greater stabilization would result when a substituted ring is maximally conjugated. For the cation the prediction is exactly the opposite.

Direct application of Martin's original synthesis of radical **1** calls for a variety of 4- and 5-substituted 1,3-dimethoxybenzenes. The range of commercially available dimethoxybenzenes is adequate if somewhat limited. In cases where the desired substituents could not tolerate Martin's

procedure

substituent

assembled

modified

systems.

functional

acid-stable

breaking

It has been

amines can

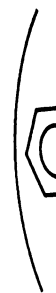
72, do

dimethyl

modified

The design

with sodium



In a less

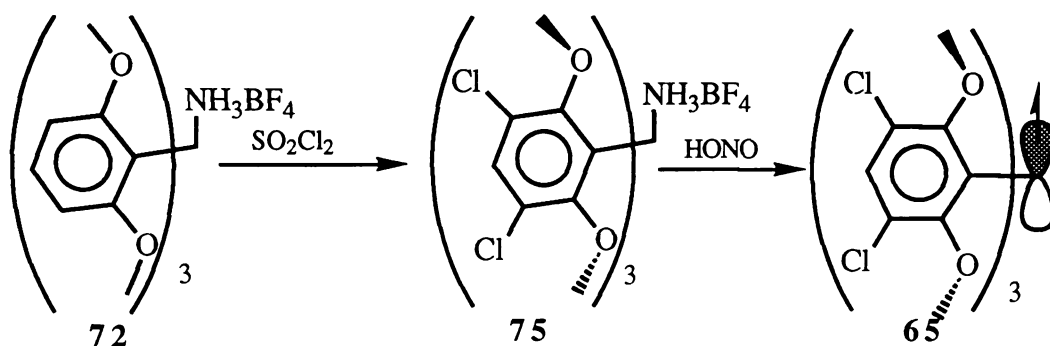
correspond

more re

electro

procedure, an alternative strategy would be desirable which would allow to substituents to be added after the triarylmethyl framework was fully assembled. The resulting intermediate could then be converted to a new modified radical, opening the way to much broader class of substituted systems. With this goal in mind, we have explored the possibility of functionalization after assembly of the triarylmethyl framework via some acid-stable derivatives in which the central carbon is sp^3 hybridized, breaking up the extended π -system.

It has been found that ammonia, as well as various primary and secondary amines can add into the central carbon in cation **62**. The ammonia adduct, **72**, does not have the proton acid sensitivities of tris(2,6-dimethoxyphenyl)methyl carbinol **71**. This ammonium salt can be modified with a wide range of halides by simple electrophilic reactions. The desired radicals can be then generated readily by a simple diazotization with sodium nitrite in acidic water.



In a less generally successful strategy, carbinol **71** can be reduced to the corresponding triarylmethane **73** using sodium cyanoborohydride which is more robust toward both treatment with organometallic reagents and electrophilic aromatic substitutions.¹⁴⁹ The corresponding hexachloro

methane

methylene

yet found

Although

unmodified

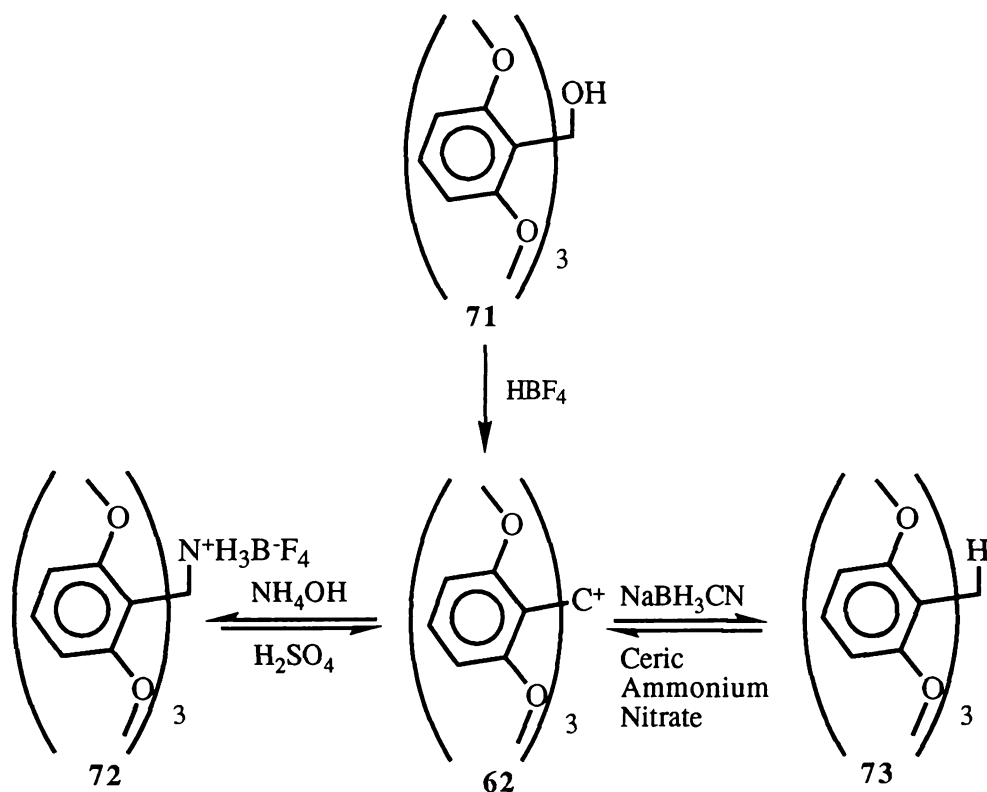
evidently

at deprot

pathways



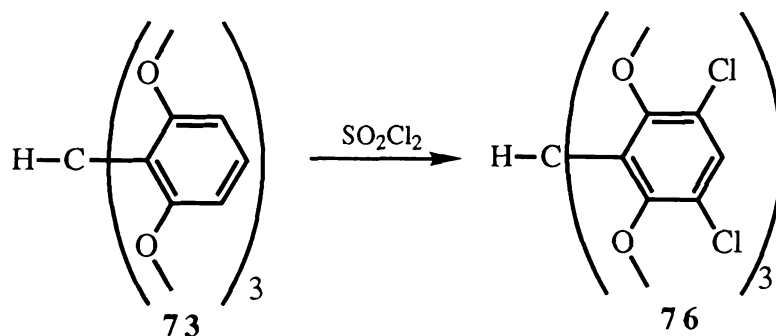
methane **76** was synthesized by a simple chlorination with SO_2Cl_2 in methylene chloride. The products are well characterized, but we have not yet found a clean conversion back to the corresponding radical or cation. Although oxidation with p-chloranil is effective at converting the unmodified methane **73** to the cation, the hexachlorinated analogue **76** is evidently too deactivated to undergo the analogous oxidation. All attempts at deprotonation were also met with failure. A variety of less general pathways were also introduced for specific substitution patterns.



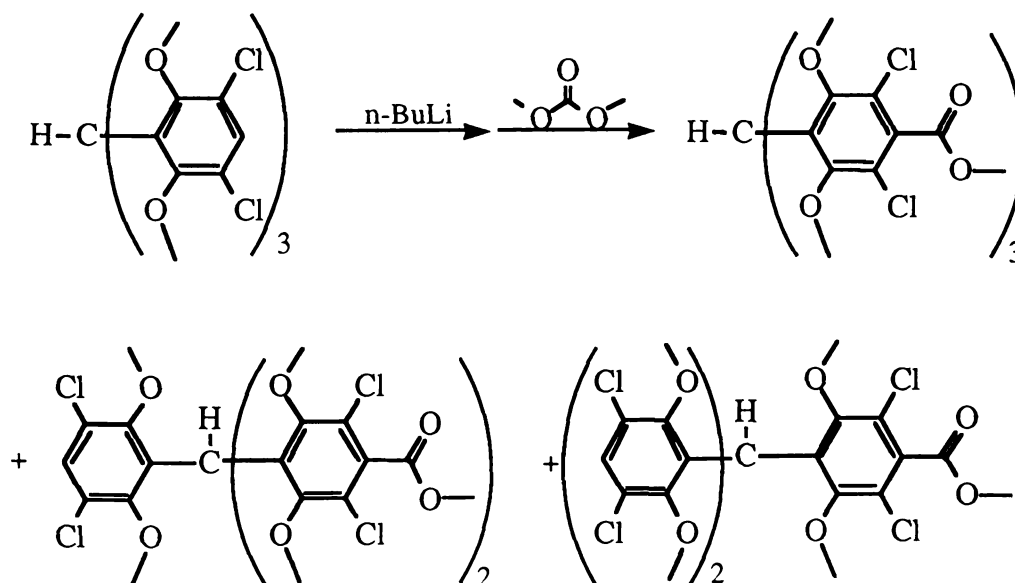
There are
can be u
could no
availabl
scheme.
mainly
carbona
for furth

F

+

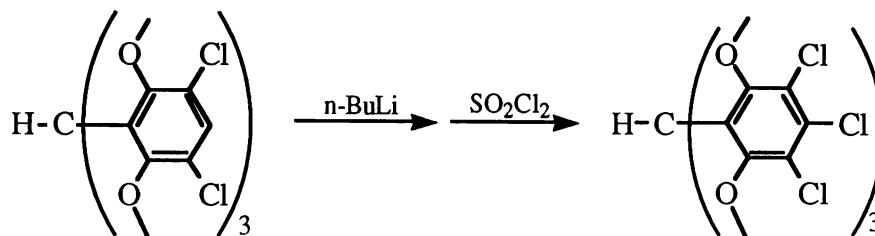


There are several more reactions worth mentioning here. The methane **76** can be used for building several substituted triphenylmethyl radicals which could not be built by the standard procedure because of side reactions or an available precursors. One example is illustrated in the following reaction scheme. The methane **76** can undergo ortho-chlorine directed lithiation mainly by the induction effect followed by quenching with dimethyl carbonate to give various substituted triaryl methanes which can be used for further functionalization of aromatic rings in the system.



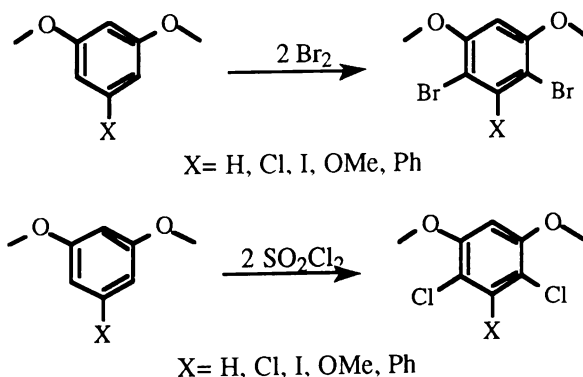
W
useful re
halogen
unsatur
These r
derivati
radicals

Electro
have b
precurs
dimeth
reactio



While building these substituted radicals, two very interesting and useful reactions were somewhat serendipitously introduced: Electrophilic halogenations of resorcinol derivatives; and condensation of α , β -unsaturated ketone and dimethyl malonate followed by aromatization. These reactions, especially the electrophilic halogenation of resorcinol derivatives, provided several key transformations in building these radicals.

Electrophilic halogen substitution and alkylation of resorcinol derivatives have been studied for decades. While pursuing the preparation of precursors for radicals, we were able to build a variety of halogenated 1,3-dimethoxy benzenes which we found later in the literature.¹⁵⁰ Some of the reactions are summarized in the following reaction schemes.



Most of t

An ether

amount

overnigh

usually

dimetho

dimethox

The co

followe

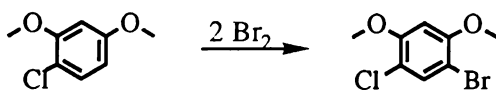
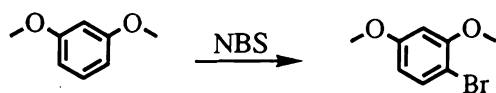
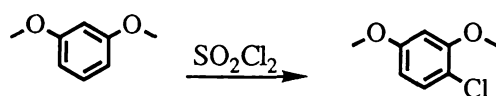
phenyl

overall

aldehy

aromat

Most of the reactions are nearly quantitative with easily purified products. An ether solution of precursors was combined with a stoichiometric amount of halogenating agent at $-78\text{ }^{\circ}\text{C}$ followed by slow warm up overnight and filtration of crystalline products. Washing with diethyl ether usually gave clean crystals of the products except 4-chloro dimethoxybenzene which we could distill under vacuum. 4-Bromo dimethoxybenzene was synthesized with aqueous NBS.



The condensation of α,β -unsaturated ketones with dimethylmalonate followed by aromatization was a key reaction in the preparation of 4-phenyl substituted triphenyl methyl radical **70**. With a good efficiency for overall reaction and wide commercial availability of a range of aryl aldehydes, these reactions have great potential for building various aromatic group substituted triphenyl methyl radicals.

All of

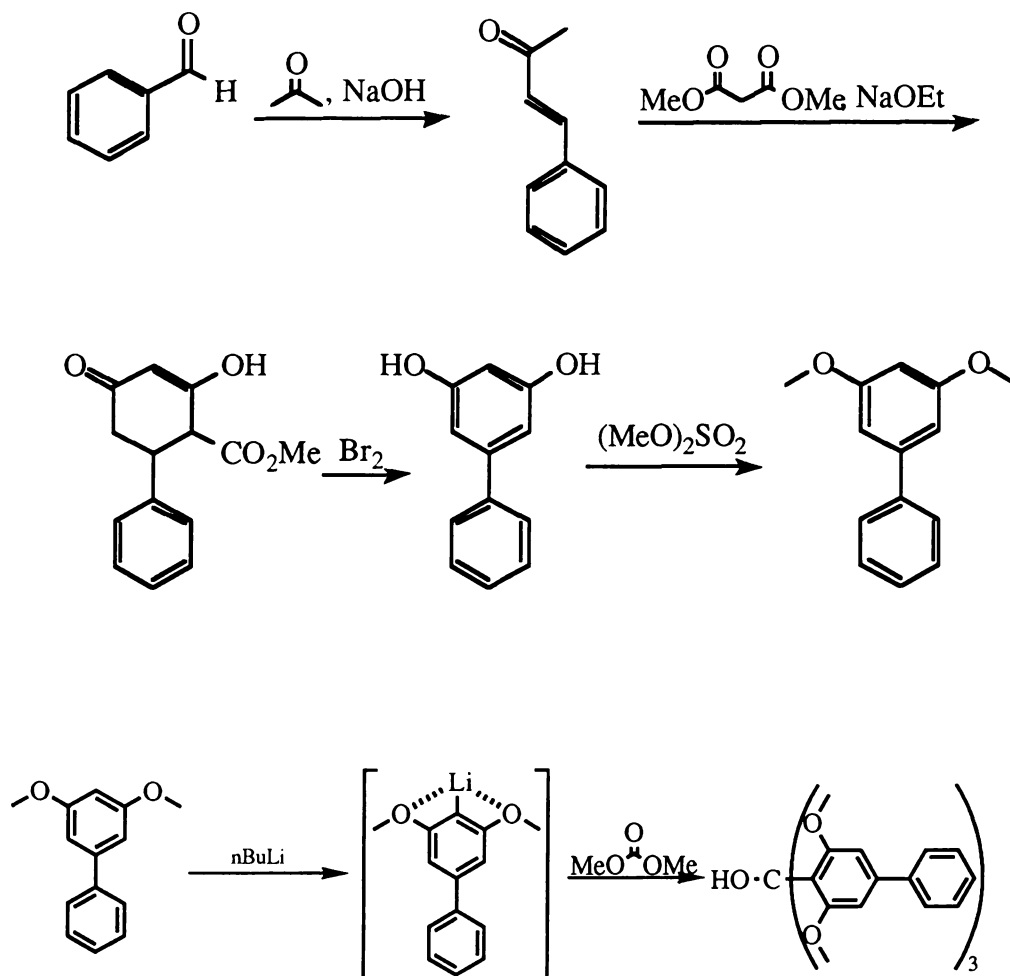
variab

been

Figur

determ

Table



All of the radicals generated have been studied by room temperature and variable temperature X-band EPR. Some ion-binding studies also have been carried out by EPR. Some of the typical EPR spectra are shown in **Figures 17, 18, and 19** along with simulations. The experimentally determined coupling constants a_i and the spin density ρ_i are summarized in **Table 5**.

Ta
fo
ra

1
1
6
6

1
3
9
3
2

Kivels
triphen
rather
substi
the m
carbo
availa
donat
may
cation

Table 5. A summary of ^1H hyperfine constants a_i (in Gauss) for coupling with meta and para proton in HMTP methyl radicals in THF.

	$a_{\text{meta}} (\#)^2$	$a_{\text{para}} (\#)^2$	$ \rho_{\text{meta}} ^1$	$ \rho_{\text{para}} ^1$
1	1.06 (6)	2.26 (3)	0.047	0.100
1⁴	1.07 (6)	2.35 (3)		
65		2.3 (3)		0.102
66³	1.0 (6)		0.044	

¹ $|\rho_{\text{exp}}| = |a / 22.5|$ ²numbers of protons in each positions.

³radicals **67**, **68**, and **69** show similar results. EPR spectra simulated with the ESRa program written by A. K. Rappé and C. J. Casewit, Calleo Scientific Software, Colorado State University.

⁴Determined by Ishizu and Mukai using ENDOR.¹³⁸

Kivelson reported that chloride substitution in the para position in triphenyl methyl increases the spin density at the ortho carbon slightly and rather more at the meta position.¹⁵¹ He suggested that methoxy substitution in the para position in triphenyl methyl radical does not affect the meta carbon spin density but increases the spin density on the ortho carbon considerably. We can follow the same arguments in estimating available spin densities on methoxy oxygen in our radicals with electron-donating *para*-substituents. The spin densities appear to be small but they may play a significant role in the magnetic interactions in our radical metal cation complexes.

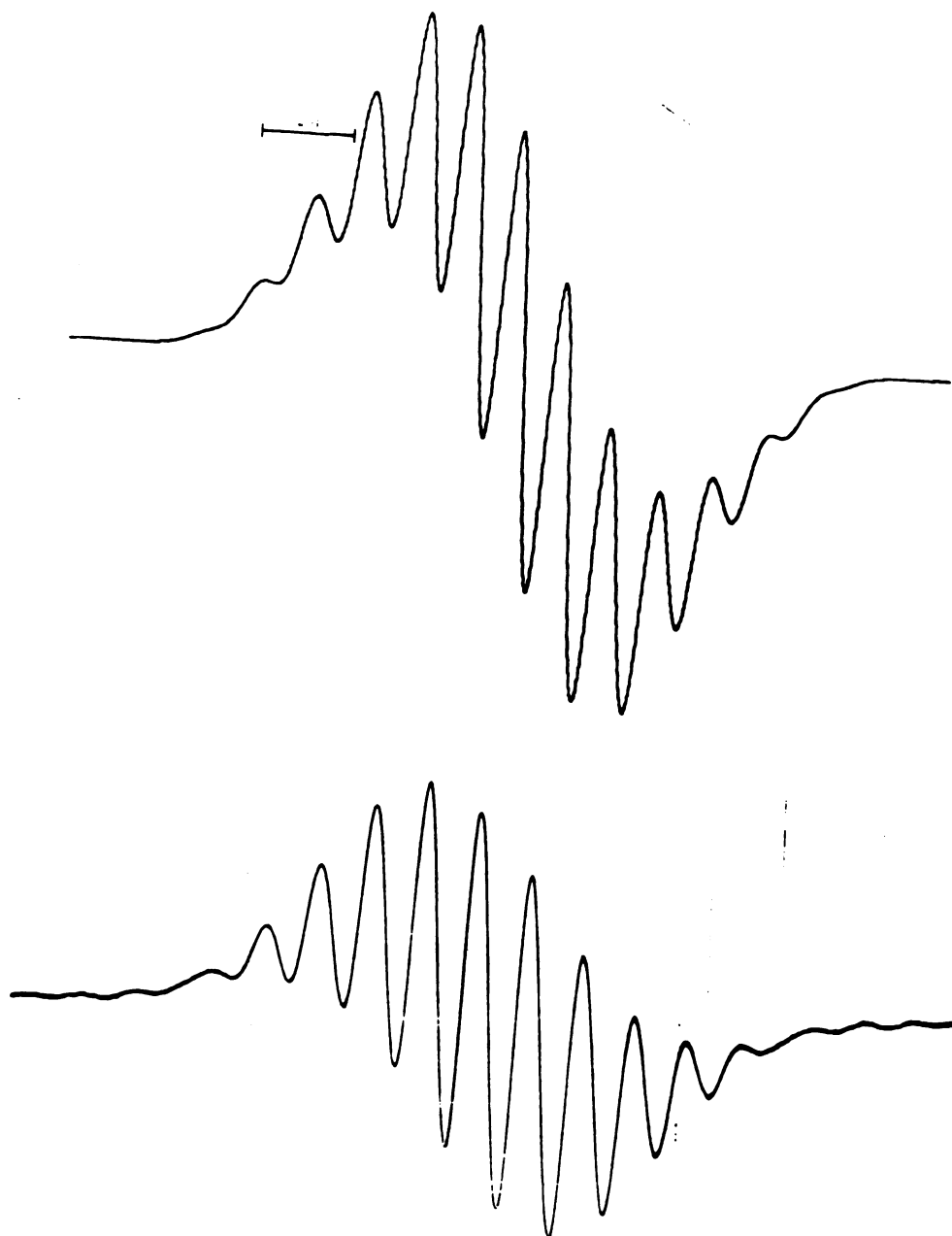


Figure 17. EPR spectrum of **1** in THF with simulation (top).

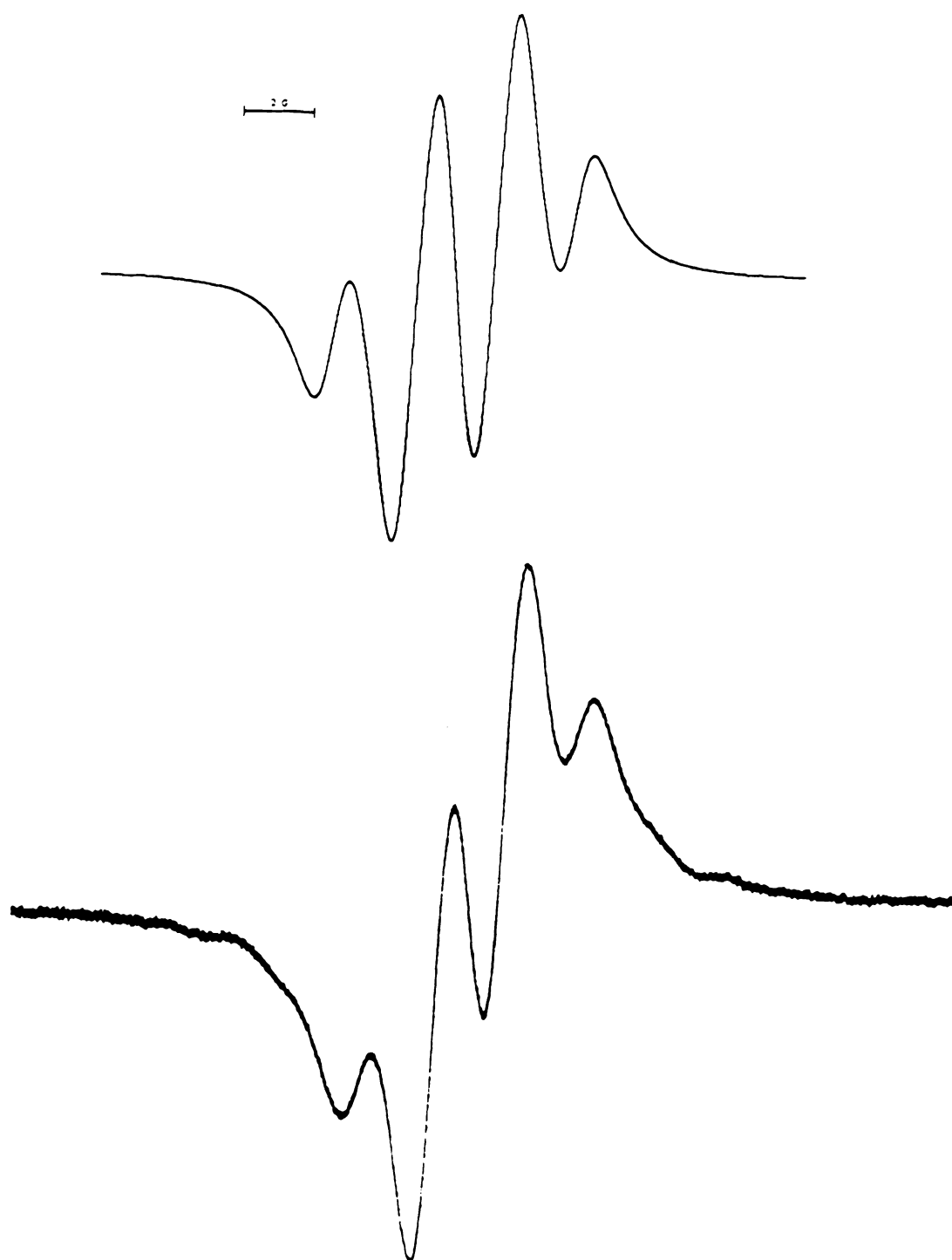


Figure 18. EPR spectrum of **65** in THF with simulation (top).

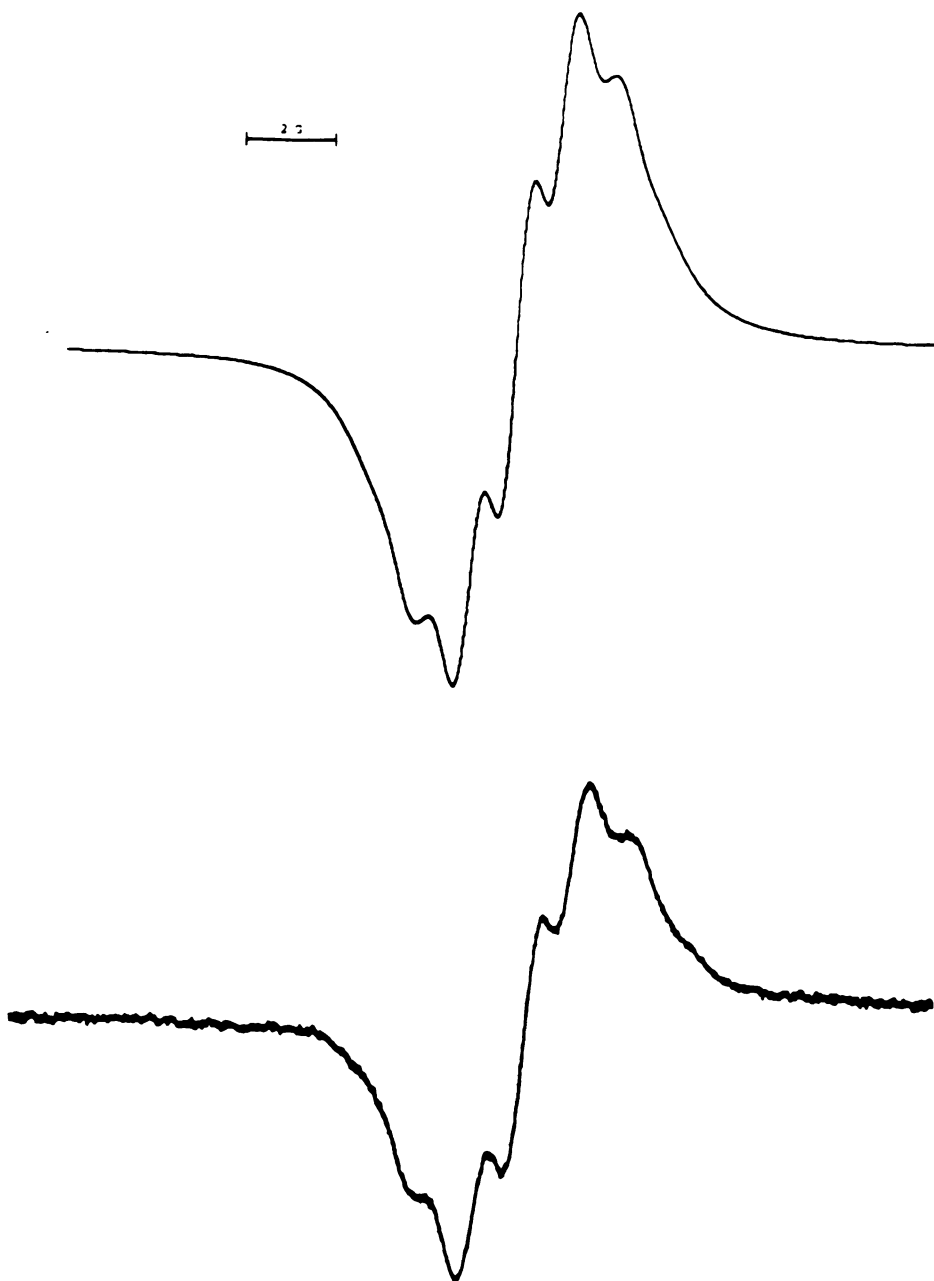


Figure 19. EPR spectrum of **66** in THF with simulation (top).

2.2. TH

So
undergo
acidic c
the cyc

Figure
cyclize

2.2. The Cyclized Xanthenol

Some of the cations which are intermediates in generating radicals undergo a cyclization to form a xanthenyl X ($= OH, NH_3^+, N^+H_2R$) under acidic conditions by way of the mechanism outlined below. We believe that the cyclization occurs when two of the rings are forced to be coplanar. **Figure 20** shows a stereo view of the X-ray crystal structure of the cyclized xanthenyl from carbinol **71**.

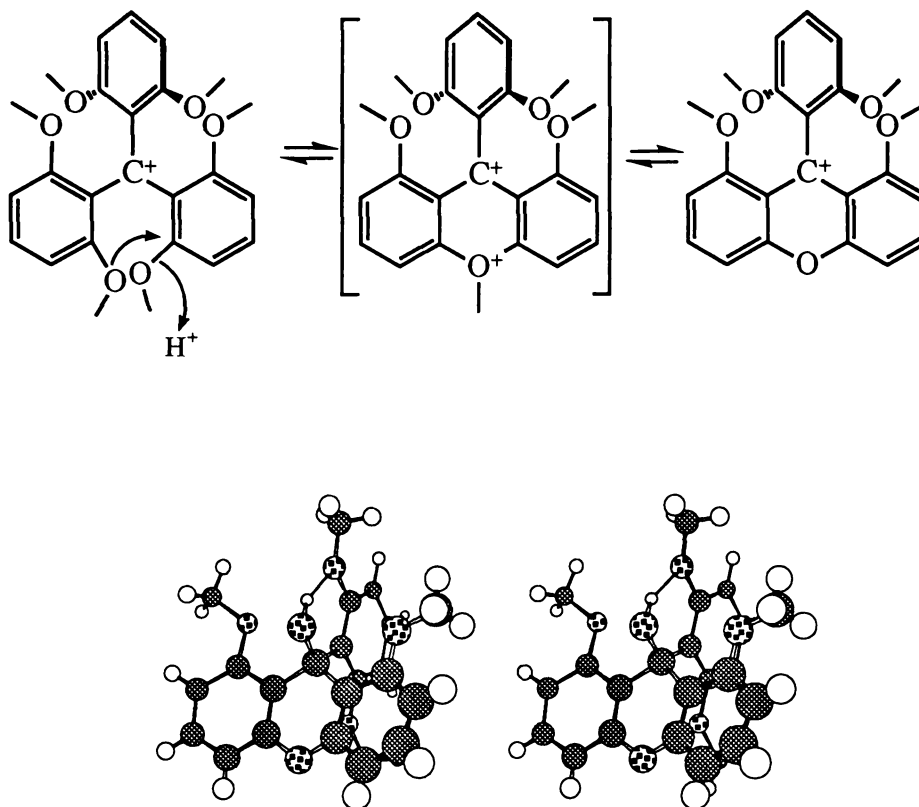


Figure 20. Stereo view of cyclized xanthenol from X-ray structure.

2.3. T

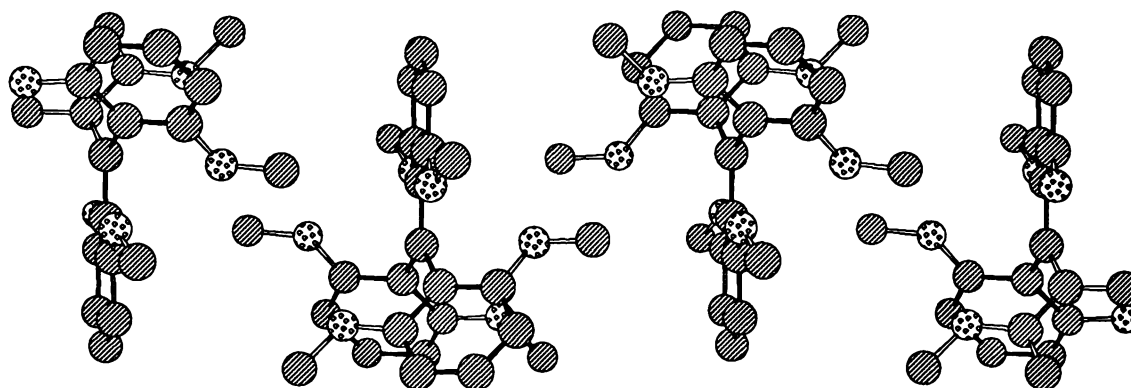
O
build lin
tripod e
ion-bin
molecu
packing
forms
the two
a roug
the sol



It o
stab
com
the
disc

2.3. Tetramethoxy Triphenylmethyl Radicals

Our purpose in using complexes of radical **1** with metal cations is to build linear chains of radicals by complexation of the metal ion with the tripod ether oxygens in the radical. Various ion-binding studies suggest that ion-binding can occur with as few as four methoxy groups in a given molecule. Furthermore, careful examination of the three-dimensional packing diagram of radical **1** shown below reveals that the radical itself forms linear chains without a metal cation. The four methoxy groups on the two more twisted rings are already placed in such a way that they form a roughly square planar ligand environment between adjacent radicals in the solid state.



It occurred to us that if a radical with only four methoxy groups would be stable enough to be handled in the usual way and could form a linear chain complex with metal cations between radicals, it should be possible to study the magnetic behavior of the resulting coordination chemistry. As I discussed earlier, the anomalous solid state structure for **1** is troublesome

even tho

amount

thought

defined

alternati

A seri

methy

modif

usual

deriva

dimet

Muka

spectr

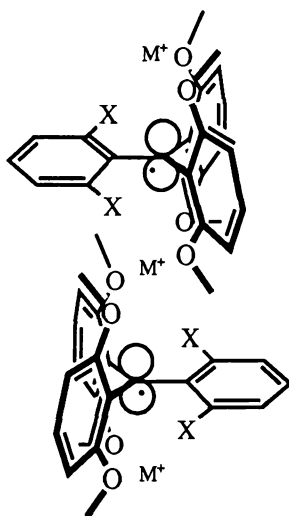
65°,

const

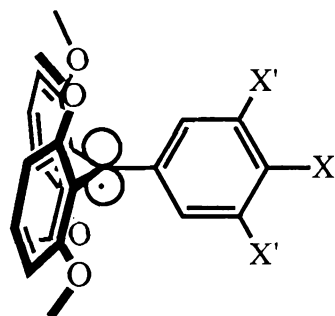
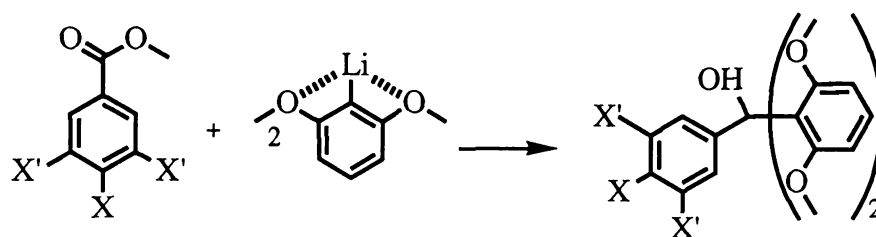
show

const

even though various calculations show that it can be explained with a small amount of crystal lattice energy (3-6 kcal/mol by AM1 calculations). We thought that if the tetramethoxy radical could also give a structurally well defined complex, and magnetic interactions, this new complex might be an alternative building block for molecular magnetic materials.



A series of *para*-substituted phenyl bis-(2,6-dimethoxyphenyl)phenyl methyl radicals was prepared as shown in next page by a simple modification of Martin's procedure. All of the radicals were studied as usual by EPR and CV as with the hexamethoxy triphenylmethyl derivatives; the results are summarized in **Tables 6** and **7**. The di-(2,6-dimethoxyphenyl)phenyl methyl radical **77** has been studied by Ishizu and Mukai using the Electron Nuclear Double Resonance (ENDOR) spectroscopy and was found to have C_2 symmetry with twist angles of 65° , 65° , and 30° in toluene. They reported almost identical hyperfine coupling constants to our values for the radical **77** in toluene.¹⁵² This spectrum shows significant solvent dependence as seen from the hyperfine coupling constants in THF (**Table 8**).



77: X = X' = H

78: X = Cl

79: X = OCH₃80: X = CH₃

81: X = OH

82: X = CO₂H83: X = NO₂84: X = H, X' = OCH₃

Table 6. Summary of electrochemical data for derivatives of radical **19** in CH₂Cl₂.

4-X	3,5-X ₂ '	$R^+ \rightleftharpoons R^\bullet$	$R^\bullet \rightleftharpoons R^-$
H	H	-0.32 V	-1.90 V
Cl	H	-0.30 V	-1.84 V
OCH ₃	H	-0.53 V	-2.04 V
CH ₃	H	-0.42 V	-1.93 V
OH	H	-0.58 V	-1.82 V
CO ₂ H	H	-0.22 V	-1.34 V
NO ₂	H	-0.25 V	-1.80 V
H	OCH ₃	-0.34 V	-1.87 V

CH₂Cl₂ Solvent; Reference: Ferrocene oxidation

As with the
half-wave po
(TMTP) met
correlations
complexities
of hydrogen
81 and 82 sh
be explained
it.

E

Figur
in CH

As with the hexamethoxy triphenylmethyl radicals, correlations between half-wave potential and literature sigma values of tetramethoxy triphenyl (TMTP) methyl radicals are poor, as shown in the least-squares fit of correlations in **Tables 7**; presumably, such difficulties reflect the complexities of reactions and conformational effects involved. The effects of hydrogen bonding in CV are not completely understood. The radicals **81** and **82** show the most dramatic departure from the series, which might be explained by the effects of hydrogen bonding and π -conjugation through it.

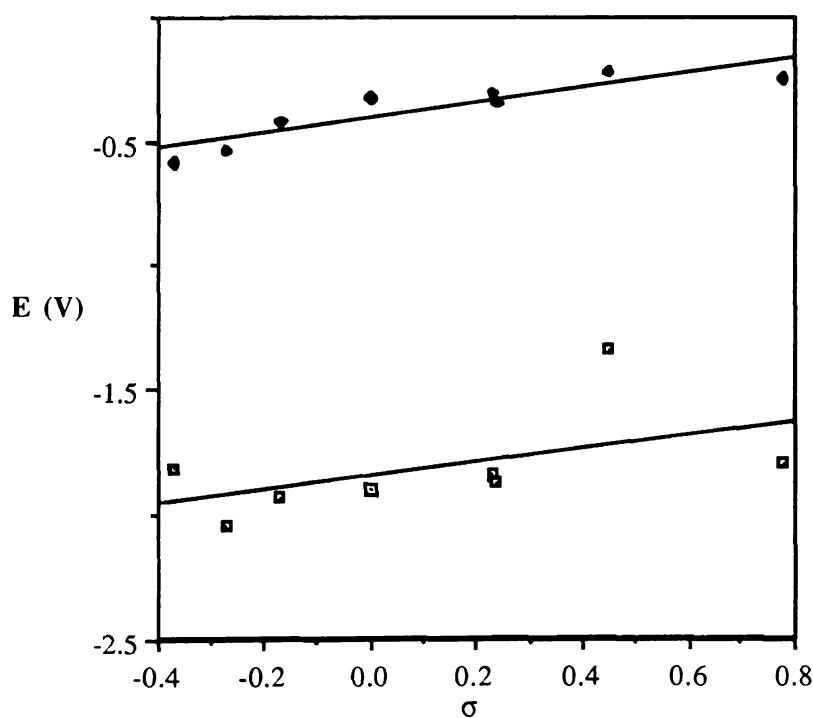


Figure 21. $\Delta E_{1/2}$ (V) vs σ in THF for TMTP methyl radicals in CH_2Cl_2 .

Table
potenti
 $E'_{1/2}$

σ (Cat

σ (Ani

^a Num

^c CH₂

Some of the
with simula
the spin der

Table 7. Least-squares fit of Correlation for half-wave potential and sigma values for derivatives of **77**. $\Delta E_{1/2} = \rho X - E'_{1/2}$

	ρ	$E'_{1/2}$	# ^a	R ^b
σ (Cation) ^c	0.2957	-0.4029	8	0.790
σ (Anion) ^c	0.2741	-1.8480	8	0.265

^a Number of experimental points used. ^b Correlation coefficient.

^c CH₂Cl₂ solvent.

Some of the typical EPR spectra are shown in **Figure 22, 23, 24** and **25** with simulations. The experimentally determined coupling constants a_i and the spin density ρ_i are summarized in **Table 8**.

Table 8. A summary of ^1H hyperfine constants a_i (in Gauss) for coupling with meta and para proton in TMTP methyl radicals.

	$a_{\text{ortho}} (\#)$	$a_{\text{meta}} (\#)^2$	$a_{\text{para}} (\#)^2$	$ \rho_{\text{ortho}} ^1$	$ \rho_{\text{meta}} ^1$	$ \rho_{\text{para}} ^1$
77		0.91 (4)	1.00 (2)		0.040	0.044
4	4.30 (2)	1.50 (2)	4.96 (1)	0.191	0.067	0.220
5	4.09 (2)	1.51 (2)	4.67 (1)			
78		0.9 (4)	1.0 (2)		0.040	0.044
4	4.2 (2)	0.7 (2)		0.187	0.031	
84 ³		0.8 (4)	1.1 (2)		0.035	0.049
4	4.8 (2)		3.2 (1)	0.187		0.142

¹ $|\rho_{\text{exp}}| = |a/22.5|$ ²numbers of protons in each position.

³Radicals **79**, **80**, and **83** shows similar results. ⁴Asymmetric ring protons coupling constants in TMTP methyl radicals.

⁵Determined by Ishizu and Mukai using ENDOR in toluene.¹³⁸



Figure 23. EPR spectrum of **77** in toluene with simulation (top).

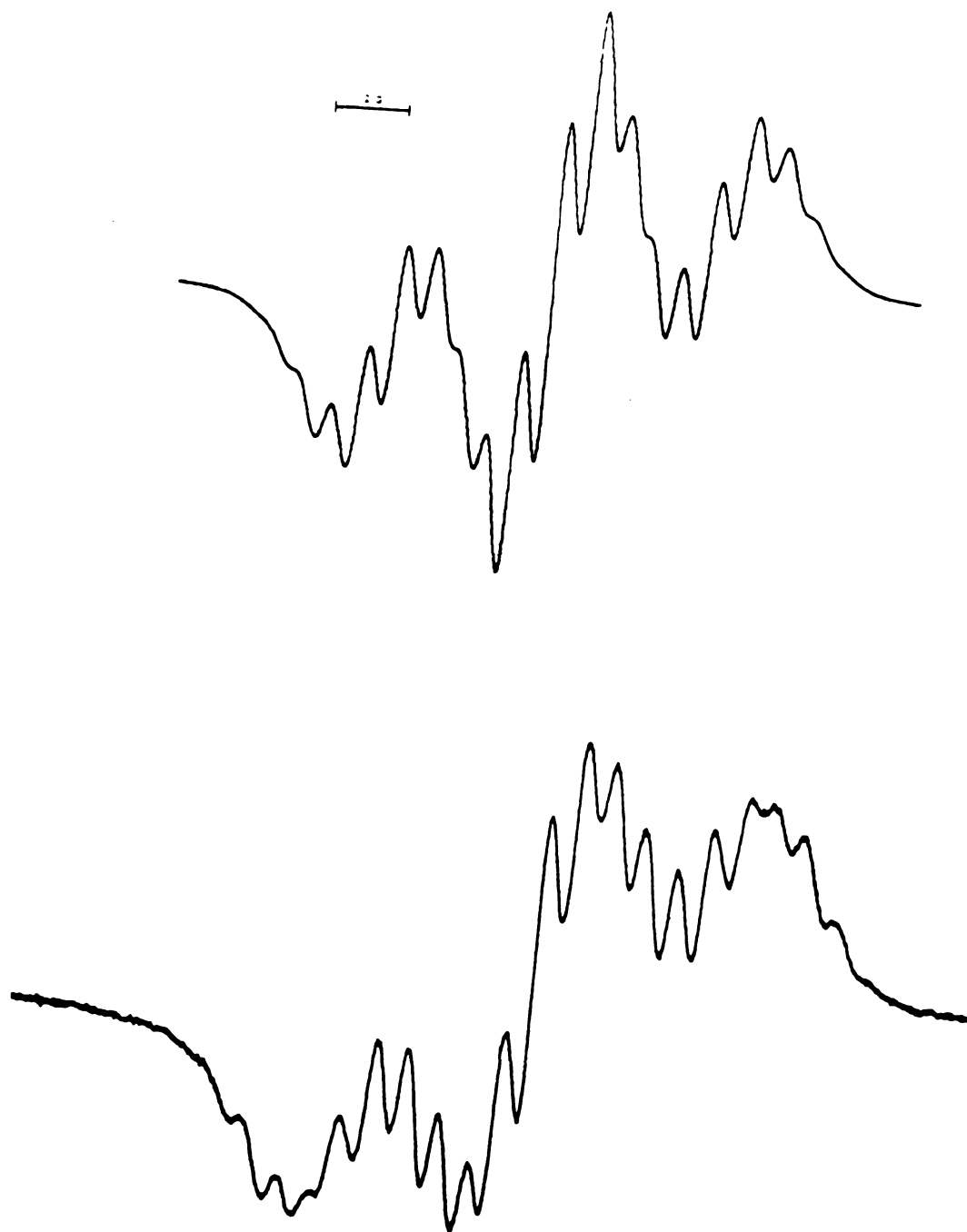


Figure 24. EPR spectrum of **78** in THF with simulation (top).

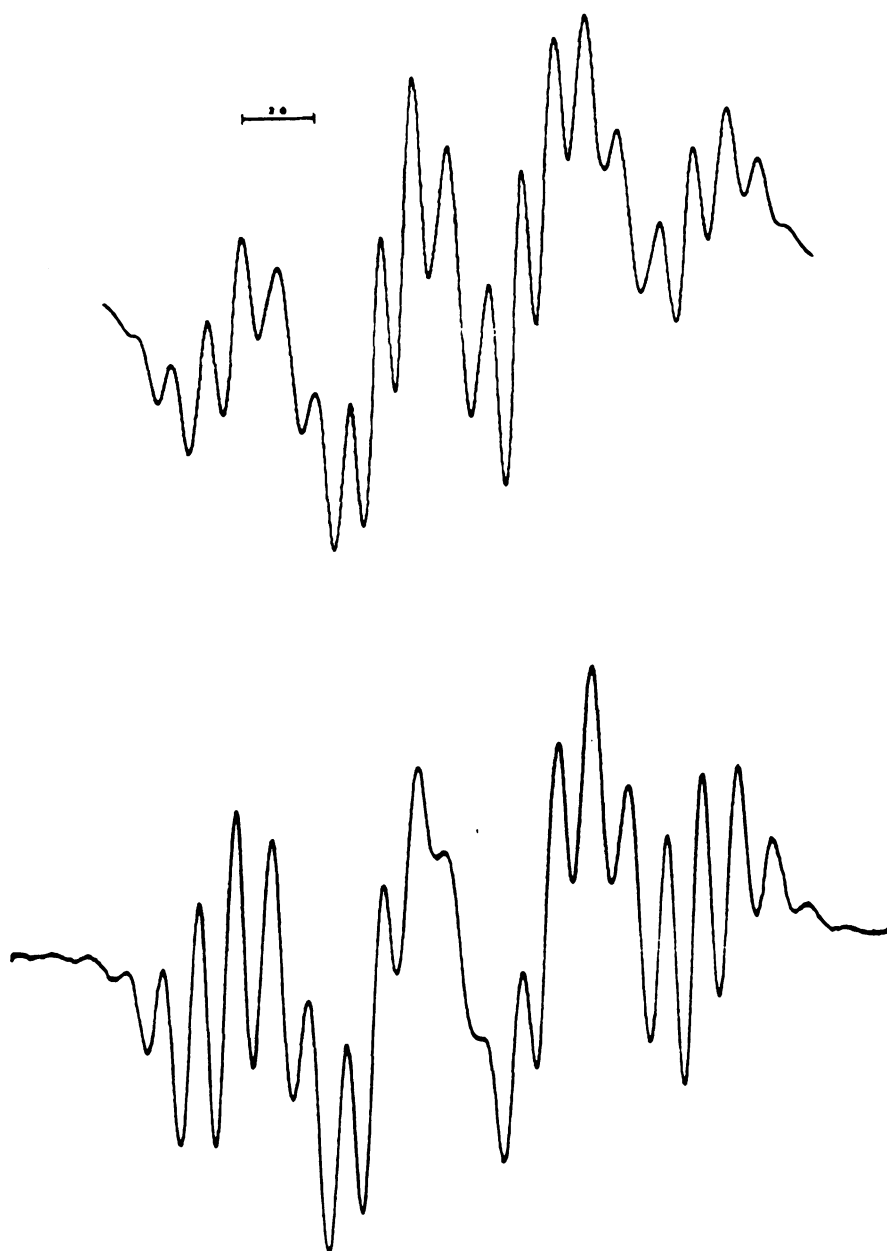


Figure 25. EPR spectrum of **84** in THF with simulation (top).

2.4. Rotational Barriers

Triaryl-X propellers, both planar and pyramidal, are well known to exhibit barriers to aryl ring rotation. Some of the triaryl systems constructed in this work and related studies show pairs of methoxy proton resonances at room temperature which are interpreted to indicate ring rotation that is slow on the NMR timescale. We thought that it would be useful to determine rotational barriers for relevant systems to have a better understanding of the structures of our systems in solutions. The rotation barriers of the aromatic rings in the **71** and **73** have been studied by Rieker and Kessler using ^1H NMR and found to be less than 8.2 kcal/mol for carbinol **71** and 11.1 kcal/mol for methane **73**.¹⁵³ The silane **74** in which the central carbon in methane **73** is replaced by Si crystallizes on a three-fold axis so that all three rings are equivalent. There are two independent molecules in the unit cell and they have twist angles of 30 and 33° respectively. It is worth adding that the methane **73** crystallizes in the same space group as the silane and has similar ring twists (27°). Due to its single intramolecular hydrogen bond (one of the methoxy groups is twisted 75° out of the ring plane because of the hydrogen bond), carbinol **71** has a lower symmetry in the solid state (Pbca space group).

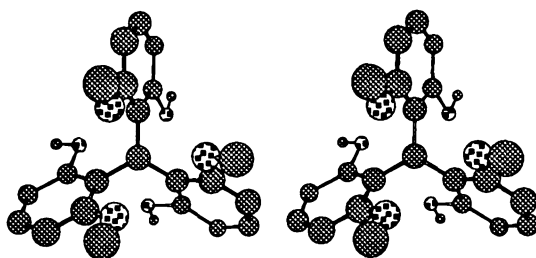


Figure 26. X-ray structure of methane **73**.

Variable temperature ^1H NMR studies have been conducted over the temperature range of -90°C to $+100^\circ\text{C}$ using the Varian VXR 300 NMR instrument in toluene- d_8 or CDCl_3 solvent to observe coalescence of two methoxy resonances in systems with doubled methoxy proton peaks at room temperature and therefore restriction of free rotation of rings. The results are consistent with a site exchange process resulting from the rapid flipping of the aryl rings on the NMR time scale. The value of the rotational barrier has been determined by applying the Gutowsky-Holm approximation to the observed methoxy group site exchange at the coalescence temperature (T_c in K).¹⁵⁴

For an exchange process between two nuclei A and B with a mutual coupling J_{AB} with peak separation of $\Delta\nu$ in Hz, the rate constant k_c at the coalescence temperature T_c is given by:

$$k_c = 2.22\sqrt{\Delta\nu^2 + 6J_{AB}^2}$$

From the Eyring equation, one can determine the free energy of activation by using the following equations. To calculate the activation barrier, we need a pair of k_c and T_c . k_B is the Boltzmann constant, κ is a transmission coefficient usually assumed to be 1, and h is Planck's constant.

$$k = \kappa \frac{k_B}{h} e^{-\Delta G^\ddagger / RT}$$

$$\Delta G_c^\ddagger = 4.58T_c(10.32 + \log \frac{T_c}{k_c}) \text{ cal / mol}$$

$$\Delta G_c^\ddagger = 19.14T_c(10.32 + \log \frac{T_c}{k_c}) \text{ J / mol}$$

The activation barriers, ΔG^\ddagger , for aryl ring rotation of tris(2,6-dimethoxyphenyl)methyl ammonium tetrafluoroborate **72**, tris(2,6-dimethoxy-3,5-dichlorophenyl)methylammonium tetrafluoroborate **75**, and tris(2,6-dimethoxy-3,5-dichlorophenyl)methane **76** were 12.67 ± 0.3 kcal/mol-1, 15.7 ± 0.8 kcal/mol, and 17.3 ± 0.8 kcal/mol, respectively.

Table 9. Variable Temperature NMR results for tris(2,6-dimethoxyphenyl)methyl ammonium tetrafluoroborate **72**, tris(2,6-dimethoxy phenyl)methane **73**, tris(2,6-dimethoxy-3,5-dichloro phenyl)methylammonium tetrafluoroborate **75**, and tris(2,6-dimethoxy-3,5-dichlorophenyl)methane **76**.

	72	73^a	75	76
$\Delta\delta\text{H (CH}_3\text{O, ppm)}$	0.63	---	0.254	0.331
(at T/K)	233	---	263	253
ΔG^\ddagger (kcal mol ⁻¹)	12.67	11.1	15.68	17.27
T_c (K)	273	216	323	358
k_c (s ⁻¹)	419	---	169	220
$\Delta\nu$ (Hz)	189	33	76.2	99.3

^aDetermined by Rieker and Kessler in CDCl₃.

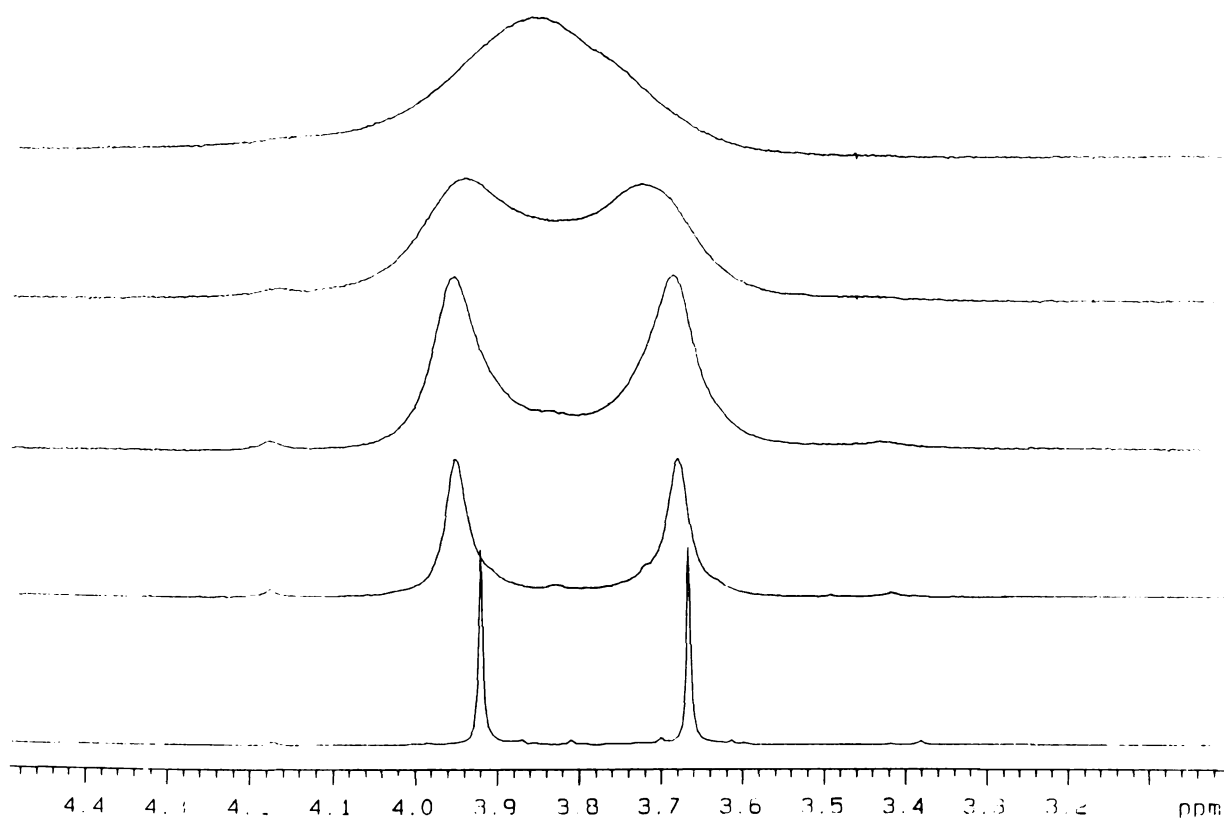


Figure 27. 300 MHz ^1H NMR signals of the methoxy protons in hexachloro tris(2,6-dimethoxyphenyl)methyl ammonium BF_4 **75**, recorded at different temperature. For slow rotation two peaks are obtained, whereas for fast exchange there is only one. In the intermediate range the signals are broadened. The coalescence temperature T_c is 50°C . (-10 , 20 , 30 , 50°C from the bottom)

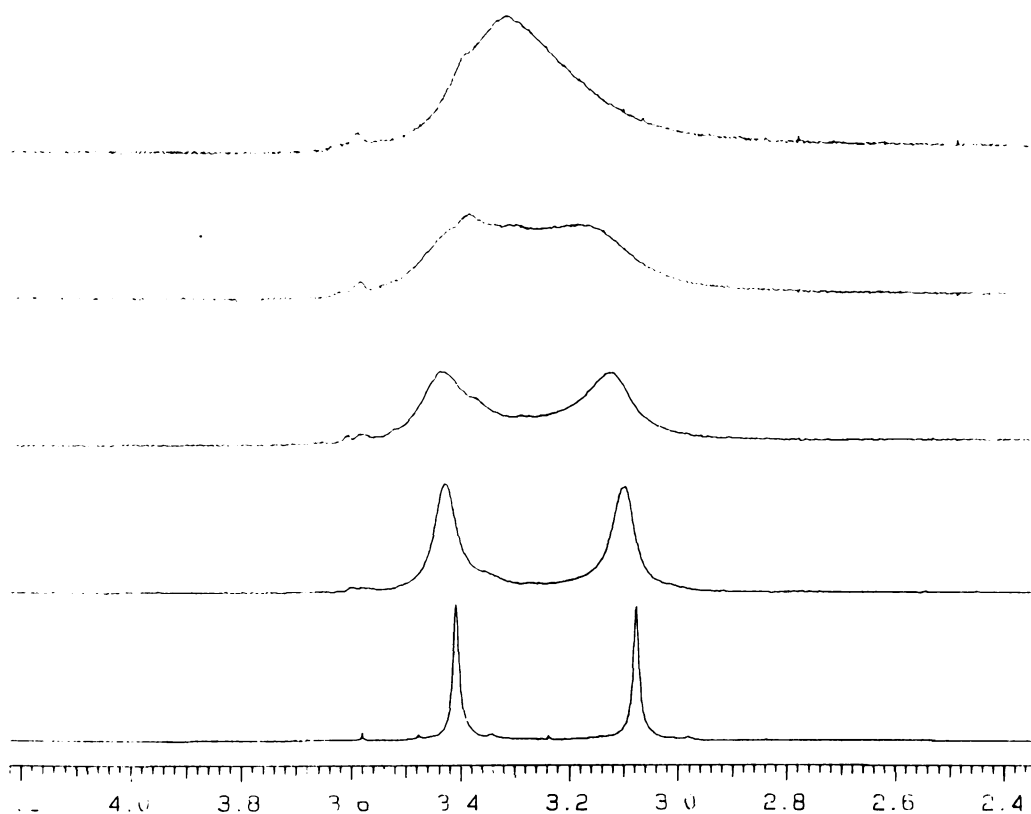
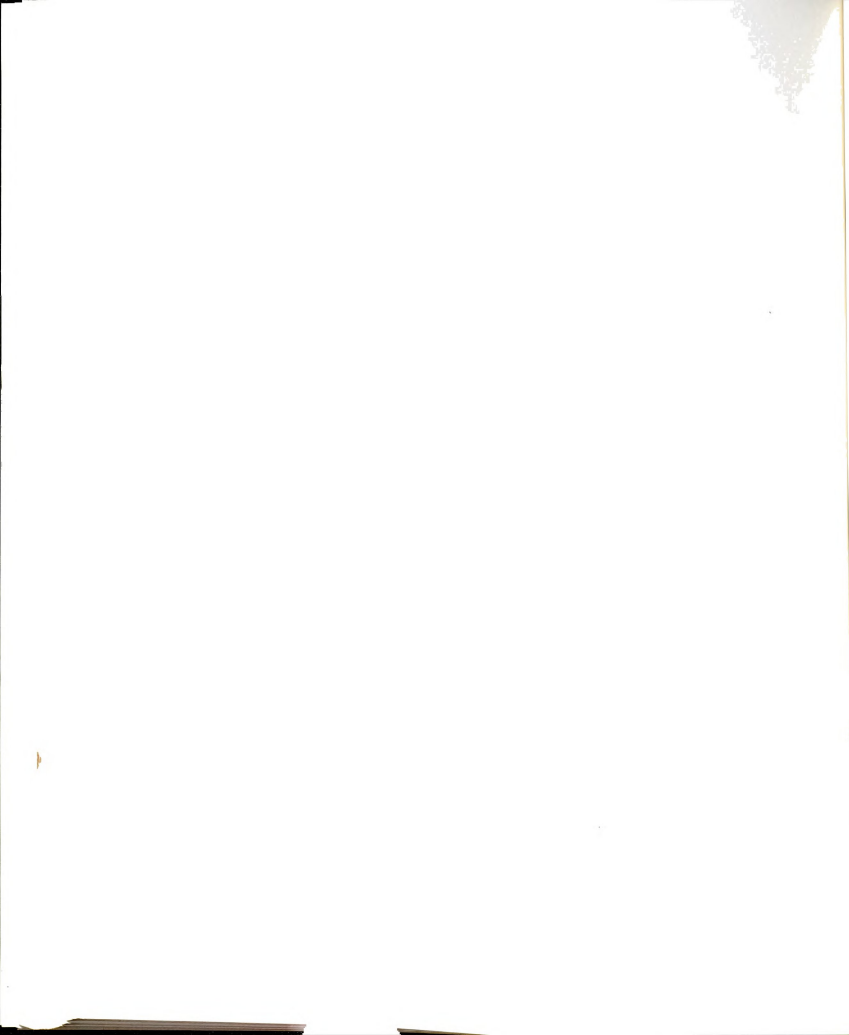


Figure 28. 300 MHz ^1H NMR signals of the methoxy protons in hexachloro tris(2,6-dimethoxyphenyl)methane **76**, recorded at different temperatures. For slow rotation two peaks are obtained, whereas for fast exchange there is only one. In the intermediate range the signals are broadened. The coalescence temperature T_c is 100°C for the methane. (20, 40, 60, 80, 100°C from the bottom)



Unlike **72**, **75**, and **76**, HMTP carbinol **71**, and HMTP silane **74** do not show splitting of methoxy ^1H resonances at 300MHz even at -90°C . These results are consistent with a faster flipping of the aryl rings than NMR timescale even in carbinol **71** in which we believe that there is a hydrogen-bond between one of the methoxy oxygens and the hydroxy proton at the temperature. We may understand why the carbinol **71** has a lower barrier for rotation than the methane **73** using "the two-ring-flip mechanism" of Mislow. The formation of the hydrogen-bond would fix the twist angle of ring in a "vertical" orientation, making it easier to rotate the other two rings appropriately in carbinol **71**. By assuming the methane **73** as a worst case of all the triaryl methyl systems studied as far as rotation barrier of rings (except the case of **72**, in which the methoxys are twisted), it would be safe to say that the activation barriers for the rotation in these systems are smaller than 11.1 kcal/mol in solution of CDCl_3 and toluene- d_8 .

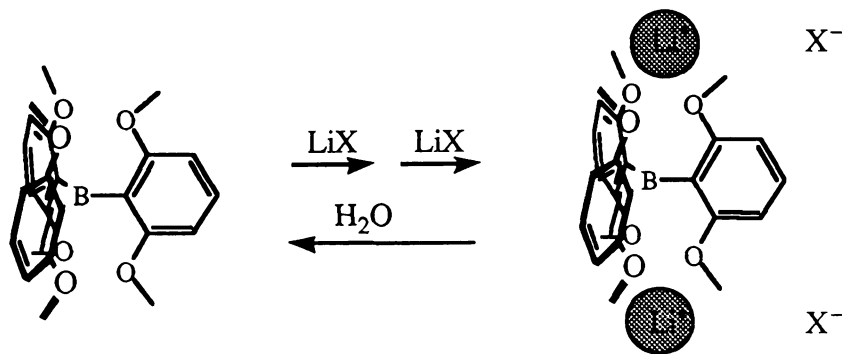
The rotation of rings in **71** and **72** would result a cleavage of the hydrogen-bonding interactions. We expected that the rotation barrier for methoxy groups in these systems will reflects the strength of these interactions. The carbinol **71** does not show any splitting of the methoxy proton signals at -90°C in toluene- d_8 . The difference between the rotation barrier of **72** and **73** is only 1.6 kcal/mol which might reflect the strength of these interactions. It is difficult to understand why they show such a small difference when **72** has three hydrogen-bonding interactions in the solid state compared to **73** which does not have any.

3. Ion-Bindings

Operating on the supposition that the relaxation of ^7Li nuclei ($S=3/2$) would be considerably shorter in the complex $\mathbf{1}\cdot\text{LiBF}_4$ than in uncomplexed mixture, Jackson and Kahr compared the line widths of the solid state ^7Li -NMR spectra for the precipitated solids with pure LiBF_4 salts. The ^7Li line widths in the reported complexes were 16 kHz at half height as opposed to 500 Hz in the pure salts. Jackson and Kahr interpreted these changes in terms of a specific binding interaction between radical $\mathbf{1}$ and the ^7Li ions in the precipitated solids; however these results do not exclude other nonspecific broadening mechanisms.

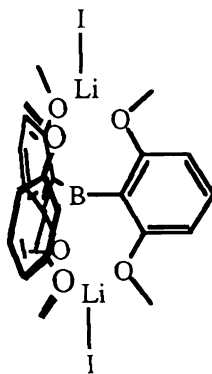
3.1. Borane

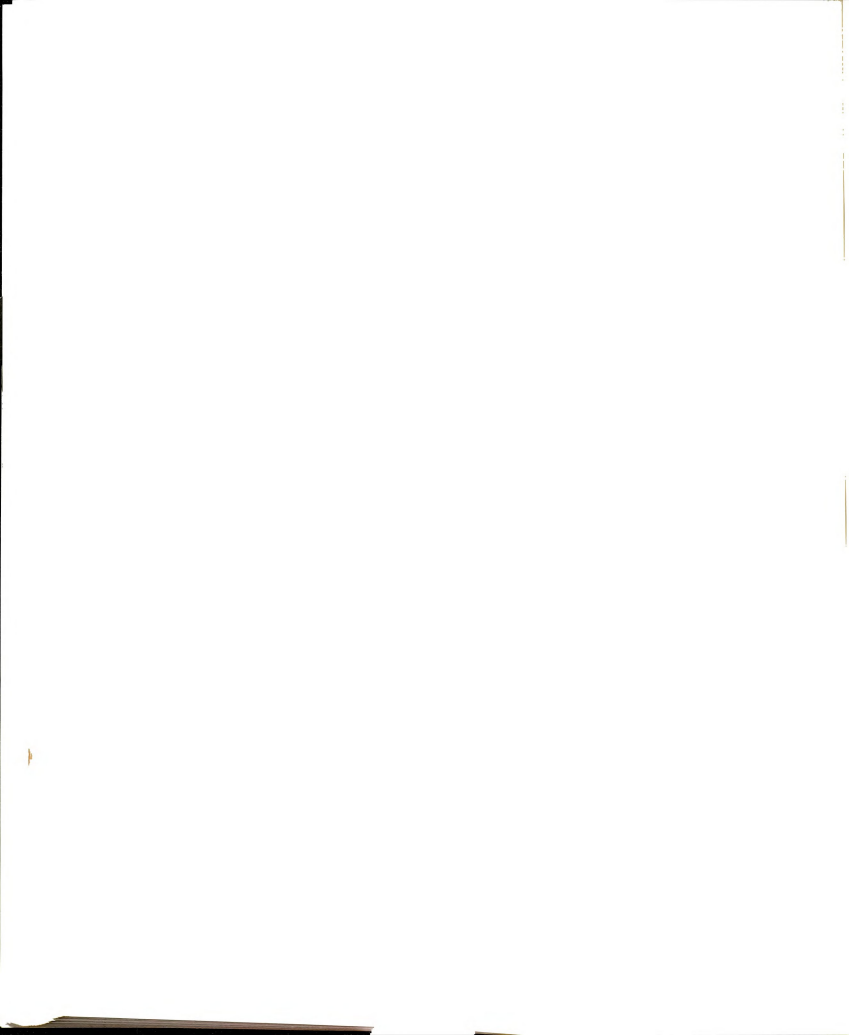
Small metal cation binding studies of borane $\mathbf{63}$ by UV-Vis spectrophotometry suggest ion-binding, consistent with the notion of stack formation. Similar UV-Vis studies of $\mathbf{1}$ are hindered by the Li^+ catalyzed oxidation reaction which yields the intensely colored cation $\mathbf{62}$.



UV-Visible spectrophotometry provides a useful probe of the binding of small metal cations by radical **1** and borane **63**. The long-wavelength maxima in each of these species in ether, THF, CH_2Cl_2 , and CH_3CN are markedly diminished in intensity by addition of solutions of lithium salts (LiBF_4 , LiClO_4 , LiSCN). Washing the complex solutions with water recovers the original species' spectra. Analogous spectral changes are not seen in solutions of anisole or *m*-methoxyanisole upon treatment with lithium salts; the only observed changes correspond to simple dilution of the sample solutions. We interpret these observations in terms of the binding of small metal cations to the triaryl propellers **1** and **63**, which alters their absorption spectra. These ligands are apparently not such efficient ion binders that they can compete with bulk H_2O ; hence the observed reversibility upon washing as shown in **Figure 29**.

Ion binding studies by NMR on the borane using various Li and Na salts in various solvents do not show significant changes except in the case of $\text{LiI} \cdot \text{Borane}$ which is still small (0.02 ppm changes under very anhydrous conditions) presumably because of the very low binding constant involved.





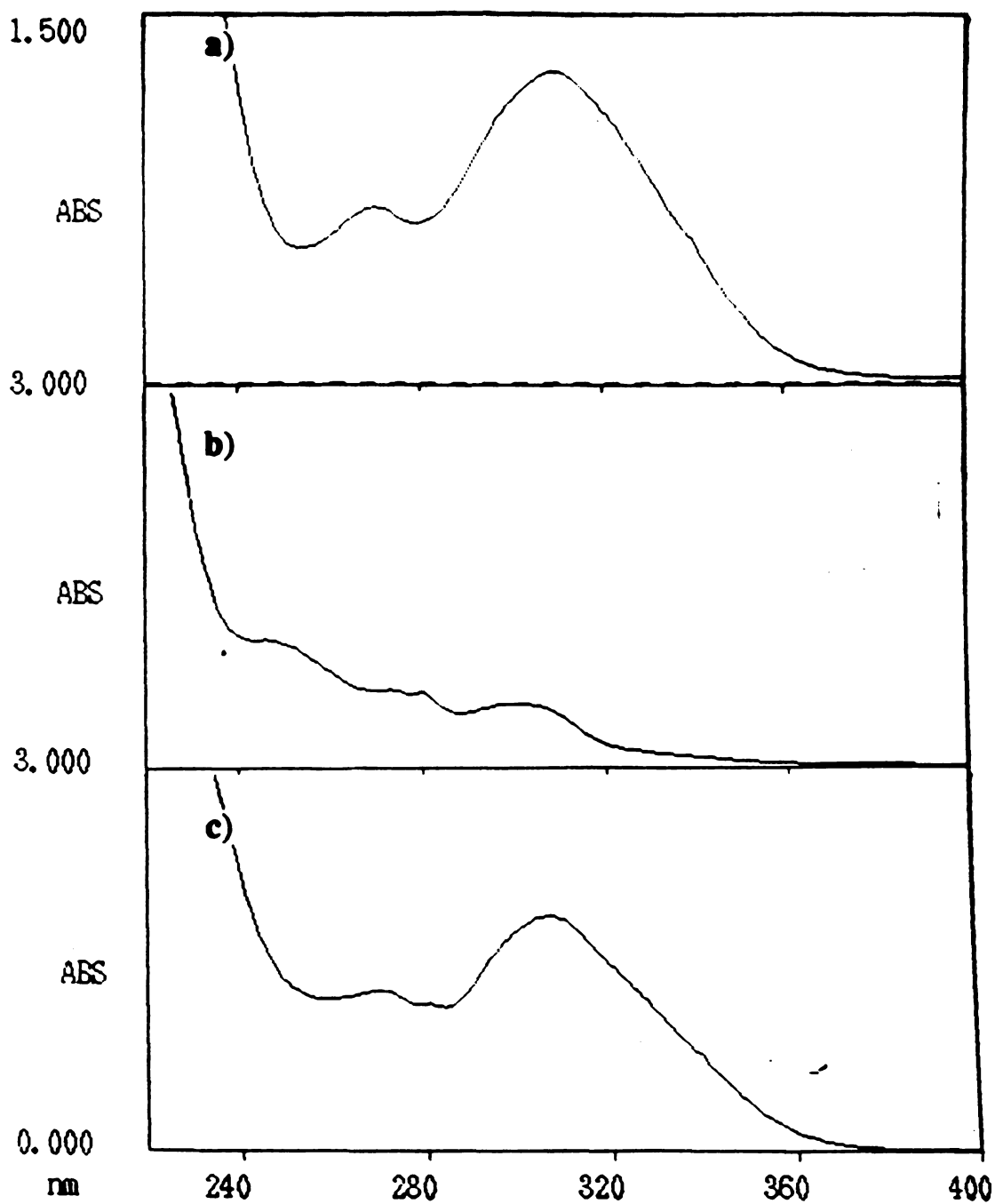
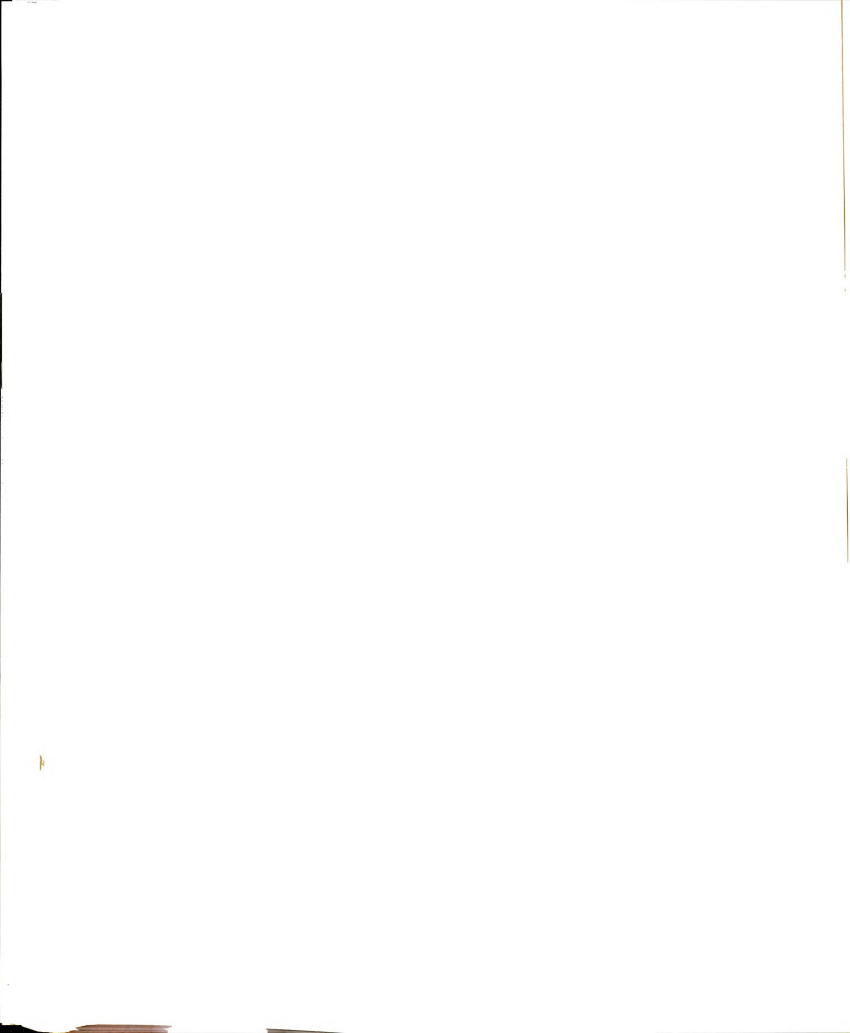


Figure 29. UV-Vis spectra illustrating reversible Li^+ binding in CH_2Cl_2 . (a) Borane **63** alone; (b) Mixture after addition of LiBF_4 solution; (c) Organic layer after H_2O wash.



The FAB Mass spectrum give one more piece of evidence for a notion of binding of radical **1** with metal cation. It shows RMR peaks in the case of NaBPh₄ complex of radicals **1** and **68** which means that the complex formed by simple mixing of salts with radical is strong enough to remain intact through the FAB ionization process even if it only shows very little changes in other spectroscopy.

JS02180005 Scan 2 RT=0:38 100% 410000 mv 19 Feb 93 14:54
Compacted SLRP +EI SA70 (NBA)

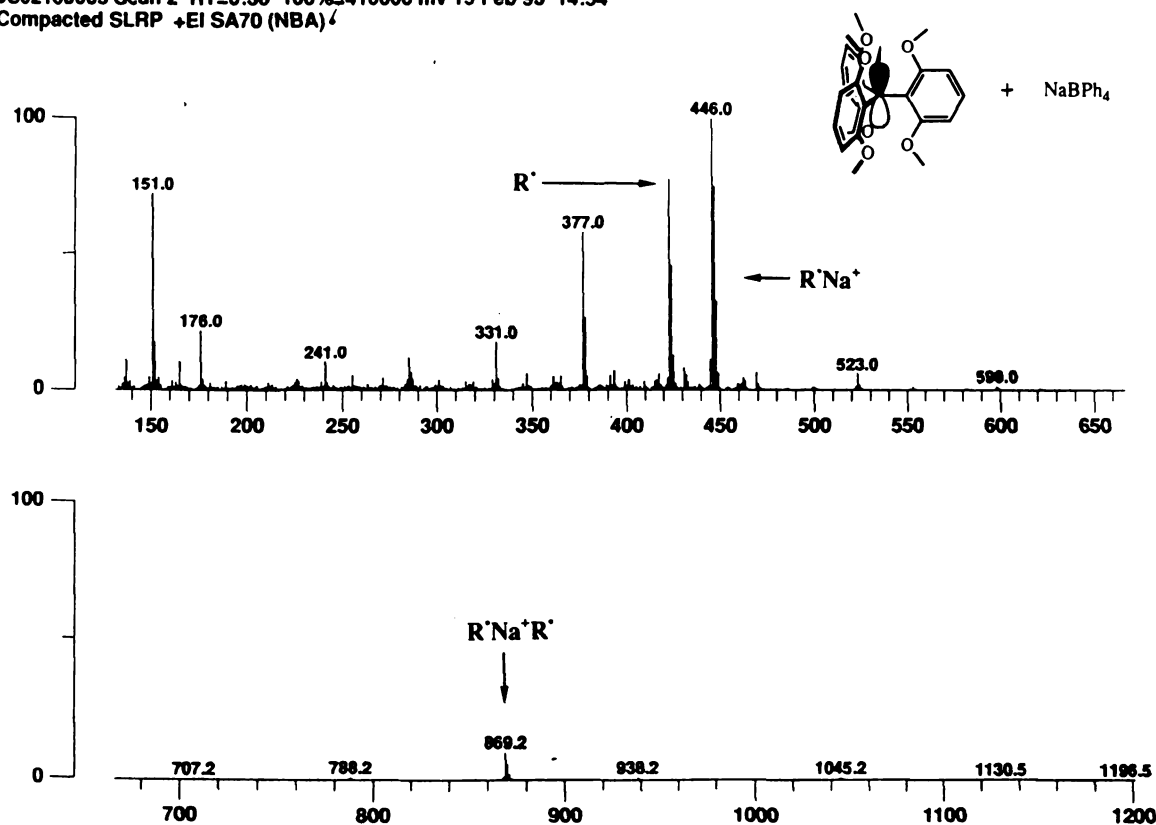
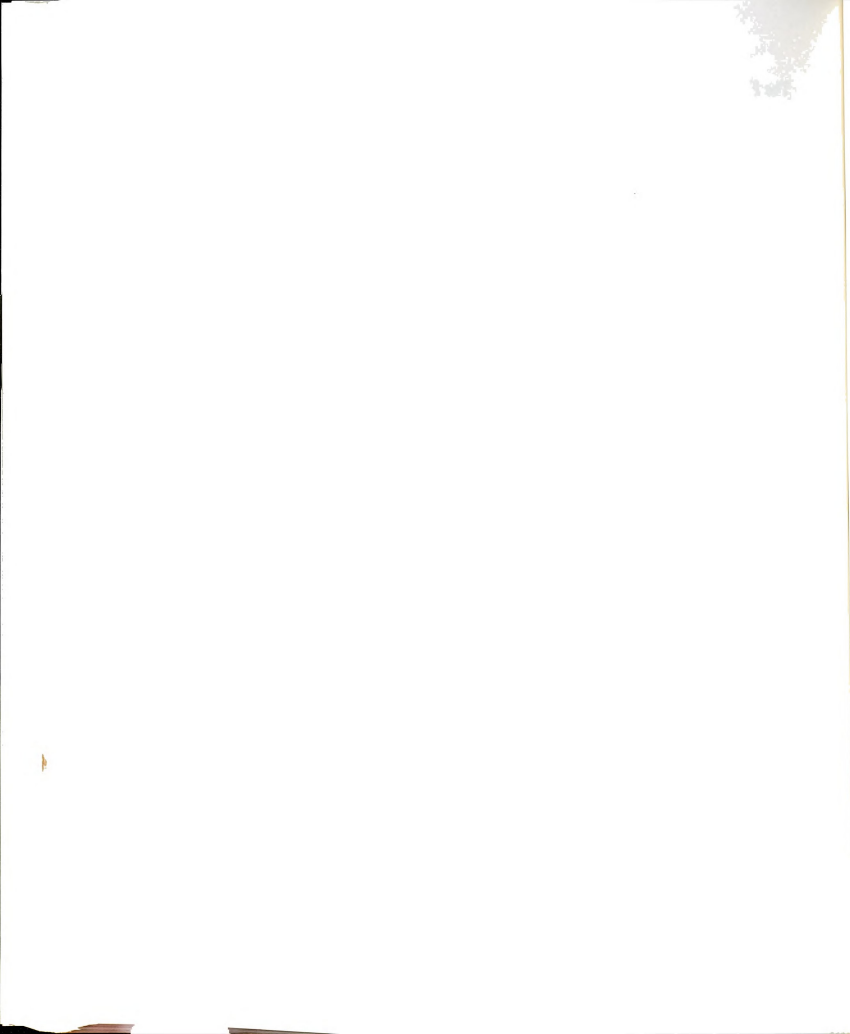
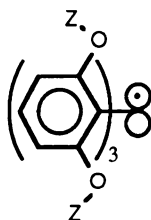


Figure 30. Mass Spectrum of dimer 2 of $1 \cdot Na^+ \cdot 1$ (869) in *m*-nitrobenzylamine matrix.



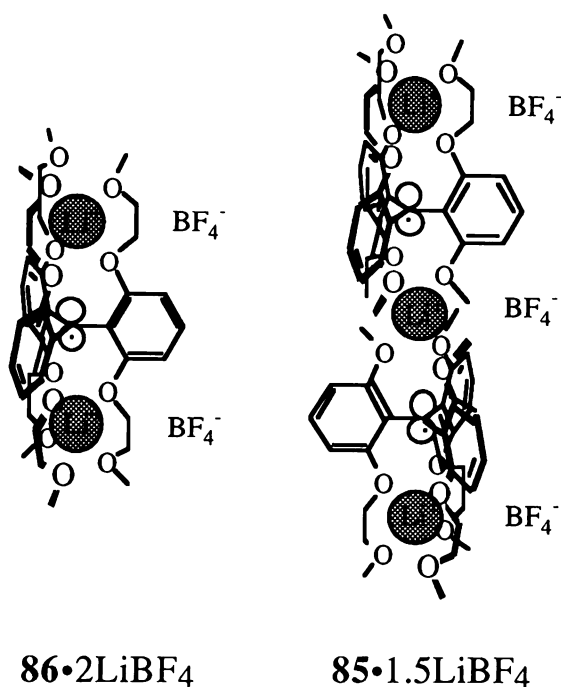
3.2. Double faced Paramagnetic Ionophore

Substitution of Z for the methyl groups shown below in **1** allows for a whole range of new radicals to be synthesized. By controlling the size, electron withdrawing/releasing properties, and ligand capabilities of Z, the ion binding properties of **1** can be varied. Synthetically, the Z-sites are certainly the easiest to substitute; resorcinol (3-hydroxyphenol) and 3-methoxyphenol are commercially available starting materials, and Williamson ether synthesis provides a straightforward means for attaching many possible Z's.



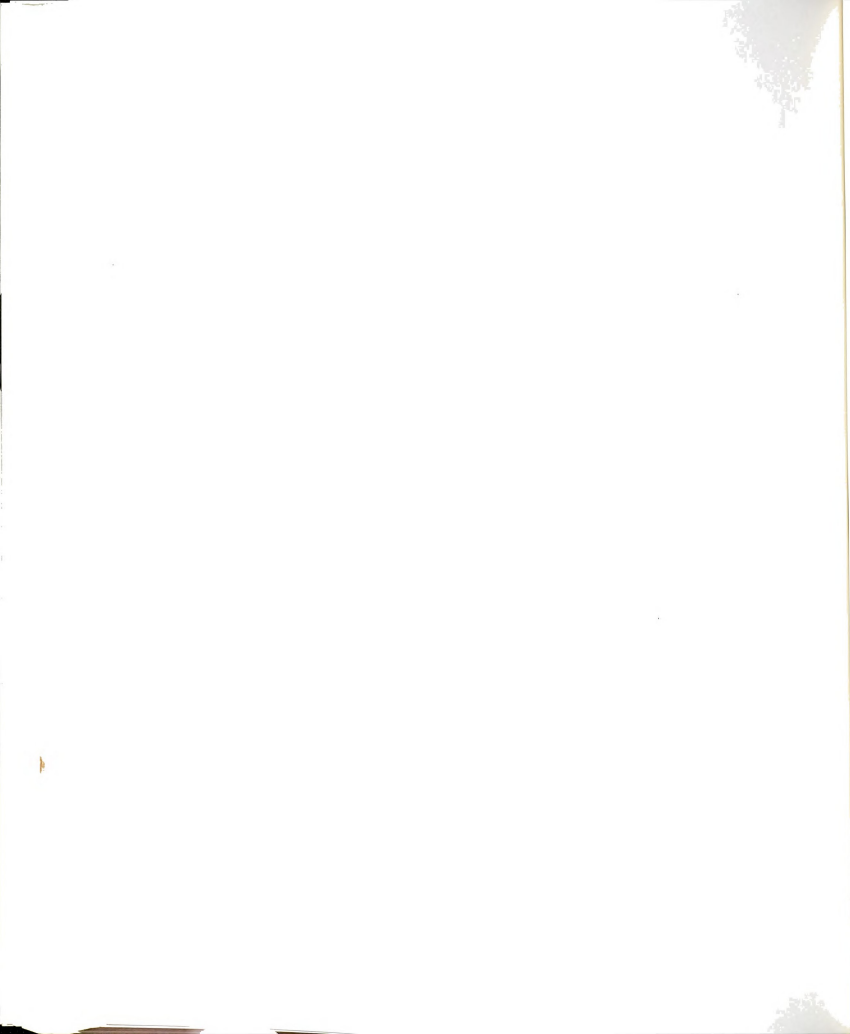
The theme of two radicals sandwiching a metal ion can be inverted in a complex with two metals fixed around a single radical center.

To evaluate the validity of our electron-coupling strategy, it would be useful to know the dimensions and the spin density on the bound metal cation. From such data it should be possible to estimate limiting magnitudes for the exchange coupling which could occur through the metal ion couplers in the hypothetical structure.



We have recently reported¹⁵⁵ the radical **86**, a double "octopus" analogue of **1**.¹⁵⁶ This work addresses the spin density questions and simultaneously provides structural insight into the novel two-faced binding properties of the hexamethoxy-triaryl complexants. In parallel with the studies of **86**, radical **85** has also been built, with the aim of making a radical with one face closed to chain formation.

Radicals **85** and **86** were synthesized by straightforward modification of Martin's original procedures. Unlike **1**, compounds **85**, **86**, and their related triarylmethanol precursors are oils. Purification in this system is most conveniently achieved by crystallizing tetrafluoroborate salts of the corresponding triarylmethyl cations; these are subsequently reduced to make the neutral radicals. CW-EPR spectra collected for **86** at -70°C showed a 13-line pattern with the splitting between consecutive lines being 1.0 gauss. **Figure 29** shows the experimental and simulated CW-EPR spectra of **86**.



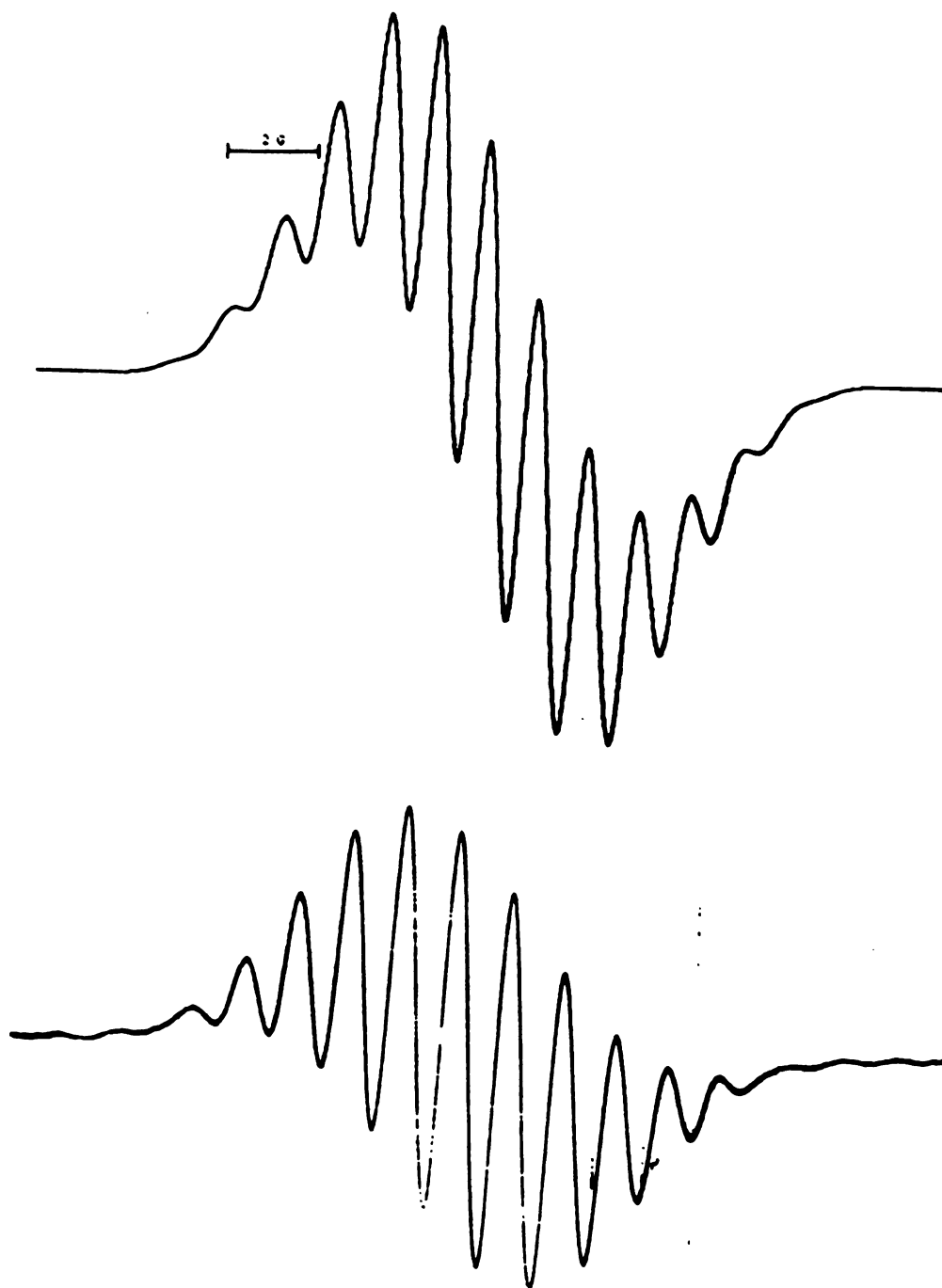
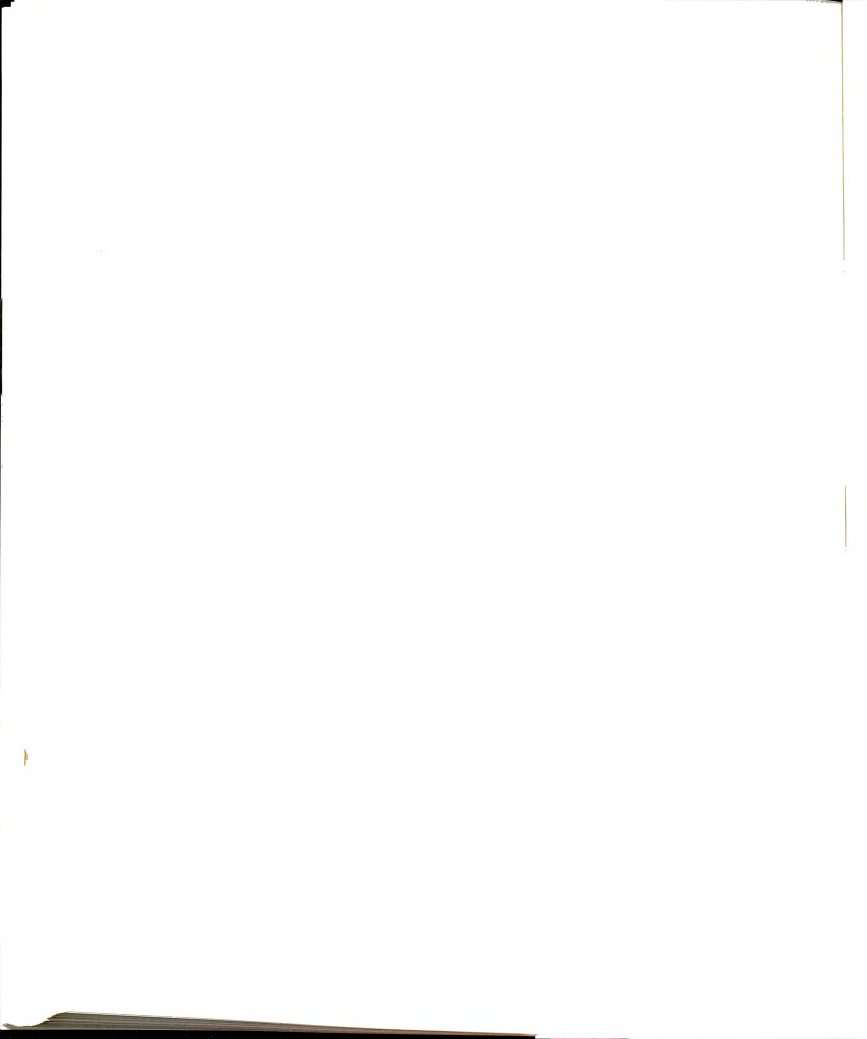
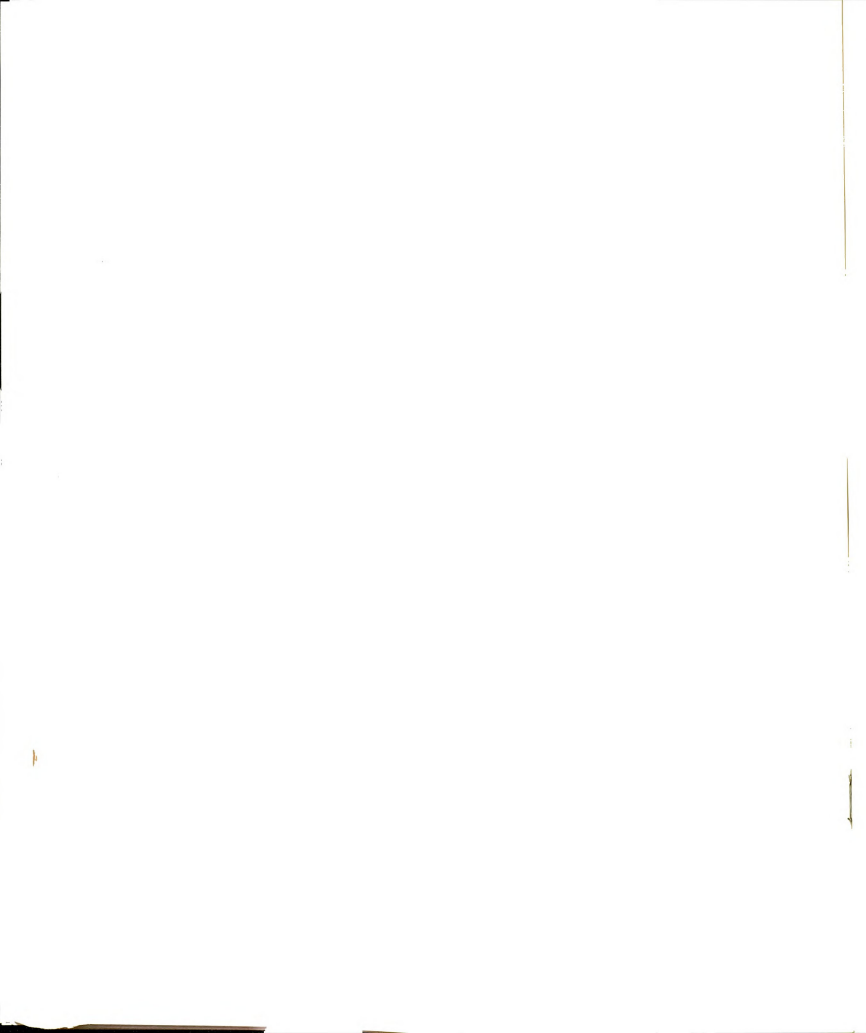


Figure 31. EPR spectrum of **86** with simulation (top).



Our purpose in synthesizing **86** was to build an analogue of **1** which could not form extended chains by pairing around metal cations as in dimer **2**. Radical **86** offers a bound Li^+ ion a full coordination sphere of six ether oxygens, effectively "capping" the radical on both faces. Thus, the radical center in $\text{86} \cdot 2\text{LiBF}_4$ is encapsulated and should behave as a completely isolated paramagnet. Like **1**, radicals **85** and **86** show some tendency toward oxidation on treatment with small metal cations in air. This behavior is evidenced by the appearance of the blue color of the corresponding triarylmethyl cation in each case.

The electron spin echo envelop modulation (ESEEM) technique of pulsed EPR spectroscopy has been used to measure weak electron-nuclear hyperfine coupling between the radical centers and coordinated metal cations in **86** in collaboration with Professor McCracken and Mr. Hong-In Lee. The ESEEM method provides structural details regarding radical-metal ion distance, the number of metal ions held near a given radical center, and an estimate of the unpaired electron spin density transferred to the metal.



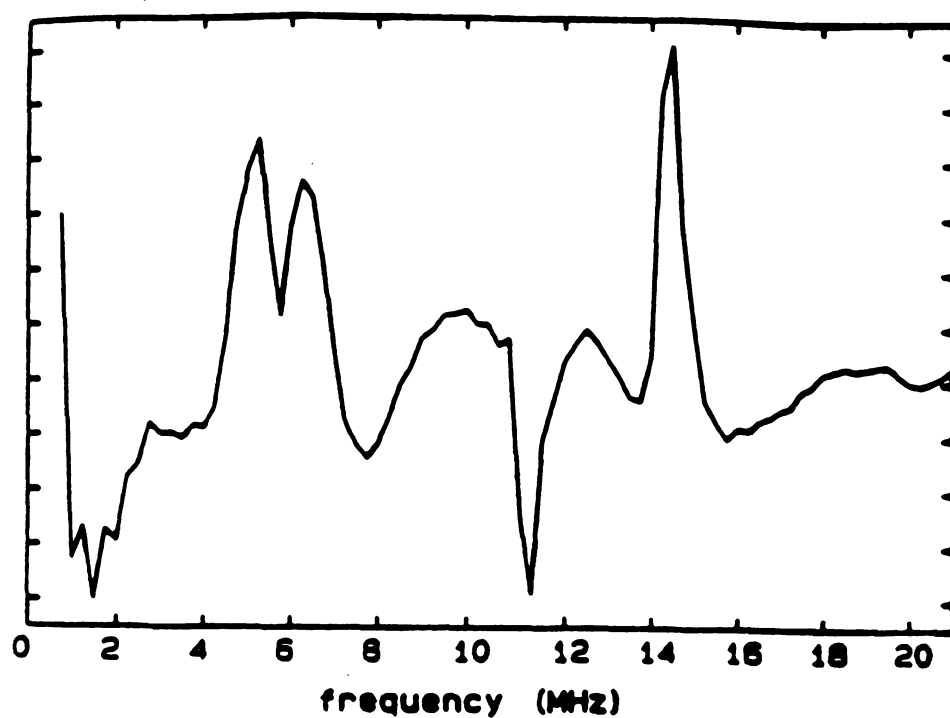


Figure 32. ESEEM spectrum of 86-LiBF_4 in 1:1 THF:Toluene at 4 K. The spectra are fourier transforms of time domain data collected under the following conditions: microwave frequency 9.346 GHz; magnetic field strength 3340 G; microwave pulse power 50W; pulse widths 16ns FWHM; two pulse excitation.



Addition of excess (10 equivalents) of LiBF_4 and NaBPh_4 to 10^{-6} M THF solutions of **86** results in complex **86**• 2LiBF_4 and **86**• 2NaBPh_4 . Because no new hyperfine couplings could be resolved in the CW-EPR spectrum after this treatment, the ESEEM technique was used to check for possible weak ^7Li hyperfine coupling to the paramagnetic center.¹⁵⁷ ESEEM data were collected on a home-built spectrometer described elsewhere.¹⁵⁸ A two-pulse (90° - τ - 180°) ESEEM spectrum collected at a microwave frequency of 9.35 GHz and a magnetic field strength of 3350 gauss is shown in **Figure 32**.

The prominent doublet centered at 5.6 MHz shows a splitting of 1.0 MHz. When ESEEM data were collected at 8.52 GHz with a field strength of 3052 gauss, the center of the doublet shifted to 5.0 MHz, consistent with its assignment to ^7Li . Also present in the spectrum of **Figure 32** are ^7Li sum and difference combination frequencies centered at 11.2 and 1.2 MHz, respectively, and a peak near 14.3 MHz due to weakly coupled protons. An analysis of modulation frequencies and depths using the formalism of Shuben and Diknov showed that this coupling arose from two $^7\text{Li}^+$ ions coupled to the radical center at an effective dipole-dipole distance of 3.5 Å and having an isotropic hyperfine coupling of 0.4 gauss.¹⁵⁹ Because the line width of the sum combination peak is independent of hyperfine anisotropy, the amplitudes and damping factors for the fundamental peaks (5.0 and 6.2 MHz) relative to that of the sum combination line can be used to determine the dipole-dipole distance.

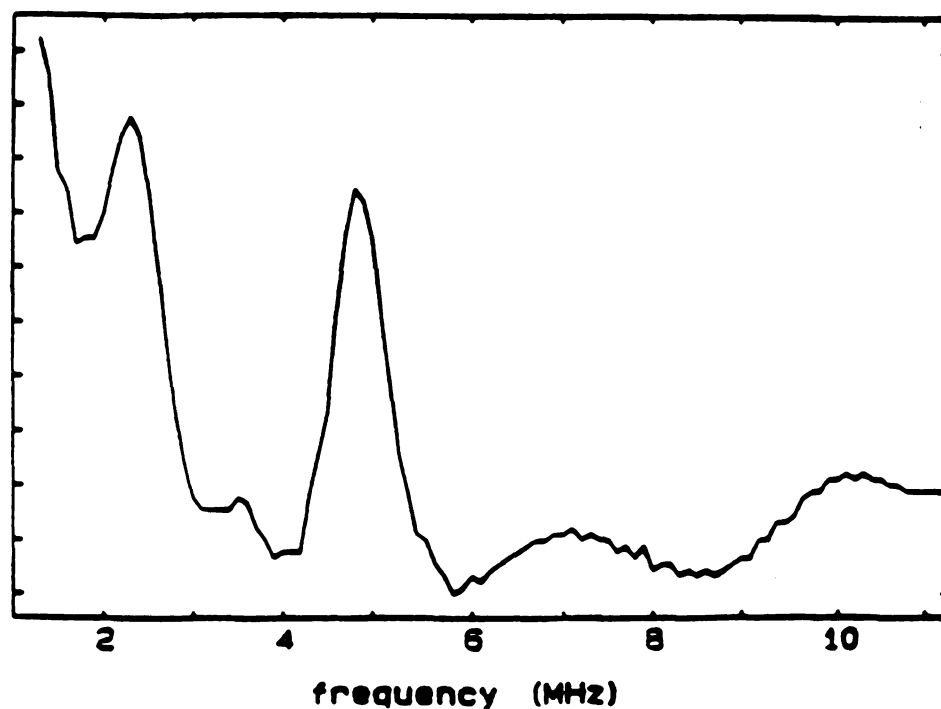
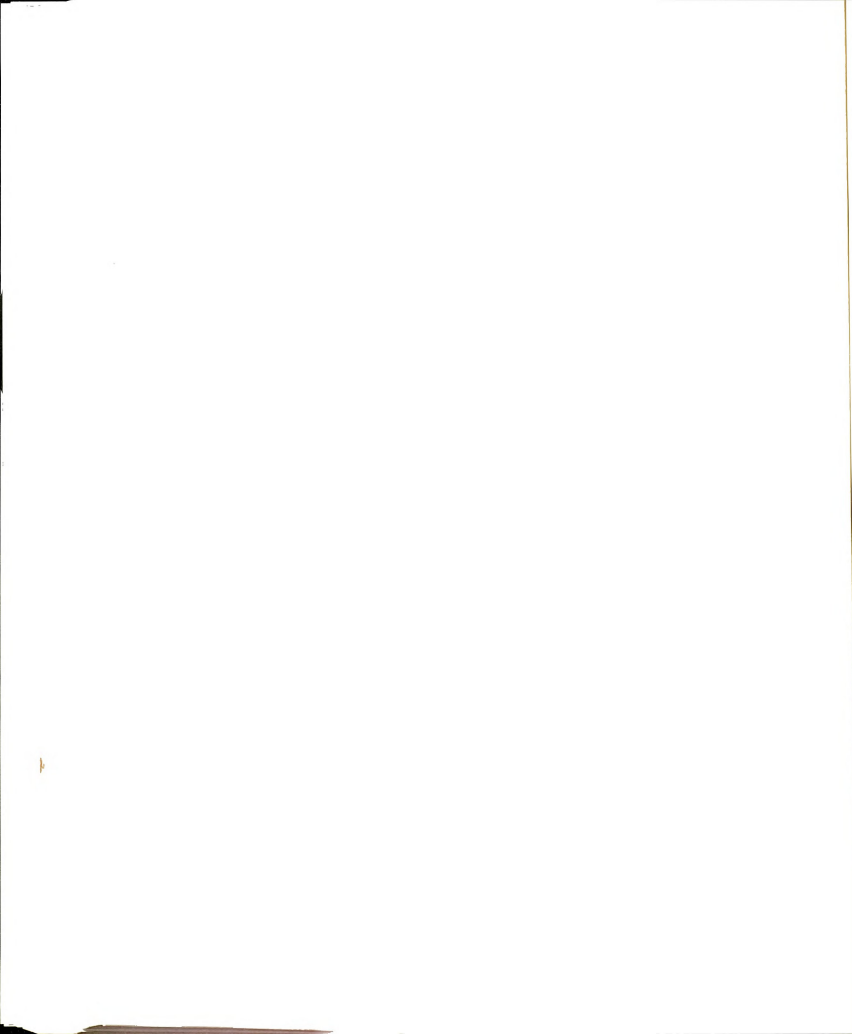


Figure 33. ESEEM spectrum of $86\text{-}2\text{NaBPh}_4$ in 1:1 THF:Toluene at 4 K. The spectra are fourier transforms of time domain data collected under the following conditions: microwave frequency 8.90 GHz; magnetic field strength 3195 G; microwave pulse power 25W; pulse widths 16 ns FWHM; and a τ value 147ns for a stimulated echo excitation sequence.

The absolute intensities of the lines can be used to determine the number of nuclei that give rise to the coupling. No coupling is seen to ^{10}B , ^{11}B , or ^{19}F nuclei of the BF_4^- counterions; thus the splittings do not simply arise via nonspecific coupling to magnetic nuclei near to the radical.

Analogous studies of $\mathbf{86} \cdot 2\text{NaBPh}_4$ and $\mathbf{86} \cdot 2\text{NaI}$ complexes gave similar findings; a stimulated echo spectrum of $\mathbf{86} \cdot 2\text{NaBPh}_4$ is shown in **Figure 33**. Two peaks centered at 3.6 MHz, the ^{23}Na larmor frequency, and split by approximately 2.5 MHz are observed. The lack of a pronounced sum combination peak in the two pulse ESEEM data precludes independent determinations of dipole-dipole distance and the number of coupled Na^+ ions. Computer simulations of these ESEEM data are consistent with an isotropic hyperfine coupling of 2.4 MHz, and an effective dipolar distance of 3.8 Å. Values for r_{eff} are calculated assuming that two Na^+ cations are coupled. If only a single Na^+ nucleus is coupled the calculated dipole-dipole distance decreases to 3.3 Å, a distance that seems unlikely based on CPK models and MNDO studies. Assuming that the ^{23}Na hyperfine coupling constants can be compared with their atomic values, unpaired spin densities of approximately 0.3% can be estimated for both Li and Na.¹⁶⁰ The Li^+ -radical center distances from ESEEM analysis using the point dipole-dipole approximation are in good agreement with those obtained from MNDO calculations. These results are summarized in **Figures 34, 35, and Table 10**.

A larger splitting of 6.0 MHz is also observed in the Na salt-treated samples of **86**. This result strongly suggests a complex with only one Na^+



bound, inducing pyramidalization at the radical center and hence decreased distance and increased overlap between radical center and Na^+ .

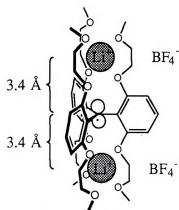


Figure 34. Summary of ESEEM spectroscopic and MNDO calculated results. CPK models yield similar geometrical characteristics.

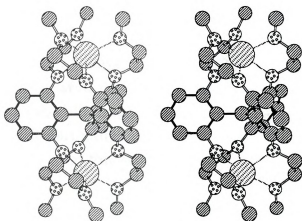


Figure 35. Stereo view of the MNDO calculated structure; the BF_4^- counterions were left out of the calculations.

Table 10. ESEEM Determined Complexation Data for **86** with Various Salts.

Salt	$A_{\text{iso}}(\text{MHz})$	$r_{\text{eff}}(\text{\AA})$	r_{MNDO}	#bound M^+	Spin Density on M^+
LiBF ₄	0.9	3.5 ± 0.2	3.45	2	0.3% ^a
LiI	1.0	3.4 ± 0.2	3.45	2	0.3% ^a
NaBPh ₄	2.4	3.8 ± 0.2^c	b	2	0.3%
NaI	2.4	3.8 ± 0.2^c	b	2	0.3%

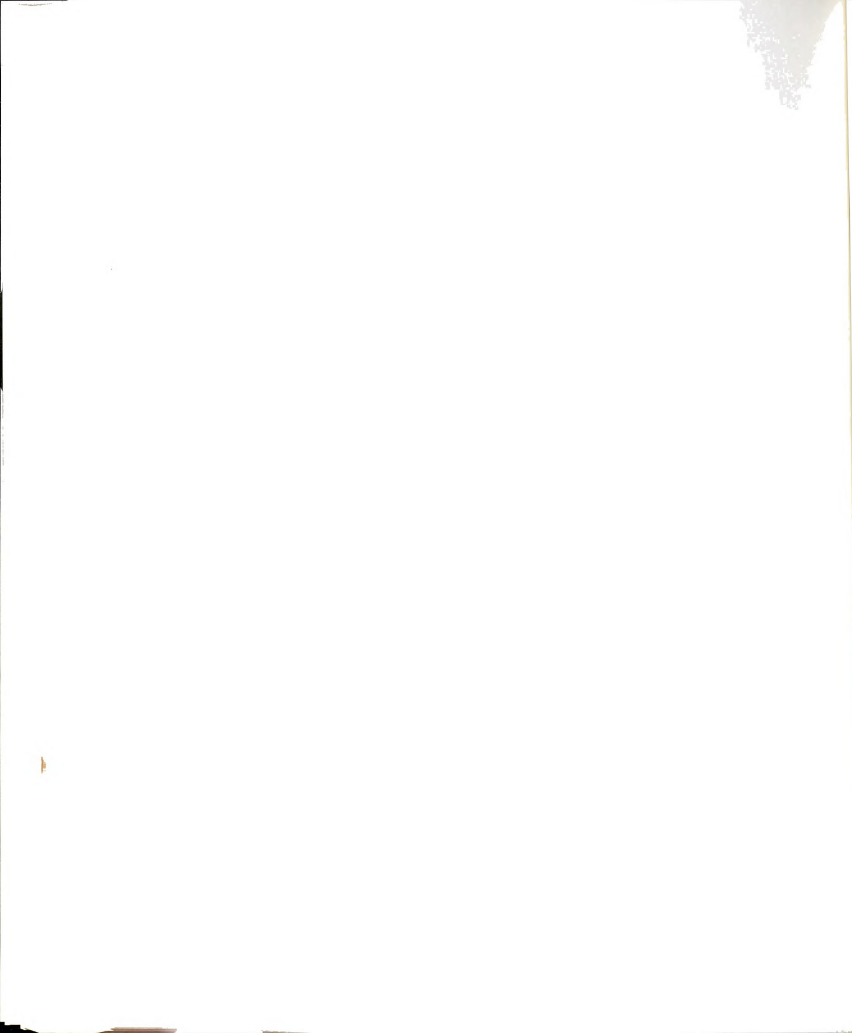
a. MNDO calculations used starting geometries generated from a simpler MNDO calculation on **1**•2LiF by "growing" the ether atoms in the expected lowest energy conformation, as evaluated using the Chem 3D molecular mechanics package. Optimization was carried out in D_3 symmetry, as suggested by calculation on **1**, the above complex, and related systems. MNDO calculates a spin density of 0.22% on the bound ^7Li ions, in reasonable agreement with experiment. Unfortunately, without suitable reference systems, we cannot judge the significance of this value.

b. MNDO parameters are not available for Na so these structures were not calculated. Attempts made using "sparkles" which represent Na^+ as a positively charged hard sphere gave unreasonable structures.

Electrochemical characterizations of **85** and **86** were accomplished via cyclic voltammetry (CV)¹⁶¹. The salts **85**⁺BF₄⁻ and **86**⁺BF₄⁻ (1 x 10⁻⁴ M) were studied in THF and methylene chloride solution using tetrabutylammonium tetrafluoroborate as a supporting electrolyte. Reversible reduction of each cation to the corresponding radical was readily measured; a second reduction wave (radical to anion) could also be observed when THF solutions of radicals were used instead of the cation salts. **Table 11** compares the observed reduction potentials for **1**, **85**, and **86**.

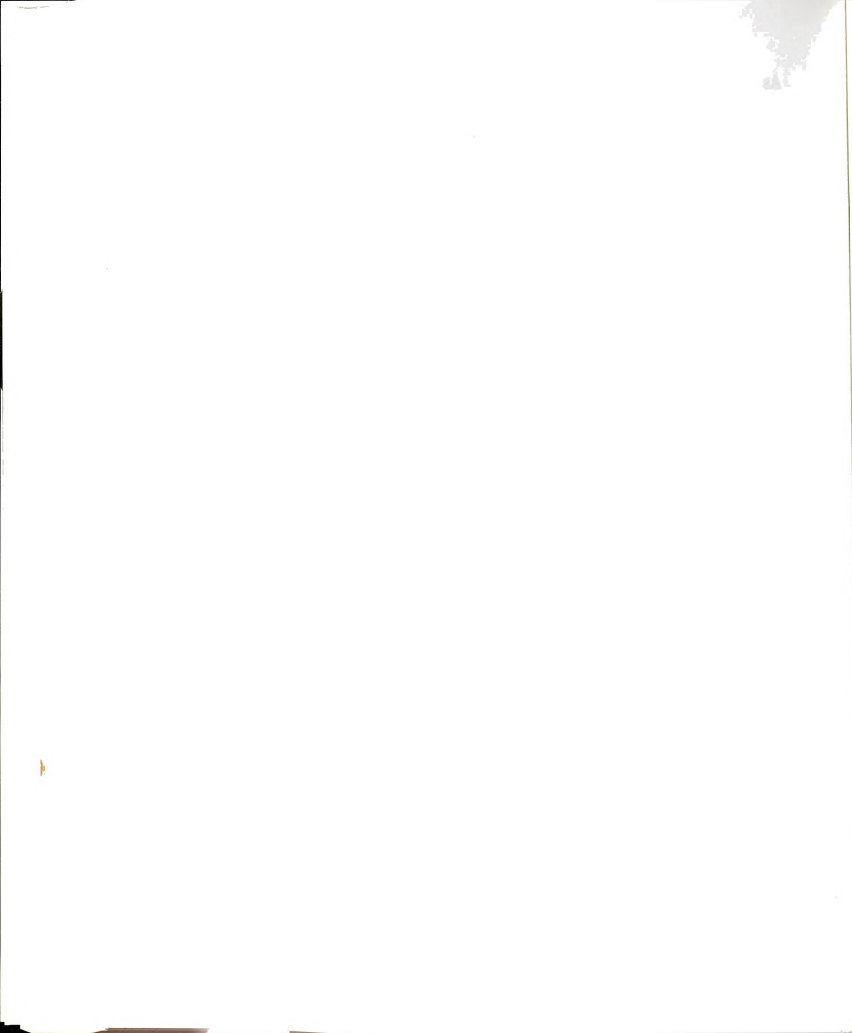
Table 11. Summary of electrochemical data for radicals **1**, **85**, and **86** with data for radical **1** for comparison. in THF a) and CH₂Cl₂ b).

a)		
	$R^+ \rightleftharpoons R^\cdot$	$R^\cdot \rightleftharpoons R^-$
1	-0.49 V	-2.05 V
85	-0.47 V	-2.10 V
86	-0.48 V	-2.04 V
THF Solvent; Reference: Ferrocene oxidation		
b)		
1	-0.44 V	-2.07 V
85	-0.50 V	-1.98 V
86	-0.48 V	-1.97 V
CH ₂ Cl ₂ Solvent; Reference: Ferrocene oxidation		



As expected, the redox potentials for **1**, **85**, and **86** are nearly identical, which shows that the added ether extensions in **86** have essentially no effect on the redox properties of the Ar_3C nucleus. The separations between cathodic and anodic peaks were large compared to the theoretical limit for Nernstian behavior (0.06 V for peak to peak distance); the wave for ferrocene/ferrocene⁺, a well-behaved reversible redox couple, showed similar separations. Thus, we believe electron transfers from an electrode to Ar_3C substrates are rapid and reversible.

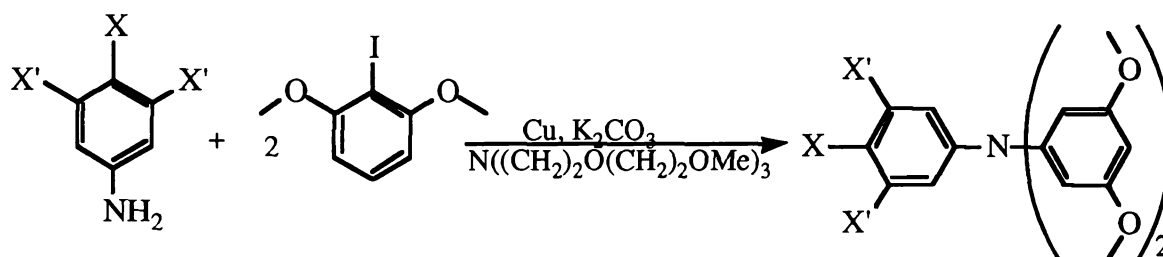
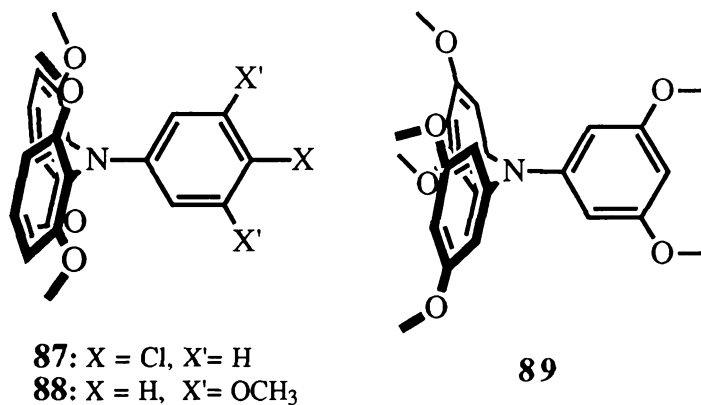
In principle, electrochemistry should be a useful probe of ion binding in triaryl-X systems such as **1** and **86**. Placement of a metal cation close to the center of radical **86** would be expected to broaden and shift both reduction waves to more positive voltages. These expectations are qualitatively borne out, but the voltammograms obtained are so poor and irreversible that we cannot identify well-defined reduction potentials for the metal cation-containing complexes. In support of the idea that specific binding is occurring, we note that no changes are observed in the cyclic voltammograms when salts of larger cations such as Na^+ or K^+ are substituted for the Li^+ .



3.3. Tetramethoxy Triphenyl amines

For the purpose of ion-binding studies of derivatives of radical **77**, structurally analogous amines in which the central carbon is replaced by nitrogen have been synthesized. In NMR ion-binding studies, it has been found that the use of metal salts with non-reducing counter anions such as BF_4^- and ClO_4^- generate significant amounts of radical cations of triaryl amine which can complicate data analysis by broadening NMR lines. However, Scott Stoudt has demonstrated that use of I^- salts effectively protects against the oxidation process of the triarylamines; I^- is easily oxidized and evidently is sacrificed to make I_2 instead of allowing the amine to be oxidized to make the persistent amine radical cations. Thus, in the case of LiI we were able to study ion-binding in CDCl_3 . Furthermore, iodide also appears to be a strong enough ligand in organic solvents that it "caps" the tripod-bound lithium cation, filling out its tetrahedral coordination geometry instead of giving way to allow a second tripod ether to make an octahedral cavity.

The amines **87** and **88** shown below are isostructural to radicals **78** and **84**. They were synthesized by a modification of Fréchet's method for building triarylamines as shown in next page.¹⁶² These amines were used in ion-binding studies with metal cations to demonstrate the abilities of four methoxy groups as coordination ligands.



They show interesting binding properties which can be detected by NMR. Similar to the ion-binding experiments with borane **63** and radical **1**, these triaryl amines can be used for more quantitative studies. Addition of salts to CDCl₃ solutions of amines in NMR tube results in significant chemical shift changes (0.2 ppm); D₂O washing regenerates the original spectrum of triaryl amines. **Figures 36 and 37** show ¹H and ¹³C NMR spectra for such experiments using amine **87**.

Other salts including Na and Cd did not induce changes in NMR spectra. **Figure 38** shows an ion-binding study of amine **88** by ¹H NMR which has internal reference built into it. Our expectation for ion-binding of tetramethoxy derivatives and dimethoxy benzene suggest that the two methoxy groups in the 3,5 positions should not participate in ion-binding. To our surprise, even those two methoxy groups show chemical shift changes after adding LiI to the CDCl₃ solution of amine **88**. These

findings may reveal conformational changes by ion-binding and suggest that the tetramethoxy amines in solution may not be preorganized for ion-binding. The possibility of participation of the central nitrogen atom's lone pair electrons is still an unresolved question.

The radical cations of these triarylaminines are isoelectronic to radicals **79** and **84** and show interesting redox properties. Those radical cations might offer alternative building blocks for magnetic chains with the required stability and structures. Their redox properties were therefore examined by cyclic voltammetry. Electrochemical data are summarized in **Table 12**; Attempts to conduct ion-binding studies by CV were unsuccessful due to the fact that the oxidations of these amines were not reversible.

Table 12. Summary of electrochemical data for oxidation of $\text{N} \rightleftharpoons \text{N}^{+\bullet}$ in amine **87**, **88**, and **89** in CH_2Cl_2 .

87	+0.50 V
88	+0.44 V
89	+0.57 V

CH_2Cl_2 Solvent; Reference: Ferrocene oxidation

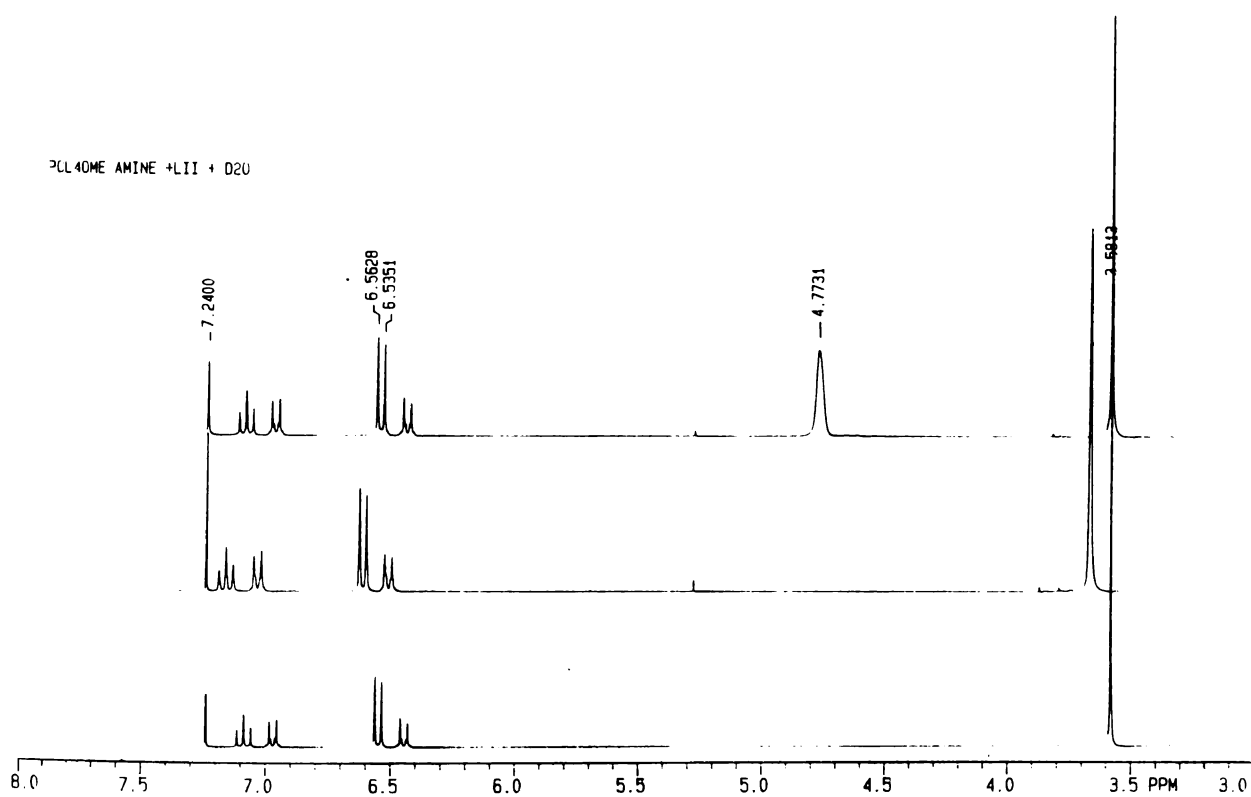


Figure 36. ^1H NMR spectra for the complexation of **87** with LiI in CDCl_3 showing chemical shifts of methoxy and corresponding aromatic protons followed by D_2O wash.

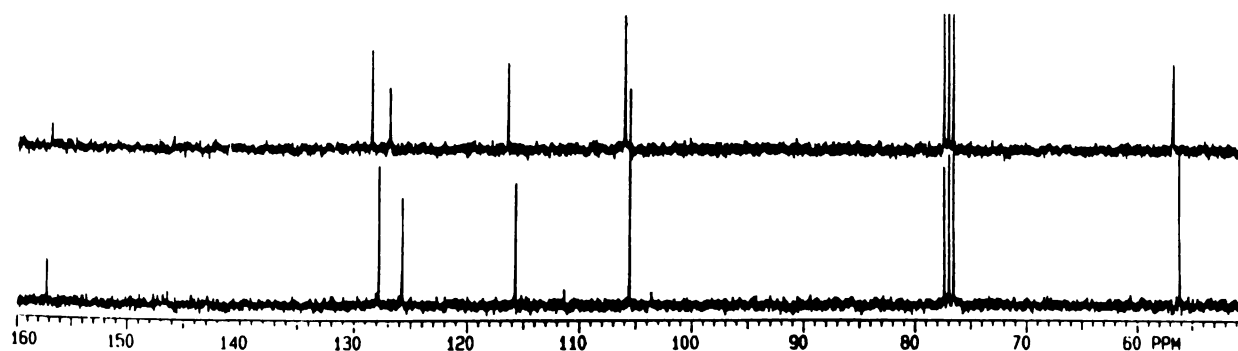


Figure 37. ^{13}C NMR spectra of **87** with LiI in CDCl_3 showing chemical shifts of methoxy and corresponding aromatic carbons.

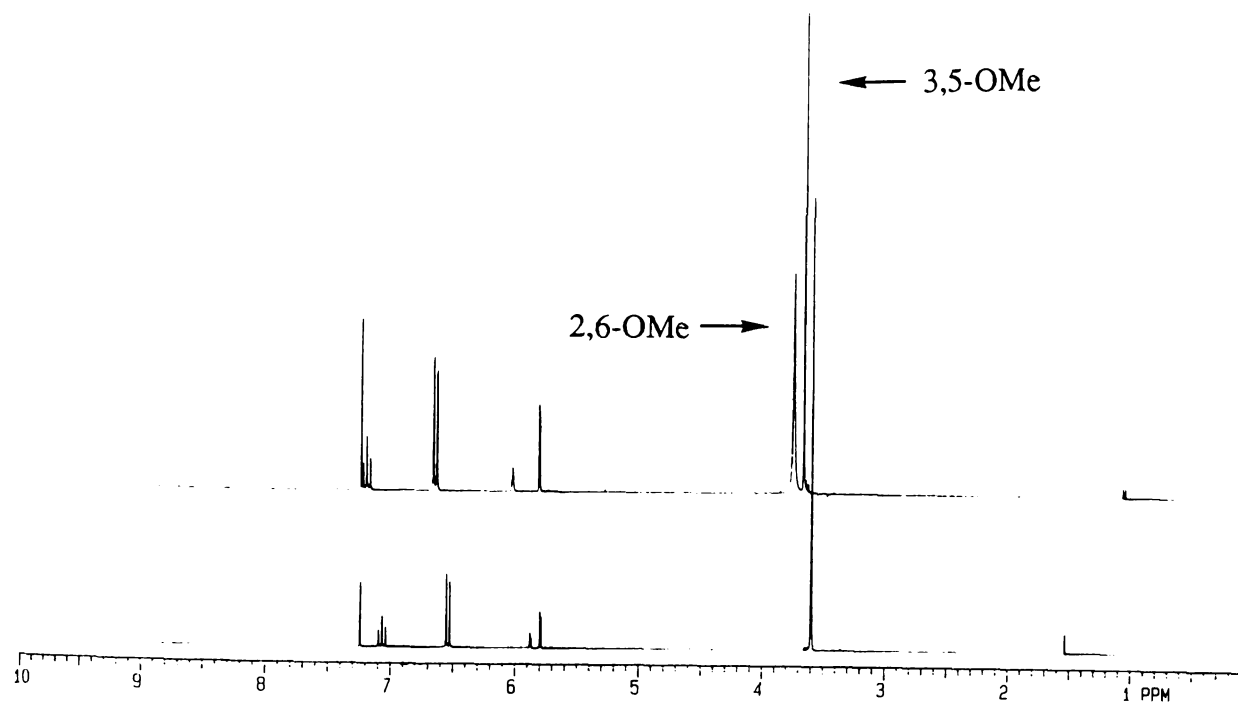


Figure 38. ^1H NMR spectra for the complexation of **88** with LiI in CDCl_3 showing chemical shifts of methoxy and corresponding aromatic protons.

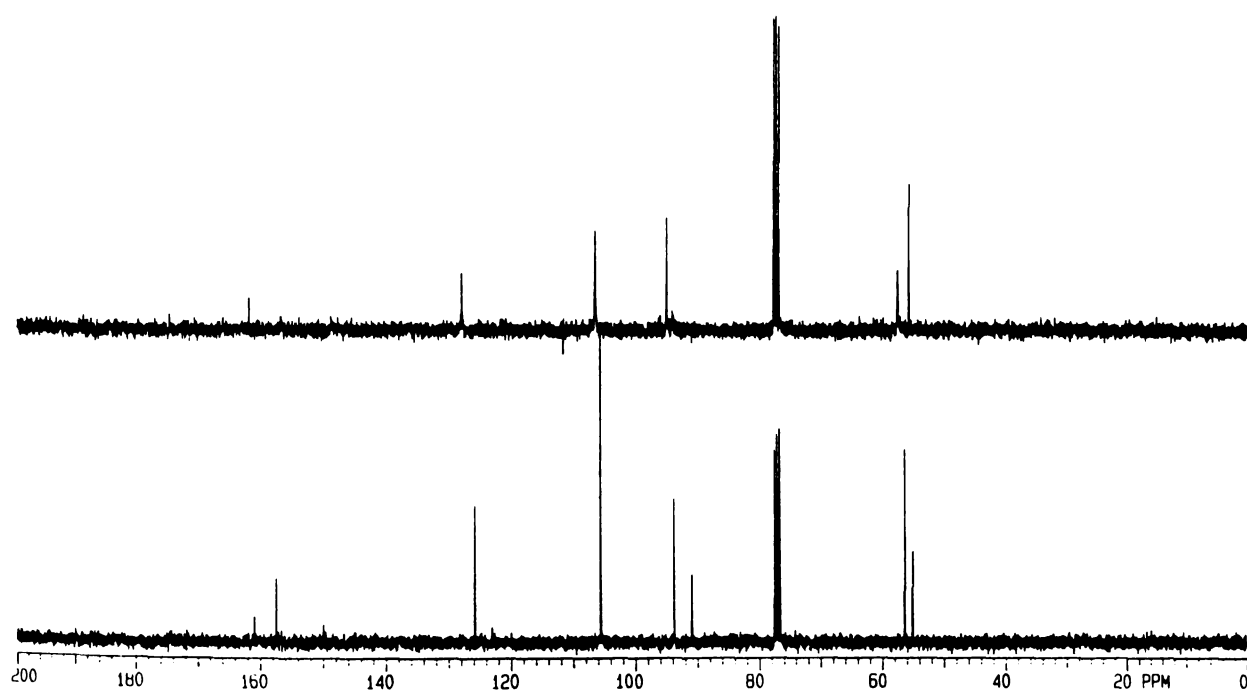
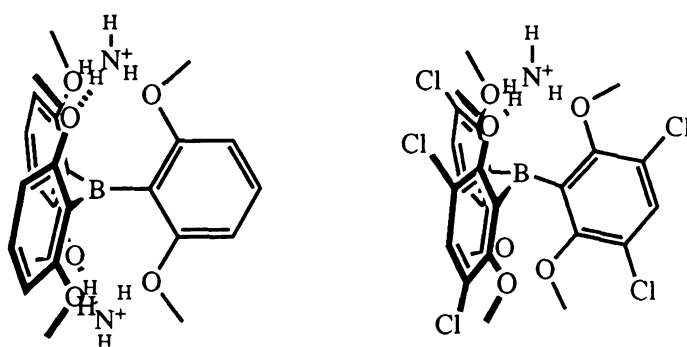


Figure 39. ^{13}C NMR spectra of **88** with LiI in CDCl_3 showing chemical shifts of methoxy and corresponding aromatic carbons.

3.4. Ammonium Complexes by Hydrogen bonding

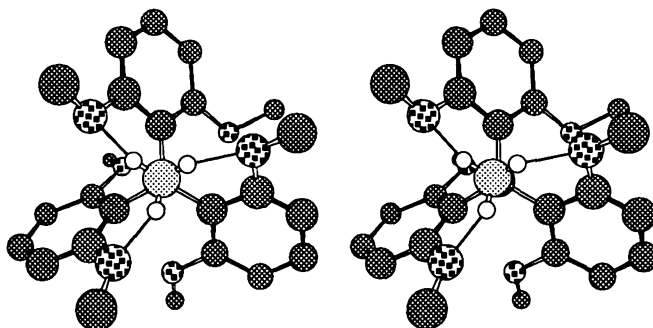
As a way to construct desirably substituted radicals like perchlororinated triarylmethyl radicals, we were working on the route for making the radical through tris(2,6-dimethoxyphenyl)methyl ammonium tetrafluoroborate **72** which is not as sensitive to protonic acids as the corresponding carbinol and can be converted into the radical by a simple diazotization reaction. The X-ray structure of the given ammonia adduct **72** shown in **Figure 40** shows three hydrogen-bonding interactions, which hint at the hydrogen bonding ability of the ether tripods in radical **1**. An attempt has been made to determine the ability of radical **1** to hydrogen bond with ammonium salts by using the borane **63** as a model compound in CD_3CN as a solvent.



To our surprise, after adding the salts into a solution of the borane **63** in a NMR tube, the characteristic proton peaks (equal-intensity triplet from coupling to N) of NH_4I appeared which corresponded to eight protons per molecule of borane from the integration of the peaks. Intrigued by this fact, we tried a similar experiment on hexachloroborane **64**, resulting in similar behavior except that in this case we can assign only four ammonium protons per molecule of the borane **64**. The X-ray structure of the hexachlorinated ammonium salt **75** has recently been solved; the aryl ring

twists have turned out to be 37, 51, and 51°. As we expected, the methoxy groups in **75** are twisted down out of the aryl ring planes, improving preorganization for binding; this twisting (the average of 67°) can be seen in the following stereo view of the X-ray crystal structure of **75**.

a)



b)

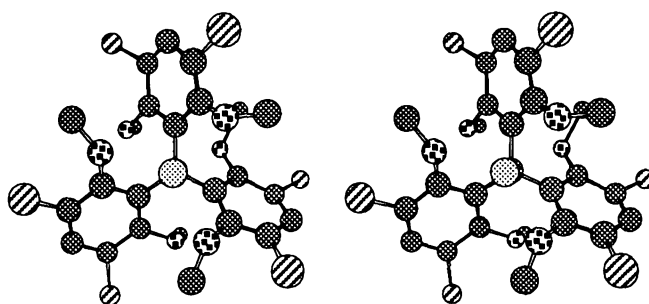


Figure 40. Stereo views of crystal structure of a) tris(2,6-dimethoxyphenyl)methyl ammonium tetrafluoroborate **72** b) tris(2,6-dimethoxy-3,5-dichlorophenyl)methyl ammonium tetrafluoroborate **75**. Note that at the time of writing, the ammonium H atom positions had not been finally refined.

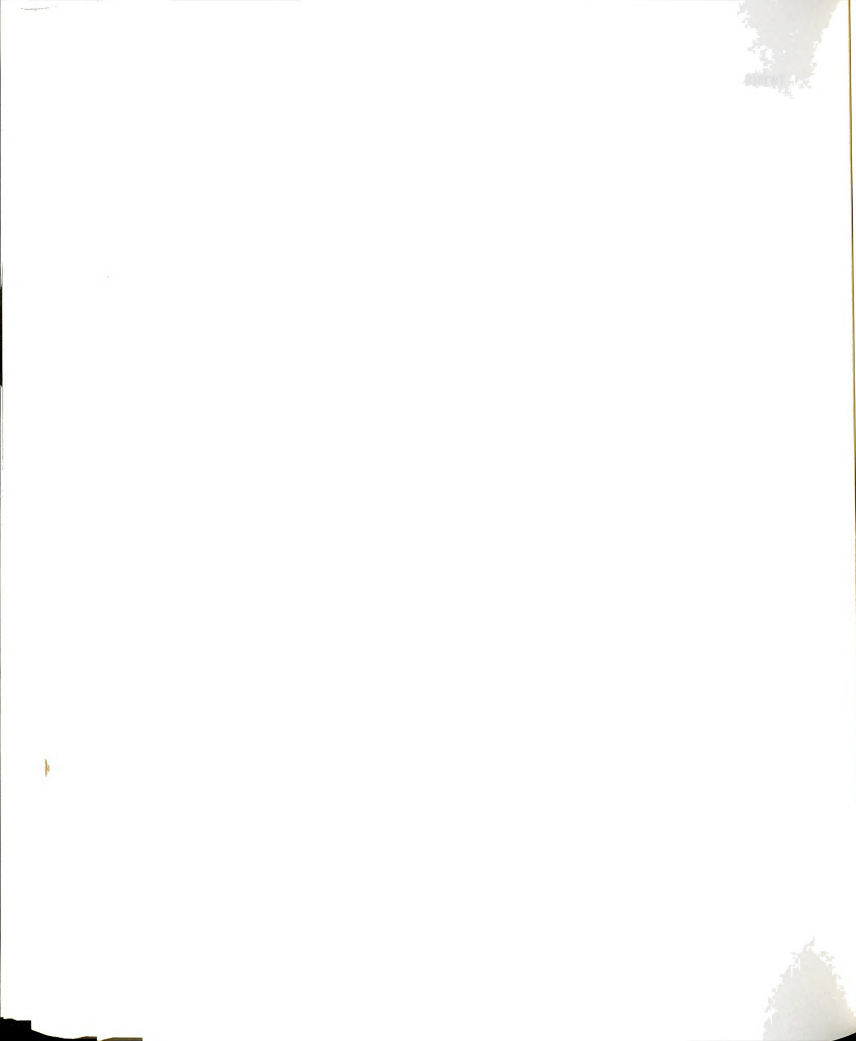


Table 13. Crystal structure determination and refinement data for tris(2,6-dimethoxyphenyl)methyl ammonium tetrafluoroborate **72** and tris(2,6-dimethoxy-3,5-dichlorophenyl)methyl ammonium tetrafluoroborate **75**.

Crystal data	72	75
Space group	P2/n	P2 ₁ /n
Z	4	4
Temperature	296 K	298K
a (Å)	15.292	12.03
b	10.796	24.07
c	15.731	12.11
β	109.99	94.38
μ (cm ⁻¹)	9.7 (Cu K α) 0.8 (Mo K α)	

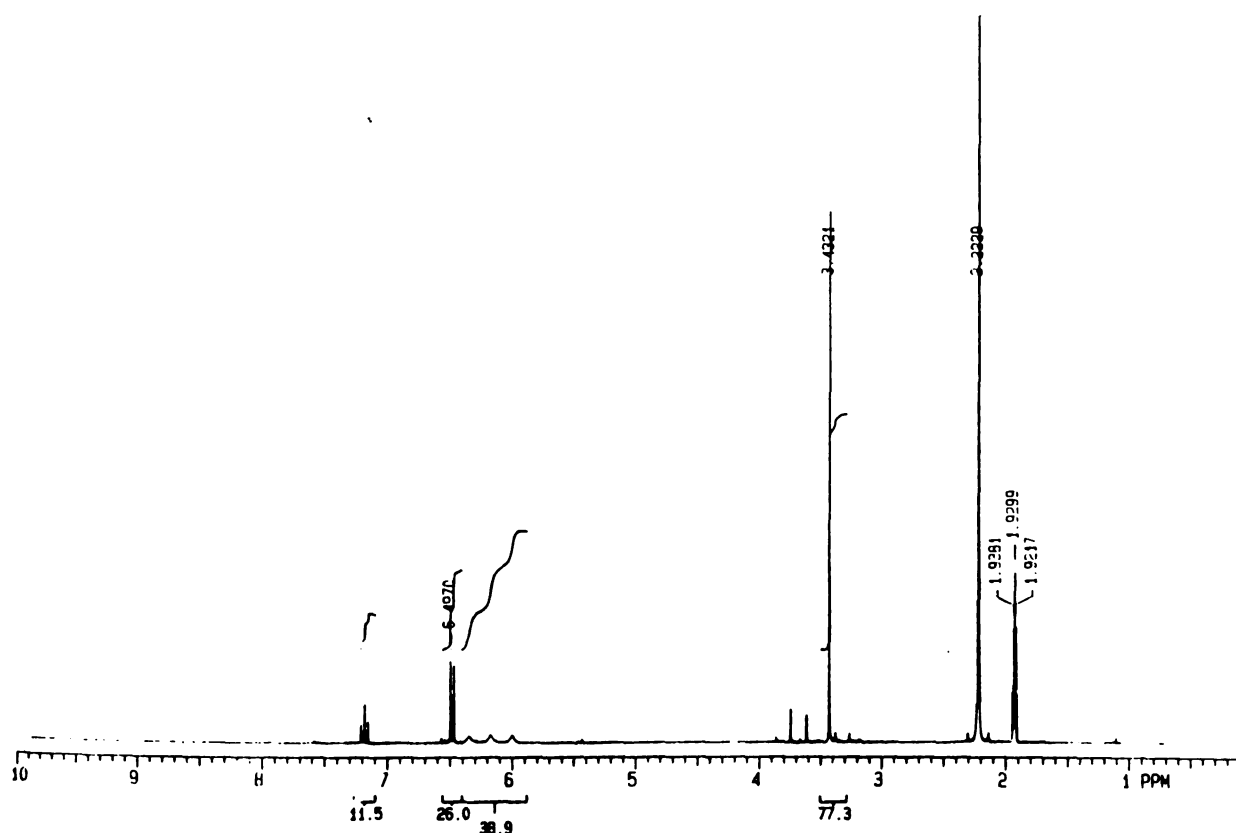


Figure 41. ^1H NMR spectrum of complex of **63**• NH_4I in CD_3CN showing characteristic triplet peaks after the addition of the salt which was not present before.

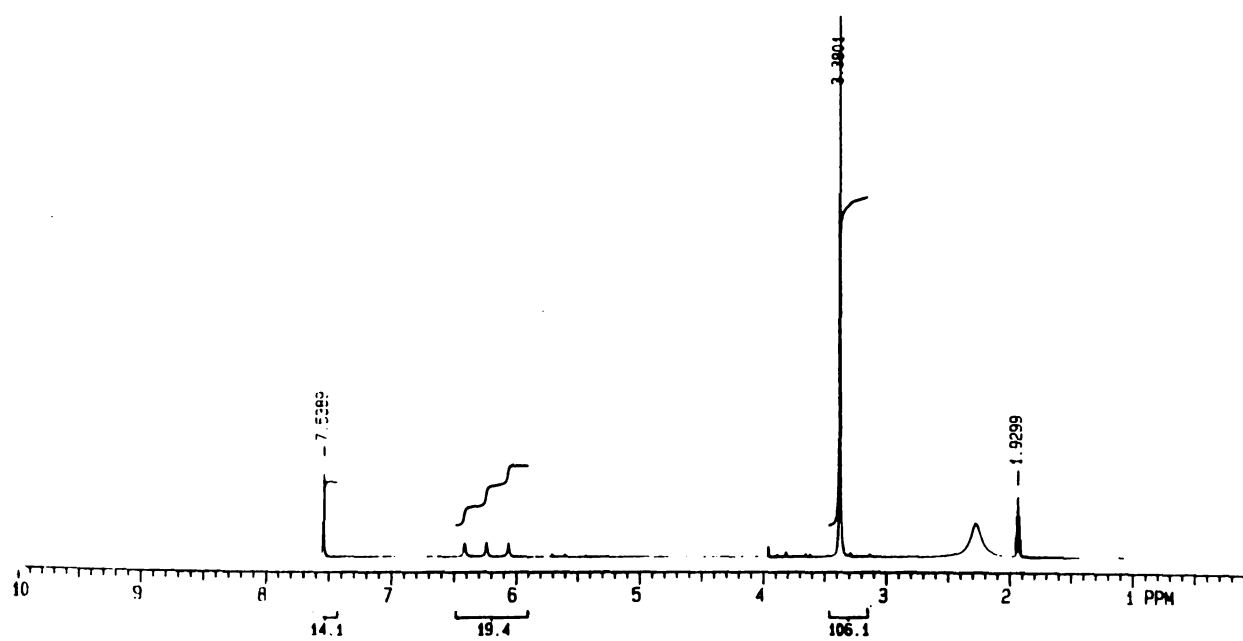


Figure 42. ^1H NMR spectrum of complex of $64\cdot\text{NH}_4\text{I}$ in CD_3CN showing characteristic triplet peaks after the addition of the salt which was not present before.

3.5. Metal Ions

A variety of new salts have been investigated in reaction with **1** and the related radicals described above. We have examined a variety of salts, varying both metal cations and their anion partners. Solid phase SQUID and EPR studies at low temperatures were performed on all complexes, giving detailed information about the magnetic properties of these materials. As with X-ray diffraction, single crystal studies would be particularly valuable, as they would provide data on the magnetic anisotropies in such crystals. However, among the magnetically interesting materials only polycrystalline solids were obtained.

Dimers and oligomers of types **2** and **3** can obviously be envisioned with metal ions other than lithium. In addition to the few salts that we have already investigated, we have examined various transition metal ions, including Cr^{3+} , Co^{3+} , Cd^{2+} , and Rh^{3+} , all ions with strong affinities for ethers and with coordination spheres of appropriate size to bind to the ether tripods in **1**. In a qualitative survey of roughly 20 alkali metal, alkaline earth, and transition metal salts, we examined the color changes due to radical oxidation in the presence of metal salts and O_2 . A clear trend emerged, with metal ions of small radius ($\leq 1.1 \text{ \AA}$)¹⁶³ promoting the rapid color change and larger ones failing. These observations are consistent with the observed size of the binding pockets in **1** and **63** and we expect such survey data to be useful in helping to select new salts for further study.

The counter anions of the salts used in our complexation studies may be critical to the successful formation and isolation of crystals for X-ray studies. Crystallization of the extended (radical-metal)_n stacks that we envision may be constrained by the requirements of fitting together such infinite charged structures in an efficiently packed lattice. Furthermore, the metal ions' charges are spaced at fixed intervals along such stacks or chains, as determined by the cation's radius and the aryl ring twist angles in the radicals. To maintain charge neutrality, the counterions must find appropriate sites with the right spacing to allow the chains to pack together in one of the relatively few simple patterns available to them. Counterion size, shape, and charge may therefore play a key role in determining which systems of salts and radicals will lead to well-formed crystals.

CHAPTER II. Magnetism of Triarylmethyl Radical Complex

1. Calculations on the Metal-Mediated Pairwise Interaction of Methyl Radicals

Professor Jackson has examined and compared the total and one-electron frontier orbital energies of calculated singlet and triplet states for the simplest model system, $\text{H}_3\text{C}\cdot\text{Li}^+\cdot\text{CH}_3$. The linear interaction of two carbon 2p-orbitals on radical centers, communicating via the 2s and 2p orbital set of a lithium cation, can be described by a simple qualitative interaction diagram, shown in **Figure 43**.

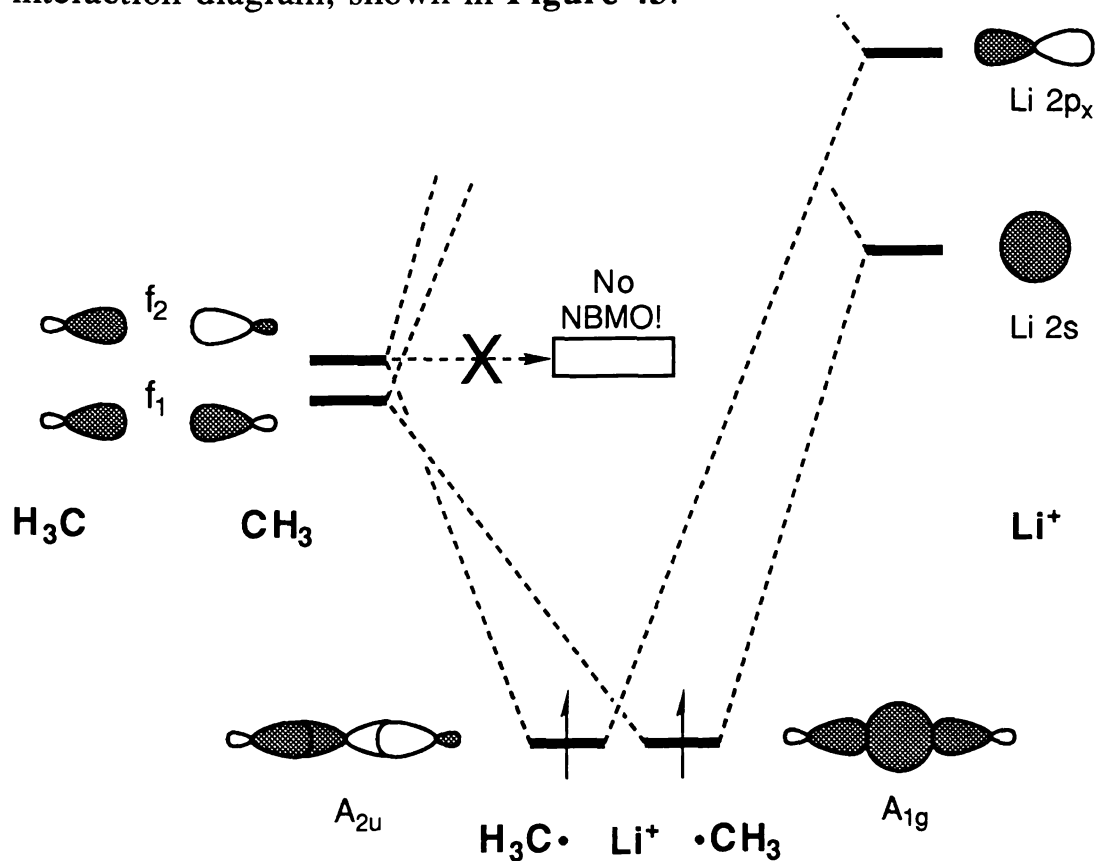
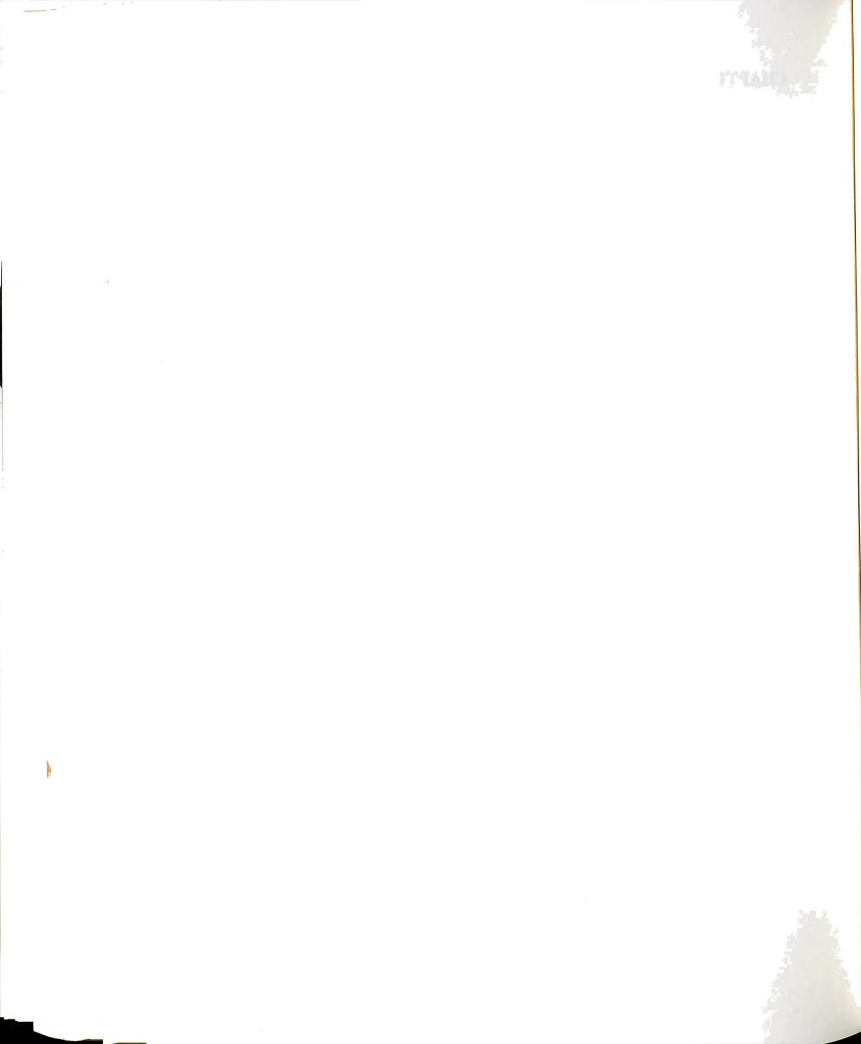


Figure 43. Qualitative MO diagram schematically indicating the coincidental near-degeneracies from mixing a pair of sp^3 hybrid orbitals with a $\text{Li } 2p_z$ orbital and a $\text{Li } 2s$ orbital.



Preliminary work on the metal-mediated radical pair $\text{H}_3\text{C}\cdot\text{Li}^+\cdot\text{CH}_3$ (3-21G and 6-31G*), suggests a triplet ground state for this model system. Geometry differences between singlet and triplet optimized structures are small, and vibrational analysis on the triplet shows that the linear form is a local minimum. The fact that the calculated total energies for the two spin states are close is surprising, and we need to pursue more complete wave functions which will determine the ordering and separation of the two spin states as a function of C-Li distance. In conjunction with our molecular mechanics and semiempirical molecular orbital modeling of the actual radicals under study, we expect these higher-level calculations ultimately to lead to a set of generalizations which will help guide the design of new paramagnetic complexants and extended structures.

Techniques such as MNDO, AM1, which are widely available and easy to use, provide a reasonable middle-ground for attempts at studying large systems such as radical **1** and its complexes. Reliable absolute predictions of preferred electronic couplings might not be possible using these methods, but they should help to predict trends and guide our choices of modified systems. Professor Jackson has fully optimized the structure of radical **1** by MNDO and AM1 within D_3 symmetry, and its structure is nearly identical with that obtained by the molecular mechanics methods using PCModel. The program PCModel¹⁶⁴ offers molecular mechanics calculations based on MM2 force field. Calculations using the program have been shown to work well in predicting geometries for the triaryl-X monomers whose structures we have studied by X-ray. As a rapid source of reasonable estimates for geometries and strain energies, this program is a valuable tool.

2. Antiferromagnetic Interaction and Peroxy dimer of The Radical 1

Magnetic susceptibility measurements on crystals of radical **1** show very weak antiferromagnetism according to Curie-Weiss behavior. It is not clear what is the mechanism responsible for the coupling, but careful examinations of the three-dimensional packing of the radical show a closest distance of 4.20 Å between para carbons of the flattened conjugated aryl rings of the radical.

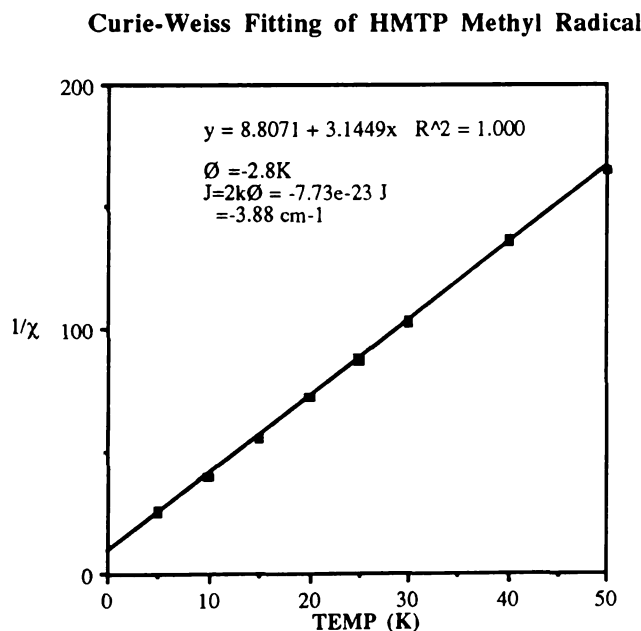


Figure 44. Curie-Weiss fitting of HMTP methyl **1** with Curie-Weiss constant of -2.8K ($J = -3.88 \text{ cm}^{-1}$) suggesting weak anti ferromagnetic interactions between radicals.

Radical **1** reacts slowly in the air to form peroxide **90** (shown on next page) as determined by ^1H NMR, FAB mass spectrometry, and elemental analysis. The formation of peroxide can be explained by the

reaction of a spin-rich para-carbon in the radical **77** with oxygen. According to McConnell's approximation there is a significant amount of unpaired electron spin density on that para-carbon which might be available for the reaction. Since it is known that oxyradicals add to *p*-positions of triarylmethyl radicals, this reaction is the point of initial oxygen addition. The tetramethoxyphenyl methyl radical **77** shows similar dimerization to form a peroxy dimer with an interesting head-to-tail connectivity which is different from the tail-to-tail mode found for radical **1**. With only four methoxy groups for steric blockage, radical **77** does not have enough steric protection against the penetration of oxygen to the central carbon so that it forms a peroxy dimer linked between a central carbon and the para carbon in that asymmetric third ring. We are in the process of determining the first step of the reaction by reaction of radical **77** in a hydrogen donating solvent; The preliminary results suggest that the first step is the attack of oxygen at the para carbon. The X-ray structure of the peroxy dimer (Jacobson's) **91** from radical **77** is shown in stereo view in **Figure 45**.

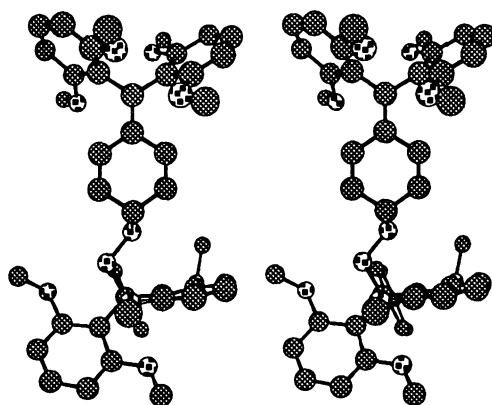


Figure 45. Stereo view of X-Ray structure of head-to-tail peroxydimer **91**.

3. Magnetic Behavior of Radicals and Complexes

We believe that we have made magnetic materials in polycrystalline form from **1** and various lithium salts. I studied these blue-black powders by standard methods (SQUID, EPR) for magnetic susceptibility determination as a function of temperature and magnetic field strength. In our experiments, ferromagnetic behavior¹⁶⁵ was reproducibly observed in the blue-black powders obtained when solutions of **1** and LiBF₄ were mixed and evaporated to dryness under an argon atmosphere. Studies of magnetic field dependence in these materials showed hysteresis (**Figure 46**) a classic signature of bulk magnetism with far less spin counts than theoretically expected. The tetrafluoroborate anion was replaced by the similar-sized perchlorate ions without qualitatively affecting the field dependent magnetic properties. This result indicated that the bulk behavior is not due to chemistry involving the counterion. Radical **1** alone, a red powder, showed weak antiferromagnetism, in contrast to the salt-treated samples; lithium salts alone showed diamagnetic behavior, suggesting that the observed ferromagnetism must somehow derive from the combination of the radical with the lithium salt.

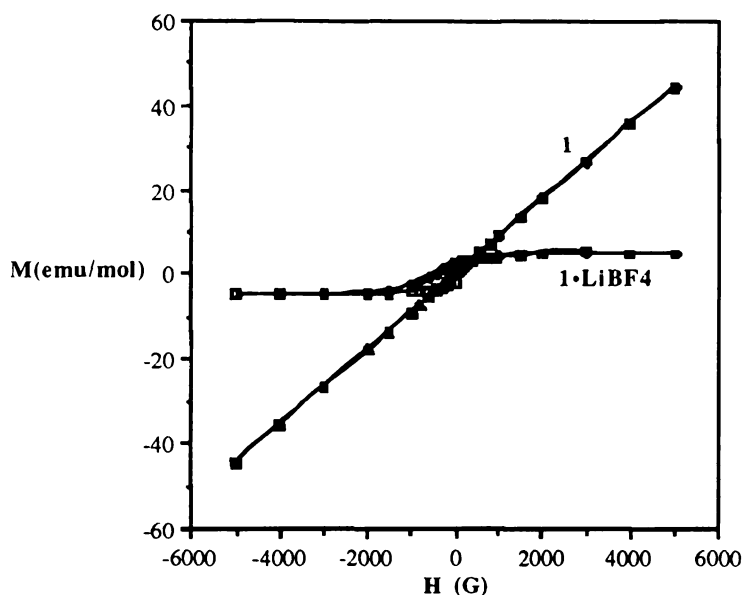


Figure 46. Plot of magnetization M (in EMU) vs. magnetic field strength H (in Gauss) at 5K for Radical **1** alone and for its complex with LiBF_4 .

Iron from the laboratory environment is a frequent ferromagnetic contaminant in studies of magnetic materials. In light of the reproducible SQUID results above and our fear that contamination with iron or other ferrous metals might be causing the observed hysteresis, we devised a metal-free synthesis of radical **1**. Martin's original synthesis used Cr(II) ion as the reducing agent; we showed that zinc works well too. However, we sought to avoid metals, such as Cr or Zn, that could carry ferrous contaminants. Ultimately, we discovered that ascorbic acid (vitamin C) and Iodide salts are both able to reduce salts of the cation in THF; the neutral radical then migrates into a nonpolar organic solvent layer, where it is easily separated and isolated. Various attempts were made to eliminate

potential iron contamination in our SQUID samples; careful filtration of radical and salt solutions before mixing, use of glass distilled solvents and high purity salts, chromatography of the starting radical solution over silica gel, etc. A series of SQUID samples were analyzed by atomic emission photometry which showed some iron at the level of the background, regardless of their SQUID behavior in all samples and controls. However, the levels found would be more than sufficient to yield the ferromagnetism observed, if the iron was in a ferromagnetic form.

3.1. Diamagnetism of Triaryl Methane **73** and Metal Salts

The Pascal constants provide an empirical method for estimation of diamagnetic corrections. For the complex **1**•LiBF₄ the diamagnetic contribution is calculated to be -2.89×10^{-4} emu/mol. Greater accuracy can be obtained by the direct measurement of the susceptibility of a diamagnetic analogue of the paramagnetic compound which is of interest.

For example, a diamagnetic correction for radical **1** can be achieved more accurately by a subtraction of magnetic measurement data from the corresponding triaryl methane **73** discussed earlier (section 2.4 of chapter I) which has one more hydrogen than the radical. Furthermore, by this process of diamagnetic correction we were able to eliminate the error factors inherent in the SQUID measurement which come from the method of sample handling, etc. The observed diamagnetic correction for radical **1** using the methane **73** gave similar diamagnetic contributions at the high temperature region. **Figure 47** shows a typical field dependence of methane **73** at 2K showing characteristic diamagnetic behavior.

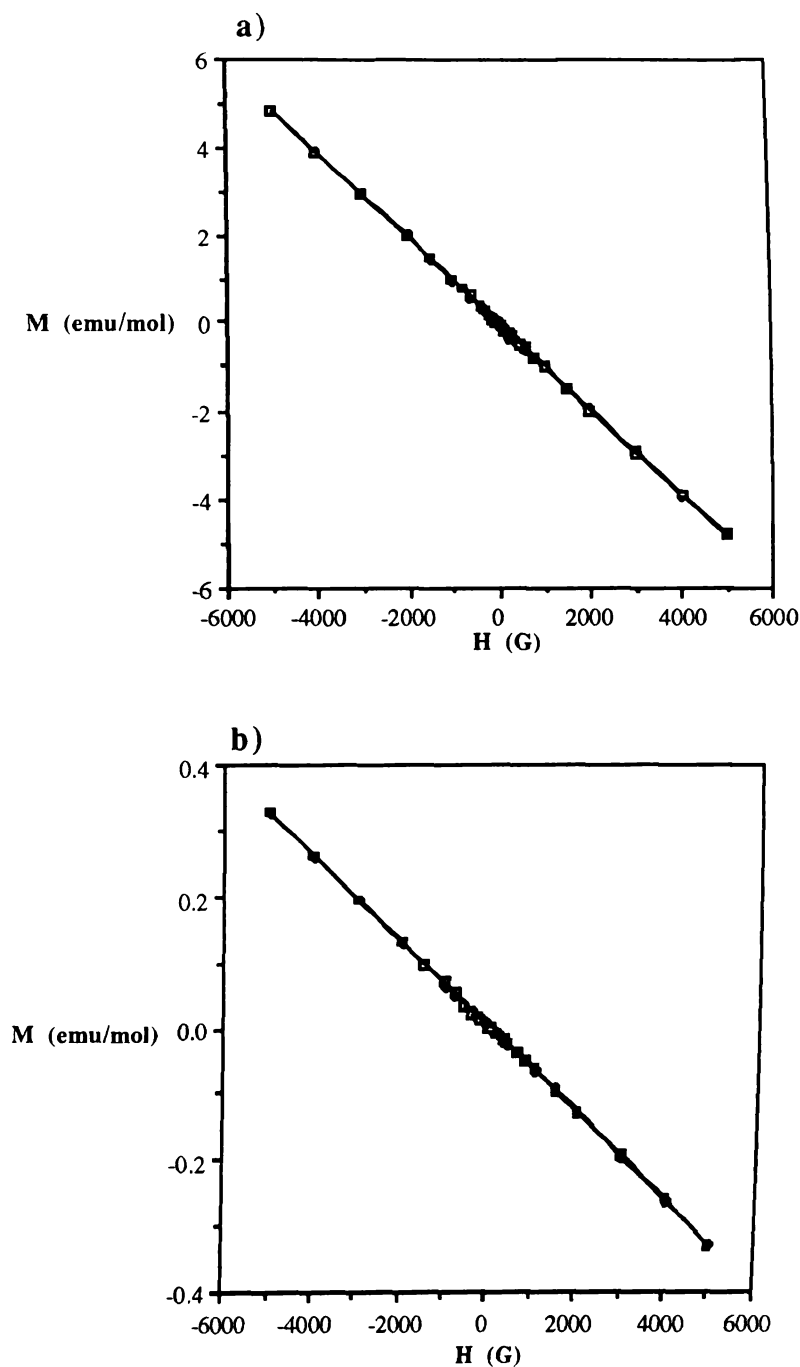


Figure 47. Field dependence of a) methane **73** at 2K and b) CdCl_2 at 5K. The induced molar magnetic moments decreases as the field strength increases which is the characteristic field dependence (inversely proportional) of a diamagnetic material.

3.2. Paramagnetism of Radicals and Radical Complexes

As I discussed in the introduction, a paramagnet concentrates the lines of force provided by an applied magnetic field and thereby moves into regions of higher field strength. Paramagnetic susceptibility is generally independent of the field strength, but shows temperature dependence according to the Curie Law.

Radical **1** shows a paramagnetic temperature dependence over a wide temperature range; it is weakly antiferromagnetic at low temperature, although the coupling is not a big one. We can show the paramagnetic properties of the radical in two different ways using the plot of $1/\chi$ vs T and χT vs T . **Figure 48** show such plots with a slight antiferromagnetic downturn at low temperature. Most of HMTP methyl radicals behave similarly to radical **1** in their temperature dependencies.

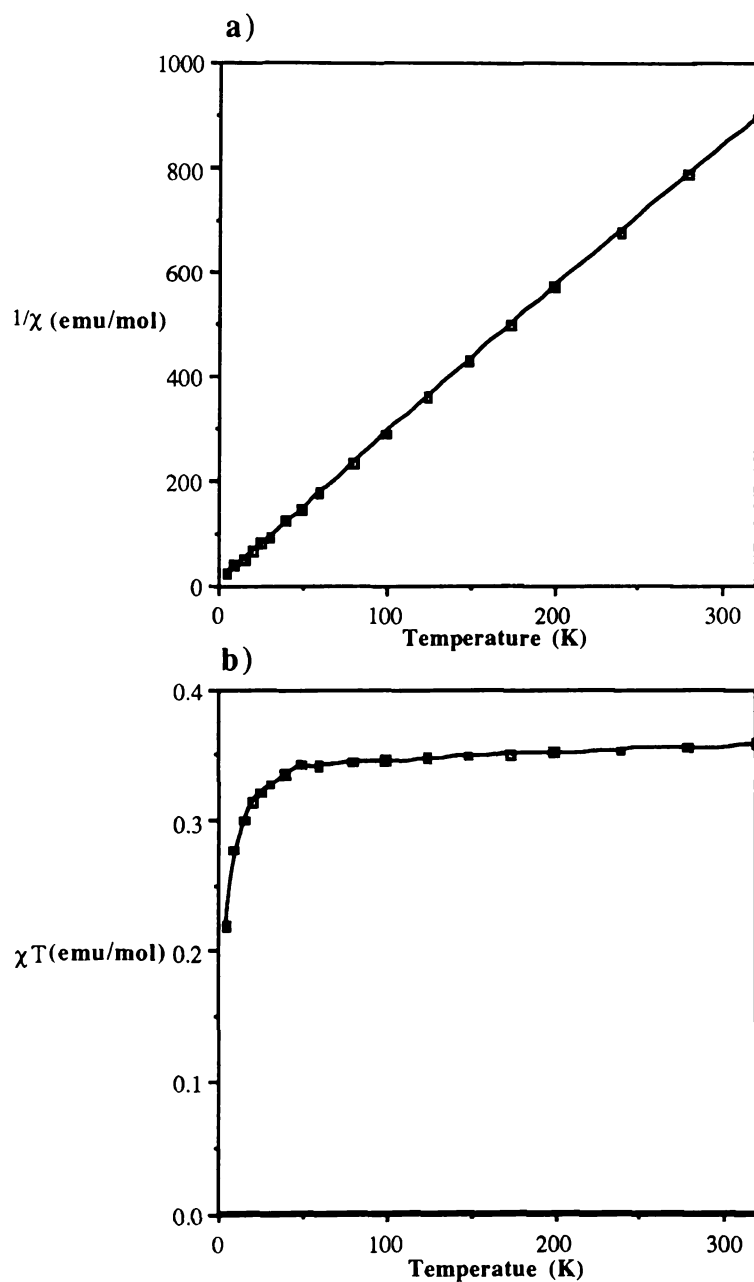
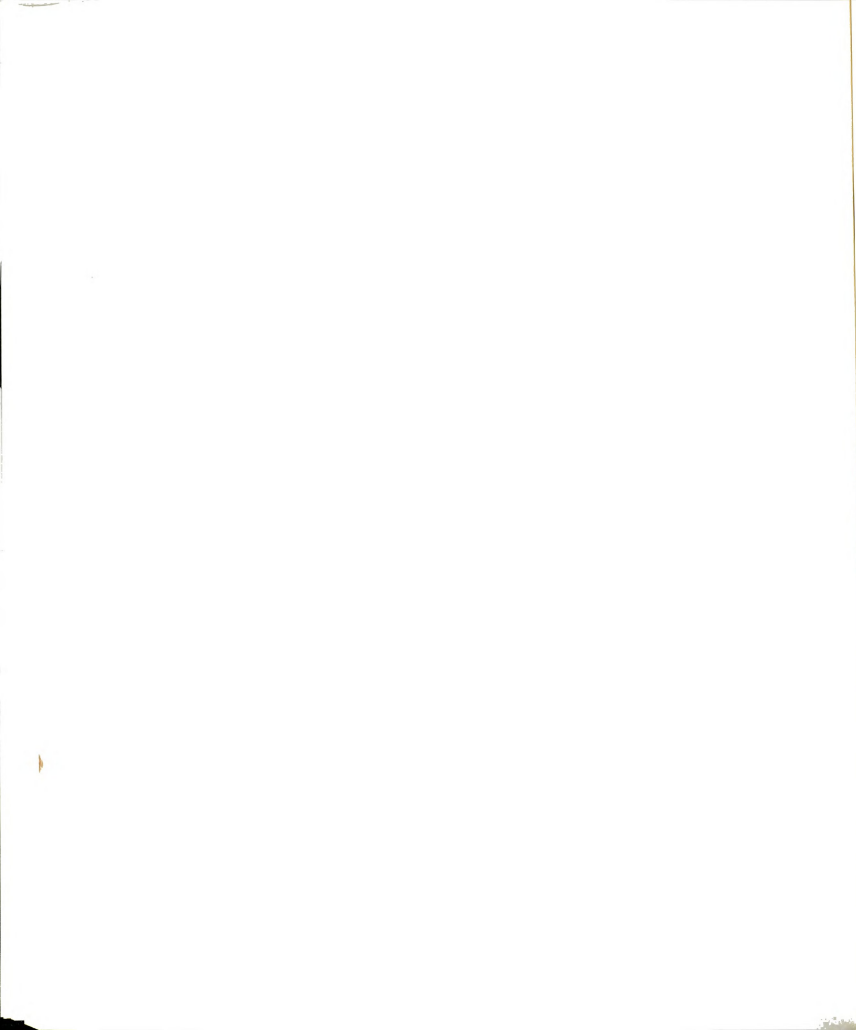
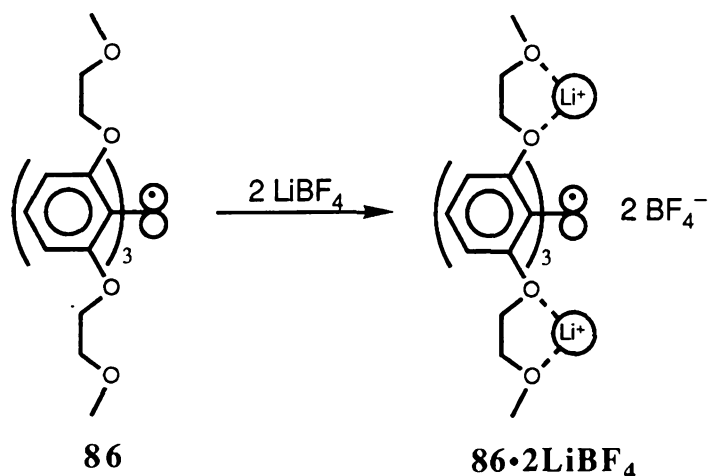


Figure 48. The temperature dependence of radical **1** analyzed in a) $1/\chi$ vs T and b) χT vs T at 5000G with Curie constant of 0.34 emu/mol which corresponds to 91% of ideal $S=1/2$ radical. Presence of the diamagnetic peroxy dimer **91** reduces the total spin count.



The radicals **86** which I discussed earlier (section 3.2 in chapter I) were synthesized to build an analogue of **1** which could not form extended chains by pairing around metal cations. Radical **86** offers a bound Li^+ ion a full coordination sphere of six ether oxygens, effectively "capping" the radical on both faces. Thus, the radical center in $\text{86} \cdot 2\text{LiBF}_4$ is encapsulated and should behave as a completely isolated paramagnet.



As shown by CV data earlier, the radicals **1** and **86** are respectable reductants with nearly identical redox potentials. Fears about impurities in our studies of radical **1** with salts led us to speculate that even though no ferromagnetism was found in our starting materials, something ferromagnetic might be generated by reduction of a diamagnetic impurity. Radical **86** should be just as likely to effect the hypothetical reduction as **1**, but magnetic measurements shows that the complex $\text{86} \cdot 2\text{LiBF}_4$ is a textbook paramagnet. In fact, these samples are among our best instances of isolated $S=1/2$ radical behavior. Thus, blocking chain formation in **1** significantly alters the nature of the LiBF_4 complex products, consistent with the notion that such chains or at least the open faces are important to the complexation chemistry of radical **1**. We have verified this

expectation by magnetic susceptibility studies of powders of the complex. **Figure 49** shows plots of magnetic susceptibilities as a function of applied magnetic field and temperature. As expected for an isolated radical, a Curie plot ($1/\chi$ vs. T) shows ideal paramagnetic behavior with a μ_{eff} of $1.56 \mu_{\text{B}}$. We attribute this slightly low value to uncertainty in the exact radical: LiBF_4 ratio, and to a small amount of radical oxidation during preparation. There is no indication that adding LiBF_4 to **86** puts the radical centers into communication. This finding is in contrast to the situation with **1**. Like **1**, radical **86** shows some tendency toward oxidation on treatment with LiBF_4 under the air. This behavior is evidenced by the appearance of the blue color of the corresponding triarylmethyl cation in each cases. This result reinforces the notion that the ferromagnetism seen from a lithium complex of radical **1** is unique to a radical which can bind metals on both open faces to form chains, and is not simply due to an artifact such as iron particle production by reduction of adventitious iron salts.

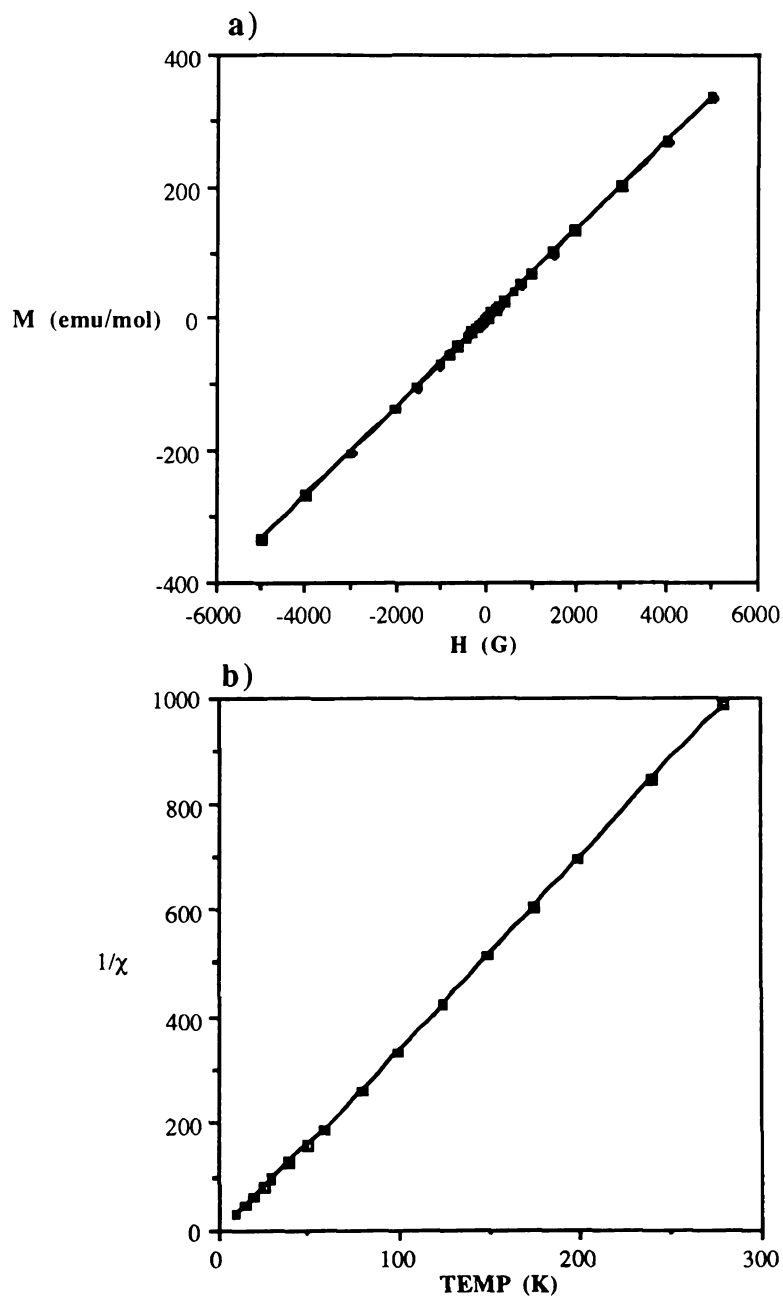


Figure 49: (a) Plot of M vs. H for $86\cdot 2\text{LiBF}_4$ at 5K; (b) Plot of $1/\chi$ vs. T for $86\cdot 2\text{LiBF}_4$ at 5000G showing paramagnetic behavior.

In the course of the NMR ion-binding studies, we developed a more detailed understanding of one counterion's role as a partner and ancillary ligand to Li^+ bound in the tripod ether's pocket. These insights have translated into an explanation of the simple $S=1/2$ paramagnetic behavior found in magnetic susceptibility studies of $\mathbf{1} \cdot 2\text{LiI}$ complexes. If the radical is capped by LiI subunits, it is sensible that it should behave as an isolated paramagnetic center like complex $\mathbf{86} \cdot 2\text{LiBF}_4$. **Figure 50** shows paramagnetic behavior of complex $\mathbf{1} \cdot 2\text{LiI}$ at 5000G.

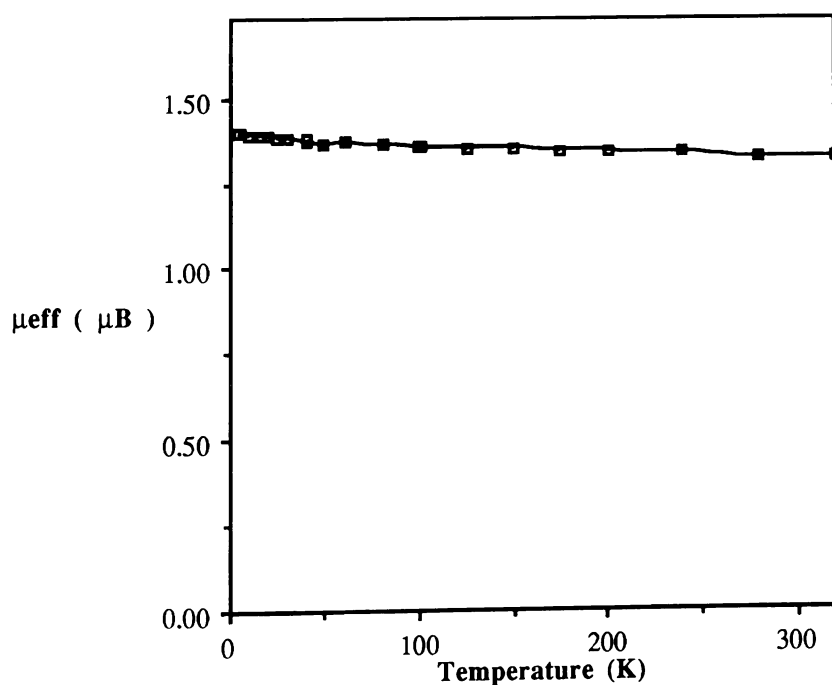


Figure 50. Temperature dependence of complex $\mathbf{1} \cdot 2\text{LiI}$ at 5000G showing simple paramagnetism of the complex (81% of spins are counted).

By the same token, if the radical is capped by NH_4I subunits, complex $1\cdot\text{NH}_4\text{I}$ should behave as an isolated paramagnetic center like the case above. The temperature dependence of this complex is shown in **Figure 51**.

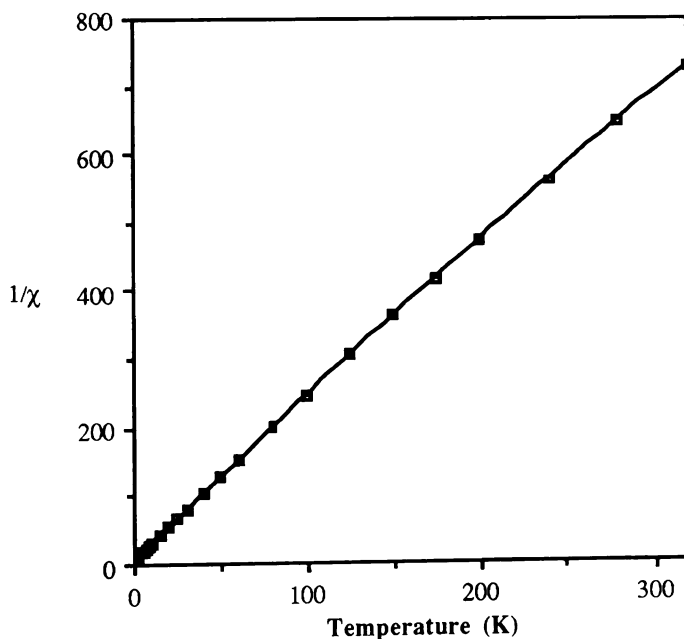


Figure 51. Temperature dependence of complex $1\cdot\text{NH}_4\text{I}$ at 500G showing simple paramagnetism of the complex by effective capping of the linear chain formation.

At very high external fields and very low temperatures, the magnetization M becomes independent of field and temperature, and approaches the maximum or saturation magnetization M_{sat} which the spin system can exhibit. This situation corresponds to the complete alignment of magnetic dipoles by the field ($M_{\text{sat}} = 5.58 \times 10^3$ erg/Os mol for $g=2$, $S=1/2$).

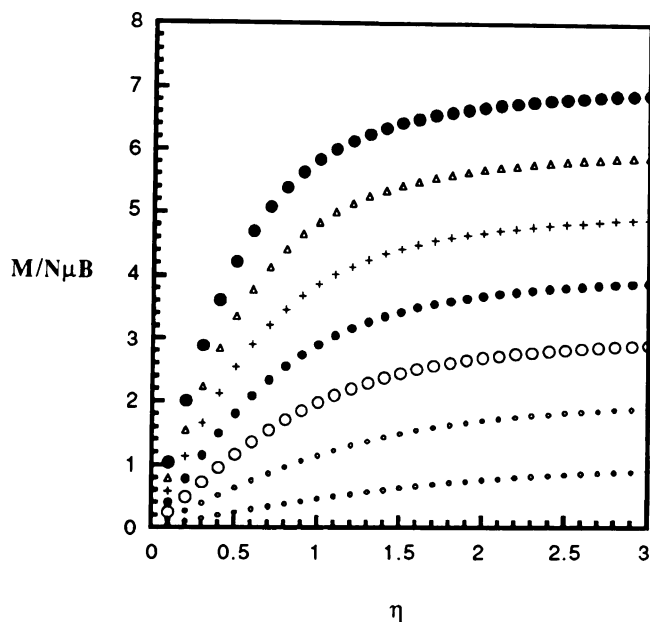


Figure 52. Plot of magnetization per radical, expressed in Bohr magnetons, against η for $S = 1/2$ to $7/2$ (bottom to top).

It is convenient to calculate the magnetic moment of a magnetic system with arbitrary spin-quantum number. The average magnetic moment of one radical can be calculated using the Brillouin function $B_S(\eta)$ which is defined below for N non-interacting atoms.

$$M_{sat} = Ng\mu_B SB_S(\eta)$$

$$\eta = \frac{g\mu_B}{k} \frac{H_z}{T}$$

$$B_S(\eta) = \frac{1}{S} \left[\left(S + \frac{1}{2} \right) \coth \left(S + \frac{1}{2} \right) \eta - \frac{1}{2} \coth \frac{\eta}{2} \right]$$

N is Avogadro's number, g is Landé's constant, S is the spin-quantum number.

The mean magnetic moment $\langle \mu_z \rangle$, or magnetization can be written as below. A plot of magnetization per radical expressed in Bohr magnetons μ_B , against η (dimensionless parameter directly proportional to field strength) for $S = 1/2$ to $7/2$ is shown in **Figure 52**.

$$\langle \mu_z \rangle = g \mu_B S B_S(\eta)$$

$$M = N \langle \mu_z \rangle = N g \mu_B S B_S(\eta)$$

Most of our radicals do not show saturation magnetization even at 55000G at 1.8K which are the field and temperature limits of our SQUID at Michigan State University. However in the case of the complex **1**•LiI, a near perfect fit is found to the Brillouin function. (**Figure 53**). Many of our radicals might show saturation at higher than 55000G using a pulsed magnet. In some of the organic radicals such as the DPPH complex with benzene which forms a linear chain in the solid state, Gervin used a pulsed magnetic field to achieve saturation of the complex at 13.4 T, more than twice of the field strength of our SQUID!¹⁶⁶

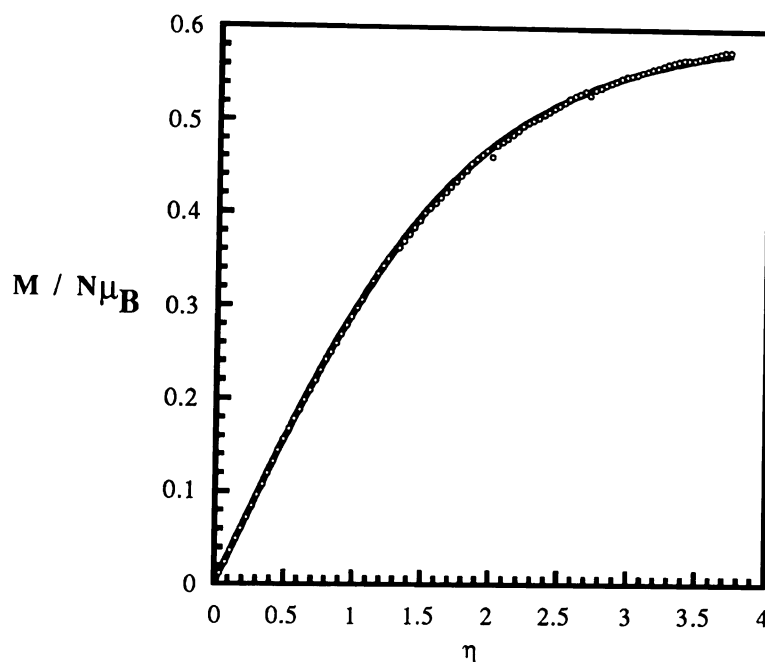
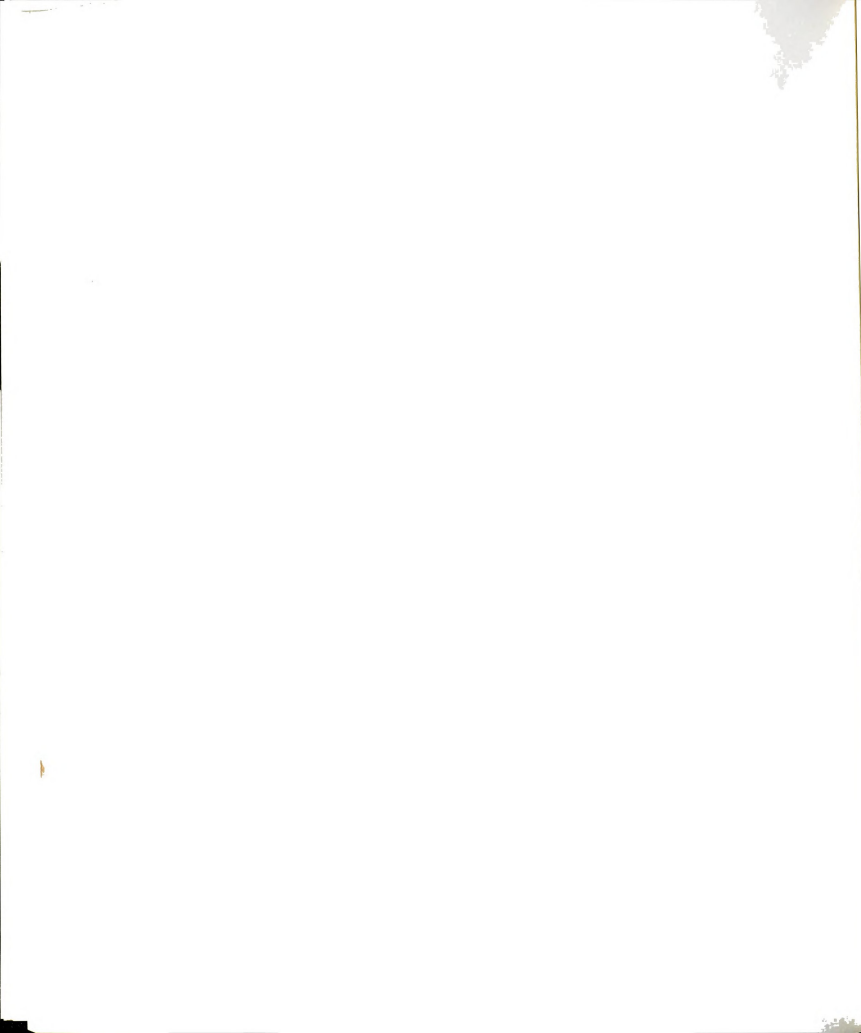


Figure 53. The saturation magnetization of the complex **1**•LiI at 1.8K. The data were fitted to Brillouin function using Kaleidagraph 3.0 with $S=0.62$ and $R=0.9999$.

3.3. Ferromagnetism of Complexes

Ferromagnetic behavior was observed in the precipitates obtained when solutions of **1** and LiBF_4 were mixed under argon atmosphere. Radical **1** alone, a red crystal, showed a weak anti ferromagnetism, in contrast to the salt-treated samples; lithium salts alone showed diamagnetic behavior, suggesting that the observed ferromagnetism must somehow derive from the combination of the radical **1** with the lithium salts. Along the same line, the complex of radical **1** with ZnCl_2 shows a hysteresis curve with less saturation than complex **1**• LiBF_4 as shown in **Figure 54**.



Our results are reproducible despite variations in synthesis of radical **1**, careful control experiments on starting materials, and filtration to remove any magnetic particulates. Atomic emission experiments yielded inconclusive results for the presence of ferromagnetic impurities. An ac susceptibility measurement, which is now available with the new SQUID at Michigan State University might also give better handles when we have structurally well defined materials.

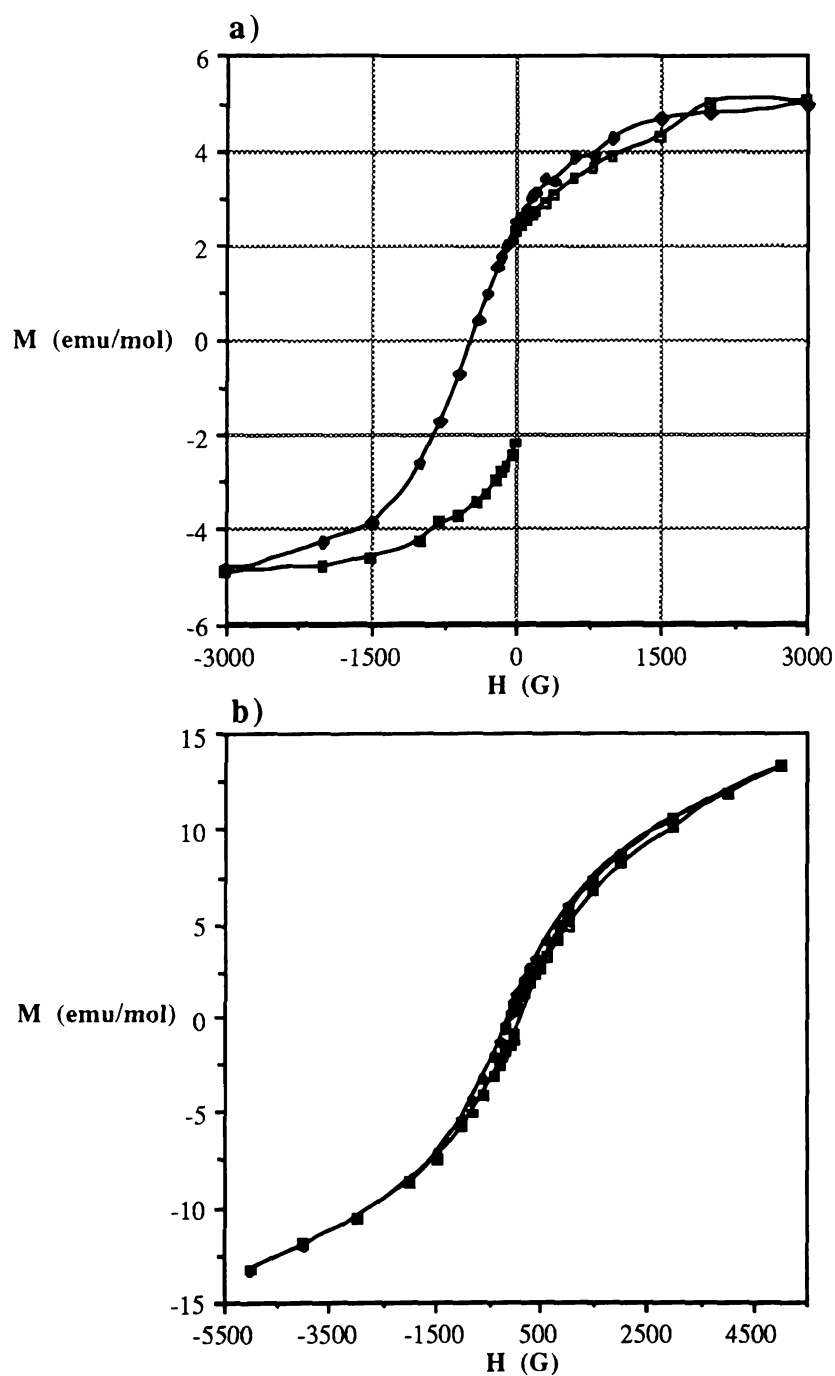


Figure 54. The field dependence of a) the complex $1 \cdot \text{LiBF}_4$ at 5K and b) the complex $1 \cdot \text{ZnCl}_2$ showing characteristic ferromagnetic hysteresis curve.

3.4. Antiferromagnetism of Radical Complexes

According to our original scheme for building magnetic chains, control over magnetic properties can be achieved by varying the metal cation, and thus, the distance between radical centers. The first consideration in selecting metal salts was the size of the metal cation and the availability of unpaired electrons in the metal. The complex of triaryl methyl radical and a paramagnetic metal cation might give us better model to study the linear combination of hetero open shell environment. Various alkali metal salts were the logical choice at first and some first row transition metal salts like CuCl_2 and CrCl_3 were tested for possible magnetic chain formation. None of the sodium or magnesium complexes with radical **1** showed any interesting magnetic behavior except simple paramagnetism which suggests that the sodium cation is unable to induce a magnetic interaction to occur. The complex of $\mathbf{1} \cdot \text{CrCl}_3$ again showed simple paramagnetic behavior with far less spin count than expected. The significance of this observation is not clear. Perhaps the metal caps the radical center as in the case of $\mathbf{1} \cdot \text{LiI}$ and $\mathbf{1} \cdot \text{NH}_4\text{I}$ and there are antiferromagnetic interactions between the unpaired electrons of the metal and the radical. It is not clear what kind of interactions are involved without knowing the solid state structure of the complex.

The complex $\mathbf{1} \cdot \text{CdCl}_2$ shows classical antiferromagnetic temperature dependencies with χ_{max} at 25K which may be explained with an alternating linear chain Heisenberg model. Attempts were made to fit the temperature dependence data with various models. The coupling constant J varies from

-10.2 to -19.7 cm^{-1} depending on the model used (Figures 55 and 56). The Bleaney-Bowers dimer model with paramagnetic impurity correction gave an inter-radical coupling constant of $J = -13.5 \text{ cm}^{-1}$ (-19.4 K) with 5% paramagnetic impurity ($R = 0.9998$). Calrin's mean field correction of the Bleaney-Bowers model (described in the introductions) with paramagnetic impurity correction gave $J = -13.6 \text{ cm}^{-1}$ (-19.5 K), $J'Z = 11.4 \text{ cm}^{-1}$ (16.5 K) where Z is number of neighboring dimers with 5.6% paramagnetic impurity ($R = 0.9998$). This alternating dimer model (chain of dimers) can be explained as an alternating Heisenberg linear chain when Z is 2 with an interdimer coupling constant of $J' = 5.7 \text{ cm}^{-1}$ (8.3 K). It is still not clear which model is the best for the complex $\mathbf{1} \cdot \text{CdCl}_2$ without having the solid state structure of the complex.

The anti-ferromagnetic behavior of the complex $\mathbf{1} \cdot \text{CdCl}_2$ was reproduced several times; this combination is unique in the sense that the complexes of radical $\mathbf{1}$ with CdBr_2 and CdI_2 only show simple paramagnetic temperature dependencies, as do those with NaBPh_4 . Numerous attempts to grow a single crystal were unsuccessful, with only polycrystalline materials obtained. X-ray powder patterns (Figure 57) of the radical and the CdCl_2 complex show clear differences but do not provide real structural information for this unique system.

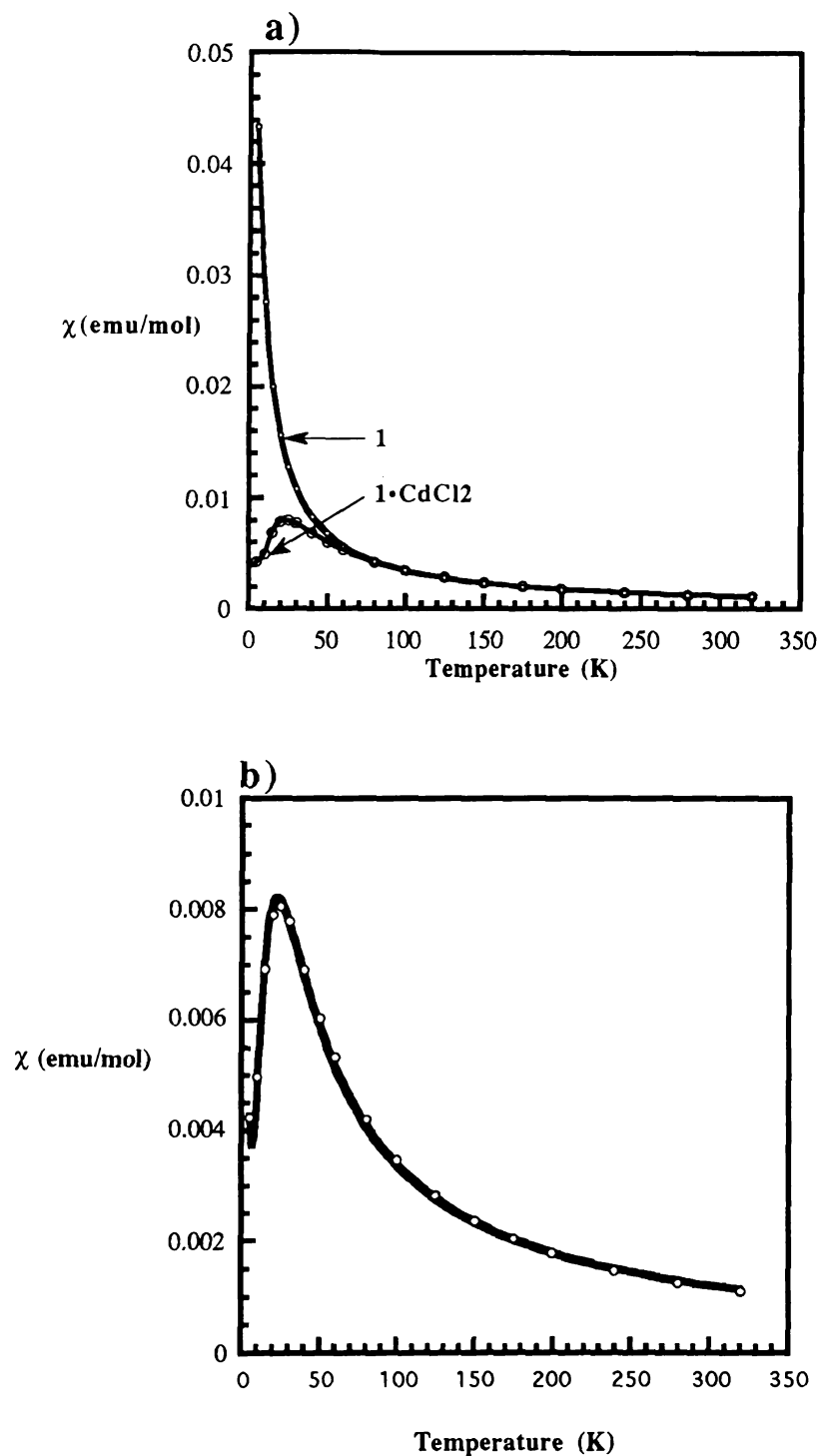


Figure 55. The temperature dependence of a) the radical **1** and complex **1**·CdCl₂ at 500G; b) with Bleaney-Bowers dimer model with $J = -13.5 \text{ cm}^{-1}$ (-19.4 K), 5% paramagnetic impurity, and $R = 0.9998$.

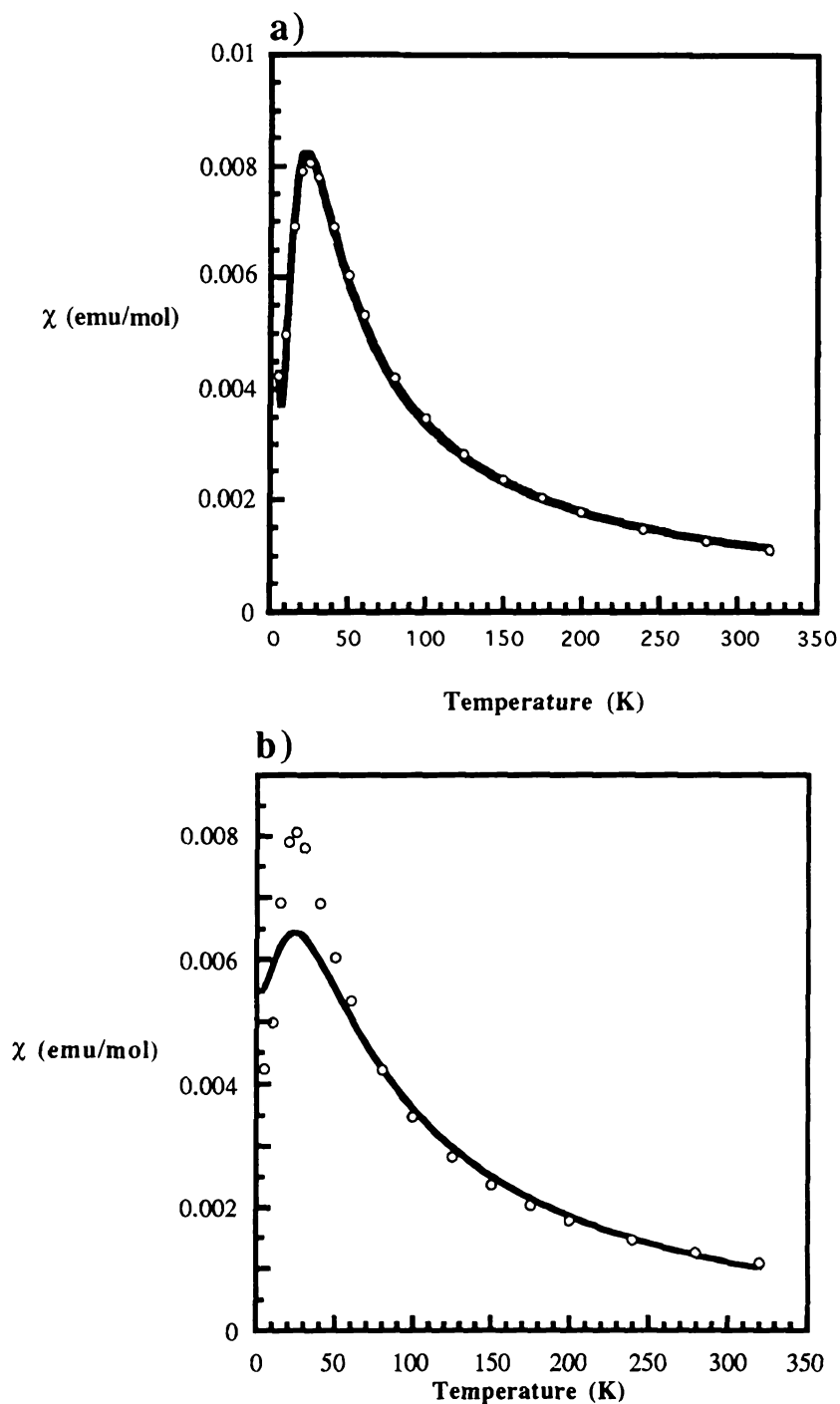
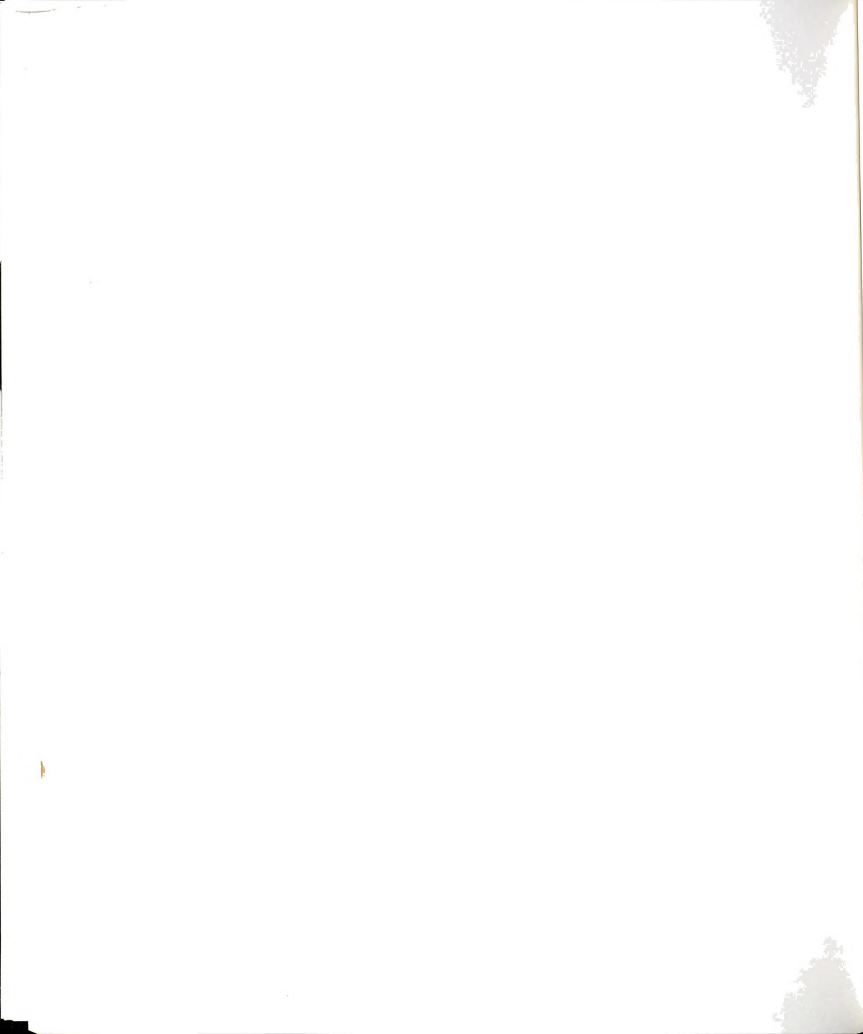


Figure 56. The temperature dependence of the complex $1 \cdot \text{CdCl}_2$ at 500G a) with alternating dimer model with $J = -13.6 \text{ cm}^{-1}$ (-19.5 K), $J' = 3.8 \text{ cm}^{-1}$ (5.5K), $Z=3$, 5.6% paramagnetic impurity, and $R = 0.9998$; b) with linear chain Heisenberg model $J = -19.7 \text{ cm}^{-1}$ (-28.5K) and $R = 0.9884$.



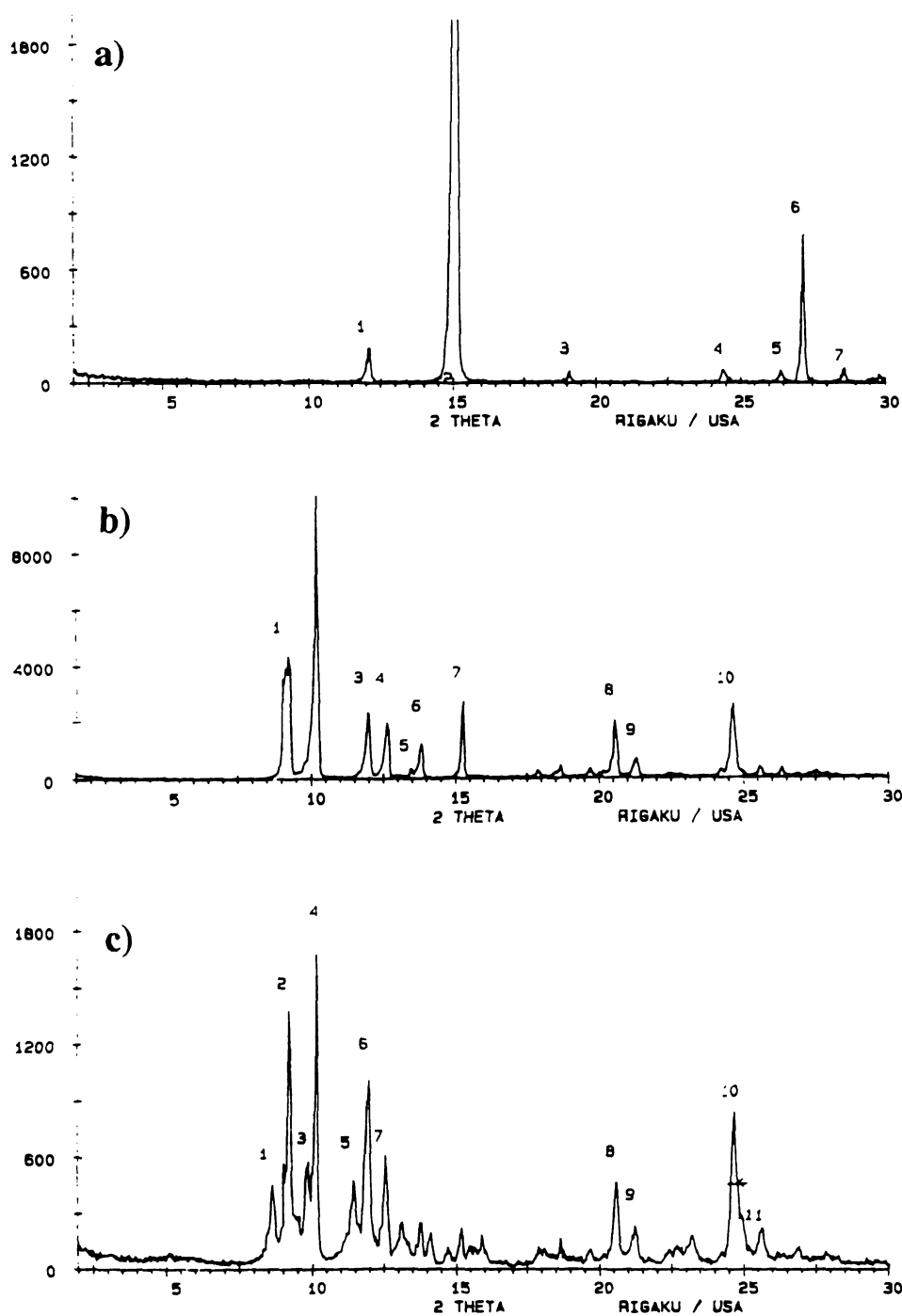
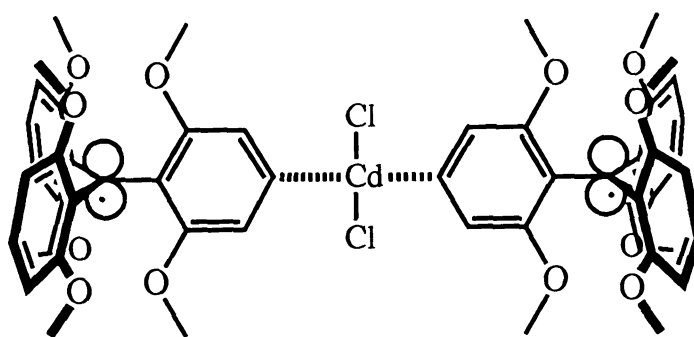


Figure 57. X-ray powder patterns of a) CdCl_2 , b) the radical 1, and c) the complex $1 \cdot \text{CdCl}_2$.

An attempt was made to find information on the electronic coupling of Cd(II) and the radical center by ESEEM using radical **86**. Although significant new features were observed, the spectra were too complex to yield any meaningful answers. The experiment is complicated by the fact that there are two different magnetic Cd isotopes (111 and 113), roughly equal in natural abundance, and a third non-magnetic isotope (112) that makes up the majority (~75%) of the element's composition. It would be very useful to have the structure of the complex in order to understand the mechanism of the magnetic coupling between CdCl₂ and **1**. There are two possible coupling routes to form an alternating dimeric chain: a) the originally intended linear chain formation through metal ion-binding oxygen pockets to form a chain; b) simple Cd-mediated linkage from para-carbon to para-carbon in two radicals as shown below; or both. The magnetic data from CdBr₂ and CdI₂ suggest that the mechanism shown below may not be the right one. The magnetic measurements on complexes of other para substituted radicals such as **78** may give more straightforward answers to this question.

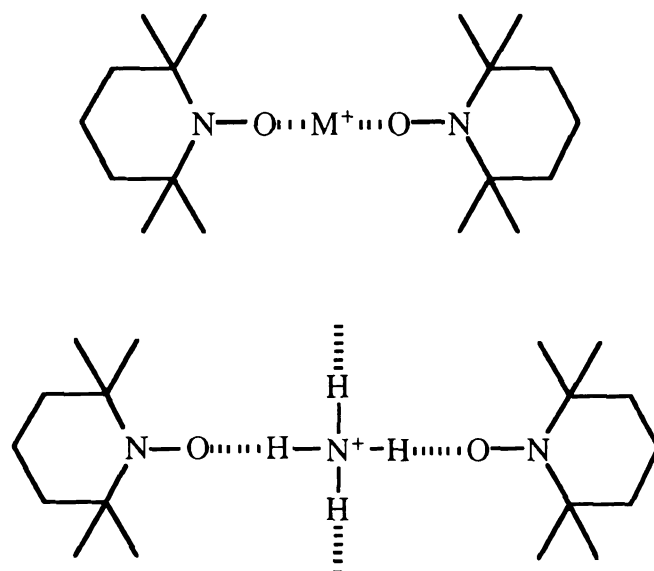


4. Design of Molecular Magnets by Other Ion-Binding

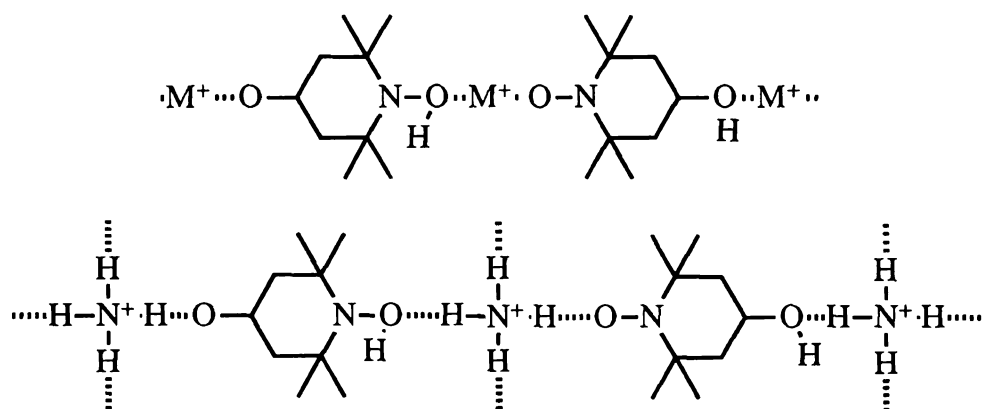
Recently, we found that treatment of TEMPO with ammonium or lithium salts leads to high-spin coupled materials. EPR spectra for these



systems show strong half-field transitions, diagnostic for high spin-coupling. No structural details are yet available, but the LiI complex of TEMPO forms crystalline long needles, and we are optimistic that it might provide a probe for the long overdue question of pairwise radical coupling directly through alkali metal cations.



It is tempting to envision pairwise radical interactions through a metal cation in the case of TEMPO and DPPH. In contrast, the resonance delocalized structures of galvinoxyl and nitronyl nitroxides suggest that these subunits may be able to participate in forming extend structures. Special attention should be paid to the search for triplet or higher spin transitions in the EPR spectra and susceptibility measurements using SQUID.



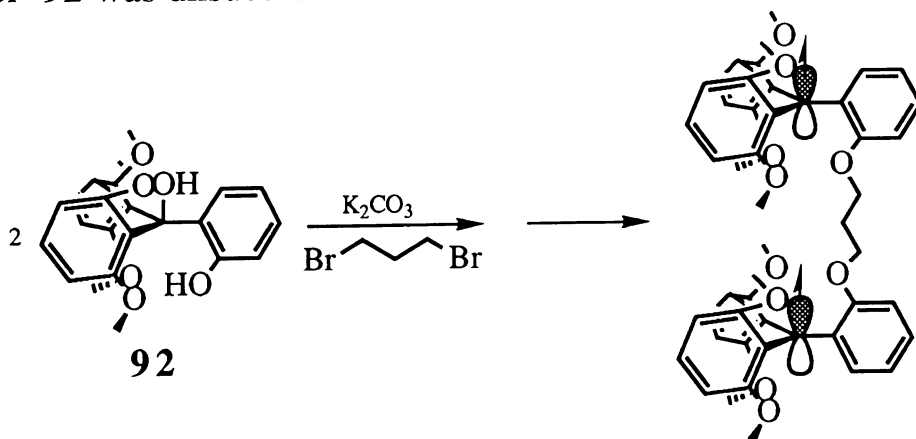
Furthermore, other commercially available stable organic radicals such as TEMPOL can be used to probe this problem including the effects of the counter anions of the coupling salts or the formation of extended structures such as those shown above.



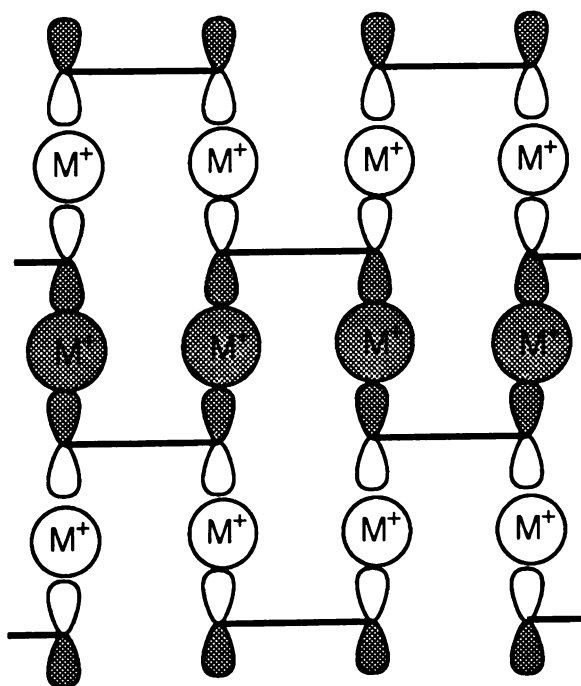
5. Introduction of Cross-Linkers

To obtain materials which exhibit bulk ferromagnetism, high-spin coupling of the constituent paramagnets must occur in three dimensions. Our picture of stacked radicals sandwiched around metal ions provides a one-dimensional coupling scheme, but how can the expected stacks be made to communicate magnetically? In the few known molecular ferromagnets, this issue has simply resolved itself without explicit action being taken to control it. However, to understand the requirements for stack-stack coupling in detail, we planned to examine both intra- and interstack types of electron-electron coupling by explicitly building biradical systems to model and/or induce these interactions.

By isolating the functional diradical unit **2** of our proposed polymeric chains, the intrastack electronic coupling can be studied. We planned to build two series of these diradical complexants; the triarylmethyl radicals linked through alkyl chains and meta-xylylene linked poly radicals. An attempt to build the alkyl chain linked biradical shown below using monomer **92** was unsuccessful.

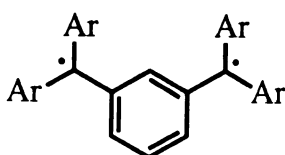


To avoid chain-chain cancellation of magnetic moments, an interchain coupling mechanism is necessary. An approach to this requirement is to build electronically and physically cross linked monomers into the chains, enforcing interchain communication. In contrast to **92**, aromatic ring linked diradicals should be fairly rigid, with little opportunity to vary the radical-radical distance, whether or not a metal ion is present in the internal cavity. There are many possible model systems which could be used in building three dimensional structures.

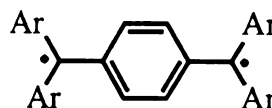


Among numerous possible aromatic linked biradicals, several phenyl linked ones, such as diradicals **93** and **94** are synthetically accessible by simple modification of usual procedure. According to the π -topology of alternant hydrocarbon discussed in the introduction, the diradical **93** should be high-spin coupled and the diradical **94** should be low-spin coupled. Radical **93** shows two reversible redox waves in the cation/radical couple of -0.12 and -0.41V, and only one redox wave in the

anion/radical couple of -2.03 V in CV (Referenced to ferrocene oxidation; Measured in CH_2Cl_2 solution of $(n\text{-Bu})_4\text{NBF}_4$). The two reversible redox waves in the diradical **93** presumably correspond to the radical cation and the diradical which is characteristic evidence for the formation of a diradical. The CW-EPR spectrum of the diradical **93** in THF was too complex to analyze for hyperfine coupling constants at present.¹⁶⁷ The half-field transition of diradical **93** was also not detected under various conditions.

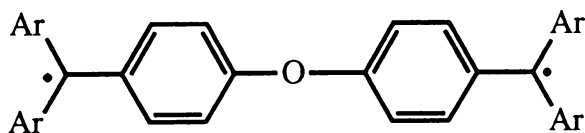


93 (Ar=2,6-dimethoxyphenyl)

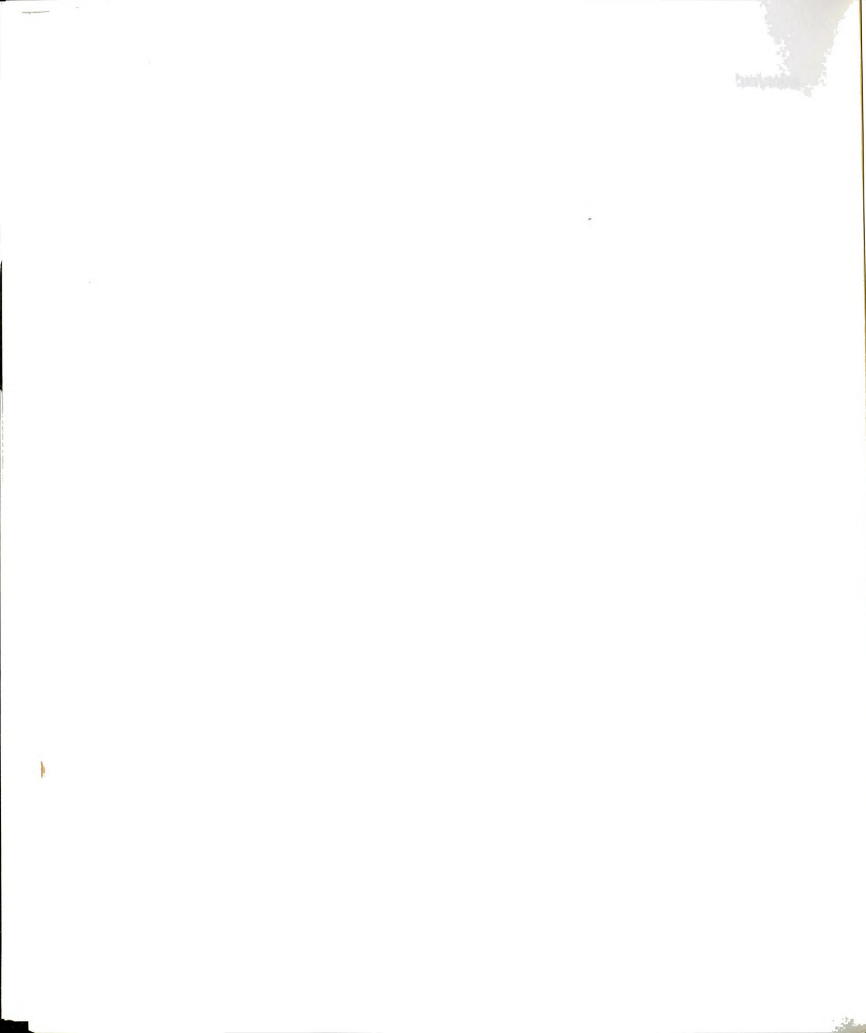


94

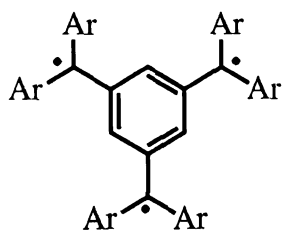
A diradical such as **95** could also be used in building three-dimensional structures with proper ion-binding ability. This system shows a reversible redox potential of -0.44 V for the cation/radical couple and -1.93 V for the anion/radical couple (Referenced to ferrocene oxidation; Measured in CH_2Cl_2 solution of $(n\text{-Bu})_4\text{NBF}_4$), and a CW-EPR spectrum which is comparable to those of other para substituted TMTP methyl radicals such as **78**, **79**, **80**, and **83** which means this radical is not antiferromagnetically coupled strongly as predicted by theory. A half-field transition was not detected.



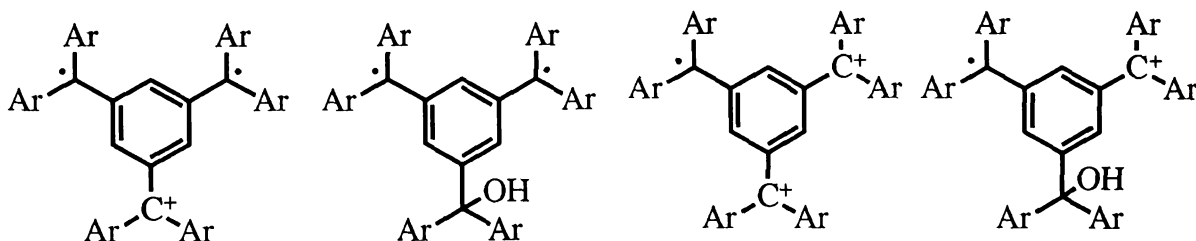
95 (Ar=2,6-dimethoxyphenyl)

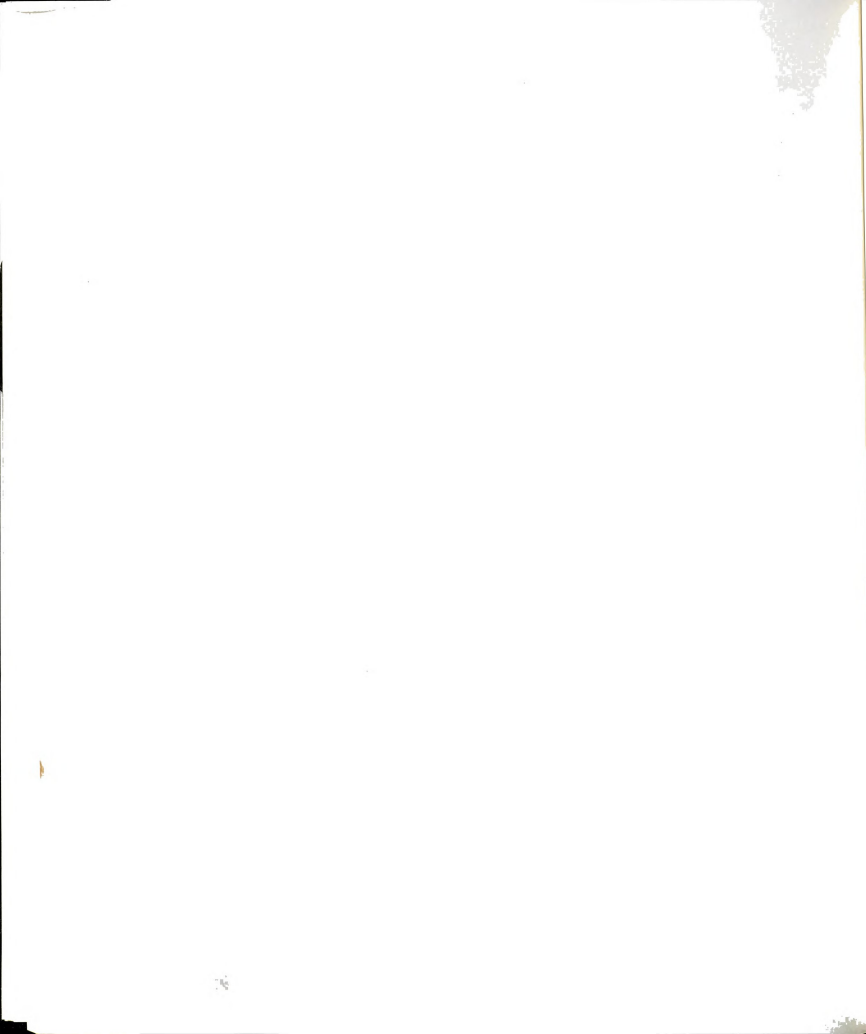


A triradical such as **96** could also be used in building extended structures by using two-dimensional frameworks extended into three-dimensional structures by ion-binding. Characterization of such systems is complex and the already detected half-field transition spectra of **96** at 77K has a problem of interpretation due to the fact that it might also be the half-field transition of the diradical cation or a diradical as shown below.



96 (Ar=2,6-dimethoxyphenyl)



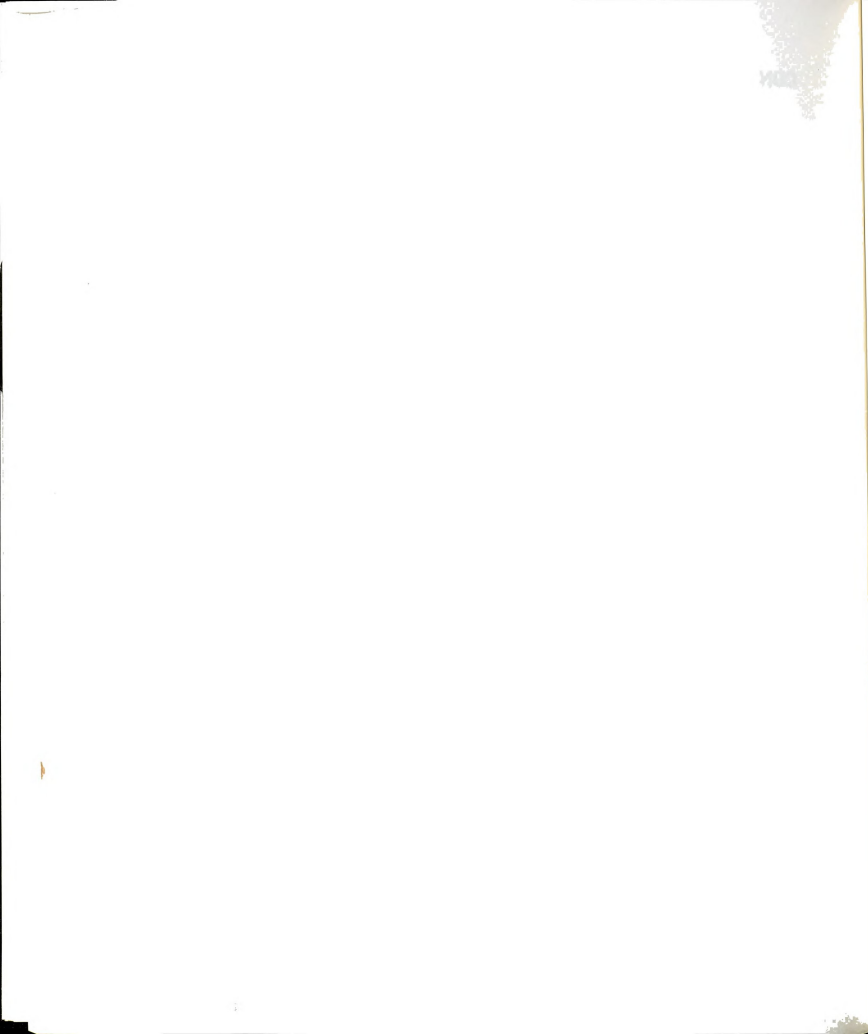


CONCLUSIONS AND SUGGESTIONS FOR FUTURE WORK

Conclusions

We have begun a new line of investigation into molecular magnetic materials, which may ultimately extend our understanding of molecular magnetism. Magnetic measurements (SQUID) suggest that we can induce ferro- and antiferro-magnetic behavior in complexes of stable organic radicals with various metal salts. Cyclic voltammetry of HMTF methyl and TMTF methyl radicals demonstrates our ability to adjust their electronic character by variation of substituents. X-ray data for radicals **1**, triarylmethyl cation **62**, triarylborane **63**, triaryl carbinol **71**, triaryl methane **73**, triarylsilane **74**, and ammonium adduct **72**, and the hexachloro ammonium adduct **75** have built a structural basis for preorganized ion-binding. Complexation studies of **63**, **64**, **87**, and **88** by UV-Vis spectrophotometry and NMR suggest complexations. ESEEM studies of the truncated complex **86**•2LiBF₄, **86**•2LiI, **86**•2NaBPh₄, and **86**•2NaI show that two metal ions are bound at the expected distance with spin densities of 0.3% on the metal cations, and molecular mechanics and semiempirical molecular orbital calculations agree on the structure of the complex. Ab Initio molecular orbital calculations offer an explanation for the high-spin coupling in radical metal radical systems.

Two critical issues have focused our efforts in this research. First, structural characterization of metal-radical complexes is essential to our understanding of the rules governing long-range organization in these new materials. Such an understanding is required for the rational construction



of organic magnetic substances. By using X-ray crystallography, we have studied *monomers* with the binding sites of interest; we have also obtained a certain amount of indirect (spectroscopic, electrochemical) evidence for ion binding. Now more detailed geometrical insights into the complexation phenomena are needed.

The second focal issue is the fundamental description of the metal ion-mediated magnetic interactions between organic paramagnets. Assuming our structural pictures of the extended complexation are correct, how is a lone radical such as **1** perturbed by metal ion binding? More importantly, how do two radicals **1**, magnetically independent in the absence of salts, couple around a metal ion to make an interrupted σ -bond? What is the sign and magnitude of the exchange integral between the two paramagnetic centers? Can it be properly understood in terms of simple molecular orbital pictures?

We have begun with magnetic, chemical, and structural characterization of various triaryl methyl radicals and their complexes with different metal cations. There is enormous structural flexibility in our ion-binding approach to building molecular magnet, where the triaryl-X platforms provide triether binding pockets for metal ions. There are several controllable variables in the basic triaryl-X structure, and in terms of the number of triether binding faces present. All of these variables should be further investigated in order to optimize the selection of the best candidates for assembly of stable extended complexes.

X-ray structures for complexes of radicals and boranes with metal salts are desperately needed. Detailed magnetic characterization of well-defined materials, ideally as single crystals, will enhance our understanding of the

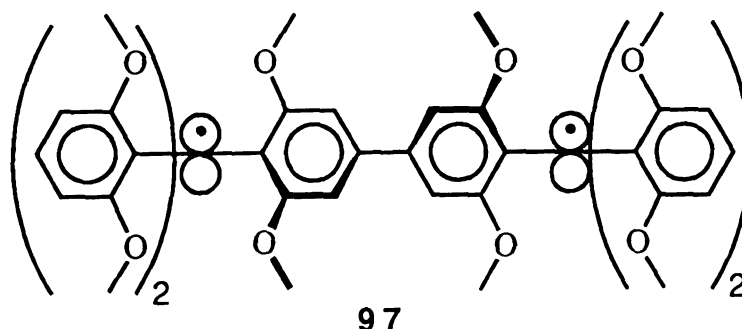
1000
1000
1000

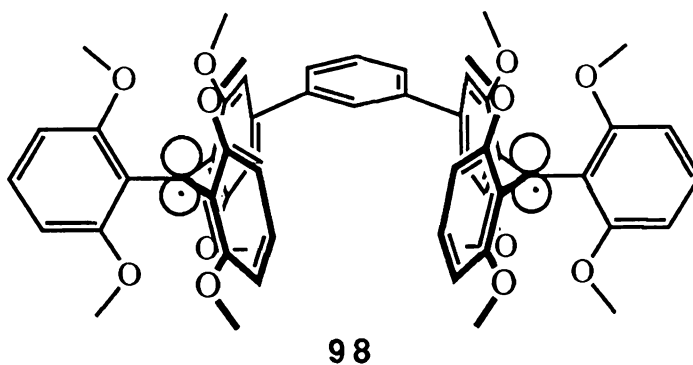
relationships of structure and odd-electron coupling. By systematically building up an understanding of the ion binding and magnetic properties of these systems, we hope to establish this new approach as an effective paradigm for the assembly of 1- and ultimately of 3-dimensional molecular magnetic materials.

Suggestions for future work

1. Aromatic Linked Biradicals

We planned to attach a second hexamethoxytriphenylmethyl radical unit at the *para* position of an aryl ring of **1** to make diradical **97**. Studies on Chichibabin's hydrocarbon¹⁶⁸ suggest that for the highly twisted **97**, open-shell paramagnetic electronic structures will be important, despite the availability of closed-shell classical structures.¹⁶⁹ In hopes of extending our studies to the rational assembly of metal-organic complex solids with bulk magnetism, the examination of the complexation and chain-forming behavior of **97**, **98**, and their derivatives will be very important.





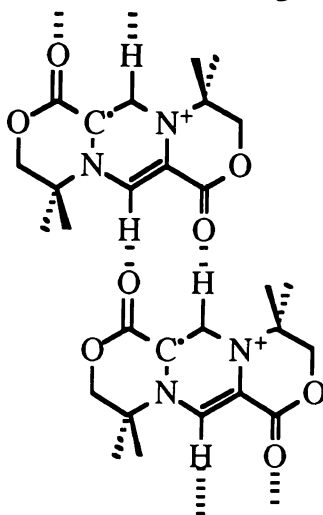
2. Magnetic Coupling through Hydrogen Bonds

Numerous examples of macromolecular chemistry have been based on frameworks of hydrogen-bonds.¹⁷⁰ Extensive studies have been reported of the structural and electronic properties of such systems. The detailed descriptions of orbital interactions through hydrogen-bonds lead us to consider a strategy in building organic magnets.

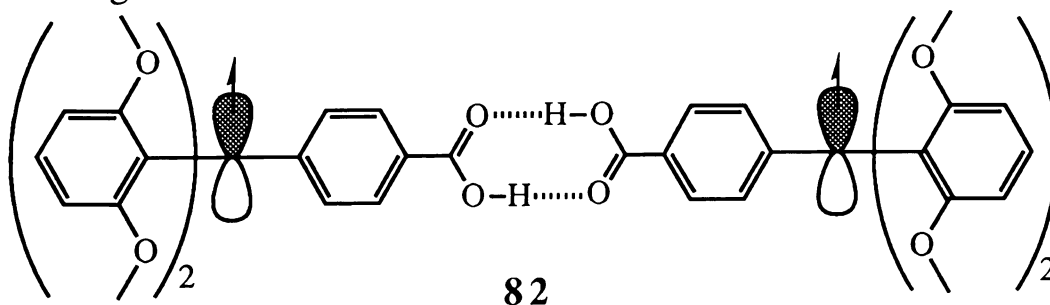
Electron transfer and energy transfer through space and through bonds, especially through hydrogen bonding have been pursued extensively in recent years, and theoretical understanding of the interactions involved can be explained by many theories.¹⁷¹

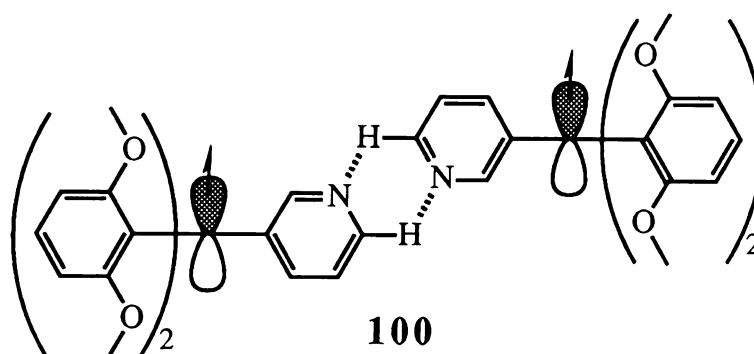
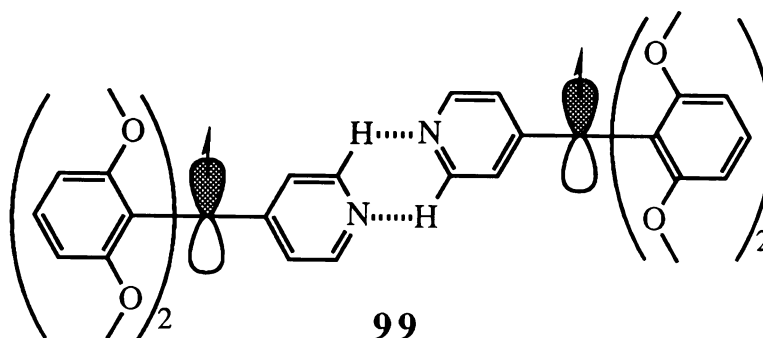
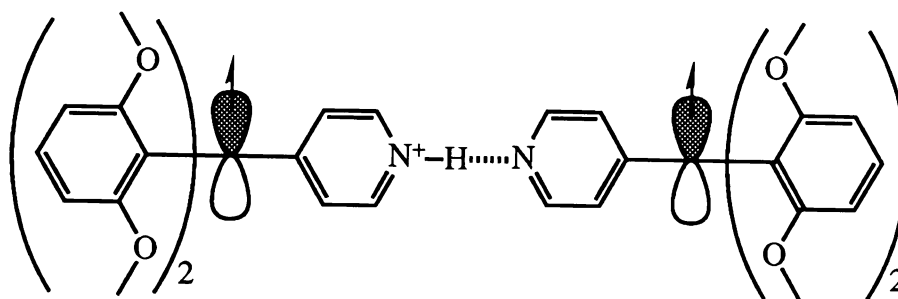
Magnetic interactions through bonds and through space have been proposed by Hoffmann and Gleiter in organic diradicals and in inorganic bimetallic bridging ligand systems and the basic theory has been accepted for more than 20 years.¹⁷² Magnetic interactions through hydrogen-bonds were suggested by Carlin in 1985 in an attempt to explain magnetic susceptibility data on a 2:1 complex of nitroxyl radical and Cu (II) complexes. In an attempt to explain the structural and magnetic behavior of a TCNQ

complex of radical cation of 1,4-hydrazine systems shown below, Koch reported at the 1993 Denver ACS meeting the first example of magnetic interactions in an infinite organic chains in which the ferromagnetic coupling was mediated by hydrogen-bonding interactions.



The possibilities of designing magnetic interaction through hydrogen bonding are endless in organic radicals as illustrated by the numerous macromolecular structures already reported. Any stable organic radicals with proper functions for hydrogen bonding can be considered to be a target for testing the proposed magnetic coupling. Simple derivatives of TMTP radical such as radicals **82**, **99**, and **100** shown below (which we have synthesized already) can serve as pairwise model systems in building organic magnets.

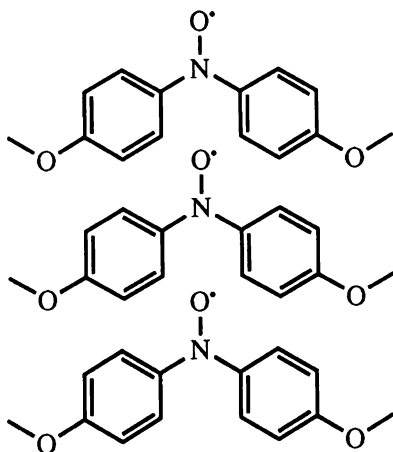




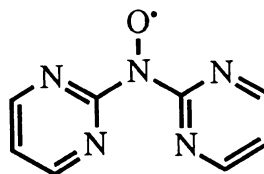
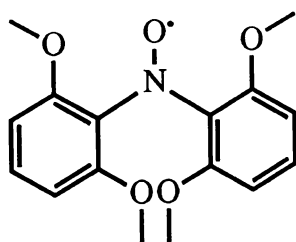
3. Ion-Binding in Various Nitroxyl Radicals

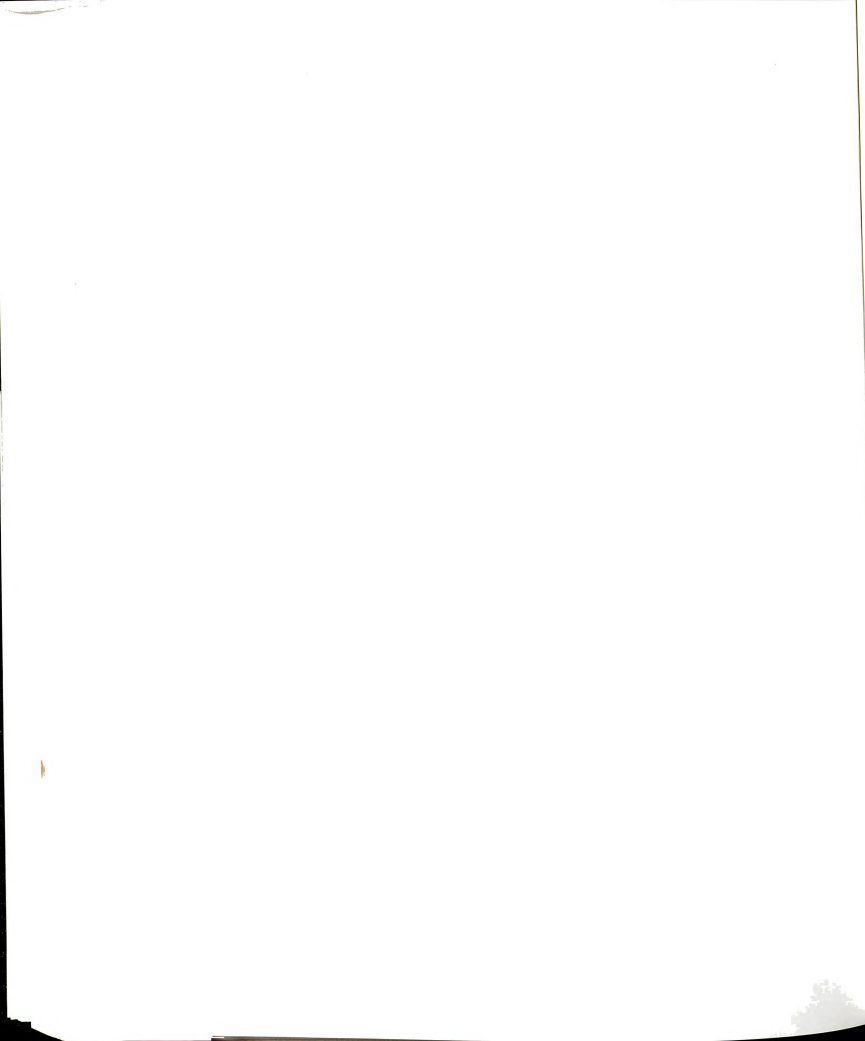
As discussed in the introduction, the study of nitroxyl radicals is one of the most active areas of molecular magnet research. The nitroxyl radicals, especially diaryl nitroxyl radicals, offer logical extensions of our strategy in building molecular magnets by ion-binding. The 4,4'-dimethoxy diphenyl nitroxide shown below has never been studied for molecular magnets even though the X-ray structure with a packing diagram has been known for more than 40 years. Magnetic measurements on a

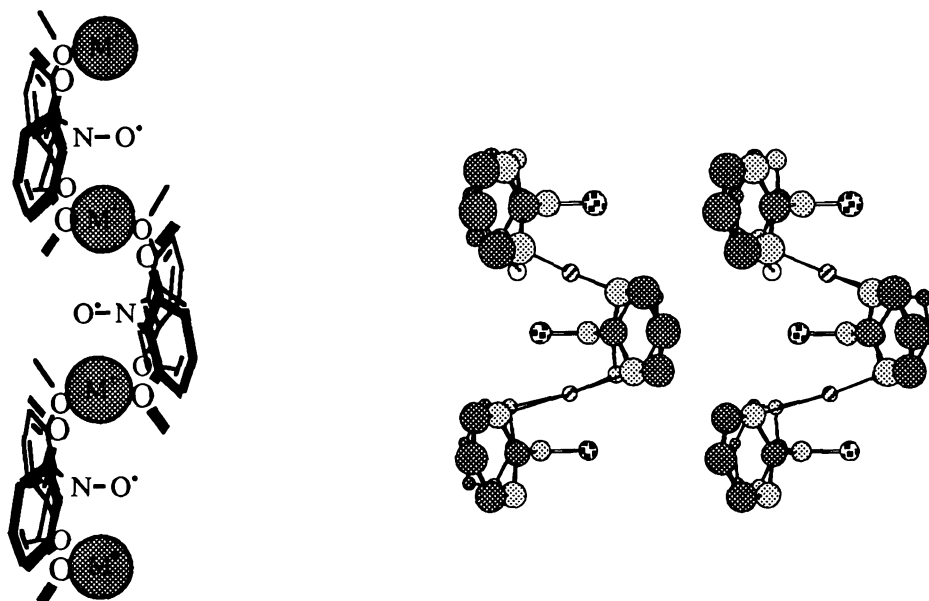
single crystals of the radical might give insight on the mechanism of inter-radical interactions in nitroxyl radicals.



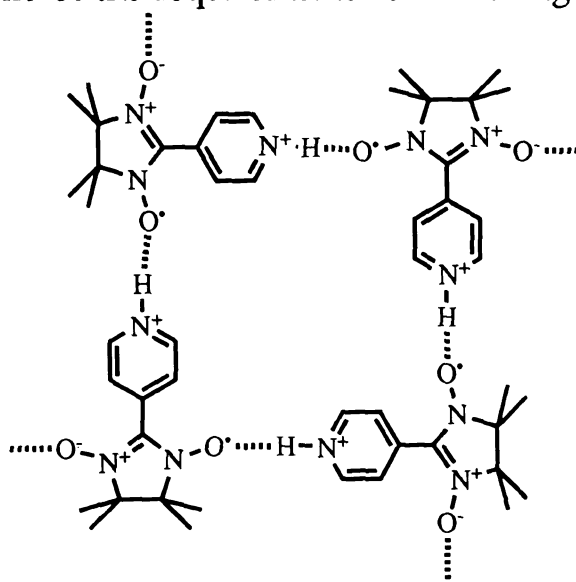
There are several advantages of using nitroxyl radicals compared to triaryl methyl radicals: The Lewis basicity of nitroxyl as demonstrated by Drago in TEMPO; spin polarizability of nitroxyls; inherent stability of diaryl nitroxyls when they are protected against CO dimerizations by para-substitution and twisting of rings by ortho-substituents. Possible linear complexes of bis-(2,6-dimethoxyphenyl nitroxyl and bis(2,6-pyrimidyl) nitroxyl with metal ions are shown on the next page.



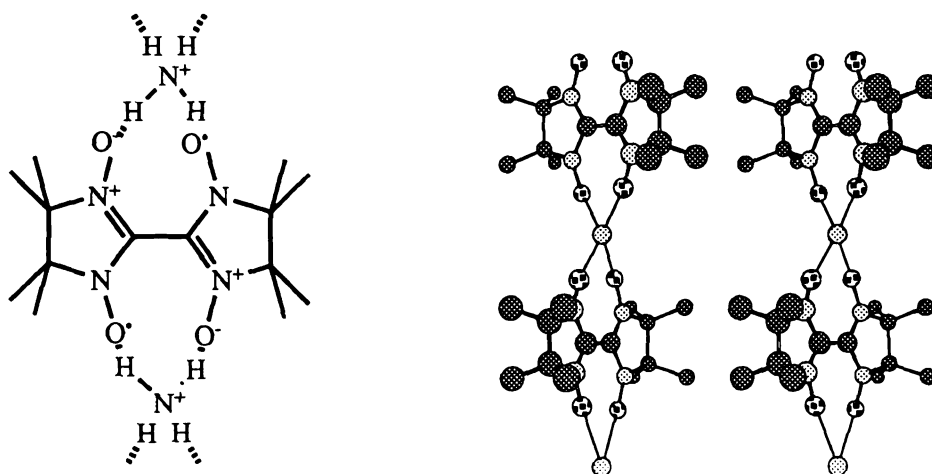




As we have seen earlier, the para-pyridyl nitronyl nitroxide is ferromagnetic in the solid state and forms linear chains through "hydrogen-bonding" interactions. The para-pyridinium nitronyl nitroxide might crystallize to give a magnetic structure with a hydrogen-bonding framework shown below. There would be little overlap in this arrangement between the SOMOs, while maintaining overlaps between other frontier orbitals which is one of the requirements for ferromagnetic coupling.



Ullman's biradical¹³⁰ is another logical precursor for an extension of our non-covalent interaction strategy. A proposed Ullman's biradical complex with NH_4^+ is shown below as a stereo view. There will be little overlap in this diradical between the SOMOs because of the orthogonality of the orbitals, while maintaining overlaps between other frontier orbitals.



EXPERIMENTAL

1. General Procedures

All ^1H NMR and ^{13}C NMR spectra were obtained with a 300MHz Varian Gemini or a 300 MHz Varian VXR-300 instrument. IR spectra were recorded using Perkin-Elmer 599 IR or Nicolet IR/42 spectrometers. UV spectra were recorded on a Shimadzu UV-160 or Hitachi U-2000 spectrophotometers. Gas Chromatography was conducted on a Perkin-Elmer 8500 using a 25-m (0.32 mm Diameter) bonded methyl silicone column with an FID detector. HPLC was conducted on a Perkin-Elmer Binary LC Pump 250 and LC-235 Diode Array Detector. Mass spectra were recorded on a Finnigan 4000 GC/MS or on a VG Trio-1 5890 GC/MS, using a 30m SE-54 Altech Capillary column. Electron Spin Echo Envelope Modulation (ESEEM) studies by pulsed EPR experiments were conducted on an instrument build by Professor John McCracken, MSU.

Powder X-ray pattern were recorded on a Phillips XRG 3000 computer-controlled powder diffractometer, operating at 40kV, 35 mA. Single crystal X-ray diffraction peaks were recorded on a Nicolet P3F diffractometer or Enraf-Nonius CAD-4 diffractometer using graphite monochromated Cu $K\alpha$ radiation and an ω -2 θ scan by Professor Kahr at Purdue University. Absorption corrections were applied using the program DIFABS (Walker & Stuart, 1983), SHELXS86 (Sheldrick, 1986), and MULTAN82 (Main, Fiske, Hull, Lessinger, Germain, Dec lercq, and

Woolfson, 1982). In each case computations were performed on a VAX computer using SDP/VAX software (Frenz, 1978).

2. Solvents and Chemicals

All chemicals used were from Aldrich Chemical Co. or Lancaster Synthesis Inc., unless otherwise noted. Some of the metal salts were from Alpha Chemical Co. Solvents were from Fisher Scientific Co., MTM Research Chemicals, J. T. Baker Chemical Co., Johnson Matthey Chemical Co, and Mallinckrodt, Inc.

THF, diethyl ether, and benzene were freshly distilled from sodium and benzophenone under argon. Dry acetonitrile and other solvents were distilled from CaH_2 under argon as needed.

3. Equipments and Procedures

CV Measurements

CV spectra were recorded on a EG & G Princeton Applied Research Scanning Potentiostat Model 273 and 362 using Bioanalytical Systems Ag/AgCl as a reference electrode. A potentiostat Model 273 was interfaced to a PC which controls the potentiometer, including data collection and plotting. The construction of the experimental cell has been described elsewhere. (P. T. Kissinger, *J. Chem. Educ.* **60**, 702, 1983.) Measurements were made under argon on a 1×10^{-4} to 1×10^{-5} M sample of substrate in 7 to 8 ml of freshly distilled dry THF or spectroscopic grade

methylen chloride containing 0.1 M tetra-n-butyl ammonium tetrafluoroborate. A platinum button was the working electrode and a platinum coil was the counter electrode. The reference electrode was a silver wire immersed in a 3M NaCl solution, separated from the bulk solution by a Vycor tip. The Vycor tip gave some water leakage problems, but it was satisfactory in determining redox potentials with ferrocene as an internal reference to determine the potentials. Pulsed differential voltammograms were obtained with a slight modification in operating programs in the PC. The scan rates were 50 to 400 mV per second and a typical one was 200 mV per second. In all cases reversibility was checked by verifying the equal height of the oxidation and reduction waves in cyclic voltammetry, and by examining peak to peak distances of the forward and reverse scans.

VT-EPR Measurements

CW-EPR spectra were recorded using a Varian E4 spectrometer with variable temperature control. The temperature range was 25 to -140 °C (temperature was controlled by a flow of nitrogen gas running through a cooling coils in liquid nitrogen). Most of the spectra for HMTP methyl derivatives and TMTP methyl derivatives gave strong enough signals without phasing problems, except in the range of -70 to -90 °C, which was evidently inherent to the spectrometers. Various conditions were studied with scan windows of 10G to 4000G, modulation amplitude of 1×10^{-2} G to 1G and receiver gain of 1×10^1 to 5×10^3 with microwave power of 1 to 5 mW.

SQUID Measurements

Magnetic susceptibility measurements in the temperature range from 1.8K to 350 K at -55kG to 55kG were performed on a MPMS Quantum Design SQUID magnetometer. Powder or polycrystalline samples were dried, weighed and placed into a capsule with a minimum amount of cotton on the top. A ventilating hole was made in the capsule with a fine needle, the capsule was placed in a normal drinking straw, and its position was fixed securely with threads up and down. The sample straw was attached to a sample rod with general centering according to the length of the sample from the top of the rod with the mass of the sample, and inserted into the evacuation chamber. The sample was lowered into an experiment chamber slowly followed by three cosecutive evacuations of air.

The sample was oriented in the 200 G to 1000 G external magnetic field according to the centering scheme built into the machine. Magnetic susceptibility measurements were conducted according to temperature and field dependence sequences. A general sequence consisted of field dependence measurements over -5000 G to 5000 G at 2 and 5 K, magnetization measurements from 0 G to 50000 G at 1.8 K and temperature dependence experiments from 0 to 320 K at 200, 500, and 5000 G field strengths. The data collected were extracted into a data file in IBM PC ASCII format consisting of temperatures in K, external field strength in gauss, induced magnetic moments in emu, and their standard deviations. The data files were converted as Macintosh format and analyzed and plotted as molar susceptibilities.

4. Synthesis

General Procedures for Generation of Radicals

Method A: The cation tetrafluoroborate salts (200 mg) were reduced by 10 ml of ~5 M CrCl_2 solution (prepared with $\text{CrCl}_3 \cdot 6\text{H}_2\text{O}$ and Zn/Hg in 10% HCl solution), extracted with 10 ml of methylene chloride, washed with water twice, and dried with magnesium sulfate. Flash column chromatography with diethyl ether over silica gel gave a solution of the radical.

Method B: The cation tetrafluoroborate salts (200 mg) were reduced by the addition of an excess (5 equivalents) solid CrCl_2 into 10 ml of methylene chloride solution of the cation and water (1:1 in volume) and the radical was extracted into methylene chloride, washed with water twice, and dried with magnesium sulfate. Flash column chromatography with diethyl ether over silica gel gave a chromatographically pure solution of radical.

Method C: The cation tetrafluoroborate salts (100 mg) were reduced by the addition of an excess iodide salt (3 equivalents) (NaI , LiI , NH_4I , and $n\text{-Bu}_4\text{NI}$) solution in 20 ml of dry THF and the radical was flash chromatographed using diethyl ether over silica gel as in Method B.

Method D: The cation tetrafluoroborate salt **4** (100 mg) was reduced to radical **1** by the addition of vitamin C (200 mg) in 20 ml of dry THF

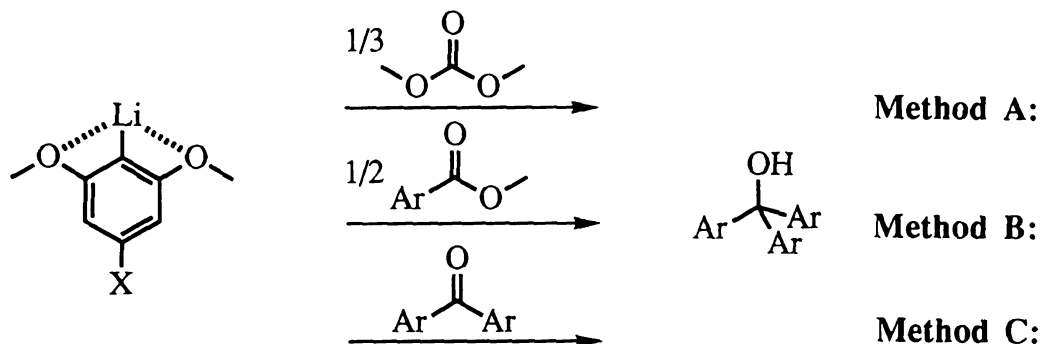
followed by stirring overnight under argon at room temperature. The radical solution was flash chromatographed as above.

Method E: Tris-(2,6-dimethoxy-3,5-dichlorophenyl)methyl ammonium tetrafluoroborate **17** was converted into a radical by diazotization. To a precooled solution of the salt (100-200 mg) in conc. HCl, a stoichiometric amount of saturated solution of NaNO₂ was added dropwise and the mixture was stirred until it warmed up to room temperature. The radical was extracted with 30 ml of diethyl ether, washed with water twice, dried with magnesium sulfate. Flash column chromatography using diethyl ether over silica gel gave a chromatographically pure solution of the radical.

General Procedures for Purification of Cations

A solution of the triaryl carbinol (200 to 500 mg.) in diethyl ether was treated with a small amount (0.1 to 0.5 ml.) of conc. HBF₄, and the dark blue precipitate was filtered, washed with diethyl ether, and dried to give cation tetrafluoroborate salt as a crystalline solid.

General Procedures for Preparation of Carbinols



Method A: To a solution of 2,6-dimethoxyphenyl lithium (0.218 mol.) in 200 ml. of dry diethyl ether, 0.3 equivalent amount (0.720 mol) of dimethyl carbonate in 300 ml. of benzene was added dropwise (using a pressure equalized dropping funnel) under argon, and the mixture was refluxed for 3 days. The reaction mixture was poured into 600 ml. of water and the organic phase was concentrated. Crystallization from ether or methylene chloride in n-hexane usually gave crystalline carbinols.

Method B: To a solution of 2,6-dimethoxyphenyl lithium (0.218 mol.) in 200 ml. of dry diethyl ether, 0.5 equivalent amounts (0.109 mol) of the esters in 400 ml. of benzene were added dropwise through a pressure equalized dropping funnel under argon and the mixture was refluxed for 3 days. The reaction mixture was poured into water and the organic phase was concentrated. Crystallization from ether or methylene chloride in n-hexane usually gave crystalline carbinols.

Method C: To a solution of 2,6-dimethoxyphenyl lithium (0.05 mol.) in 60 ml. of dry diethyl ether, an equivalent amount of the ketone (0.05 mol) was added dropwise through a pressure equalized dropping funnel under argon and the mixture was refluxed for 3 days. The reaction mixture was poured into 100 ml of ice water and the organic phase was concentrated to yield a gray residue. Crystallization from ether or methylene chloride in n-hexane gave carbinols.

2,6,2',6',2'',6''-Hexamethoxytriphenyl methyl, HMTP 1:

2,6-dimethoxymethylbenzoate: 2,6-dimethoxybenzoylchloride (100 g.) in 1 liter of methanol with 5% 2,6-dimethoxybenzoic acid was refluxed overnight under argon with stirring. (Commercially available 2,6-dimethoxybenzoyl chloride contains 5% 2,6-dimethoxybenzoic acid and it has been used as a catalyst for the reaction.) The solvent was evaporated and the residue was extracted with diethyl ether, washed with 5% NaHCO₃ solution, dried with magnesium sulfate, and crystallized to give the theoretical amounts of ester as white crystals. ¹H NMR (CDCl₃, 299.95 MHz): 3.80 (s, 6H), 3.89 (s, 3H), 6.54 (d, J=8 Hz, 2H), 7.26 (t, J=8 Hz, 1H) ¹³C NMR (75.43 MHz): 52.04, 55.58, 77.02, 103.43, 130.68, 156.86.

di-(2,6-dimethoxyphenyl)methanone: A solution of phenyl lithium was prepared by the addition of bromobenzene (39.2g., 0.250 mol.) in 125 ml. of ether to lithium wire (4.0 g., 0.577 mol.) and 60 ml. of ether. Resorcinol dimethyl ether (30.0 g., 0.218 mole) was added and the reaction mixture was allowed to stand at room temperature under nitrogen for 60 hours. The reaction mixture was poured into 43.75 g. (218 mmol.) of 2,6-dimethoxy benzoilchloride in 400 ml. of cold diethyl ether and the reaction mixture was stirred for 3 hours at -78°C. The reaction mixture was poured into 300 ml. of ice water and the organic phase was dried and concentrated to yield a gray residue. Recrystallization from ether gave 25 g. of the product (38%). ¹H NMR (CDCl₃, 299.95 MHz): 3.67 (s, 12H), 3.50 (d, J=8 Hz, 4H), 7.21 (t, J=8 Hz, 2H) ¹³C NMR (75.43 MHz): 56, 104, 111, 131, 158 m/z 302 (M⁺), found 302.

Tris-(2,6-dimethoxyphenyl)methyl carbinol 71: A solution of phenyl lithium was prepared by the addition of bromobenzene (39.2g., 0.250 mole) in 125 ml. of ether to lithium wire (4.0 g., 0.577 mol.) and 60 ml. of ether. Resorcinol dimethyl ether (30.0 g., 0.218 mole) was added and the reaction mixture was allowed to stand at room temperature under nitrogen for 60 hours. Dimethyl carbonate (6.49 g., 0.072 mole) in 400 ml. of benzene was added and the reaction mixture was refluxed for 3 days under nitrogen. The reaction mixture was poured into 600 ml. of water and the organic phase was concentrated to yield a gray residue. Recrystallization from ether gave 22.4 g. of the carbinol. (71 %) ^1H NMR (CDCl_3 , 299.95 MHz): 3.42 (s, 18H), 6.46 (d, $J=8$ Hz, 6H), 6.82 (s, 1H), 7.02 (t, $J=8$ Hz, 3H) ^{13}C NMR (75.43 MHz): 56.21, 78.22, 105.98, 126.11, 126.85, 158.49, m/z 440 (M^+), found 440.

A solution of the radical in diethyl ether was prepared according to general Method A.

Tris-(2,6-dimethoxyphenyl) borane 63: A solution of phenyl lithium was prepared by the addition of bromobenzene (39.2 g., 0.250 mole) in 125 ml. of ether to lithium wire (4.0 g., 0.577 mol.) and 60 ml. of ether. Resorcinol dimethyl ether (30.0 g., 0.218 mole) was added and the reaction mixture was allowed to stand at room temperature under nitrogen for 60 hours. 10.22 g. (8.85 ml., 72 mmol.) of $\text{BF}_3 \cdot \text{OEt}_2$ in 300 ml. of benzene was added and the reaction mixture was refluxed for 3 days under nitrogen. The reaction mixture was poured into 400 ml. of water and the organic phase was concentrated to yield a gray residue. Recrystallization from diethyl ether gave 11 g. of the borane (36%). ^1H NMR (CDCl_3 ,

299.95 MHz): 3.43 (s, 18H), 6.46 (d, $J=8$ Hz, 6H), 7.16 (t, $J=8$ Hz, 3H) ^{13}C NMR (75.43 MHz): 56.52, 105.09, 130.17, 162.54 m/z 422 (M^+), found 422.

Tris-(2,6-dimethoxyphenyl-3,5-dichlorophenyl) borane 64: To a precooled solution of 3.7 g. (8.77 mmol.) of tris-(2,6-dimethoxyphenyl) borane in dry diethyl ether (to act as a base) and methylene chloride solution (10 ml. ether, 30 ml. methylene chloride), 4.5 ml. (7.1 g., 55 mmol.) of sulfonylchloride was slowly added through syringe at -78°C and refluxed overnight with stirring under argon. The reaction mixture was washed with water twice, dried with magnesium sulfate, concentrated, and chromatographed with 10% ethyl acetate in n-hexane to give white crystals (3.0 g., 54%). ^1H NMR (CDCl_3 , 299.95 MHz): 3.42 (s, 18H), 7.42 (s, 3H) ^{13}C NMR (75.43 MHz): 61.09, 129.87, 133.00, 156.20 m/z 629 (M^+), found 629.

Tris-(4-chloro-2,6-dimethoxyphenyl)methanol 66: To a cooled solution of 5.0 g. (29 mmol.) of 3-chloro-dimethoxybenzene in 50ml of diethyl ether, 11.6 ml. (29 mmol.) of 2.5M n-BuLi in n-hexane was added slowly at -78°C under argon with stirring. The mixture was stirred at the room temperature for 2 days, 862 mg. (9.6 mmol.) of dimethyl carbonate in 50 ml. of benzene was added, and the reaction mixture was refluxed for 3 days under nitrogen. The reaction mixture was poured into 100 ml. of water and the organic layer was separated, dried with sodium sulfate, and the solvent was evaporated (200 mg., 4%). Cation: ^1H NMR (CDCl_3 , 299.95 MHz): 3.64 (s, 18H), 6.47 (s, 6H) ^{13}C NMR (75.43 MHz): 56.90, 77.05, 105.63, 149.16, 162.30.

Tris-(2,4,6-trimethoxyethoxyphenyl)methanol 67: To a cooled solution of 20 g. (119 mmol.) of trimethoxybenzene in 100ml of diethyl ether, 48.4 ml. (121 mmol.) of 2.5 M n-BuLi in n-hexane was added slowly at -78°C under argon with stirring. The mixture was stirred at the room temperature for 2 days, 3.57g (39.6 mmol.) of dimethyl carbonate in 200 ml. of benzene was added, and the reaction mixture was refluxed for 3 days under nitrogen. The reaction mixture was poured into 300 ml. of water and the organic layer was separated, dried with sodium sulfate, and the solvent was evaporated (13.4g, 64%). ^1H NMR (CDCl_3 , 299.95 MHz): 3.44 (s, 18H), 3.75 (s, 9H), 6.04 (s, 6H), 6.66 (s, 1H). ^{13}C NMR (75.43 MHz): 54.65, 77.02, 91.94, 157.77, 158.66. Cation: ^1H NMR (CDCl_3 , 299.95 MHz): 3.57 (s, 18H) 3.97 (s, 9H) 6.03 (s, 6H).

Tris-(2,6-dimethoxy-4-methylphenyl)methanol 68: A solution of phenyl lithium was prepared by the addition of 11.85 g. (75.4 mmol.) of bromobenzene in 60 ml. of ether to 1.21 g. (174.1 mg. atom) of lithium and 30 ml. of ether. 10 g. (65.8 mmol.) of dimethoxy toluene was added and the reaction mixture was allowed to stand at room temperature under nitrogen for 60 hours. 1.95 g. (21.7 mmol.) of dimethyl carbonate in 200 ml. of benzene was added dropwise and the reaction mixture was refluxed for 3 days under nitrogen. The reaction mixture was poured into 200 ml. of water and the organic phase was concentrated to yield a gray residue. Recrystallization from ether gave 5.9 g. of the carbinol (56 %). ^1H NMR (CD_3CN , 299.95 MHz): 2.23 (s, 9H), 3.37 (s, 12H), 6.32 (s, 6H) 6.54 (s, 1H) ^{13}C NMR (75.43 MHz): 21.37, 56.67, 107.67, 118.30, 125.30, 136.78, 159.32.

Tris-(2,6-dimethoxy-4-phenylphenyl)methyl 69:

2-hydroxy-4-oxo-6-phenyl-2-cyclohexenecarboxylate : To a solution of 3.5 g. of NaOH in 150 ml. of methanol, 9.8 g. of dimethyl malonate (75 mmol.) was added and the mixture stirred for 30 min. at room temperature under argon. 10 g. (68 mmol.) of *trans*-4-phenyl-3-buten-2-one was added portion wise with stirring. The reaction mixture was refluxed for 3 hours under argon and allowed to cool to room temperature. The solvent was distilled under reduced pressure. The oily residue was treated with acidic (pH=5) water and extracted with dichloromethane. The solution was dried over magnesium sulfate, the solvent was evaporated, and the product mixture was dried under vacuum. The crude mixture was submitted to the next reaction without purification.

5-Phenyl Resorcinol : 20 g. (81.3 mmol.) of crude phenylcarboxylate 2-hydroxy-4-oxo-6-phenyl-2-cyclohexenecarboxylate was dissolved in 150 ml. of DMF and 4.13 ml. (12.8g, 80 mmol.) of bromine was added dropwise with dry ice cooling under argon. The mixture was heated for three hours at about 80 °C until the evolution of CO₂ ceased followed by continued refluxing for 2 days. The solvent was distilled off under reduced pressure and the mixture was extracted with 300 ml. of 5% NaOH solution twice. The combined solution was treated with conc. HCl carefully with cooling and the 5-Phenyl resorcinol mixture was extracted with 500 ml. of methylene chloride. The solution was dried with magnesium sulfate and the solvent was evaporated under vacuum to give crystalline product. (5.6g, 43%) ¹H NMR (CD₃CN, 299.95 MHz): 6.36 (t, J=2 Hz, 1H), 6.61

(d, $J=2$ Hz, 2H), 7.31 (m, 1H), 7.40 (m, 2H), 7.55 (m, 2H), 8.35 (s, 2H), ^{13}C NMR (CD_3CN , 75.43 MHz): 102.48, 106.32, 107.11, 127.56, 128.10, 129.50, 144.05, 159.77.

3,5-dimethoxy-phenyl benzene : 10 g. (53.76 mmol.) of 5-phenylresorcinol was dissolved in 300 ml. of 5% NaOH solution, 12.72 ml. (16.95g, 134.4 mmol.) of dimethylsulfate was added using a separatory funnel, the mixture was mixed vigorously with shaking, and left for 30 min. followed by an extraction with 200 ml. of diethyl ether. The organic layer was dried, the solvent was evaporated, and the mixture was chromatographed over a silica gel using 30% ethyl acetate in hexane to give NMR clean product (8.9g, 78%). ^1H NMR (CDCl_3 , 299.95 MHz): 3.84 (s, 6H), 6.46 (t, $J=2$ Hz, 1H), 6.73 (d, $J=2$ Hz, 2H), 7.34 (m, 1H), 7.42 (tm, 2H), 7.56 (dm, 2H) ^{13}C NMR (75.43 MHz): 54.99, 98.83, 105.01, 126.77, 127.13, 128.27, 140.76, 143.01, 160.59.

Tris-(2,6-dimethoxy-4-phenyl phenyl)methanol : To a cooled solution of 2 g. (9.345 mmol.) of 5-phenyl-dimethoxybenzene in 100ml of diethyl ether, 4.11 ml. of 2.5 M n-BuLi in n-hexane was added slowly at -78°C under argon with stirring. The mixture was stirred at the room temperature for 2 days, 279 mg. (3.10 mmol.) of dimethyl carbonate in 100 ml. of benzene was added, and the reaction mixture was refluxed for 3 days under nitrogen. The reaction mixture was poured into 100 ml. of water, the organic layer was separated, dried with sodium sulfate, and the solvent was evaporated (4.4g, 71 %). ^1H NMR (CDCl_3 , 299.95 MHz): 3.54 (s, 18H), 6.75 (s, 6H), 6.95 (s, 1H), 7.32 (m, 3H), 7.41 (m, 6H), 7.59 (m, 6H) ^{13}C

NMR (75.43 MHz): 56.43, 56.48, 105.02, 125.85, 126.83, 127.12, 128.64, 139.23, 141.40, 157.00, 158.79 m/z 668 (M⁺), found 668.

A solution of carbinol in diethyl ether was treated with a small amount of conc. HBF₄ and the blue precipitates were filtered and dried to give the cation tetrafluoroborate salt as crystalline solids. Cation: ¹H NMR (CDCl₃, 299.95 MHz): 3.71 (s, 18H), 6.78 (s, 6H), 7.52 (m, 9H), 7.75 (d, J=7 Hz, 6H) ¹³C NMR (75.43 MHz): 56.48, 102.97, 126.95, 128.87, 129.94, 138.43, 192.29.

A solution of the radical in diethyl ether was prepared according to general Method A.

Di-(2,6-dimethoxyphenyl)-2,6-dimethoxy-4-methyl phenyl methyl 70:

A solution of phenyl lithium was prepared by the addition of 19.6 g. (125 mmol.) of bromobenzene in 60 ml. of ether to 2 g. (289 mol.) of lithium and 30 ml. of ether. 15g (109.6 mmol.) of 1,3-dimethoxybenzene was added and the reaction mixture was allowed to stand at room temperature under nitrogen for 60 hours. 20.3 g. (96.8 mmol.) of 2,6-dimethoxy,5 methyl benzoate in 200 ml. of benzene was added and the reaction mixture was refluxed for 3 days under argon. The reaction mixture was poured into 200 ml. of water and the organic phase was concentrated to yield gray residues. Recrystallization from ether gave a crude carbinol. A solution of the carbinol in diethyl ether was treated with a small amount of conc. HBF₄ and the blue precipitate was filtered and dried to give the cation tetrafluoroborate salt as crystalline solids (12g, 27%). Cation: ¹H NMR (CDCl₃, 299.95 MHz): 2.48 (s, 3H), 3.54 (s, 12H), 3.59 (s, 6H), 6.36 (s,

2H), 6.48 (d, $J=9$ Hz, 4H), 7.41 (t, $J=9$ Hz, 2H) ^{13}C NMR (75.43 MHz): 24.65, 56.60, 57.14, 104.75, 106.21, 138.03, 152.20, 160.63, 164.83, 165.71.

Tris-(2,6-dimethoxyphenyl) methyl ammonium tetrafluoroborate 72: To a 10 ml. THF solution of tris-(2,6-dimethoxyphenyl)methanol (500 mg., 1 mmol.), 0.2 ml. of conc. HBF_4 was added followed by the addition of conc. aqueous ammonia until the color of the mixture turned red. 30 ml. of diethyl ether was added and the mixture was left to give red precipitates which were filtered and dried to give NMR (and X-ray) clean crystals of the product (380 mg., 72%). ^1H NMR (CDCl_3 , 299.95 MHz): 3.44 (s, 18H), 6.58 (d, $J=8$ Hz, 6H), 7.21 (t, $J=8$ Hz, 3H) 8.45 (s, 3H) ^{13}C NMR (75.43 MHz): 56.25, 105.93, 106.02, 117.5, 129.06, 145.50, 157.50.

Tris-(2,6-dimethoxyphenyl)methane 73: To a solution of 5 g. (6.82 mmol.) of tris-(2,6-dimethoxyphenyl)methanol in 100 ml. of THF, 30 ml. of 10% HCl solution, 496.4 mg. (7.90 mmol.) of solid NaBH_3CN was added slowly and the mixture was stirred for 2 hours at the room temperature. 100 ml. of water was added to the mixture and the product filtered, washed with water, and dried under vacuum to give 2.7 g. of clean products (93.4%). ^1H NMR (CDCl_3 , 299.95 MHz): 3.41 (s, 18H), 6.45 (s, 1H), 6.48 (d, $J=8$ Hz, 6H), 7.02 (t, $J=8$ Hz, 3H) ^{13}C NMR (75.43 MHz): 56.82, 106.37, 124.00, 125.64, 159.51 m/z 424 (M^+), found 424.

Tris-(2,6-dimethoxyphenyl) silane 74: A solution of phenyl lithium was prepared by the addition of bromobenzene (39.2g., 0.250 mole) in 125 ml. of ether to lithium wire (4.0 g., 0.577 mol.) and 60 ml. of ether.

Resorcinol dimethyl ether (30.0 g., 0.218 mole) was added and the reaction mixture was allowed to stand at room temperature under nitrogen for 60 hours. 11.8 g. of triethoxysilane (0.072 mole) in 400 ml. of benzene was added and the reaction mixture was refluxed for 3 days under nitrogen. The reaction mixture was poured into 600 ml. of water and the organic phase was concentrated to yield gray residues. Recrystallization from diethyl ether gave 13.4 g. of the silane (42%). ^1H NMR(CDCl_3 , 299.95 MHz): 3.46 (s, 18H), 5.52 (s, 1H), 6.44 (d, $J=8$ Hz, 6H), 7.19 (t, $J=8$ Hz, 3H) ^{13}C NMR (75.43 MHz): 55.41, 77.1, 103.80, 103.80, 129.69, 164.90.

Tris-(2,6-dimethoxyphenyl-3,5-dichlorophenyl)methyl ammonium tetrafluoroborate 75: To a solution of 5 g. of tris-(2,6-dimethoxyphenyl)-methyl ammonium tetrafluoroborate in 10 ml. of diethyl ether and 50 ml. of dichloromethane, 10 ml. of sulfurylchloride was added and the mixture was refluxed under argon overnight. The organic layer was separated, dried with magnesium sulfate, the solvent was evaporated, and chromatographed over silica gel using methylene chloride to yield 2.75 g. of hexachloro-ammonium tetrafluoroborate as white crystals (37.5 %). ^1H NMR (CDCl_3 , 299.95 MHz): 3.38 (s, 9H), 3.66 (s, 9H), 7.53 (s, 3H), 8.69 (s, 3H).

Tris-(2,6-dimethoxyphenyl-3,5-dichlorophenyl) methane 76: To a solution of the methane 73 (2 g., 4.71 mmol.) in 10 ml. of diethyl ether and 50 ml. of dichloromethane, 33 mmol. of sulfurylchloride was added and the mixture was refluxed under argon overnight. The organic layer was separated, dried with magnesium sulfate, and the solvent was evaporated. Chromatography over silica gel using dichloromethane gave

hexachloromethane as white crystals (2.2g, 75%). ^1H NMR (CDCl_3 , 299.95 MHz): 3.07 (s, 9H), 3.73 (s, 9H), 6.65 (s, 1H), 7.31 (s, 3H) ^{13}C NMR (75.43 MHz): 59.34, 61.00, 122.43, 123.94, 129.43, 133.32, 153.05, 156.93.

Di-(2,6-dimethoxyphenyl)-phenyl methanol 77: A solution of dimethoxyphenyllithium was prepared by the addition of 34.8 ml. (86.9 mmol.) of 2.5 M n-BuLi in n-hexane to a solution of 10 g. (72.4 mmol.) of dimethoxybenzene in sodium-dried diethyl ether at -78°C and the mixture was stirred at room temperature under argon for 48 hours. 3.13 g. (23.0 mmol.) of methyl benzoate in 200 ml. of benzene was added and the reaction mixture was refluxed for 3 days under argon. The reaction mixture was poured into 200 ml. of water, the organic phase was washed with 200 ml. of water twice, dried, and concentrated to yield carbinol as gray residues. The carbinol was crystallized in dichloromethane and hexane to give 9 g. of NMR clean carbinol (65%). A solution of carbinol (500 mg., 1.31 mmol.), in 150 ml. of diethyl ether was treated with 0.1 ml. of conc. HBF_4 and the blue precipitates were filtered and dried to give the cation tetrafluoroborate salt as a crystalline solid quantitatively. 200 mg. of the cation tetrafluoroborate salt in 20 ml. of dichloromethane was reduced by 20 ml. of 5M CrCl_2 solution (prepared with $\text{CrCl}_3 \cdot 6\text{H}_2\text{O}$ and Zn/Hg in 10% HCl solution) and extracted with dichloromethane and washed with water twice, dried with magnesium sulfate, and chromatographed with diethyl ether over silica gel to give a chromatographically pure solution of the radical (35%, based on SQUID measurement, μ_{eff}). ^1H NMR (CDCl_3 , 299.95 MHz): 3.38 (s, 12H), 6.43 (s, 1H), 6.54 (d, $J=8$ Hz, 4H), 7.11 (t, $J=8$ Hz, 2H), 7.13 (m, 1H), 7.21 (m, 2H), 7.46 (m, 2H) ^{13}C NMR

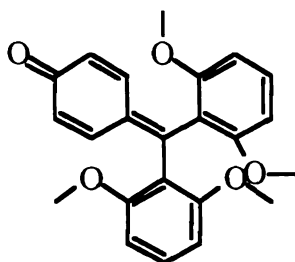
(75.43 MHz): 56.50, 78.50, 106.74, 125.37, 126.31, 126.50, 126.63, 127.28, 149.50, 158.00, mp. =104 -105°C.

Cation: ^1H NMR (CDCl_3 , 299.95 MHz): 3.54 (s, 12H), 6.63 (d, $J=8$ Hz, 4H), 7.44 (m, 4H), 7.61 (m, 1H), 7.79 (t, $J=8$ Hz, 2H) ^{13}C NMR (75.43 MHz): 56.83, 105.36, 125.00, 129.09, 134.59, 137.02, 145.90, 163.79, 191.58 m/e=364.44116 mp. =142 -144°C.

Di-(2,6-dimethoxyphenyl)(4-chlorophenyl)-methanol 78: A solution of phenyl lithium was prepared by the addition of bromobenzene (39.2g., 0.250 mole) in 125 ml. of ether to lithium wire (4.0 g., 0.577 mol.) and 60 ml. of ether. Resorcinol dimethyl ether (30.0 g., 0.218 mole) was added and the reaction mixture was allowed to stand at room temperature under nitrogen for 60 hours. 14.8 g. (86.8 mmol.) of methyl 4-chlorobenzoate in 400 ml. of benzene was added and the reaction mixture was refluxed for 3 days under nitrogen. The reaction mixture was poured into 600 ml. of water and the organic phase was concentrated to yield gray residues. Recrystallization from methylene chloride in n-hexane gave 31.3 g. of NMR clean crystals of carbinol (87%). ^1H NMR (CDCl_3 , 299.95 MHz): 3.39 (s, 12H), 6.49 (s, 1H), 6.53 (d, $J=8$ Hz, 4H), 7.12 (t, $J=8$ Hz, 2H), 7.15 (dq, $J=8$ Hz, 2H), 7.37 (dq, $J=8$ Hz, 2H) ^{13}C NMR (75.43 MHz): 56.29, 79.12, 106.625, 125.73, 126.64, 127.53, 128.11, 130.88, 148.01, 157.93. Cation ^1H NMR (CDCl_3 , 299.95 MHz): 3.55 (s, 12H), 6.62 (d, $J=8$ Hz, 4H), 7.40 (dd, 4H), 7.78 (t, $J=8$ Hz, 2H) ^{13}C NMR (75.43 MHz): 56.87, 105.42, 124.40, 129.50, 135.54, 142.65, 144.04, 146.23, 163.71, 189.04.

Di-(2,6-dimethoxy phenyl)(4-methoxyphenyl)methanol 79: A solution of phenyl lithium was prepared by the addition of bromobenzene (39.2 g., 0.250 mole) in 125 ml. of ether to lithium wire (4.0 g., 0.577 mol.) and 60 ml. of ether. Resorcinol dimethyl ether (30.0 g., 0.218 mole) was added and the reaction mixture was allowed to stand at room temperature under argon for 60 hours. 14.4 g. (98.6 mmol.) of methyl 4-methoxybenzoate in 400 ml. of benzene was added and the reaction mixture was refluxed for 3 days under argon. The reaction mixture was poured into 600 ml. of water and the organic phase was concentrated to yield gray residues. Recrystallization from methylene chloride in n-hexane gave 24.6 g. of NMR clean crystals of carbinol (61%). ^1H NMR (CDCl_3 , 299.95 MHz): 3.38 (s, 12H), 3.76 (s, 3H), 6.36 (s, 1H), 6.53 (d, $J=8$ Hz, 4H), 6.75 (dq, $J=8$ Hz, 2H), 7.10 (t, $J=8$ Hz, 2H), 7.34 (dq, $J=8$ Hz, 2H) ^{13}C NMR (75.43 MHz): 55.12, 56.47, 79.17, 106.88, 111.96, 126.65, 127.20, 127.73, 141.60, 157.40, 158.03, mp=105 °C.

A solution of carbinol in diethyl ether was treated with a small amount of conc. HBF_4 and the blue precipitates were filtered and dried to give the cation tetrafluoroborate salt as a crystalline solid. The cation tetrafluoroborate salt was reduced by CrCl_2 solution (prepared with $\text{CrCl}_3 \cdot 6\text{H}_2\text{O}$ and Zn/Hg in 10% HCl solution) and extracted with dichloromethane, washed with water twice, dried with magnesium sulfate, and chromatographed using diethyl ether over silica gel to give a chromatographically pure solution of radical (76%).



The radical solution was left under the air for 3 days to give crystals of bis-(2,6-dimethoxy phenyl)methyl quinone methide shown above. ^1H NMR (CDCl_3): 3.62 (s, 12H), 6.29 (dq, $J=8$ Hz, 2H), 6.56 (d, $J=8$ Hz, 4H), 7.20 (dq, $J=8$ Hz, 2H), 7.24 (t, $J=8$ Hz, 2H) ^{13}C NMR (75.43 MHz): 55.98, 104.17, 117.5, 127.51, 130.24, 139.56, 150.00, 158.36, 188.00.

Di-(2,6-dimethoxy phenyl)(4-methyl phenyl)methanol **80**: A solution of phenyl lithium was prepared by the addition of bromobenzene (39.2g., 0.250 mole) in 125 ml. of ether to lithium wire (4.0 g., 0.577 mol.) and 60 ml. of ether. Resorcinol dimethyl ether (30.0 g., 0.218 mole) was added and the reaction mixture was allowed to stand at room temperature under nitrogen for 60 hours. 14.8 g. (98.6 mmol.) of methyl 4-methylbenzoate in 400 ml. of benzene was added and the reaction mixture was refluxed for 3 days under nitrogen. The reaction mixture was poured into 600 ml. of water and the organic phase was concentrated to yield gray residues. Recrystallization from methylene chloride in n-hexane gave 32 g. of NMR clean crystals of carbinol (83%). ^1H NMR (CDCl_3 , 299.95 MHz): 2.29 (s, 3H), 3.38 (s, 12H), 6.38 (s, 1H), 6.53 (d, $J=8$ Hz, 4H), 7.00 (d, $J=8$ Hz, 2H), 7.10 (t, $J=8$ Hz, 2H), 7.32 (d, $J=8$ Hz, 2H) ^{13}C NMR (75.43 MHz): 21.00, 56.46, 79.38, 106.88, 126.47, 126.61, 127.19, 127.37, 134.65, 146.23, 158.07.

Di-(2,6-dimethoxy phenyl)(4-hydroxyphenyl)methanol 81: Bis-(2,6-dimethoxy phenyl)methyl quinone in THF was treated with conc. HBF_4 and crystallized by slow evaporation to give needles of di-(2,6-dimethoxy phenyl)(4-hydroxyphenyl)methyl cation tetrafluoroborate (60% by nmr). ^1H NMR (CDCl_3): 3.56 (s, 12H), 6.56 (d, $J=8$ Hz, 4H), 7.17 (dq, $J=8$ Hz, 2H), 7.46 (t, $J=8$ Hz, 2H), 7.82 (dq, $J=8$ Hz, 2H).

Di-(2,6-dimethoxy phenyl)(4-nitrophenyl)methanol 83: A solution of dimethoxyphenyllithium was prepared by the addition of 70 ml. (175 mmol.) of 2.5 M n-Butyl lithium in n-hexane to a solution of 20 g. (145 mmol.) of dimethoxybenzene in sodium-dried diethyl ether at -78°C and the mixture was stirred at room temperature under argon for 48 hours. 6.56 g. (36.2 mmol.) of methyl 4-nitrobenzoate in 300 ml. of benzene was added and the reaction mixture was refluxed for 3 days under nitrogen. The reaction mixture was poured into 300 ml. of water and the organic phase was dried and concentrated to yield brown residues. A solution of carbinol in diethyl ether was treated with a small amount of conc. HBF_4 and the blue precipitates were filtered and dried to give the cation tetrafluoroborate salt as a crystalline solid. (<1%) Cation: ^1H NMR (CDCl_3 , 299.95 MHz): 3.56 (s, 12H), 6.63 (d, $J=9$ Hz, 4H), 7.40 (dd, $J=8$ Hz, 4H), 7.79 (t, $J=9$ Hz, 2H) ^{13}C NMR (75.43 MHz): 56.88, 105.43, 124.41, 129.52, 135.55, 142.66, 144.01, 146.25, 163.73, 189.05.

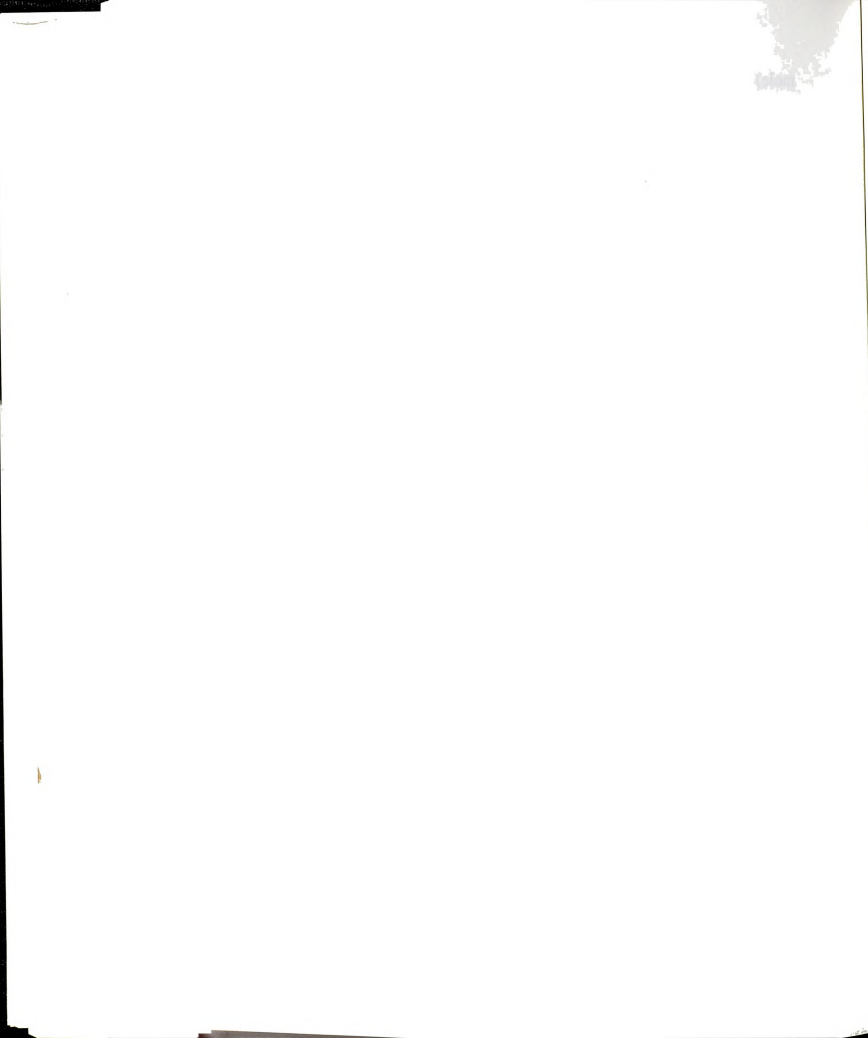
Di-(2,6-dimethoxy phenyl)-(3,5-dimethoxyphenyl)methanol 84: A solution of phenyl lithium was prepared by the addition of bromobenzene (39.2g., 0.250 mole) in 125 ml. of ether to lithium wire (4.0 g., 0.577 mol.) and 60 ml. of ether. Resorcinol dimethyl ether (30.0 g., 0.218

mole) was added and the reaction mixture was allowed to stand at room temperature under nitrogen for 60 hours. 17 g. (98.6 mmol.) of methyl 3,5-dimethoxybenzoate in 400 ml. of benzene was added and the reaction mixture was refluxed for 3 days under nitrogen. The reaction mixture was poured into 600 ml. of water and the organic phase was concentrated to yield gray residues. Recrystallization from methylene chloride in n-hexane gave 24 g. of NMR clean crystals of carbinol. (55%). ^1H NMR (CDCl_3 , 299.95 MHz): 3.40 (s, 12H), 3.70 (s, 6H), 6.27 (t, $J=2$ Hz, 1H), 6.46 (s, 1H), 6.52 (d, $J=8$ Hz, 4H), 6.69 (d, $J=2$ Hz, 2H), 7.09 (t, $J=8$ Hz, 2H), ^{13}C NMR (75.43 MHz): 55.17, 56.43, 97.75, 105.25, 106.76, 127.28, 152.21, 158.06, 159.50.

Tris-(6-methoxy-2-(2-methoxyethoxy)phenyl) methanol 85:

1-(2-methoxyethoxy)-3-methoxy benzene : A solution of 50 g. (400 mmol.) of methoxyphenol, 38.12 g. (400 mmol.) of chloromethoxyethane, 38.12g (400 mmol.) of chloromethoxyethane in 700ml of acetone was refluxed overnight under argon. The solution was filtered, evaporated, extracted with diethyl ether, dried with magnesium sulfate, concentrated, and chromatographed using 10% ethyl acetate in n-hexane to give the product as a clear oil (60%). ^1H NMR (CDCl_3): 3.42 (d, $J=2$ Hz, 3H), 3.70 (d, $J=2$ Hz, 2H), 3.74 (d, $J=2$ Hz, 3H), 4.07 (d, $J=2$ Hz, 2H), 6.50 (m, 3H), 7.16 (t, $J=2$ Hz, 1H) ^{13}C NMR (75.43 MHz): 54.48, 58.45, 66.55, 70.37, 100.59, 106.01, 129.45, 159.75, 160.53. m/z 182 (M^+), found 182.

To a cooled solution of 14.82 g. (81.4 mmol.) of methoxyethoxy benzene in 100 ml. of diethyl ether, 39.1 ml. (97.7 mmol.) of 2.5 M n-BuLi in n-



hexane was added slowly at -78°C under argon with stirring. The mixture was stirred at room temperature for 2 days and 2.42 g. (26.86 mmol.) of dimethyl carbonate in 200 ml. of benzene was added and the reaction mixture was refluxed for 3 days under nitrogen. The reaction mixture was poured into 300 ml. of water and the organic layer was separated, dried with sodium sulfate, and the solvent was evaporated.

A solution of carbinol in diethyl ether was treated with a small amount of conc. HBF_4 and the blue precipitates were filtered and dried to give the cation tetrafluoroborate salt as a crystalline solid. The cation tetrafluoroborate salt was reduced by CrCl_2 solution (prepared with $\text{CrCl}_3 \cdot 6\text{H}_2\text{O}$ and Zn/Hg in 10% HCl solution), extracted with dichloromethane, washed with water twice, dried with magnesium sulfate, and chromatographed with diethyl ether over silica gel to give a chromatographically pure solution of the radical.

^1H NMR (CDCl_3): 3.17 (t, 6H), 3.19 (s, 9H), 3.39 (s, 9H), 3.81 (t, $J=2$ Hz, 6H), 6.47 (dd, 6H), 6.63 (s, 1H), 7.04 (t, $J=2$ Hz, 3H) ^{13}C NMR (75.43 MHz): 55.68, 58.44, 68.27, 70.31, 105.93, 107.18, 125.78, 157.09, 158.57. Cation: ^1H NMR (CDCl_3): 3.14 (s, 9H), 3.21 (s, 6H), 3.55 (s, 9H), 3.93 (s, 6H), 6.50 (d, $J=2$ Hz, 6H), 7.57 (t, $J=2$ Hz, 3H) ^{13}C NMR (75.43 MHz): 56.3, 58.4, 68.5, 69.7, 105.3, 121.0, 142.0, 156.6.

Tris-(2,6-di(2-methoxyethoxy)phenyl) methanol **86**:

1,3-di(2-methoxyethoxy)benzene : A solution of 70 g. (636 mmol.) of resorcinol, 185.2 g. (1340 mmol.) of potassium carbonate, 126.2 g. (1340 mmol.) of 2-chloroethyl methyl ether, 20 g. (120 mmol.) of potassium

iodide in 700 ml. of acetone was refluxed overnight under argon. The solution was filtered, evaporated, extracted with diethyl ether, dried with magnesium sulfate, concentrated, and chromatographed with 10% ethyl acetate in n-hexane to give the product as a clear oil (42.4%). ^1H NMR (CDCl_3 , 299.95 MHz) 3.42 (s, 6H), 3.72 (m, 4H), 4.07 (m, 4H), 6.51 (m, 3H), 7.13 (m, 1H) ^{13}C NMR (75.43 MHz): 58.75, 66.74, 70.54, 101.24, 106.65, 129.34, 159.48. m/z 226 (M^+), found 226.

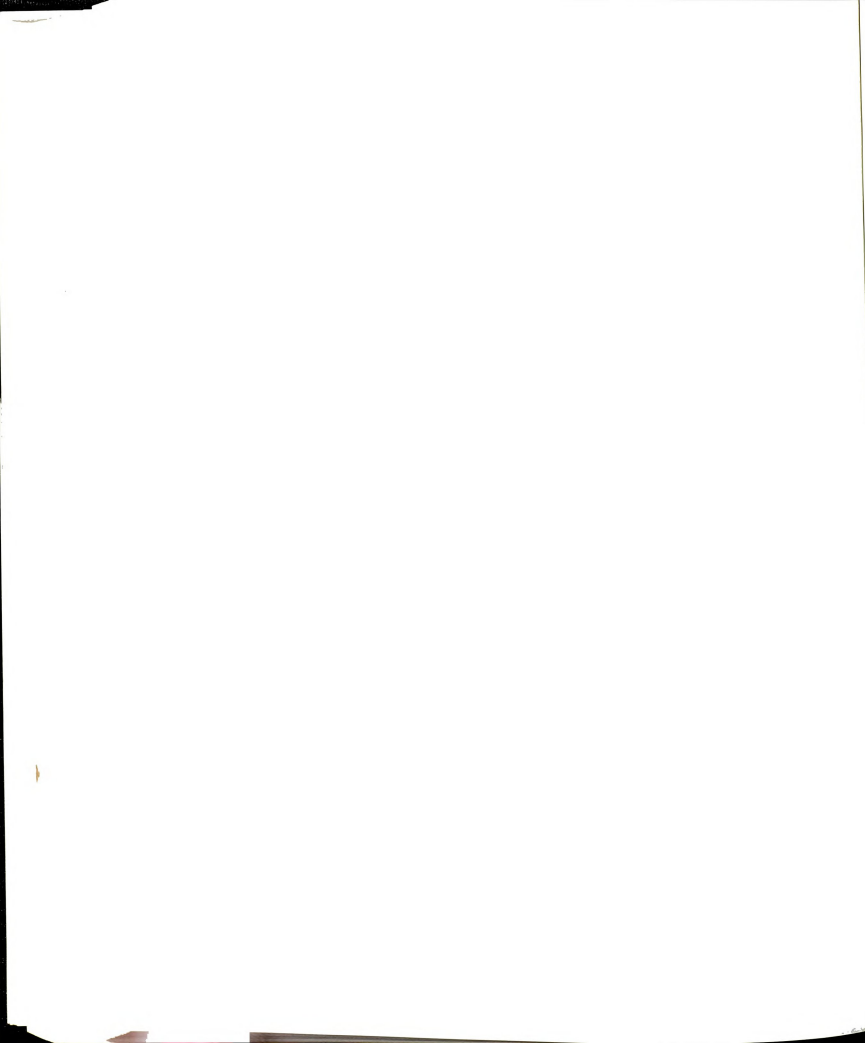
Tris-(2,6-di(2-methoxyethoxy)phenyl)methanol: 1,3-di(2-methoxyethoxy)-benzene was prepared by the reaction of resorcinol and 2-chloroethyl methyl ether with K_2CO_3 in refluxing acetone. A solution of 1,3-di(2-methoxyethoxy) phenyl lithium was prepared by the addition of n-Butyl lithium in n-hexane to a solution of 1,3-di-(2-methoxyethoxy)benzene in sodium-dried diethyl ether at -78°C and the mixture was stirred at room temperature under argon for 48 hours. Dimethyl carbonate in benzene was added and the reaction mixture was refluxed for 3 days under argon. The reaction mixture was poured into ice water and the organic phase was concentrated to yield an oil (11.9%). ^1H NMR (CDCl_3 , 299.95 MHz): 3.15 (s, 18H), 3.20 (m, 12H), 3.92 (m, 12H), 6.50 (d, $J=9$ Hz, 6H), 7.56 (t, $J=9$ Hz, 3H) ^{13}C NMR (75.43 MHz): 58.37, 68.39, 69.80, 105.35, 111.50, 141.19, 161.82.

A solution of the carbinol in diethyl ether was treated with a small amount of conc. HBF_4 and the blue precipitates were filtered and dried to give the cation tetrafluoroborate salt as a crystalline solid. The cation tetrafluoroborate salt was reduced by CrCl_2 solution (prepared with $\text{CrCl}_3 \cdot 6\text{H}_2\text{O}$ and

Zn/Hg in 10% HCl solution), extracted with dichloromethane, washed with water twice, dried with magnesium sulfate, and chromatographed with diethyl ether over silica gel to give a chromatographically pure solution of the radical **86**.

Bis-(2,6-dimethoxyphenyl)-4-chlorophenyl amine **87**: The mixture of 950 mg. (7.6 mmol.) of 4-chloroaniline, 5 g. (18.9 mmol.) of 2,6-dimethoxyiodobenzene, 6.9 g. (50 mmol.) of potassium carbonate, 2.54 g. (40 mg. atom) of copper, and 248 mg. (0.767 mmol.) of tris-(2-methoxyethoxy) amine was refluxed in 50 ml. of o-dichlorobenzene for 48 hours under argon. Inorganic salts and copper were removed by filtration of the hot reaction mixture. The solvent was distilled off under reduced pressure and the residue freed from the impurities by passing through a short silica gel column. Chromatography over silica gel using 20% ethyl acetate in hexane gave the product as white crystals (2.4g, 78%). ^1H NMR (CDCl_3 , 299.95 MHz): 3.58 (s, 12H), 6.40 (d, $J=8$ Hz, 2H), 6.56 (d, $J=8$ Hz, 4H), 6.97 (d, $J=2$ Hz, 2H), 7.20 (t, $J=8$ Hz, 2H) ^{13}C NMR (75.43 MHz): 56.16, 104.00, 105.51, 111.5, 115.69, 125.75, 127.79, 157.22.

Bis-(2,6-dimethoxyphenyl)-3,5-dimethoxyphenyl amine **88**: The mixture of 1.16 g. (7.6 mmol.) dimethoxyaniline, 5 g. (18.9 mmol.) 2,6-dimethoxyiodobenzene, 6.9 g. (50 mmol.) of potassium carbonate, 2.54 g. (40 mmol.) of copper, and 248 mg. (0.767 mmol.) of tris-(2-methoxyethoxy) amine was refluxed in 50 ml. of o-dichlorobenzene for 48 hours under argon. Inorganic salts and copper were removed by filtration of the hot reaction mixture. The solvent was distilled off under reduced pressure and the residue freed from the impurities by passing through a



short silica gel column. Chromatography over silica gel using 20 % ethyl acetate in hexane gave the product as white crystals. (2.61g, 81%). ^1H NMR (CDCl_3 , 299.95 MHz): 3.59 (s, 12H), 3.60 (s, 6H), 5.80 (d, $J=2$ Hz, 2H), 5.87 (t, $J=2$ Hz, 1H), 6.53 (d, $J=8$ Hz, 4H), 7.15 (t, $J=8$ Hz, 2H) ^{13}C NMR (75.43 MHz): 55.00, 56.50, 90.82, 93.66, 105.50, 125.70, 157.37, 160.78.

Tris-(3,5-dimethoxyphenyl)amine 89: The mixture of 460 mg. (3.80 mmol.) of 3,5-dimethoxyaniline, 2.51 g. (9.50 mmol.) of 2,6-dimethoxyiodobenzene, 4.21 g. (30.54 mmol.) of potassium carbonate, 970 mg. (15.30 mmol.) of copper, and 248 mg. (0.767 mmol.) of tris-(2-methoxyethoxy) amine was refluxed in 20 ml. of *o*-dichlorobenzene for 24 hours under argon. Inorganic salts and copper were removed by filtration of the hot reaction mixture. The solvent was distilled off under reduced pressure and the residue freed from the impurities by passing through a short silica gel column. Chromatography over silica gel using 20 % ethyl acetate in hexane gave the product as white crystals (880 mg., 55%). ^1H NMR (CDCl_3 , 299.95 MHz): 3.68 (s, 18H), 6.14 (t, $J=2$ Hz, 3H), 6.24 (d, $J=8$ Hz, 6H) ^{13}C NMR (75.43 MHz): 54.8, 54.9, 95.0, 102.6, 148.6, 160.7 m/z 425 (M^+), found 425.

Jacobson's (head-to-tail) peroxy dimer 91: A fresh solution of radical 77 was allowed to stand for 3 days under air to give the peroxy dimers. The peroxy dimer was crystallized by slow evaporation of a diethyl ether solution of the radical (65%, based on SQUID measurement, μ_{eff}) (the peroxydimer can be made almost quantitatively with an O_2 saturated

solution of the radical in methylene chloride). ^1H NMR (CDCl_3 , 299.95 MHz): 3.40 (s, 12H), 3.58 (d, $J=3$ Hz, 12H), 4.82 (m, 1H), 5.54 (dd, $J=12,2$ Hz, 2H), 6.12 (dd, $J=10,2$ Hz, 2H), 6.44 (dd, $J=8,2$ Hz, 8H), 6.55 (m, 2H), 7.03 (t, $J=8$ Hz, 4H), 7.05 (m, 1H), 7.11 (t, $J=3$ Hz, 2H), 7.68 (d, $J=8$ Hz, 2H). mp=108-111 °C.

Martin's (tail-to-tail) peroxy dimer 90: A fresh solution of radical **1** was allowed to stand for 3 days under air to give tail-to-tail peroxy dimer. (7% yield, based on SQUID measurement of the best radical, μ_{eff}) (20%, based on average SQUID measurement of the radical, μ_{eff}) (we can increase the yield of the peroxydimer significantly with O_2 saturated solution of the radical in methylene chloride.) ^1H NMR (CDCl_3 , 299.95 MHz): 3.13 (s, 12H), 3.51 (d, $J=3$ Hz, 24H), 5.05 (d, $J=2$ Hz, 4H), 5.33 (t, $J=2$ Hz, 2H), 6.39 (dd, $J=2,2$ Hz, 8H), 7.00 (t, $J=8$ Hz, 4H). mp=>300 °C.

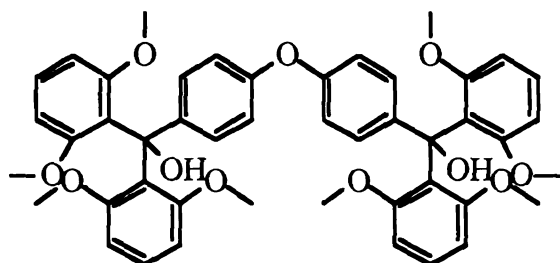
Di-(2,6-dimethoxyphenyl)(2-hydroxyphenyl)methyl carbinol 92: A solution of phenyl lithium was prepared by the addition of bromobenzene (19.6g., 0.12 mole) in 75 ml. of ether to lithium wire (2.0 g., 0.288 mol.) and 30 ml. of ether. Resorcinol dimethyl ether (15.0 g., 0.109 mole) was added and the reaction mixture was allowed to stand at room temperature under nitrogen for 60 hours. 8.5 g. (56 mmol.) of methyl salicylate in 300 ml. of benzene was added and the reaction mixture was refluxed for 3 days under nitrogen. The reaction mixture was poured into 400 ml. of water and the organic phase was concentrated to yield a gray residue. Recrystallization from methylene chloride in n-hexane gave 10.1 g. of NMR clean crystals of carbinol (45%). ^1H NMR (CDCl_3 , 299.95 MHz): 3.40 (s, 12H), 6.58 (d, $J=8$ Hz, 4H), 6.64 (m, 2H), 6.86 (dd, $J=8,2$ Hz, 1H),

7.09 (m, 1H), 7.16 (t, $J=8$ Hz, 2H), 9.15 (s, 1H) ^{13}C NMR (75.43 MHz): 56.62, 81.37, 107.00, 115.74, 118.51, 123.89, 127.21, 127.93, 128.00, 131.73, 157.37, 158.25.

Bis-1,3-(tetra-(2,6-dimethoxyphenyl)methyl dicarbinol 93: A solution of 2,6-dimethoxyphenyl lithium was prepared by the addition of 34.8 ml. (86.9 mmol.) of 2.5 M n-BuLi in n-hexane to a solution of 10 g. (72.4 mmol.) of dimethoxy benzene in sodium-dried diethyl ether at -78°C , and the mixture was stirred at room temperature under argon for 48 hours. 3.10 g. (16.0 mmol.) of dimethylisophthalate in 200 ml of benzene was added and the reaction mixture was refluxed for 3 days under argon. The reaction mixture was poured into 200 ml. of ice water and the organic layer was separated, dried with sodium sulfate, and concentrated to yield a gray residue. Recrystallization from ether gave 2.23 g. of the dicarbinol as white crystals (21%). ^1H NMR (CDCl_3 , 299.95 MHz): 3.26 (s, 24H), 6.37 (s, 2H), 6.30 (d, $J=8$ Hz, 8H), 7.02 (t, $J=8$ Hz, 4H), 7.08 (m, 1H), 7.32 (dd, $J=8,2$ Hz, 2H), 7.44 (t, $J=2$ Hz, 1H) ^{13}C NMR (75.43 MHz): 55.77, 79.42, 106.23, 123.56, 124.53, 126.37, 126.53, 146.88, 157.60.

Bis-1,4-(tetra-(2,6-dimethoxyphenyl)methyl dicarbinol 94: A solution of 2,6-dimethoxyphenyl lithium was prepared by the addition of 34.8 ml. (86.9 mmol.) of 2.5 M n-BuLi in n-hexane to a solution of 10.0 g. (72.4 mmol.) of dimethoxy benzene in sodium-dried diethyl ether at -78°C and the mixture was stirred at room temperature under argon for 48 hours. 3.10 g. (16.0 mmol.) of dimethyl terephthalate in 200ml of benzene was added and the reaction mixture was refluxed for 3 days under argon. The reaction mixture was poured into 200 ml. of ice water and the organic

layer was separated, dried with sodium sulfate, and concentrated to yield a gray residue. Recrystallization from ether gave dicarbinol as white crystals. (4g, 37 %). ^1H NMR (CDCl_3 , 299.95 MHz): 3.33 (s, 24H), 6.18 (s, 2H), 6.48 (d, $J=8$ Hz, 8H), 7.06 (t, $J=8$ Hz, 4H), 7.16 (m, 2H), 7.34 (m, 4H) ^{13}C NMR (75.43 MHz): 56.22, 79.50, 106.73, 124.50, 125.02, 126.95, 128.00, 128.50, 158.03.



Oxy-4,4' dicarbinol 95: A solution of phenyl lithium was prepared by the addition of bromobenzene (39.2g., 0.250 mol.) in 125 ml. of ether to lithium wire (4.0 g., 0.577 mol.) and 60 ml. of ether. Resorcinol dimethyl ether (30.0 g., 0.218 mole) was added and the reaction mixture was allowed to stand at room temperature under nitrogen for 60 hours. 14.3 g. (50 mmol.) of 4-oxy-dimethylbenzoate in 400 ml. of benzene was added and the reaction mixture was refluxed for 3 days under nitrogen. The reaction mixture was poured into 600 ml. of water and the organic phase was concentrated to yield a gray residue. Recrystallization from methylene chloride in n-hexane gave 12.8 g. of NMR clean crystals of the dicarbinol (33%). ^1H NMR (CDCl_3 , 299.95 MHz): 3.40 (s, 24H), 6.38 (s, 2H), 6.53 (d, $J=8$ Hz, 8H) 6.83 (d, $J=8$ Hz, 4H), 7.10 (t, $J=8$ Hz, 4H), 7.34 (d, $J=8$ Hz, 4H) ^{13}C NMR (75.43 MHz): 56.45, 79.24, 106.84, 116.96, 126.48, 127.32, 127.89, 143.96, 155.41, 158.09.

Tris-1,3,5-(bis-2,6-dimethoxyphenyl)hydroxymethyl benzene 96: A solution of phenyl lithium was prepared by the addition of bromobenzene (3.92g., 0.0250 mole) in 12.5 ml. of ether to lithium wire (0.4 g., 0.058 mol.) and 10 ml. of ether. Resorcinol dimethyl ether (3.0 g., 0.0218 mole) was added and the reaction mixture was allowed to stand at room temperature under nitrogen for 60 hours. 1.5 g. (5.9 mmol.) of 1,3,5-trimethylbenzoate in 400 ml. of benzene was added and the reaction mixture was refluxed for 3 days under argon. The reaction mixture was poured into 100 ml. of water and the organic phase was concentrated to yield 1.2 g. of gray residue (21%). ^1H NMR (CDCl_3 , 299.95 MHz): 3.20 (s, 36H), 6.35 (d, $J=8$ Hz, 12H), 6.95 (t, $J=8$ Hz, 6H), 7.33 (s, 3H), 7.45 (s, 3H).

4, 4'-biphenyl linked dicarbinol 97:

1-(3,5-dimethoxyphenyl)-3,5-dimethoxybenzene : A solution of 2 g. (7.6 mmol.) of 3,5-dimethoxy-iodobenzene, Mg (7.6 mmol.), CuI (7.6 mmol.), dibromoethane (0.01 mmol.) in 30 ml. of THF was refluxed for 3 hours under argon. Iodo-2,6-dimethoxybenzene was added and the reaction mixture was refluxed further overnight. The solution was filtered, evaporated, extracted with methylene chloride, dried with magnesium sulfate, concentrated, and chromatographed with 10% ethyl acetate in n-hexane to give 870 mg. of white solid (83%). ^1H NMR (CDCl_3 , 299.95 MHz): 3.82 (s, 12H), 6.45 (t, $J=8$ Hz, 2H), 6.69 (d, $J=8$ Hz, 4H) ^{13}C NMR (75.43 MHz): 54.99, 99.02, 105.06, 143.00, 160.51 m/z 274 (M^+), found 274.

1-(3,5-dimethoxyphenyl)-3,5-dimethoxy dimethylbenzoate: 1-(3,5-dimethoxyphenyl)-3,5-dimethoxybenzene was lithiated with n-BuLi in dry THF and quenched with 10 fold excess of dimethyl carbonate and washed with water twice and extracted with diethyl ether followed by drying and evaporation of solvent. Chromatography over silica gel using 20 % ethyl acetate in hexane gave the product as white solids (23%). ^1H NMR (CDCl_3 , 299.95 MHz): 3.87 (s, 12H), 3.91 (s, 6H), 6.64 (s, 4H) ^{13}C NMR (75.43 MHz): 52.51, 56.21, 103.45, 144.76, 157.49, 166.72.

1,3-benzenedicarboxaldehyde : A solution of 1,3-phenylene diamine (50g, 379 mmol.), hexamethylene tetraamine (188.3g, 1.345 mol.) in 90 ml. of conc. HCl and 600 ml. of 50% acetic acid in a 2 liter round bottom flask was refluxed for 3 hours with stirring. The hot amber reaction mixture is poured into a flask and a solution of 56.2 g. of NaOH in 750 ml. of water was slowly added with stirring. The mixture was covered and allowed to stand overnight at 5°C. The product was collected and washed with 10 ml. of cold water and dried (37.2g, 73 %). ^1H NMR (CDCl_3 , 299.95 MHz): 7.72 (t, $J=3$ Hz, 1H), 8.14 (dd, $J=4,1$ Hz, 2H), 8.36 (m, 1H), 10.12 (s, 2H) ^{13}C NMR (75.43 MHz): 129.50, 130.60, 134.22, 136.54, 190.65.

4-(3-(3-oxo-1-butenyl)phenyl)-3-buten-2-one: To a stirred solution of 10 g. (57.4 mmol.) of 1,3-benzenedicarboxaldehyde in 200 ml. of water and 200 ml. of diethyl ether, 100 ml. of acetone and 5 g. of NaOH were added and the mixture was stirred at the room temperature for 2 days. The organic layer was separated by adding 200 ml. of diethyl ether and 100 ml. of acetone and dried with magnesium sulfate. The combined organic

solution was evaporated and chromatographed over silica gel using 20% ethyl acetate in n-hexane to give the diketone as white crystals. (5.5 g., 45%). ^1H NMR (CDCl_3 , 299.95 MHz): 2.37 (s, 6H), 6.73 (d, $J=16$ Hz, 2H), 7.46 (m, 2H), 7.54 (m, 3H), 7.67 (s, 1H) ^{13}C NMR (75.43 MHz): 27.70, 127.86, 127.93, 129.58, 129.80, 135.19, 142.22, 198.05 m/z 214 (M^+), found 214.

2-hydroxy-6-(3-(3-hydroxy-2-methoxycarbonyl-5-oxo-3-cyclohexenyl)phenyl)-4-oxo-2-cyclohexenecarboxylate: To a solution of sodium methoxide (2.3g, 100 mg. atom) in 200 ml. of methanol, dimethyl malonate (12.36g, 93.63 mmol.) was added and the mixture stirred for 30 min at room temperature under argon. 4-(3-(3-oxo-1-butenyl)phenyl)-3-buten-2-one (6.68g, 31.21 mmol.) was added portion wise with stirring. The reaction mixture was refluxed for 3 hours under argon and allowed to cool to room temperature. The solvent was distilled under reduced pressure, the oily residue was treated with acidic ($\text{pH}=5$) water, and extracted with methylene chloride. The solution was dried over magnesium sulfate, solvent was evaporated, and the product mixture was dried under vacuum. The crude mixture was crystallized with methanol (10.7g, 83%) m/z 414 (M^+), found 414.

1,3-Bis-(3,5-dimethoxyphenyl)benzene:

^1H NMR (CDCl_3 , 299.95 MHz): 3.84 (s, 12H), 6.47 (t, $J=2$ Hz, 2H), 6.75 (d, $J=2$ Hz, 4H), 7.50 (m, 3H), 7.74 (s, 1H).

Di-(2,6-dimethoxy phenyl)-(4-pyridyl) methanol 99: A solution of phenyl lithium was prepared by the addition of bromobenzene (39.2g., 0.250

mole) in 125 ml. of ether to lithium wire (4.0 g., 0.577 mol.) and 60 ml. of ether. Resorcinol dimethyl ether (30.0 g., 0.218 mole) was added and the reaction mixture was allowed to stand at room temperature under nitrogen for 60 hours. 13.5 g. (98.6 mmol.) of methyl isonicotinate in 400 ml. of benzene was added and the reaction mixture was refluxed for 3 days under nitrogen. The reaction mixture was poured into 600 ml. of water and the organic phase was concentrated to yield a gray residue. Recrystallization from methylene chloride in n-hexane gave 14 g. of NMR clean crystals of carbinol (37 %). ^1H NMR (CDCl_3 , 299.95 MHz): 3.39 (s, 12H), 6.52 (d, $J=8$ Hz, 4H), 6.65 (s, 1H), 7.13 (t, $J=8$ Hz, 2H), 7.36 (dd, $J=8,2$ Hz, 2H), 8.40 (dd, $J=8,2$ Hz, 2H) ^{13}C NMR (75.43 MHz): 56.02, 78.80, 106.30, 121.55, 124.41, 127.82, 148.31, 157.74, 158.50.

Di-(2,6-dimethoxy phenyl)-(3-pyridyl) methanol 100: A solution of phenyl lithium was prepared by the addition of bromobenzene (39.2g., 0.250 mole) in 125 ml. of ether to lithium wire (4.0 g., 0.577 mol.) and 60 ml. of ether. Resorcinol dimethyl ether (30.0 g., 0.218 mole) was added and the reaction mixture was allowed to stand at room temperature under nitrogen for 60 hr. 13.5g (98.6 mmol.) of methyl nicotinate in 400 ml. of benzene was added and the reaction mixture was refluxed for 3 days under nitrogen. The reaction mixture was poured into 600 ml. of water and the organic phase was concentrated to yield a gray residue. Recrystallization from methylene chloride in n-hexane gave 15.5 g. of NMR clean crystals of the carbinol (41 %). ^1H NMR (CDCl_3 , 299.95 MHz): 3.40 (s, 12H), 6.51 (d, $J=8$ Hz, 4H), 6.63 (s, 1H), 7.12 (t, $J=8$ Hz, 3H), 7.70 (dt, $J=8,2$ Hz, 1H), 8.34 (dd, $J=6,2$ Hz, 1H), 8.64 (d, $J=2$ Hz, 1H) ^{13}C NMR (75.43 MHz):

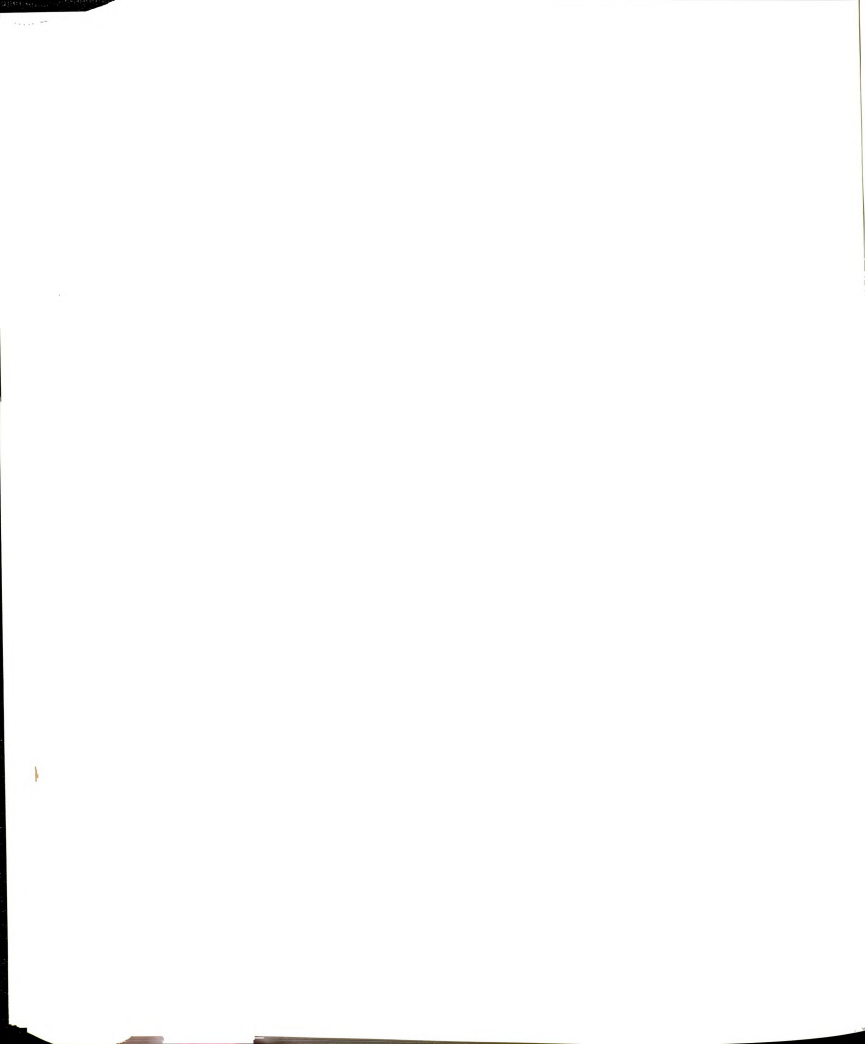
^{13}C NMR (75.43 MHz): 56.16, 78.20, 106.36, 121.73, 124.82, 127.76, 133.73, 144.46, 146.39, 148.93, 157.83.

Di-(2,6-dimethoxy phenyl)(2-pyridyl) methanol **101**: A solution of phenyl lithium was prepared by the addition of bromobenzene (39.2g., 0.250 mole) in 125 ml. of ether to lithium wire (4.0 g., 0.577 mol.) and 60 ml. of ether. Resorcinol dimethyl ether (30.0 g., 0.218 mole) was added and the reaction mixture was allowed to stand at room temperature under nitrogen for 60 hours. 13.5 g. (98.6 mmol.) of methyl picolinate in 400 ml. of benzene was added and the reaction mixture was refluxed for 3 days under nitrogen. The reaction mixture was poured into 600 ml. of water and the organic phase was concentrated to yield a gray residue. Recrystallization from methylene chloride in n-hexane gave 23 g. of NMR clean crystals of the carbinol (61 %). ^1H NMR (CDCl_3 , 299.95 MHz): 3.39 (s, 12H), 6.49 (d, $J=8$ Hz, 4H), 6.56 (s, 1H), 7.00(m, 1H), 7.09 (t, $J=8$ Hz, 2H), 7.50 (m, 2H), 8.45 (m, 1H) ^{13}C NMR (75.43 MHz): 56.30, 79.44, 106.24, 120.45, 121.70, 127.32, 134.73, 146.71, 158.07, 168.46.

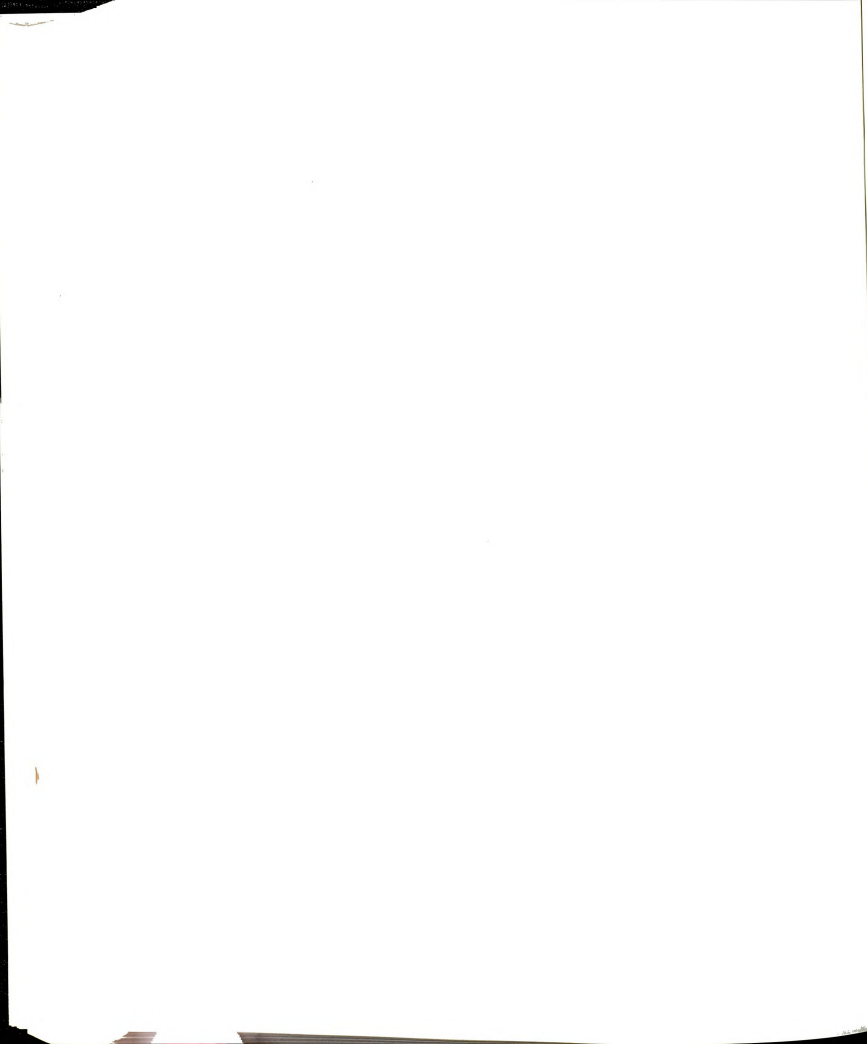
REFERENCES

1. C. J. Pedersen, *J. Am. Chem. Soc.* **89**, 7017, **1967**. D. J. Cram, *Angew. Chem. Int. Ed. Engl.*, **25**, 1039, **1986**. D. J. Cram, *Science*, **240**, 760, **1988**. J.-M. Lehn, *Angew. Chem. Int. Ed. Engl.*, **27**, 89, **1988**.
2. H. G. Viehe, R. Merényi, L. Stella, Z. Janousek, *Angew. Chem. Int. Ed. Engl.* **18**, 917, **1979**; M. Ballester, *Acc. Chem. Res.* **18**, 380, **1985**.
3. For carbenes with particular relevance to organic ferromagnets, see: A. M. Trozzolo, R. W. Murray, G. Smolinsky, W. A. Yager, E. Wasserman, *J. Am. Chem. Soc.* **85**, 2526, **1963**; K. Itoh, *Chem. Phys. Lett.* **1**, 235, **1967**; T. Takui, K. Itoh, *Chem. Phys. Lett.* **19**, 120, **1973**. A. Izuoka, S. Murata, T. Sugawara, H. Iwamura, *J. Am. Chem. Soc.* **107**, 1786, **1985**; Y. Teki, T. Takui, K. Itoh, H. Iwamura, K. Kobayashi, *J. Am. Chem. Soc.* **108**, 2147, **1986**; I. Fujita, Y. Teki, T. Takui, T. Kinoshita, K. Itoh, F. Miko, Y. Sawaki, H. Iwamura, A. Izuoka, T. Sugawara, *J. Am. Chem. Soc.* **112**, 4074, **1990**.
4. W. T. Borden, Ed., *Diradicals*; John Wiley & Sons, Inc., **1982**; G. L. Closs, R. J. Miller, O. D. Redwine, *Acc. Chem. Res.* **18**, 196, **1985**; M. Platz (Ed.) Symposia-in-Print No. 4, *Tetrahedron*, **38**, 733-867; J. A. Berson, *Acc. Chem. Res.* **11**, 446, **1978**; C. Doubleday, Jr.; N. J. Turro, J.-F. Wang, *Acc. Chem. Res.* **22**, 199, **1989**.
5. For an excellent discussion of exchange phenomena in bimetallic systems see: R. D. Willett, D. Gatteschi, O. Kahn Ed., "Magneto-Structural Correlations in Exchange-Coupled Systems," NATO ASI Series C, V. 140, D. Reidel, Boston, **1985**; O. Kahn, *Structure and Bonding*, **68**, 91, **1987**; A. Bencini, D. Gatteschi, *Electron Paramagnetic Resonance of Exchange Coupled Systems*, Springer-Verlag, Berlin, **1990**.
6. V. Bonacic-Koutecky', J. Koutecky', J. Michl, *Angew. Chem. Int. Ed. Engl.* **26**, 170, **1987**.
7. H. McConnell, *J. Chem. Phys.* **39**, 1910, **1963**; *Proc. Robert A Welch Found.* **108**, 11, **1967**.
8. C. M. Hurd *Contemporary Physics* **23**, 469 **1982**.
9. 197th National American Chemical Society meeting in Dallas, Texas, April 10-14, **1989**. Proceedings of the Symposium on Ferromagnetic and High Spin Molecular Based Materials in *Mol. Cryst. Liq. Cryst.* **176**, 1-562 (**1989**); J. S. Miller; D. A. Dougherty, *Angew. Chem. Int. Ed. Engl., Adv. Mater.* **28**, 961 (**1989**).
10. W. E. Broderick, J. A. Thompson, E. P. Day, B. M. Hoffman, *Science*, **249**, 402 (**1990**); J. S. Miller, A. J. Epstein, in: Z. Yoshida, T. Shiba, Y. Oshiro (Eds.) *New Aspects of Organic Chemistry I*, VCH, Weinheim, **1989**; p 237; J. S.

- Miller, A. J. Epstein, W. M. Reiff, *Chem. Rev.* **88**, 201 (1988). J. S. Miller, A. J. Epstein, W. M. Reiff, *Science* **240**, 40 (1988). *Chem. Eng. News*, p. 5 (Mar. 30, 1987) and p. 28 (Nov. 9, 1987). J. S. Miller, J. C. Calabrese, H. Rommelmann, S. R. Chittipeddi, J. J. Zhang, W. M. Reiff, A. J. Epstein, *J. Am. Chem. Soc.* **109**, 769 (1987). J. S. Miller, A. J. Epstein, *J. Am. Chem. Soc.* **109**, 3850 (1987).
- 11 P. W. Selwood, *Magnetochemistry*, Interscience, New York, 1943; A. P. Cracknell, *Magnetism in Crystalline Materials*, Pergamon Press, Oxford, 1975; R. L. Carlin, *Magnetochemistry*, Springer-Verlag, Berlin, 1986.
- 12 For early musings on organic ferromagnetism see ref. 9 and: N. Mataga, *Theoret. Chim. Acta* **10**, 372 (1968); A. A. Ovchinnikov, *Theoret. Chim. Acta*, **47**, 297 (1978); A. L. Buchachenko, *Doklady Nauk Acad. SSSR* **244**, 1146 (1979); I. A. Misurkin, A. A. Ovchinnikov, *Russ. Chem. Rev. (Engl. Trans.)* **46**, 967 (1977); R. Breslow, B. Jaun, R. Q. Klutz, C.-Z. Xia, *Tetrahedron*, **38**, 863 (1982).
- 13 For some more recent magnetic models see: H. Fukutome; A. Takahashi; M. Ozaki, **133**, 34 (1987); L. Dulog, J. S. Kim, *Angew. Chem. Int. Ed. Engl.*, **29**, 415 (1990); K. Yamaguchi, Y. Toyoda, T. Fueno, *Synthetic Metals*, **19**, 81 (1987); K. Yamaguchi, Y. Toyoda, M. Nakano, T. Fueno, *ibid.*, **19**, 87 (1987); K. Awaga, T. Sugano, M. Kinoshita, *J. Chem. Phys.*, **85**, 2211 (1986). K. Awaga, T. Sugano, M. Kinoshita, *Chem. Phys. Lett.*, **141**, 540 (1987). P. M. Lahti, A. S. Ichimura, *Mol. Cryst. Liq. Cryst.*, **176**, 125 (1989). P. M. Lahti, A. S. Ichimura, J. A. Berson, *J. Org. Chem.*, **54**, 958 (1989); K. M. Chi, J. C. Calabrese, J. S. Miller, *Mol. Cryst. Liq. Cryst.*, **176**, 173 (1989). K. M. Chi, J. C. Calabrese, J. S. Miller, S. I. Khan, *Mol. Cryst. Liq. Cryst.*, **176**, 185 (1989).
- 14 D.J. Cram, *Angew. Chem. Int. Ed. Engl.*, **27**, 1009 (1988); J.-M. Lehn, *Angew. Chem. Int. Ed. Engl.* **27**, 89 (1988).
- 15 CPK models are particularly faithful for ion binding ligands and their interactions and have consistently provided insights into complexant design. In the present case, two CPK models of radical **1** neatly encapsulate a marble of appropriate size to represent a Li⁺ ion.
- 16 The methoxy groups in the analogous tris(2,6-dimethoxyphenyl)phosphine participate in the ligation of a variety of metal species. See: K.R. Dunbar, S. C. Haefner, L. E. Pence, *J. Am. Chem. Soc.*, **111**, 5504 (1989).
- 17 J.-M. Lehn, *Angew. Chem. Int. Ed. Engl.*, **27**, 89, 1988.
- 18 E. Weber, *Top. Curr. Chem.*, **140**, 1, 1987. S. Kamitori, K. Hirotsu and T. Higuchi, *J. Am. Chem. Soc.*, **109**, 2409, 1987. W. Saenger, *Angew. Chem.*, **92**, 343, 1980, F. Vögtle and W. M. Müller, *Angew. Chem. Int. Ed. Engl.*, **18**, 628, 1979.
- 19 K. Odashima and K. Koga, in *Cyclophanes*, Vol. 2. Academic Press, New York, 629, 1983. K. Odashima, A. Ita, Y. Litaka and K. Koga, *J. Org. Chem.*, **50**, 4478, 1985.

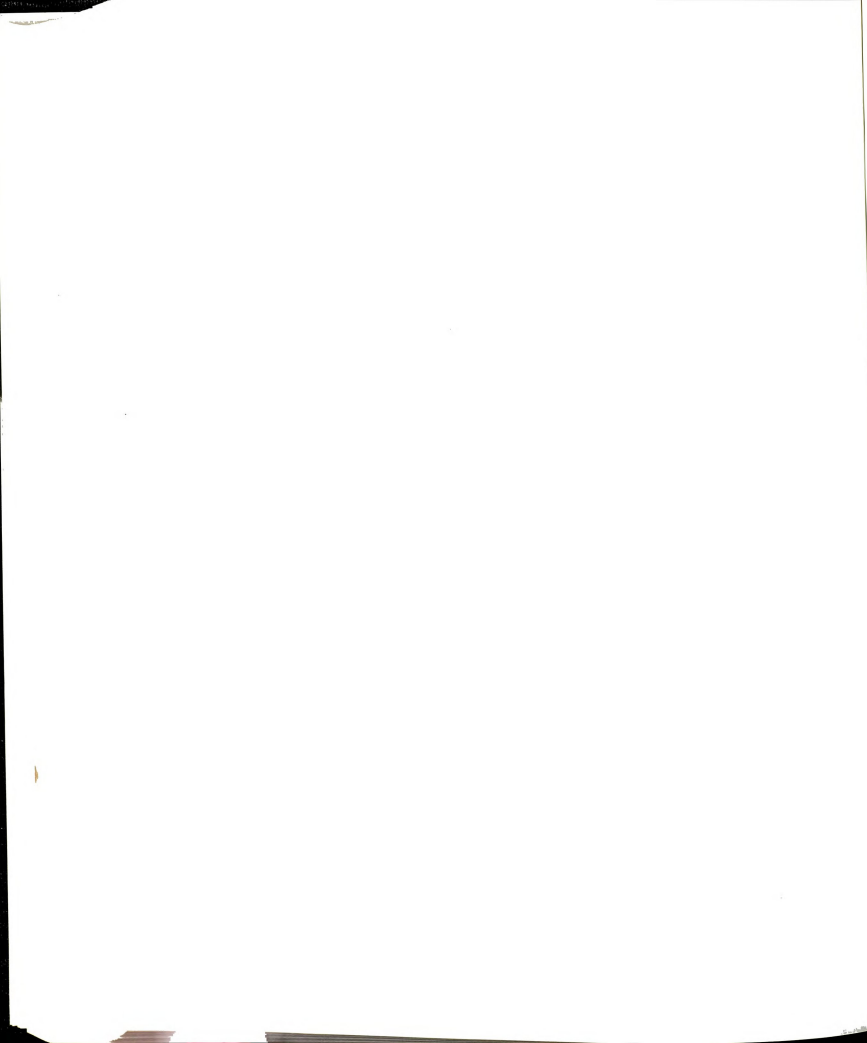


-
- 20 F. Vögtle and W. M. Müller, *Angew. Chem.* **96**, 711, **1984**, F. Vögtle and W. M. Müller *Angew. Chem. Int. Ed. Engl.*, **25**, 567, **1986**.
- 21 H. J. Schneider and T. Blatter *Angew. Chem.* **100**, 1211, **1988**. H. J. Schneider and T. Blatter *Angew. Chem. Int. Ed. Engl.*, **27**, 1163, **1988**. H.-J. Schneider and I. Theis, *Angew. Chem., Int. Ed. Engl.*, **28**, 753, **1989**. H.-J. Schneider, D. Guttes and U. Schneider, *J. Am. Chem. Soc.* **110**, 6449, **1988**. F. Diederich and K. Dick, *Angew. Chem. Int. Ed. Engl.* **22**, 715, **1983**. F. Diederich and K. Dick, *Angew. Chem. Int. Ed. Engl.* **23**, 810, **1984**. F. Diederich and D. R. Carcanague, *Angew. Chem. Int. Ed. Engl.* **29**, 769, **1990**.
- 22 G. R. Desiraju "Crystal Engineering: the Design of Organic Solids" *Materials Science Monographs*, 54, Elsevier, New York, NY. **1989**.
- 23 G. M. J. Schmidt, *Pure Appl. Chem.*, **27**, 647, **1971**. and references therein.
- 24 H. R. Ott *Nature* **363**, 56, **1993**.
- 25 M. A. Beno, H. H. Wang, K. D. Carson, A. M. Kini, G. M. Frankenbach, J. R. Ferraro, N. Larson, G. D. McCabe, J. Thomson, C. Purnama, M. Vashon, J. M. Williams, D. Jung, M. -H. Whangbo., *Mol. Cryst. Liq. Cryst.* **1990**, 181, 145. M. A. Beno, H. H. Wang, A. M. Kini, K. D. Carson, U. Geiser, W. K. Kwok, J. E. Thompson, J. M. Williams, J. Ren, M. -H. Whangbo, *Inorganic. Chem.* **1990**, **29**, 1599.
- 26 D. Griller and K. U. Ingold *Acc. Chem. Res.* **9**, 13, **1976**.
- 27 S. W. Benson "Thermochemical Kinetics", Wiley, New York, N.Y., **1968**, D. M. Golden and S. W. Benson, *Chem. Rev.* **69**, 125, **1969**, H. E. O'Neal and S. W. Benson in "Free Radicals", Vol II. J. K. Kochi, Ed., Wiley, New York, N.Y. **1973**.
- 28 "The History of Organic Chemistry in the United States, 1875-1955" D. S. Tarbell and A. T. Tarbell, K & S Press, Nashville, TN, **1986**.
- 29 H. Lankamp, W. Th. Nauta, C. MacLean, *Tett. Lett.* 249, **1968**. P. Jacobson, *Ber. Dtsch. Chem. Ges.* **38**, 196, **1905**.
- 30 M. Stein, W. Winter, and A. Rieker *Angew. Chem. Int. Ed. Engl.* **17**, 692, **1978**. B. Kahr, D. V. Engen, and K. Mislow *J. Am. Chem. Soc.* **108**, 8305, **1986**.
- 31 W. Schlenk and M. Brauns, *Ber. Dtsch. Chem. Ges.* 48, 661, **1915**.
- 32 G. Kothe, K.-H. Denkel, W. Sümmermann *Angew. Chem. Int. Engl. Ed.*, **9**, 906, **1970**.
- 33 A. E. Chichibabin, *Chem. Ber.* 40, 1810, **1907**.



-
- 34 M. S. Platz, *Diradicals*, W. T. Borden, Ed., Wiley, New York, **1982**, Chapter 5.
- 35 L. K. Montgomery, J. C. Huffman, E. A. Jurczak, M. P. Grendze, *J. Am. Chem. Soc.* **108**, 6004, **1986**.
- 36 J. Thiele, H. Balhorn, *Chem. Ber.* **37**, 1463, **1904**.
- 37 M. Ballester, C. Molinet, *Chem. Ind. (London)* 1290, **1954**. M. Ballester, C. Molinet, J. Castaner, *J. Am. Chem. Soc.*, **82**, 4254, **1960**, M. Ballester, R. Riera, *J. Am. Chem. Soc.*, **86**, 4505, **1964**.
- 38 M. Ballester, *Pure Appl. Chem.* **15**, 123, **1967**.
- 39 M. Ballester, J. Castaner, J. Riera, *J. Am. Chem. Soc.* **88**, 957, **1966**.
- 40 M. J. Sabacky, C. S. Johnson, Jr., R. G. Smith, H. S. Gutowsky, J. C. Martin, *J. Am. Chem. Soc.* **89**, 2054 (**1967**).
- 41 While EPR spectra observed by Jackson and Kahr remain unassigned at least one feature is clear; the spectral dispersion—as large as 800 Gauss in some cases—is too great to be due solely to hyperfine interactions and must be fine structure resulting from long-range magnetic coupling of pairs of radicals. The temperature dependence of the signal intensity indicates that its carrier might be species with a high spin ground state. The spectra were unchanged when LiBF₄ was replaced by LiClO₄ or 99% ⁶LiBF₄.
- 42 For the status of research on molecular magnetism in 1985, see H. Iwamura, T. Sugawara, K. Itoh, T. Takui, *Mol. Cryst. Liq. Cryst.* **125**, 251 (**1985**) R. Breslow, *Mol. Cryst. Liq. Cryst.* **125**, 261 (**1985**)
- 43 For a valuable enumeration of these models, see D. Dougherty and J. S. Miller in *Mol. Cryst. Liq. Cryst.* **176**, 25 (**1989**).
- 44 S. Goldschmidt, *Ber.* **53**, 44, **1920**, S. Goldschmidt and K. Euler *Ber.* **55**, 616, **1922**. S. Goldschmidt and K. Renn, *Ber.* **55**, 628, **1922**. S. Goldschmidt, and F. Graef, *Ber.* **61**, 1858, **1928**. R. H. Poirier, E. J. Kahler, and F. Benington, *J. Org. Chem.* **17**, 1437, **1952**.
- 45 L. S. Singer, and C. Kikuchi, *J. Chem. Phys.* **23**, 1738, **1955**.
- 46 G. Fraenkel and P.D. Bartlett, *J. Am. Chem. Soc.* **81**, 5582, **1959**.
- 47 F. L. Allen and S. Sugden, *J. Chem. Soc.* 440, **1936**. W. Duffy., *J. Chem. Phys.* **36**, 490, **1962**, W. Duffy and D. L. Strandburg, *J. Chem. Phys.* **46**, 457, **1967**.
- 48 C. A. Hutchison, R.C. Pastor, and A.G. Kowalsky *J. Chem. Phys.* **20**, 534, **1952**. N. W. Lord and S. M. linder, *J. Chem. Phys.* **34**, 1693, **1961**. R. M. Deal and W. S. Koski, *J. Chem. Phys.* **31**, 1138, **1959**. R. W. Holmberg, R. Livingston, and W. T. Smith, *J. Chem. Phys.* **33**, 541, **1960**. R. I. Walter, *J.*

- Am. Chem. Soc.* **88**, 1923, **1966**, R. I. Walter, *J. Am. Chem. Soc.* **88**, 1930, **1966**.
- 49 J. Heidberg and J. Weil, *J. Am. Chem. Soc.* **86**, 5173, **1964**. A. L. Buchachenko, "*Stable Radicals*", Consultants Bureau, New York. **1965**.
- 50 O. Piloty and B.G. Schwerin. *Ber.* **34**, 1870, **1901**. O. Piloty and B. G. Schwerin *Ber.* **34**, 2354, **1901**.
- 51 K. H. Meyer and H. G. Bilbroth *Ber.* **52**, 1476, **1919**. K. H. Meyer and W. Reppe, *Ber.* **52**, 1476, **1919**.
- 52 Y. Y. Lim and R. S. Drago, *J. Am. Chem. Soc.* **93**, 891, **1970**. Y. Y. Lim and R. S. Drago, *Inorganic Chem.* **11**, 1334, **1972**.
- 53 R. Briere, H. Lemaire, and A. Rassat, *Bull. Soc. Chim. France*, 3273, **1965**. L. Chapelet, H. Lemaire, and A. Rassat, *Bull. Soc. Chim. France*, 3283, **1965**. E. G. Rozantsev, *Bull. Acad. Sci. USSR*. 2085, **1964**.
- 54 A.M. Feldman and A. K. Hoffmann *Chem. Abst.* **61**, 13289, **1964**. A. W. Hanson, *Acta Cryst.* **6**, 32, **1953**.
- 55 K. H. Meyer and W. Reppe *Ber.* **54**, 327, **1921**. A. K. Hoffmann, A. M. Feldman, and E. Gelblum, *J. Am. Chem. Soc.* **86**, 646, **1964**.
- 56 C. D. Cook, *J. Org. Chem.* **18**, 261, **1953**. C. D. Cook and R. C. Woodworth, *J. Am. Chem. Soc.* **75**, 6242, **1953**.
- 57 N. C. Yang and A. Castro, *J. Am. Chem. Soc.* **82**, 6208, **1960**. E. A. Chandross *J. Am. Chem. Soc.* **86**, 1263, **1964**.
- 58 F. A. Neugebauer, H. Tischmann, and M. Jenne, *Angew. Chem. Int. Ed.*, **6**, 362, **1967**. E. A. Chandross, *J. Am. Chem. Soc.* **86**, 1263, **1964**. K. Mukai and J. Sakamoto *J. Chem. Phys.* **68**, 1432, **1978**.
- 59 A. Earnshaw, *Introduction to Magnetochemistry*, Academic Press, New York, **1968**. R. L. Carlin, *Magnetochemistry*, Springer-Verlag, New York, **1986**.
- 60 B. Morosin and E. J. Graeber. *Acta Cryst.* **16**, 1176, **1963**. L. J. de Jongh and A. R. Miedema, *Adv. Phys.* **23**, 1, **1974**. D.W. Hone and P. M. Richards, *Ann. Rev. Material Sci.* **4**, 337, **1974**. R. Dingle, M. E. Lines, and S. L. Holt, *Phys. Rev.* **187**, 643, **1969**.
- 61 T. Oguchi, *Prog. Theor. Phys.*, **13**, 148, **1955**. H. Ohya-Nishiguchi, *Bull. Chem. Soc. Japan.* **52**, 3480, **1979**. J. C. Bonner, M. E. Fisher, *Phys. Rev.* **135**, A640, **1964**. J. C. Bonner, H. W. J. Blote, J. W. Bray, and I. S. Jacobs, *J. App. Phys.* **50**, 1810, **1979**. M. Verdaguer, A. Gleizes, J. P. Renard, and J. Seiden, *Phys. Rev. B.* **29**, 5144, **1984**. W. Duffy, Jr. and K. P. Barr, *Phys. Rev.* **165**, 647, **1968**.



- 62 M. E. Fisher, *J. Phys.* **32**, 343, **1964**. A. van der Bilt, K. O. Joungh, and R. C. Carlin, *Phys. Rev. B* **24**, 445, **1981**. M. M. Olmstead, W. K. Musker, L. W. Ter Haar, and W. E. Hatfield, *J. Am. Chem. Soc.* **104**, 6627, **1982**. J. W. Hall, W. E. Marsh, R. R. Weller, and W. E. Hatfield, *Inorg. Chem.* **20**, 1033, **1981**., W. E. Hatfield, R. R. Weller, and J. W. Hall, *Inorg. Chem.* **19**, 3825, **1980**., W. H. Crawford and W. E. Hatfield, *Inorg. Chem.* **16**, 1336, **1977**. A. Bencini, C. Benelli, D. Gatteschi, and C. Zanchini, *J. Am. Chem. Soc.* **106**, 5813, **1984**. C. Benelli, D. Gatteschi, D. W. Carnegie, Jr., and R. L. Carlin, *J. Am. Chem. Soc.* **107**, 2560, **1985**.
- 63 A. S. Edelstein, M. Mandel, *J. Chem. Phys.* **35**, 1130, **1961**.
- 64 H. M. McConnell *J. Chem. Phys.* **37**, 1910, **1963**.
- 65 H. McConnell, *Proc. of the Robert A. Welch Foundation Conf. on Chem. Res.* **11**, 144, **1967**.
- 66 N. Mataga, *Theoret. Chim. Acta (Berl.)* **10**, 372, **1968**.
- 67 A. A. Ovchinnikov, *Theoret. Chim. Acta. (Berl.)* **47**, 297, **1978**. A. A. Ovchinnikov, V. N. Spector *Synthetic Metals*, **27**, B615, **1988**.
- 68 R. Breslow *Pure & Appl. Chem.* **54**, 927, **1982**. R. Breslow, B. Jaun, R. Q. Kluttz, C.-Z. Xia *Tetrahedron*, **38**, 863, **1982**.
- 69 T. LePage, R. Breslow, *J. Am. Chem. Soc.* **109**, 6412, **1987**. R. Breslow. *Mol. Cryst. Liq. Cryst.*, **176**, 199, **1989**.
- 70 J. B. Torrance, S. Oostra, A. Nazzal, *Synthetic Metals*, **19**, 709, **1987**.
- 71 C. Kollmar, O. Kahn, *J. Am. Chem. Soc.* **113**, 7987, **1991**, C. Kollmar, M. Couty, and O. Kahn, *J. Am. Chem. Soc.* **113**, 7994, **1991**.
- 72 C. Kollmar and O. Kahn, *Acc. Chem. Res.* **26**, 259, **1993**. A. Caneschi, D. Gatteschi, and R. Sessoli, *Acc. Chem. Res.* **22**, 392, **1989**, J. S. Miller, A. J. Epstein, and W. M. Reiff, *Acc. Chem. Res.* **21**, 114, **1988**, J. S. Miller, A. J. Epstein, and W. M. Reiff, *Chem. Rev.* **88**, 201, **1988**. O. Kahn, *Angew. Chem. Int. Ed. Engl.* **24**, 834, **1985**.
- 73 B. Bleaney, K. D. Bowers, *Proc. R. Soc. London A* **214**, 451, **1952**.
- 74 D. Gatteschi, O. Kahn, R. D. Willett (eds): *Magneto Structural Correlations in Exchange Coupled Systems*, D. Reidel, Dordrecht **1984**.
- 75 M. Verdaguer, M. Julve, A. Michalowicz, and O. Kahn, *Inorg. Chem.* **22**, 2624, **1983**. Y. Pei, O. Kahn, J. Sletten., *J. Am. Chem. Soc.* **108**, 3143, **1986**., Y. Pei, M. Verdaguer, O. Kahn, J. Sletten, and J. P. Renard, *J. Am. Chem. Soc.* **108**, 7428, **1986**. Y. Pei, M. Verdaguer, O. Kahn, J. Sletten, and J. P. Renard, *Inorg. Chem.* **26**, 138, **1987**. O. Kahn, *Angew. Chem. Int. Ed. Engl.* **24**, 834, **1985**. K. Nakatani, O. Kahn. C. Mathoniere, T. Pei, and C. Zakine, *New. J.*



- Chem.* **14**, 861, **1990**. O. Kahn, Comments *Inorg. Chem.* **3**, 105, **1984**. M. Julve, M. Verdaguer, A. Gleizes, M. P. Levisalles, and O. Kahn. *Inorg. Chem.* **23**, 3808, **1984**.
- 76 D. Beltram, E. Escriva, and M. Drillon, *J. Chem. Soc., Faraday Trans. 2*, **78**, 1773, **1982**. M. Drillon, E. Coronado, D. Beltran, J. Curely, R. Georges, P. R. Nugteren, L. J. de Hongh, and J. L. Genicon, *J. Magn. Magn. Mater.*, **54-57**, 1507, **1986**. M. Drillon, E. Coronado, A. Fuertes, D. Beltran, and R. Georges, *Chem. Phys.* **79**, 449, **1983**. E. Coronado, M. Drillon, A. Fuertes, D. Beltran, A. Mosset, and J. Galy, *J. Am. Chem. Soc.* **108**, 900, **1986**.
- 77 O. Kahn Comments *Inorg. Chem.* **3**, 105, **1984**. R. D. Willett, D. Gatteschi, O. Kahn Eds., *Magnetostructural Correlations in Exchange Coupled Systems* (NATO Advanced Study Institute Series), D. Reidel, Dordrecht, The Netherlands, **1984**.
- 78 D. Y. Jeter, D. L. Lewis, J. C. Hemplel, D. J. Hodgson, and W. E. Hatfield, *Inorg. Chem.* **11**, 1958, **1972**.
- 79 M. Julve, M. Verdaguer, A. Gleizes, M. P. Levisalle, and O. Kahn, *Inorg. Chem.* **23**, 3808, **1984**. Y. Pei, K. Nakatani, J. Sletten, J. P. Renard, *Inorg. Chem.* **16**, 3170, **1986**.
- 80 L. R. Carlin, A. Kopinga, O. Kahn, and M. Verdaguer, *Inorg. Chem.* **25**, 1786, **1986**.
- 81 S. K. Shakhathreh, E. G. Bakalbassis, I. Brüdgam, H. Hartl, J. Mrozinski, and C. A. Tsipis, *Inorg. Chem.* **30**, 2801, **1991**.
- 82 A. Bencini, C. Benelli, D. Gatteschi, and C. Zanchini, *J. Am. Chem. Soc.* **106**, 5813, **1984**. C. Benelli, D. Gatteschi, and C. Zanchini, *Inorg. Chem.* **23**, 798, **1984**. C. Benelli, D. Gatteschi, D. W. Carnegie, Jr., and R. Carlin, *J. Am. Chem. Soc.* **107**, 2560, **1985**. A. Caneschi, D. Gatteschi, J. Laugier, P. Rey, R. Sessoli, and C. Zanchini, *J. Am. Chem. Soc.* **110**, 2795, **1988**. A. Caneschi, D. Gatteschi, J. Laugier, P. Rey, and C. Zanchini, *Inorg. Chem.* **28**, 1969, **1989**. A. Caneschi, D. Gatteschi, J. P. Renard, P. Rey, and R. Sessoli, *Inorg. Chem.* **28**, 1976, **1989**. A. Caneschi, D. Gatteschi, J. P. Renard, P. Rey, and R. Sessoli, *Inorg. Chem.* **28**, 3314, **1989**. A. Caneschi, D. Gatteschi, and R. Sessoli, *Mol. Cryst. Liq. Cryst.* **176**, 329, **1989**. A. Caneschi, D. Gatteschi, J. P. Renard, P. Rey, and R. Sessoli, *J. Am. Chem. Soc.* **111**, 785, **1989**. P. Rey, J. Laugier, A. Caneschi, D. Gatteschi, *Mol. Cryst. Liq. Cryst.* **176**, 337, **1989**. A. Caneschi, F. Ferraro, D. Gatteschi, P. Rey, and R. Sessoli, *Inorg. Chem.* **29**, 4217, **1990**. A. Caneschi, D. Gatteschi, R. Sessoli, and P. Rey, *Acc. Chem. Res.* **22**, 392, **1989**. A. Caneschi, D. Gatteschi, P. Rey, and R. Sessoli, *Chem. Mater.*, **4**, 204, **1992**.
- 83 S. S. Eaton, G. R. Eaton, *Coord. Chem. Rev.* **26**, 207, **1978**. S. Eaton, S. S. G. R. Eaton, *Coord. Chem. Rev.* **83**, 29, **1988**.
- 84 A. Caneschi, D. Gatteschi, A. Grand, J. Laugier, L. Pardi, and P. Rey, *Inorg. Chem.* **27**, 1031, **1988**. A. Caneschi, D. Gatteschi, J. Laugier, L. Pardi, P. Rey, and C. Zanchini, *Inorg. Chem.* **27**, 2027, **1988**.

-
- 85 A. Bencini, C. Benelli, D. Gatteschi, C. Zanchini, *J. Am. Chem. Soc.* **106**, 5813, **1984**. C. Benelli, D. Gatteschi, and C. Zanchini, *Inorg. Chem.* **23**, 798, **1984**.
- 86 A. Caneschi, D. Gatteschi, J. Laugier, and P. Rey, "*Organic and Inorganic Low Dimensional Crystalline Materials*", P. Delhaes, M. Drilon, Eds.; Plenum Press, New York, London, p109, p389, **1987**.
- 87 A. Caneschi, D. Gatteschi, P. Rey, R. Sessoli, *Inorg. Chem.* **27**, 1756, **1988**, A. Caneschi, D. Gatteschi, J. P. Renard, P. Rey, and R. Sessoli, *J. Am. Chem. Soc.* **111**, 785, **1989**.
- 88 J. S. Miller, J. C. Calabrese, H. Rommelmann, S. R. Chittipeddi, J. H. Zhang, W. M. Reiff, and A. J. Epstein, *J. Am. Chem. Soc.* **109**, 769, **1987**, J. S. Miller and A. J. Epstein, *J. Am. Chem. Soc.* **109**, 3850, **1987**. J. S. Miller, *Acc. Chem. Res.*, **21**, 114, **1988**. J. S. Miller, A. J. Epstein, W. M. Reiff, *Chem. Rev.*, **88**, 201, **1988**. J. S. Miller, A. J. Epstein, and W. M. Reiff, *Science*, **240**, 40, **1988**. A. Chakraborty, A. J. Epstein, W. N. Lawless, and J. S. Miller, *Phys. Rev. B*, **40**, 11 422, **1989**. J. S. Miller and A. J. Epstein, *Phil Trans. R. Soc. Lond. A*, **330**, 205, **1990**.
- 89 C. Kollmar, O. Kahn, *J. Am. Chem. Soc.* **113**, 7987, **1991**, C. Kollmar, M. Couty, and O. Kahn, *J. Am. Chem. Soc.* **113**, 7994, **1991**. C. Kollmar and O. Kahn, *Acc. Chem. Res.* **26**, 259, **1993**. , C. M. Hurd, *Contemporary Physics* **23**, 469, **1982**.
- 90 K. Mukai, H. Nishiguchi, and Y. Deguchi, *J. Phys. Soc. Japan*, **23**, 125, **1967**, K. Awaga, T. Sugano, and M. Kinoshita, *Solid State Comm.* **57**, 453, **1986**. K. Awaga, T. Sugano, and M. Kinoshita, *Chem. Phys. Lett.* **128**, 587, **1986**. K. Awaga, T. Sugano, and M. Kinoshita, *J. Chem. Phys.* **85**, 2211, **1986**. K. Awaga, T. Sugano, and M. Kinoshita, *Chem. Phys. Lett.* **141**, 540, **1987**. M. Kinoshita, *Mol. Cryst. Liq. Cryst.* **176**, 163, **1989**.
- 91 D. E. Williams, *Mol. Phys.* **16**, 145, **1969**.
- 92 K. M. Chi, J. C. Calabrese, J. S. Miller, and S. I. Khan, *Mol. Cryst. Liq. Cryst.* **176**, 185, **1989**.
- 93 K. Mukai, *Bull. Chem. Soc. Jpn.* **42**, 40, **1969**.
- 94 K. Awaga and Y. Maruyama, *Chem. Phys. Lett.* **158**, 556, **1989**. K. Awaga, T. Inabe, U. Nagashima, and Y. Maruyama, *J. Chem. Soc. Chem. Comm.* 1617, **1989**. M. Kinoshita, P. Turek, M. Tamura, K. Nozawa, D. Shiomi, Y. Nakazawa, M. Ishikawa, M. Takahashi, K. Awaga, T. Inabe, and Y. Maruyama, *Chem. Lett.* 1225, **1991**. P. Turek, K. Nozawa, D. Shiomi, K. Awaga, T. Inabe, Y. Maruyama, and M. Kinoshita. *Chem. Phys.* **180**, 327, **1991**.
- 95 L. Pauling "*The Nature of the Chemical Bond*", Cornell University Press, New York, p343, **1960**. J. W. Linnett, *J. Am. Chem. Soc.* **83**, 2643, **1961**.

1944-45
A. J. Jones

1945-46
A. J. Jones

1946-47
A. J. Jones

1947-48
A. J. Jones

1948-49
A. J. Jones

1949-50
A. J. Jones

1950-51
A. J. Jones

-
- 96 Y. Y. Lim and R. S. Drago, *J. Am. Chem. Soc.* **93**, 891, **1970**. A. M. Vasserman and A. L. Buchachenko, *J. Struct. Chem.* **7**, 633, **1966**.
- 97 T. Sugano, M. Tamura, M. Kinoshita, Y. Sakai, and Y. Ohashi, *Chem. Phys. Lett.* **200**, 235, **1922**.
- 98 H. Iwamura, 197th National Meeting of the American Chemical Society, Dallas, TX, April 9-14, **1989**.
- 99 W. T. Borden, Diradicals; W. T. Borden, Ed.; Wiley, New York, **1982**, W. T. Borden and E. R. Davidson, *J. Am. Chem. Soc.* **99**, 4587, **1977**.
- 100 E. E. Seeger, P. M. Lahti, A. R. Rossi, and J. A. Berson, *J. Am. Chem. Soc.* **108**, 1251, **1986**.
- 101 S. Kato, K. Morokuma, D. Feller, E. Davidson, W. T. Borden, *J. Am. Chem. Soc.* **105**, 1791, **1983**. B. B. Wright, M. S. Platz, *J. Am. Chem. Soc.* **105**, 628, **1983**. J. L. Goodman, J. A. Berson *J. Am. Chem. Soc.* **106**, 1867, **1984**, M. Rule, A. Matlin, D. E. Seeger, E. F. Hilinski, and D. A. Dougherty *Tetrahedron* **38**, 787, **1982**.
- 102 T. Matsumoto, T. Ishida, N. Koga, and H. Iwamura. *J. Am. Chem. Soc.* **114**, 9952, **1992**.
- 103 A. J. Novak, R. Jain, and D. A. Dougherty, *J. Am. Chem. Soc.* **111**, 7618, **1989**. J. A. Berson, *Acc. Chem. Res.* **11**, 446, **1978**, P. Dowd., *Acc. Chem. Res.* **5**, 242, **1972**, R. Jain, M. B. Sponsler, F. D. Combs, D. A. Dougherty, *J. Am. Chem. Soc.* **110**, 1356, **1988**. J. A. Berson, *Acc. Chem. Res.* **11**, 446, **1978**.
- 104 M. Ballester, J. Castaner, J. Riera, A. Ibanez, and J. Pujadas, *J. Org. Chem.* **47**, 259, **1982**. M. Ballester, J. Riera, J. Castaner, A. Rodriguez, C. Rovira, and J. Veciana, *J. Org. Chem.* **47**, 4498, **1982**. M. Ballester, J. Castaner, J. Riera, J. Pujadas, O. Armet, C. Onrubia, and J. A. Rio, *J. Org. Chem.* **49**, 770, **1984**. M. Ballester, *Acc. Chem. Res.* **18**, 380, **1985**.
- 105 J. Veciana, A. D. Martinez and O. Armet, *Rev. Chem. Intermediates*, **10**, 35, **1988**, J. Veciana and A. Duran. *J. Inclus. Pheno.* **5**, 173, **1987**.
- 106 O. Armet, J. Veciana, C. Rovira, J. Riera, J. Castaner, E. Molins, J. Rius, C. Miravittles, S. Olivella, and J. Brichfeus. *J. Phys. Chem.* **91**, 5608, **1987**.
- 107 J. Veciana, C. Rovira, M. I. Crespo, O. Armet, V. M. Domingo, and F. Palacio, *J. Am. Chem. Soc.* **113**, 2552, **1991**. J. Carilla, L. Julia, J. Riera, E. Brillas, J. A. Garrido, A. Labarta, and R. Alcala. *J. Am. Chem. Soc.* **113**, 8281, **1991**, J. Veciana, C. Rovira, N. Ventosa, M. I. Crespo, and F. Palacio *J. Am. Chem. Soc.* **115**, 57, **1993**.
- 108 A. Rajca, *J. Am. Chem. Soc.* **112**, 5889, **1990**, A. Rajca, *J. Org. Chem.* **56**, 2557, **1991**, A. Rajca, S. Utamapanya, and J. Xu, *J. Am. Chem. Soc.* **113**,

- 9235, **1991**. S. Utamapanya and A. Rajca, *J. Am. Chem. Soc.* **113**, 9242, **1991**., A. Rajca, S. Utamapanya, and S. Thayumanavan *J. Am. Chem. Soc.* **114**, 1884, **1992**.
- 109 Crystal Structure and Magnetic Susceptibility of a Hydrocarbon Free Radical: Tris (3,5-di-t-butylphenyl)methyl B. Kahr, D. V. Engen, and P. Gopalan, *submitted for publication*.
- 110 A. Izuoka, S. Murata, T. Sugawara, and H. Iwamura, *J. Am. Chem. Soc.* **107**, 1786, **1985**., H. Iwamura, *Pure & Appl. Chem.* **58**, 187, **1986**. A. Izuoka, S. Murata, T. Sugawara, and H. Iwamura, *J. Am. Chem. Soc.* **109**, 2631, **1987**.
- 111 K. Itoh, *Chem. Phys. Lett.* **1**, 235, **1967**., Y. Teki, T. Takui, K. Itoh, H. Iwamura, and K. Kobayashi *J. Am. Chem. Soc.* **108**, 2147, **1986**., K. Itoh, T. Takui, Y. Teki, and Takamasa *Mol. Cryst. Liq. Cryst.* **176**, 49, **1989**. N. Nakamura, K. Inoue, H. Iwamura, T. Fujioka, and Y. Sawaki, *J. Am. Chem. Soc.* **114**, 1484, **1992**. H. Iwamura and N. Koga, *Acc. Chem. Res.* **26**, 346, **1993**.
- 112 S. Murata and H. Iwamura, *J. Am. Chem. Soc.* **113**, 5547, **1991**. K. Inoue, N. Koga, and H. Iwamura, *J. Am. Chem. Soc.* **113**, 9803, **1991**.
- 113 C. Ling, M. Minato, P. M. Lahti, and H. van Willigen, *J. Am. Chem. Soc.* **114**, 9959, **1992**.
- 114 M. Kato, H. B. Jonassen, and J. C. Fanning, *Chem. Rev.* **64**, 99, **1964**.
- 115 G. J. Sloan and W. R. Vaughan *J. Org. Chem.* **22**, 750, **1957**, G. J. Sloan and W. R. Vaughan *J. Chem. Phys.* **25**, 697, **1956**.
- 116 E. G. Rozantsev, V. A. Golubev, M. B. Neiman, and Y. V. Kokhanov, *Bull. Acad. Sci. USSR.* 559, **1965**. E. G. Rozantsev, and V. A. Golubev, *Bull. Acad. Sci. USSR.* 695, **1965**. R. M. Dupeyre, H. Lemaire, and A. Rassat *J. Am. Chem. Soc.* **87**, 3771, **1965**. E. G. Rozantsev, V. A. Golubev and V. A. Golubev *Bull. Acad. Sci. USSR.* 382, **1965**.
- 117 D. F. Evans, *J. Chem. Soc.*, 2003, **1959**.
- 118 D. G. B. Boocock, R. Darcy and E. F. Ullman, *J. Am. Chem. Soc.* **90**, 5445, **1968**, D. G. B. Boocock and E. F. Ullman *J. Am. Chem. Soc.* **90**, 6873, **1968**. E. F. Ullman and D. G. B. Boocock *Chem. Comm.* 1161, **1969**, P. W. Kopf, R. Kreilick, D.G. B. Boocock, and E. F. Ullman, *J. Am. Chem. Soc.* **92**, 4531, **1970**. F. Alies, D. Luneau, J. Laugier, and P. Rey, *J. Phy. Chem.* **97**, 2922, **1993**.
- 119 P. M. Lahti and A. S. Ichimura *Mol. Cryst. Liq. Cryst.* **176**, 125, **1989**.
- 120 O. H. Griffith and A. S. Waggoner, *Acc. Chem. Res.* **2**, 17, **1969**, H. Dugas *Acc. Chem. Res.* **10**, 47, **1977**. E. Ullman, J. H. Osiecki, D. G. B. Boocock, and R. Darcy *J. Am. Chem. Soc.* **94**, 7049, **1972**.

-
- 121 K. Mukai, T. Yano, and K. Ishizu, *Tett. Lett.* **22**, 4661, **1981**. K. Ishizu, H. Kohama, and K. Mukai, *Chem. Lett.* **227**, **1978**, K. Mukai, N. Iida, Y. Kumamoto, H. Kohama, and K. Ishizu, *Chem. Lett.* **613**, **1980**, K. Mukai, M. Yamashita, K. Ueda, K. Tajima, and K. Ishizu, *J. Phys. Chem.* **87**, 1338, **1983**. K. Mukai, M. Tanii, Y. Yurugi, K. Tajima, and K. Ishizu *Bull. Chem. Soc. Jpn.*, **58**, 322, **1985**.
- 122 P. J. Hay, J. C. Thibeault, and R. Hoffmann, *J. Am. Chem. Soc.*, **97**, 4884, **1975**.
- 123 R. Hoffmann, *Acc. Chem. Res.*, **4**, 1, **1971**, R. Gleiter, *Angew. Chem.*, **86**, 770, **1974**.
- 124 O. Kahn, *Angew. Chem. Int. Ed. Engl.* **24**, 834, **1985**. J. B. Goodenough, "*Magnetism and the Chemical Bond*", Interscience, New York, N.Y., **1963**. J. Kanamori, *Phys. Chem. Solid*, **10**, 87, **1959**, P. W. Anderson, *Solid State Phys.*, **14**, 99, **1963**.
- 125 See also perchlorotriphenylmethyl: M. Ballester, J. Riera, J. Castaner, C. Badía, M.J. Monsó, *J. Am. Chem. Soc.*, **93**, 2215, **1971**.
- 126 The ferromagnetic coupling of a pair of nitroxyl substituted benzo-15-crown-5-ethers was accomplished with potassium ions. See: K. Ishizu, H. Kohama, K. Mukai, *Chemistry Letters*, **227**, **1978**. See also: K. Mukai, N. Iida, Y. Kumamoto, H. Kohama, K. Ishizu, *Chem. Lett.*, **613** **1980**; K. Mukai, M. Yamashita, K. Ueda, K. Tajima, K. Ishizu, *J. Phys. Chem.* **87**, 1338, **1983**; J. F. W. Keana, J. Cuomo, L. László, S. E. Seyerdrezai, *J. Org. Chem.* **48**, 2647, **1983**; K. Mukai, M. Tanii, Y. Yurugi, K. Tajima, *Bull. Chem. Soc. Jpn.* **58**, 322, **1985**.
- 127 In related work, glasses of tris(biphenyl)methyl gave triplet coupling, presumably due to stacking of radicals pairwise to form $D_3 \pi$ -complexes. See: W. Broser, H. Kurreck, W. Niemeier, *Tetrahedron*, **32**, 1183, **1976**.
- 128 For a review of one-dimensional ferromagnetism in inorganic solids see: R. D. Willett, R. M. Gaura, C. P. Landee in J. S. Miller (Ed.) *Extended Linear Chain Compounds*, V. 3, Plenum, New York, **1983**; p143.
- 129 C. Kollmar and O. Kahn *Acc. Chem. Res.* **26**, 259, **1993**.
- 130 K. Nath, P. L. Taylor, *Mol. Cryst. Liq. Cryst.*, **180B**, 389, **1990**; K. Yamaguchi, H. Namimoto, T. Fueno, *Mol. Cryst. Liq. Cryst.*, **176**, 151 **1989**; H. Iwamura, S. Murata, *Mol. Cryst. Liq. Cryst.*, **176**, 33, **1989**; J. Veciana, C. Rovira, O. Armet, V. M. Domingo, M. I. Crespo, F. Palacio, *Mol. Cryst. Liq. Cryst.*, **176**, 77, **1989**; D. J. Klein, S. A. Alexander, M. Randic, *Mol. Cryst. Liq. Cryst.*, **176**, 109 **1989**. T. Hughbanks, M. Kertesz, *Mol. Cryst. Liq. Cryst.*, **176**, 115, **1989**; J. S. Miller, A. J. Epstein, *Mol. Cryst. Liq. Cryst.*, **176**, 347, **1989**.

- 131 H. M. McConnell, *J. Chem. Phys.*, **24**, 764, **1956**., D. J. E. Ingram, "*Free Radical as Studied by Electron Spin Resonance*," Butterworths, p.111, **1958**. H. Jukeikis and D. Kivelson *J. Am. Chem. Soc.* **84**, 1132, **1962**.
- 132 O. Armet, J. Veciana, C. Rovira, J. Riera, J. Castaner, E. Molins, J. Rius, C. Maravittles, S. Olivella, and J. Brichfeus *J. Phys. Chem.* **91**, 5608, **1987**.
- 133 A. G. de Mesquita, C. M. Gillarvy, and E. Eriks, *Acta Cryst.* **18**, 437, **1965**; P. Andersen and B. Klewe *Acta Chem. Scand.* **21**, 2599, **1967**; A. Port, M. M. Olmstead, and P. P. Power *J. Am. Chem. Soc.* **107**, 2174, **1985**; J. Veciana, J. Riera, J. Castaner, and N. Ferrer, *J. Organomet. Chem.* **297**, 131, **1985**.
- 134 K.M. Mislow, *Acc. Chem. Res.* **9**, 26 (**1976**).
- 135 M. Ballester, J. Riera, J. Castaner, C. Badia, and J. M. Monso, *J. Am. Chem. Soc.* **93**, 2215, **1971**. K. S. Hayes, M. Nagamo, J. F. Blount, and K. Mislow, *J. Am. Chem. Soc.* **102**, 2773, **1980**.
- 136 "Comparison of Twists in Isosteric Propellers: X-ray Structures of Tris(2,6-dimethoxy-phenyl)borane, Tris(2,6-dimethoxyphenyl)methyl cation, and Tris(2,6-dimethoxyphenyl)methyl Radical"; B. E. Kahr, J. E. Jackson, D. Ward, S. -H. Jang, and J. Blount, *Acta Cryst.*, **B48**, 324, **1992**. "Aryl Ring Twists in Tris(2,6-dimethoxyphenyl)-Z Tripod Ethers: Why is the Radical Different?" S. J. Stout, P. Gopalan, J. E. Jackson, and B. Kahr, Submitted for publication.
- 137 M. M. Olmstead and P. E. Power, *J. Am. Chem. Soc.* **108**, 4235, **1986**.
- 138 K. Ishizu, K. Mukai, A. Shibayama, and K. Kondo, *Bull. Chem. Soc. Jpn.* **50**, 2269, **1977**.
- 139 R. Terrence, O. Toole, N. Janet, B. Younathan, P. Sullivan, and T. J. Meyer *Inorg. Chem.* **28**, 3923, **1989**.
- 140 See F. A. Cotton, G. Wilkinson, "Advanced Inorganic Chemistry" Fifth Ed., Wiley, N.Y. **1988**, pp. 1288 ff., 1388 ff.
- 141 T. P. Radhakrishnan, Z. G. Soos, H. Endres, L. J. Azevado, *J. Chem. Phys.* **85**, 1126 (**1986**).
- 142 H. Volz, W. Lotsch, *Tetrahedron Lett.*, **27**, 2275, **1969**. S. Bank, C. L. Ehrlich, J. A. Zubieta, *J. Org. Chem.*, **44**, 1454, **1979**. S. Bank, C. L. Ehrlich, M. Mazur, J. A. Zubieta, *J. Org. Chem.*, **46**, 1243, **1981**.
- 143 For a general overview, see "Organic Electrochemistry," 2nd Ed., M. M. Baizer, H. Lund, Eds. Marcel Dekker, New York, **1983**, Chap. 2.
- 144 R. W. Brockman and D. E. Pearson, *J. Am. Chem. Soc.* **74**, 4128, **1952**, P. Zuman, *Chem. Listy*, **47**, 1234, **1953**. I. R. Fox, R. W. Taft, Jr., and I. C. Lewis, *J. Am. Chem. Soc.* **81**, 5343, **1959**.

- 145 T. Berzins and P. Delahay, *J. Am. Chem. Soc.* **75**, 5716, **1953**. W. H. Reinmuth, L. B. Rogers and L. E. I. Hummelstedt, *J. Am. Chem. Soc.* **81**, 2947, **1959**.
- 146 C. D. Ritchie, W. F. Sager *Prog. Phys. Org. Chem.* **2**, 323, **1964**. C. G. Swain, S. H. Unger, N. R. Rosenquist, and M. S. Swain, *J. Am. Chem. Soc.* **105**, 492, **1983**, C. Hansch, A. Leo, S. Unger, K. H. Kim, D. Nikaitani, and E. Liem, *J. Med. Chem.* **16**, 1207, **1973**, R. Popielarz and D. R. Arnold, *J. Am. Chem. Soc.* **112**, 3068, **1990**.
- 147 C. D. Ritchie, "*Physical Organic Chemistry*", Marcel Dekker, New York, 102, **1975**. T. H. Lowry and K. S. Richardson, "*Mechanism and Theory in Organic Chemistry*", Harper & Row, New York, 149, **1987**.
- 148 J. J. Brooks and G. D. Stucky *J. Am. Chem. Soc.* **94**, 7333, **1972**.
- 149 M. M. Kreevoy and D. C. Johnston, *Croatica Chemica Acta* **45**, 511, **1973**.
- 150 D. Masilamani and M. M. Rogic *J. Org. Chem.* **46**, 4486, **1981**, W. D. Watson, *J. Org. Chem.* **50**, 2145, **1985**, U. Wriede, M. Fernandez, K. F. West, D. Harcourt, and H. W. Moore, *J. Org. Chem.* **52**, 4485, **1987**. E. Bay, D. A. Bak, P. E. Timony, and A. Leone-Bay, *J. Org. Chem.* **55**, 3415, **1990**. E. Iiehlmann and R. W. Lauener *Can. J. Chem.* **67**, 335, **1989**. R. A. Eade, F. J. McDonald and H. P. Pham, *Asust J. Chem.* **31**, 2699, **1978**. D. C. Schlegel, C. D. Tipton, and K. L. Rinehart, Jr. *J. Org. Chem.* **35**, 849, **1970**, T. L. Davis and V. F. Harrington *J. Am. Chem. Soc.* **56**, 129, **1934**.
- 151 H. Jukeikis and D. Kivelson *J. Am. Chem. Soc.* **84**, 1132, **1962**.
- 152 K. Ishizu, K. Mukai, A. Shibayama, and K. Kondo, *Bull. Chem. Soc. Jpn.* **50**, 2269, **1977**.
- 153 A. Rieker and H. Kessler, *Tett. Lett.* 1227, **1969**; H. Kessler, A. Moosmayer, and A. Rieker, *Tetrahedron*, **25**, 287, **1969**.
- 154 H. S. Gutowsky, C. H. Holm, *J. Chem. Phys.* **25**, 1228, **1956**., D. Kost, E. H. Carlson, and M. Raban, *J. Chem. Soc. Chem. Comm.* 656, **1971**, J. Sandström, *Dynamic NMR Spectroscopy*; Academic Press, New York, 97, **1982**. H. Freibolin, *Basic One- and Two- Dimensional NMR Spectroscopy*, VCH, New York, 263, **1991**.
- 155 Pulsed EPR studies of Ion Binding in a Double-faced Paramagnetic Ionophore: Tris(2,6-dimethoxyethoxy)phenyl)methyl Radical S. -H. Jang, H. -I. Lee, J. MaCracken, and J. E. Jackson. *Accepted for publication in J. Am. Chem. Soc.*
- 156 H. G. Lohr and F. Vögtle *Acc. Chem. Res.* **18**, 65, **1985**.
- 157 L. Kevan, in "*Time Domain Electron Spin Resonance*" L. Kevan & R. N. Schwartz, edit. Chapter 8, Wiley-Interscience, New York, **1979**.

-
- 158 J. MaCracken, D.-H. Shin, and J. L. Dye, *Appl. Magn. Reson.* **3**, 305, **1992**.
- 159 A. A. Shuben and S. A. Dikanov, *J. Magn. Reson.* **52**, 1, **1983**.
- 160 W. Weltner, "*Magnetic Atoms and Molecules*", Dover, New York, **1983**.
- 161 M. M. Baizer and H. Lund. "*Organic Electrochemistry*", 2nd Edition, Chapter 2, Marcel Dekker, New York, **1983**. S. Bank, C. L. Ehrlich, M. Mazur, and J. A. Zubieta *J. Org. Chem.*, **46**, 1243, **1981**. G. Kothe, W. Summerrmann, H. Baumgartel and H. Zimmermann, *Tett. Lett.* 2185, **1969**.
- 162 S. Gauthier and J. M. Fréchet *Synthesis* , 383, **1987**.
- 163 See for example F. A. Cotton, G. Wilkinson, "Advanced Inorganic Chemistry" 5th Ed., Wiley Interscience, NY, **1988**, p. 1385. J. E. Huheey, "Inorganic Chemistry; Principles of structure and reactivity" 2nd E. Harper & Row, NY, **1978**, p71.
- 164 "PCModel Molecular Modeling Software", K. E. Gilbert, J. J. Gajewski, M. M. Midland; Serena Software, Bloomington, IN 47402, (**1987**).
- 165 There have been a number of reports of organic ferromagnetism. The more substantial accounts are those of the well-characterized crystalline metallocene derivatives cited. For other examples of purported organic ferromagnets in less well-characterized polymeric materials see: H. Tanaka, K. Tokuyama, T. Sato, T. Ota, *Chemistry Letters*, 1813, **1990** ; J. B. Torrance, S. Oostra, A. Nazzal *Syn. Met.* **19**, 708 ,**1987** ; Y. V. Korshak, T. V. Medvedeva, A. A. Ovchinnikov, V. N. Spektor, *Nature*, **326**, 370 **1987** ; Y. Cao, P. Wang, Z. Hu, S. K. Zhang, J. Zhao, *Syn. Met.* **27**, B625, **1988** ; M. Ota; S. Otani; K. Kobayashi, *Chem. Lett.* 1179 , **1989**.
- 166 P. Grobet, L. V. Gerven, A. V. D. Bosch, and J. Vansumneren, *Physica* 86-86B, 1132, **1977**. W. Boon and L. V. Gerven, *Physica B* **155**, 437, **1989**.
- 167 We have been unable to obtain any commercially available simulation programs for multiradical CW-EPR spectra.
- 168 A careful structure determination with a review of the history of Chichibabin's hydrocarbon appeared recently: Montgomery, J. C. Huffman, E. A. Jurczak, M. P. Grendze, *J. Am. Chem. Soc.* **108**, 6004, **1986**.
- 169 Although the singlet-triplet splitting in Chichibabin's hydrocarbon has not been unambiguously determined, it is clear that the (singlet) wavefunction of the crystalline material studied by Montgomery has a significant biradical component.
- 170 G. A. Jeffrey and W. Saenger in "*Hydrogen Bonding in Biological Structures* " Springer-Verlag, Berlin Heidelberg New York, **1991** and references therein.
- 171 J. Herbich, J. Karpikuk, Z. R. Grabowski, N. Tamai, and K. Yoshihara *J. Luminescence* **54**, 165, **1992**. H. Tamiaki and K. Maruyama *J. Chem. Soc.*

-
- Perkin. Trans.* 2431, **1992**. C. Turrò, C. K. Chang, G. E. Leroi, R. I. Cukier, and D. G. Nocera, *J. Am. Chem. Soc.* **114**, 4013, **1992**. A. Harriman, Y. Kubo, J. L. Sessler, *J. Am. Chem. Soc.* **114**, 388, **1992**. D. N. Beratan, J. N. Betts, and J. N. Onuchic *Science*, **252**, 1285, **1991**. Y. Aoyama, M. Asakawa, Y. Matsui, and H. Ogoshi, *J. Am. Chem. Soc.* **113**, 6233, **1991**.
- 172 R. Hoffmann *Acc. Chem. Res.* **4**, 1, **1971**, P. J. Hay, J. C. Thibeault, and R. Hoffmann, *J. Am. Chem. Soc.* **97**, 4884, **1975**. R. Gleiter, *Angew. Chem.* **86**, 770. **1974**.

MICHIGAN STATE UNIV. LIBRARIES



31293010190910